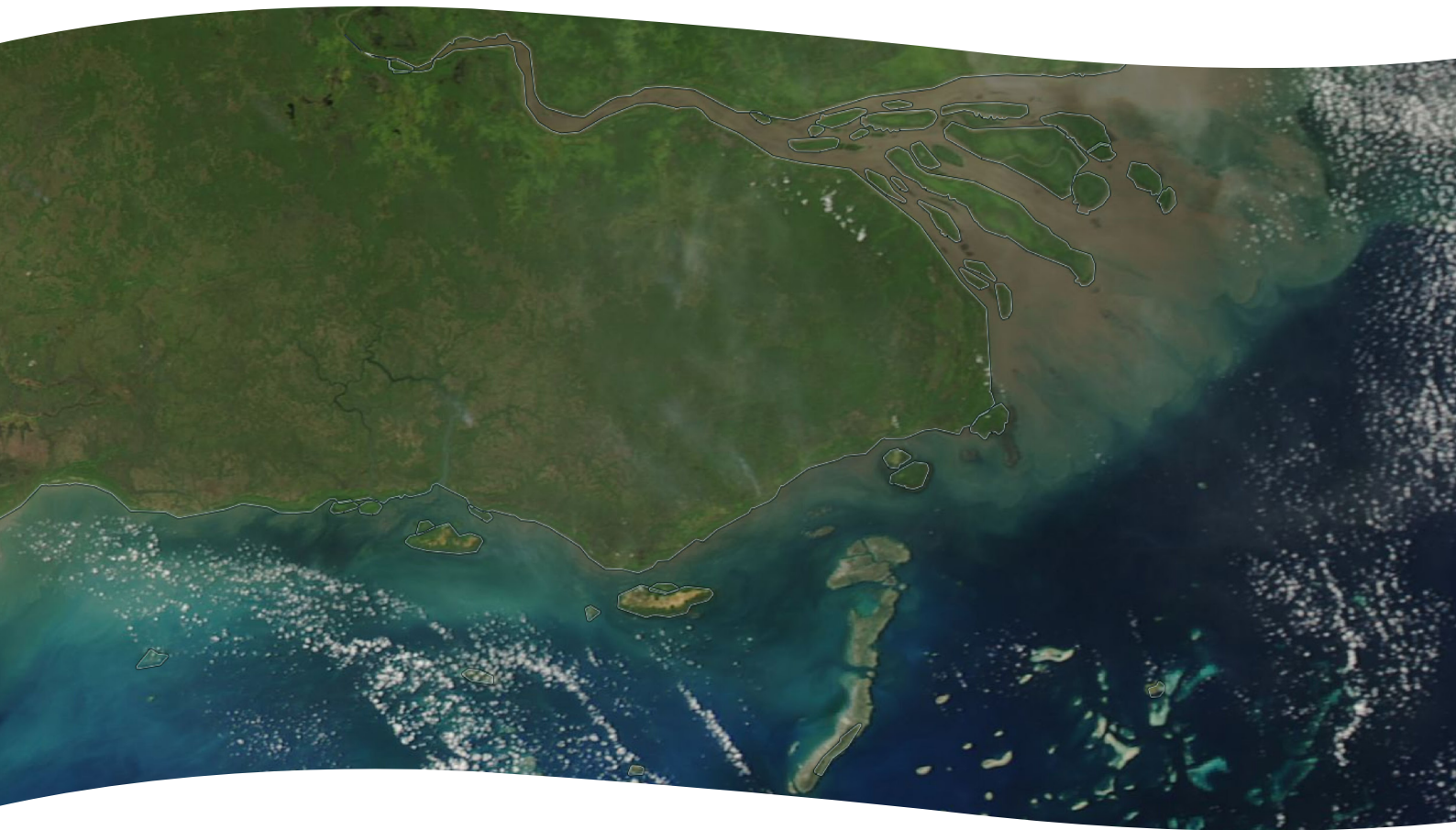# Assessing the influence of the Fly River discharge on the Torres Strait

Jane Waterhouse, Simon C. Apte, Caroline Petus, Brad M. Angel, Eric Wolanski, Scott Bainbridge, Dieter Tracey, Chad V. Jarolimek, Joshua King, Jane Mellors and Jon Brodie

JAMES COOK UNIVERSITY
AUSTRALIA

Assessing the influence of the Fly River discharge on the Torres Strait

Jane Waterhouse[1], Simon C. Apte[2], Caroline Petus[1], Brad M. Angel[2], Eric Wolanski[1], Scott Bainbridge[3], Dieter Tracey[1], Chad V. Jarolimek[2], Joshua King[2], Jane Mellors[1] and Jon Brodie[4]

[1] TropWATER, James Cook University, Townsville, Australia
[2] CSIRO Land & Water, Sydney, Australia
[3] Australian Institute of Marine Science, Townsville, Australia
[4] Centre of Excellence for Coral Reef Studies, James Cook University, Australia

National **Environmental** Science Programme

Cover photographs: (front) MODIS-Aqua true colour image, 12 Oct 2016 showing influence of Fly River discharge. Image: © NASA Worldview application. (back) Herbert Warusam, Mura Buway Ranger, Saibai Island collecting sediment cores with the gravity sediment corer. Image: Jane Mellors.

This report is available for download from the NESP Tropical Water Quality Hub website:
http://www.nesptropical.edu.au

CONTENTS

LIST OF TABLES

LIST OF FIGURES

ACRONYMS AND ABBREVIATIONS

AIMS.............. Australian Institute of Marine Science

ANZG .... Australian and New Zealand Guideline

ANOVA.......... Analysis of variance

CDOM............ Coloured dissolved organic matter

Chl-a.............. Chlorophyll-a

C/N .... Carbon/Nitrogen

CSIRO .... Commonwealth Scientific and Industrial Research Organisation

DOC .... Dissolved organic carbon

DGV............... Default guideline value

EDS .... Energy dispersive X-ray spectroscopy

ENSO .... El Niño–Southern Oscillation

EOSDIS .... Earth Observing System Data and Information System (A NASA utility)

GBR .... Great Barrier Reef

GPS............... Geographical positioning system

GV .... Guideline value

HCl .... Hydrochloric acid

JCU .... James Cook University

MA................. MODIS Aqua

MODIS........... Moderate resolution imaging spectroradiometer

MOHID........... Modelo Hidrodinamico ('hydrodynamic' in Portuguese)

MQ water ...... High purity deionised water

MSL............... Mean sea level

NATA............. National Association of Testing Authorities

NERP............. National Environment Research Program

NESP............. National Environmental Science Program

NOAA .... National Oceanic and Atmospheric Administration (USA)

NE .... Northeast

NTU .... Nephelometric turbidity units

NW .... Northwest

OLCI.............. Ocean and Land Colour Instrument

PNG............... Papua New Guinea

Sd................. Standard deviation

WQGV .... Water quality guideline value

SLIM.............. Second-generation Louvain-la-Neuve Ice-ocean Model

S2 .... Sentinel 2

S3 .... Sentinel 3

SE................. Southeast

SEM.............. Scanning electron microscopy

SSC .... Suspended sediment concentration

SSD .... Species sensitivity distribution

SW.................Southwest

TC.................True colour

TSRA.............Torres Strait Regional Authority

TSS ....Total suspended solids

TWQ ....Tropical Water Quality

UPGMA ....Unweighted pair group method with arithmetic mean

WS.................Wet season

ΔMSL ....Difference in mean sea level (MSL) across the Strait. ΔMSL is > 0 when the MSL in the Gulf of Papua is greater than the MSL in the Gulf of Carpentaria

TRACE METALS

Al...................aluminium

Fe ....iron

S....................sulfur

Ca..................calcium

Ag..................silver

As..................arsenic

Cd..................cadmium

Ce..................cerium

Co..................cobalt

Cr ....chromium

Cu..................copper

Mn ....manganese

Mo ....molybdenum

Ni...................nickel

Pb..................lead

T ....titanium

U....................uranium

V ....vanadium

Zn ....zinc

UNITS OF MEASUREMENT

h .... hour

km .... kilometre

m .... metre

mg .... milligram

Mt/yr .... Million tonnes per year

ng .... nanogram

NTU .... Nephelometric turbidity unit

µg .... microgram

PSU .... Practical Salinity Units

µL .... microlitre

µm .... micrometre

ISLAND NAMES

Traditional name	Other references
Maizab Kaur	Bramble Cay
Erub	Darnley
Masig	Yorke
Iama	Yam
Ugar	Stephens
Warraber	Sue
Murray	Mer
Poruma	Coconut
Saibai	Saibai
Boigu	Talbot
Duaun	Mt Cornwallis
Waiben	Thursday
Ngurupai	Horn

ACKNOWLEDGEMENTS

EXECUTIVE SUMMARY

The Torres Strait is an area of Australia that has relatively few anthropogenic inputs of trace metals, however, concerns have been raised about the impacts of mining occurring in Papua New Guinea (PNG) and the transboundary transport of metal contaminants into the Torres Strait. Under certain climatic conditions, dilute Fly River plume waters have been detected across the northern Torres Strait, east of the Warrior Reefs, as far west as Saibai Island and south to Masig Island. It is important to note that this is a natural process that has been occurring for several thousand years. However, in 1984 the Ok Tedi copper mine opened in the headwaters of the Fly River and the Porgera gold mine opened in 1990 in the headwaters of the Strickland River (a major tributary of the Fly River) in PNG. This has resulted in significant impacts on the river system including widespread contamination of the Fly River by copper (which is highly toxic to aquatic life), increased turbidity and changes to river geomorphology through widespread deposition of sediments. Estimates suggest that mining operations have increased sediment discharge from the whole of the Fly River by 40%. Given the close proximity of the Torres Strait to the mouth of the Fly River, concerns have been raised since the start of mine operations that trans-boundary pollution may occur.

To enhance our understanding of the Fly River plume intrusion into the Torres Strait and identify its potential impacts on the region's marine ecosystems and dependent communities, two phases of projects were undertaken through the National Environmental Science Program (NESP). These projects built on previous work to determine: (i) the spatial extent, temporal patterns of the Fly River plume and the water and sediment quality of the Torres Strait region; and (ii) which ecosystems in the Torres Strait are exposed to the Fly River discharge. The studies were conducted by James Cook University (including TropWATER and the Centre of Excellence for Coral Reef Studies) and CSIRO in collaboration with scientists from the Australian Institute of Marine Science, University of New South Wales, Macquarie University, University of Algarve, the Yantai Institute of Coastal Zone Research China and C_2O Consulting. It was outside the scope of this project to conduct a full assessment of the (environmental) impact of Fly River discharges on Torres Strait ecosystems, and the current studies focused only on identifying when and where the influence from this discharge is likely to occur.

The studies which commenced in 2015 as part of NESP Project 2.2.1 and 2.2.2 (2015 to 2018) have utilised a range of tools. This included weekly salinity monitoring conducted by local Rangers, real time marine observations for salinity and turbidity supported by local weather data, hydrodynamic and sediment transport modelling, remote sensing to assess plume intrusions and to conduct turbidity and suspended sediment concentration assessments, and collection of field data for dissolved trace metal concentrations, and for metal concentrations in suspended sediment, benthic sediment and in seagrasses across the region. The additional work in NESP TWQ Hub Project 5.14 (2019 - 2020) also included a tracing component to provide further evidence of potential sources of elevated trace metal concentrations in areas of the Torres Strait. Using these multiple lines of evidence, a more complete assessment of the potential influence of the Fly River discharge in the Torres Strait region was able to be gained. This information is important for ensuring the protection of these regions given their importance as ecosystems, to Torres Strait Islander communities and to turtle and dugong populations, and their connectivity with the Great Barrier Reef Marine Park. The key findings of the study were:

1. Data collected through salinity monitoring, turbidity loggers, remote sensing and modelling predictions further confirmed previous findings that habitats located in the northeast corner of the Torres Strait Protected Zone, including the northern Warrior Reef, as far west as Saibai Island and as far east as Bramble Cay, are located in an area of higher exposure to sediments from the Fly River. The evidence also reinforced that there is a turbid coastal boundary layer along the PNG coast of the Torres Strait with maximum turbidity found inshore and decreasing seaward.

2. The source of highly turbid Torres Strait waters cannot be fully attributed to the Fly River and is likely to include other sources of sediments associated with smaller streams (including the Wassi Kussa and Mai Kussa Rivers around Boigu Island), as well as resuspension of sediment deposited in the Torres Strait mud wedge via currents, wind and wave action.

3. The Fly River plume intruded into the Torres Strait to the greatest extent during the southeast trade wind season and less so during the monsoon season. Satellite images and logger data collected at Warrior Reef suggested that the plume intrusion is greater between June and September, with a likely maximum in July to August.

4. Salinity at the northern Warrior reef monitoring site showed a strong monthly cycle with low salinity events that cannot be explained by localised rainfall or run-off. These may represent tidally driven brackish waters from coastal PNG flowing into the northern Warrior Reef area.

5. Sediment transport modelling demonstrated that contaminated new mud intrudes Torres Strait from the Fly River discharge and is diluted by the non-contaminated mud of the long-term mud wedge. Daru and Bristow Islands, located close to the PNG coast, form a hydrodynamic barrier that restricts the circulation pattern and slows down the intrusion of Fly River contaminated material further west into the Torres Strait. The time scales for the pollution spread in Torres Strait are probably of the order of 100 years.

6. Water quality across the Torres Strait is generally very good, however elevated concentrations of some trace metals are observed in waters, sediments and seagrasses in the northeast areas of the Torres Strait including Bramble Cay and also around the northern Warrior Reefs, Boigu and Saibai Islands. The highest copper concentrations (along with other metals) were found around Saibai Island. The concentrations of dissolved trace metals measured in the Torres Strait were all below the Australia and New Zealand marine water quality guideline values for 95% species protection which are the main guideline values applied in Australia for coastal management. However, the concentrations of dissolved copper detected in the Boigu and Saibai regions consistently exceeded the Australian and New Zealand Guideline Value of 99% that is applicable for pristine, uncontaminated waters. This is significant because copper is the primary trace metal of concern that is linked to the Ok Tedi mine discharge. It is important to note that the concentrations of dissolved copper measured in the Torres Strait are orders of magnitude below those reported to cause direct impacts on coral and seagrass ecosystems.

7. The enrichment of metals in waters and sediments in the Boigu and Saibai region is likely to result from natural inputs of metals from the PNG mainland such as river runoff from various coastal rivers which are periodically augmented by contributions from the Fly River plume. The relative contributions from these sources is hard to assess without data on the contributions of metals from the PNG coastal rivers in the Boigu/Saibai region. Sediment core data indicates relatively homogenous distributions of metals with depth and does not indicate increases in metals concentrations with time. Sulphide mineral particles indicative of mine-derived sediments were detected in suspended sediment particles in samples from Boigu and Saibai but confirmation of their origin requires further work.

8. The concentrations of dissolved trace metals found around the northeast Torres Strait, Boigu and Saibai are higher than those found in other Australian coastal environments, especially for cobalt and cadmium, but are far lower than the concentrations observed in contaminated locations such as industrialised harbours.

9. The elevation of metal concentrations in the northeast Torres Strait at locations such as Bramble Cay is most likely associated with the influence of the Fly River plume. This is evident from the elevated dissolved copper concentrations and copper concentrations in suspended sediments. The association is also supported by salinity and turbidity logger data and remote sensing results. However, benthic sediments do not appear to be accumulating mine-derived contaminants as only extremely low particulate trace metal concentrations were detectable along with an absence of sulphide mineral particles (used for tracing). This is also consistent with the findings from the hydrodynamic and mud transport modelling.

10. Seagrass trace metal concentrations were significantly higher in the northeast Torres Strait (Bramble Cay), and then Boigu and Saibai islands. Markedly higher concentrations of cobalt, chromium, copper, lead and zinc were found in seagrasses from the Boigu and Saibai sites. Copper lead and zinc were also higher at Bramble Cay compared to the remaining sites. These results are in broad agreement with the patterns of the metal analysis in water, suspended sediments and benthic sediment. Seagrass trace element concentrations were generally low compared with literature values reported for other unpolluted environments.

11. Comparison of benthic sediment metals data collected over the course of the NESP Tropical Water Quality Hub Torres Strait projects (2016 to 2020) with data from the Torres Strait Baseline Study conducted in the early 1990's did not suggest any marked increase in metals concentrations that could be associated with mine-derived sediment inputs. Indeed the recent concentrations of copper (indicative of mine-related inputs) in sediments measured at Bramble Cay, the monitoring site closest to the mouth of the Fly River, were over an order of magnitude lower than measured during the baseline study. This difference was linked to the presence of a far larger proportion of fine sediments at Bramble Cay during the baseline study compared to the current day. The data may reflect geomorphological changes at Bramble Cay over the last 30 years or transient deposition of fine sediments at this location.

12. Based on multiple lines of evidence derived from the investigations conducted, six 'areas of relative exposure' to Fly River discharge were defined (Table i). The highest relative exposure areas (to freshwater, turbid waters and trace metals) were located in North East (Bramble Cay - Zone 1) and North West (Saibai, Boigu - Zone 3). While the North Central areas (Warrior Reefs - Zone 2) were also within the higher area of exposure, the degree of exposure - and link to the Fly River specifically - was lower than Saibai and Boigu islands (Zone 3) and Bramble Cay (Zone 1), but still high relative to other areas. The North Central–south area (Masig and Ugar - Zone 4) was considered to be a transitional area and was therefore assessed as moderate to low exposure. The Central (Iama, Warraber, Poruma – Zone 5) and South East areas (Erub, Mer – Zone 6) were the lowest exposure areas, with limited or no evidence of Fly River discharge influencing these areas. Data confidence varied for each zone and assessment (Table i). This was a *relative* assessment of the exposure of the Torres Strait region to Fly River discharge, and even the highest concentrations of dissolved trace metals measured in the study were below the Australian and New Zealand Guideline (ANZG) default guideline values for 95% species protection. However, the concentrations of dissolved copper detected in the Boigu and Saibai regions consistently exceeded the ANZG of 99% that is applicable for pristine, uncontaminated water. An Overall Assessment, synthesising the above results and adding an assessment of Ecological significance, took this into account. None of the zones were assessed as being in the highest Overall Assessment category as the ecological significance of the results in all locations was assessed as being relatively low to moderate, and with low data confidence. Zone 1, Zone 2 and Zone 3 were in the moderate category, Zone 4 was in the moderate to lowest category, and Zone 5 and 6 were in the lowest category.

Water Quality Implications for Torres Strait

The implications of these changes to water quality in the Torres Strait are not well known, but potential impacts can be extrapolated from knowledge derived from other marine ecosystems including the Great Barrier Reef. For example, increased sediment inputs can result in increased turbidity and reduced water clarity in receiving waters, which in turn reduces light availability for marine ecosystems, leading to local and regional scale changes and potential degradation of coral reef and seagrass ecosystems. Increases in trace metal concentrations above National Water Quality Guidelines could also have direct toxicological impacts on coral reef and seagrass health as well as direct effects on local marine species such as turtles, dugongs and fish. However, the concentrations of trace metals that are documented to cause adverse effects on corals are orders of magnitude higher than those measured in this study. Impacts of trace metals on seagrass are understood to be of a lower threat to the plant itself, however, bioaccumulation can also have flow-on effects for other species such as seagrass-feeding animals such as green turtle and dugong. These animals also have an important dietary role in some local islander communities as well as being iconic and vulnerable species in the region. The trace metal concentrations measured in this study are relatively low, and the environmental risk associated with exposure to these concentrations is not of concern. However, there were limitations to the study (due to COVID-19 restrictions) in terms of the temporal variability in the results that may warrant further investigation in terms of potential 'flow on' effects of the bioaccumulation of trace metals in marine plants and animals. Further discussion of the limitations of this study and the areas of greatest uncertainty in the results is included in Section 8.5.

Of critical importance to the local communities, this study confirms that almost 30 years on from the 1991-1992 Torres Strait Baseline Study, there have not been any detectable increases in the concentrations of trace metals in benthic sediments at locations in the Torres Strait that are potentially impacted by mine-derived sediments. The current study also extended this evidence to include analysis of dissolved trace metals in the water and suspended sediment (not just benthic sediment), highlighting some areas of greater exposure, as well as areas of uncertainty in terms of potential contributions from smaller PNG mainland rivers. In addition, this study has strengthened the knowledge of the extent of influence of Fly River discharge on turbidity dynamics in the region through detailed analysis of long-term (11 years) remote sensing datasets, the sediment transport model and *in-situ* monitoring.

The results provide spatially explicit information that can help to prioritise areas which need further investigation and/or where management effort should be focused in the Torres Strait. It is however important to note that this study did not explicitly evaluate ecological impacts or possible sub-lethal effects of low-level contaminant exposure on organisms. Investigation of ecological impact of exposure to metals was outside the scope of the current study. Accordingly, the analysis of trace metals in seafood that was conducted in the 1991-1992 Torres Strait Baseline Study would need to be repeated to enable comprehensive comparison of the potential changes over time.

Results from this project underline the importance of integration of data from a range of sources to provide a comprehensive assessment of water quality and environmental conditions. In this study, the remote sensing data utilised results from the *in-situ* monitoring studies (salinity, *in-situ* loggers and metal concentrations) to strengthen the conclusions by providing match up of results with satellite images and verification of the potential source of influence. Furthermore, the modelling also cross-referenced the remote sensing outputs and *in-situ* data. Without these links between datasets, the ability to draw conclusions with a relatively high level of confidence would not be possible. This study also highlights the value of long-term datasets, and the important role that the Torres Strait Baseline Study played in setting a baseline for comparison of results in the region. It has demonstrated that the multiple lines of evidence approach to exposure assessment may be essential in remote, complex and data poor marine environments such as the Torres Strait.

Recommendations

1. Future water quality monitoring of the Torres Strait would be best conducted jointly between Australia and PNG. This would allow access to areas such as the rivers that drain the South Fly district of PNG and also enable monitoring of the sources of mine derived contamination that originate from the Fly River. It is also important to track changes of mining operations in PNG such as mine expansions and shutdowns and use this information as a trigger to inform future monitoring.

2. Future sediment and water quality monitoring should focus on Bramble Cay, the Warrior Reef complex and the PNG coastline (Daru to Boigu). Prior to long term monitoring, a pilot study should assess temporal variability (e.g. seasonal variations) and spatial heterogeneity at these locations. Given the slow rates of sediment accumulation, a monitoring frequency of every 5 to 10 years would be sufficient to track environmental change.

3. Further field monitoring should be conducted to explain the low salinity events observed at the northern Warrior Reef. This information would enable a better understanding of water circulation and a better understanding of the freshwater contributions from the rivers in the South Fly district.

4. This study has illustrated the benefits of utilising multiple lines of evidence (e.g. field monitoring, remote sensing, modelling, biomonitoring and geochemical investigations) to assess environmental impacts. It is recommended that future studies adopt this integrative approach.

5. Involvement of local Rangers has also provided significant benefits to the project in terms of access to local support, and engagement and upskilling of the Ranger teams; continuation of their involvement is recommended in any future monitoring programs.

Table i: Summary of the lines of evidence assessing the intrusion of Fly River discharge in the Torres Strait

Relative assessment score	Confidence in dataset/assessment	Assessment
🟠 Highest	▪▪▪ High	🔶 Exposure to Fly River discharge. Elevated trace metal concentrations, above guideline values. Ecological risk likely, but high uncertainty. **Further investigation recommended.**
🟡 Moderate	▪▪ Moderate	🔶 Exposure to diluted Fly River discharge. Slighly elevated or elevated trace metal concentrations, but below guideline values. Ecological risk likely to be low, but high uncertainty. **Further investigation recommended.**
🔵 Lowest	▪ Low	🔷 Low exposure, low trace metal levels, low ecological risk. **No need for further investigations***

*** Further investigations include:** *Examination of biological indicators + Salinity monitoring + Long-term continuous in-situ measurements of temperature, salinity and turbidity supported by satellite data and sediment transport modelling + Periodic monitoring (every five to ten years) of water and sediment quality including trace metal analysis.*

Zone	In-situ data – loggers and salinity	Modelling data suggests that:	Remote sensing data suggests that:	Additional evidence	Metals in sediment, water & seagrass	Ecological significance	Overall assessment
1 — North central (Warrior Reef)	Pulses of low salinity water detected, appear correlated to monthly tidal flows and may represent low salinity PNG coastal water intruding down to the northern Warrior Reefs.	The influence of Fly River waters is a common occurrence during the SE trade wind season.	The influence of Fly River waters is likely to reach the Warrior Reefs during the SE trade wind season.	Oceanographic studies in April-May 1982 and August-September 1994 show a major intrusion of Fly River water and mud at Warrior Reef.	Some evidence of slightly elevated trace metal concentrations in benthic sediments, waters and suspended sediments. Relatively low trace metals concentrations in seagrass - consistent with other unpolluted environments.	Presence of key ecosystems (coral, seagrass). Dissolved trace metals below guideline values for species protection.	Very likely periodic influence of Fly River waters during the SE trade wind season. Turbid plume waters likely diluted (low salinity, higher but still moderate turbidity levels). Measurable likely influence of contaminated materials. Ecological significance likely to be low, but there is high uncertainty in this assessment.
	Exposure to Fly River discharge and/or derived sediments 🟠 ▪▪▫				*Mine derived pollution* 🟡 ▪▪▫	*Potential threats* 🔵 ▪▫▫	🔶
2 — North east (Bramble Cay)	Higher than expected levels of field turbidity and exposure to turbid waters in satellite data for a remote offshore reef.	The influence of Fly River waters is a common occurrence throughout the year, but especially in the SE trade wind season with events lasting 2-3 weeks.	Intermittent influence of the Fly River plume on Bramble Cay captured by medium resolution (MODIS and Sentinel) and high resolution satellite images (Sentinel-2) during the trade wind season. Period of highest exposure is likely between June and September.	Coral cores showed freshwater influence and several pulses of freshwater each year (1781-1993). Oceanographic studies in April-May 1982 and August-September 1994 show a major intrusion of Fly River water and mud.	Elevated dissolved copper and elevated suspended sediment associated copper concentrations detected. Also some evidence of elevated trace metal concentrations in benthic sediments. Some elevation of trace metals (copper, silver, lead, zinc) in seagrass.	Presence of Key ecosystems (coral, seagrass) + fisheries. Dissolved trace metals below guideline values for species protection.	Regular 'pulses' of Fly River waters potentially driven by wind intensity and direction (inter-annual variability) with higher chance of exposure during periods of intense SE trade winds. Measurable likely influence of contaminated materials. Ecological significance likely to be low, but there is high uncertainty in this assessment.
	Exposure to Fly River discharge and/or derived sediments 🟠 ▪▪▪				*Mine derived pollution* 🟠 ▪▪▫	*Potential threats* 🔵 ▪▫▫	🔶
3 — North west (Boigu,Saibai)	Lower field salinity and higher salinity ranges measured.	The influence of Fly River waters is a common occurrence during the SE trade wind season. Signature diluted at Boigu Island.	The influence of Fly River waters is likely to reach Saibai Island. Wassi Kussa and Mai Kussa Rivers likely contribute to turbidity levels in the areas east and west of Boigu Island. The contribution of Mai and Wassi Kussa rivers varied seasonally and is expected to reach a maximum around May to August with turbid riverine water mainly flowing westward during this period.	An oceanographic study in April-May 1982 and August-September 1994 show a major intrusion of Fly River water and mud. Historically, extensive salinity intrusion in August-September 1994.	Elevated trace metal concentrations in waters and sediments. Highest metal concentrations in waters and sediments detected in this zone. Highest concentrations of several metals, including copper, lead and zinc, in seagrass found in this area.	Presence of Key ecosystems (coral, seagrass). Dissolved copper concentrations exceed the 99% species protection guideline value indicating some potential stress on ecosystems.	Likely influence of Fly River waters and mud at Saibai but this is diluted by the original mud along the PNG coast; potential influence of Fly River waters at Boigu but likely highly diluted. The time scale of influence of contaminated materials may be 100 years. Likely influence of southern PNG mainland inputs (especially at Boigu – Mai and Wassi Kussa rivers) requires quantification. Ecological significance likely to be low, but there is high uncertainty in this assessment.
	Exposure to Fly River discharge and/or derived sediments 🟠 ▪▪▫				*Mine derived pollution* 🟡 ▪▪▫	*Potential threats* 🔵 ▪▫▫	🔶

Relative assessment score

- 🟠 Highest
- 🟡 Moderate
- 🔵 Lowest

Confidence in dataset/assessment

- ▪▪▪ High
- ▪▪ Moderate
- ▪ Low

Assessment

- 🔶 Exposure to Fly River discharge. Elevated trace metal concentrations, above guideline values. Ecological risk likely , but high uncertainty. **Further investigation recommended.**
- 🔶 Exposure to diluted Fly River discharge. Slightly elevated or elevated trace metal concentrations, but below guideline values. Ecological risk likely to be low, but high uncertainty. **Further investigation recommended.**
- 🔷 Low exposure, low trace metal levels, low ecological risk. **No need for further investigations***

* Further investigations include: Examination of biological indicators + Salinity monitoring + Long-term continuous in-situ measurements of temperature, salinity and turbidity supported by satellite data and sediment transport modelling + Periodic monitoring (every five to ten years) of water and sediment quality including trace metal analysis.

Zone	In-situ data – loggers and salinity	Modelling data suggests that:	Remote sensing data suggests that:	Additional evidence	Metals in sediment, water & seagrass	Ecological significance	Overall assessment
4 — North central (south) (Ugar, Masig)	Salinity measurements at Masig Island are similar to average values for marine waters. Occasional reductions in salinity (to 33 PSU) were measured in the SE trade wind seasons.	Frequent intrusion of Fly River water, but diluted with seawater. Probably minimal Fly River mud reaches there.	Limited exposure to turbid waters and greatest variability between years in the SE trade wind season.	Oceanographic studies in 1979, 1981, 1982 and 1994 shows a frequent intrusion of the Fly River plume, but well diluted by oceanic water.	Some evidence of elevated trace metal concentrations in waters. Relatively low trace metals concentrations in sediments and seagrass - consistent with other unpolluted environments.	Presence of Key ecosystems (coral, seagrass) + fisheries. Dissolved trace metals below guideline values for species protection.	Likely event-driven influence of Fly River waters in the SE trade wind season, likely to be highly diluted with seawater. Comparison of salinity data with local rainfall data and satellite images and modelling results indicate that the periods of lower salinity may be influenced by Fly River waters. Small influence of water-borne contaminated materials. Ecological significance likely to be low, but there is high uncertainty in this assessment.
		Exposure to Fly River discharge and/or derived sediments			*Mine derived pollution*	*Potential threats*	
		🟡🔵 ▪			🟡🔵 ▪▪	🔵 ▪	🔷🟡
5 — Central (Iama, Warraber, Poruma)	Highest mean salinities and lowest salinity ranges were measured at these sites. Data indicates minimal freshwater inputs.	Minimal intrusion of Fly River water.	Very limited exposure to turbid waters.	Oceanographic studies in 1979, 1981, 1982 and 1994 shows an intrusion of the Fly River plume highly diluted by oceanic water.	No evidence of elevated trace metal concentrations in waters and sediments. Relatively low trace metals concentrations in seagrass - consistent with other unpolluted environments.	Presence of Key ecosystems (coral, seagrass). Dissolved trace metals below guideline values for species protection.	Likely no influence from Fly River waters. No evidence of contaminated materials. Low ecological significance.
		Exposure to Fly River discharge and/or derived sediments			*Mine derived pollution*	*Potential threats*	
		🔵 ▪▪			🔵 ▪▪▪	🔵 ▪▪	🔷
6 — South east (Erub, Mer)	Insufficient salinity measurements collected to undertake assessment.	Limited Fly River water reaches Erub Island.	Limited exposure to turbid waters and greatest variability between years in the SE trade wind season.	Coral cores showed no freshwater influence at Erub (1781-1993). Previous modelling studies (1979, 1981, 1982 and 1994) show no intrusion of Fly River waters at Mer Island, but a more frequent intrusion of Fly River water at Erub Island (but no mud), and it was well diluted with seawater.	No evidence of elevated trace metal concentrations in waters and sediments. Relatively low trace metals concentrations in seagrass - consistent with other unpolluted environments.	Presence of Key ecosystems (coral, seagrass). Dissolved trace metals below guideline values for species protection.	Influence of Fly River waters unlikely to be significant at Mer Island, but further investigation is required at Erub Island due to modelling results and proximity to Zone 4. Limited influence of contaminated materials. Low ecological significance.
		Exposure to Fly River discharge and/or derived sediments			*Mine derived pollution*	*Potential threats*	
		🔵 ▪▪			🔵 ▪▪▪	🔵 ▪▪	🔷

PART A: INTRODUCTION

1.0 BACKGROUND

Torres Strait Islanders depend on local marine resources for food, livelihoods, and cultural activities. The Torres Strait is an area of Australia that has relatively few anthropogenic inputs of contaminants such as trace metals. However, concerns have been raised over the last couple of decades about the impacts of mining occurring in Papua New Guinea (PNG) and trans-boundary transport of metal contaminants into the Torres Strait.

The Ok Tedi copper mine in PNG has been operating since 1984 and discharges copper contaminated sediments in the form of mine tailings and waste rock into the Fly River which ultimately flow into the Fly River Estuary and Gulf of Papua. This has resulted in significant impacts on the river system including widespread contamination of the Fly River by copper (which is highly toxic to aquatic life), increased turbidity and changes to river geomorphology through widespread deposition of sediments (Bolton 2008). Estimates made during the early stages of mining suggested that mining operations had increased sediment discharge from the whole of the Fly River by 40% (Wolanski et al. 1995a). Given the close proximity of the Torres Strait to the mouth of the Fly River (Figure 1-1), concerns have also been raised since the start of mine operations that trans-boundary contamination may also be occurring.

Most of the water from the Fly River estuary discharges into the Gulf of Papua. Under certain tidal and weather conditions it has been observed that plumes of water from the Fly River estuary may extend into the north east Torres Strait (Wolanski et al. 1999; Li et al. 2017). This is a natural process which has been occurring for several thousand years. However, over the last 30 years, intrusion of plumes of water originating from the Fly River now provide a mechanism for transporting mine sediments into the north east Torres Strait. Fly River plume waters have been detected across the northern Torres Strait, east of the Warrior Reefs, as far west as Saibai Island and south to Masig Island (Figure 1-1) (Wolanski et al. 2013a, 2013b; Martins and Wolanski 2015; Li et al. 2017; Petus et al. 2018). These areas contain complex and important seagrass and reef communities that are potentially threatened by changes in water quality (Carter et al. 2014). The Commonwealth Scientific and Industrial Research Organisation (CSIRO) has conducted various studies on the impacts of mine contamination in the Fly River system over the last 25 years that indicate a significant increase in the copper content of waters and sediments in the Fly River estuary (Angel et al. 2010a and 2014), thus giving rise to further concerns about potential impacts in Torres Strait.

The implications of these changes to water quality in the Torres Strait are not well known, but potential impacts can be extrapolated from knowledge from other marine ecosystems including the Great Barrier Reef. For example, increased sediment inputs can result in increased turbidity and reduced water clarity in receiving waters (e.g. Fabricius et al. 2014, 2016), which in turn reduces light availability for marine ecosystems (e,g. Collier et al. 2016; Chartrand et al. 2018). Coral reef and seagrass ecosystems have minimum light requirements for healthy growth and reproduction, and prolonged exposure to reduced light conditions can result in changes in community composition, increased incidence of disease and in extreme cases, fatalities and/or ecosystem collapse (e.g. Jones et al. 2015). Reef fish can be impacted by reduced water clarity and sedimentation indirectly via water quality induced changes to their

coral and seagrass habitats, or directly, as increased sediment loadings can have behavioural, sub-lethal, and lethal impacts on fish (e,g. Wenger et al. 2017). Increases in trace metal concentrations above National Water Quality Guidelines could also have direct toxicological impacts on coral reef and seagrass meadow health as well as direct effects on particular species such as corals, turtles, dugongs and fish (Pratchett and Hoogenboom, 2019). Impacts on seagrass can also have flow-on effects for other species such as seagrass-feeding animals (e.g. green turtle and dugong) which have an important dietary role in some local islander communities as well as being iconic and vulnerable species in the region.
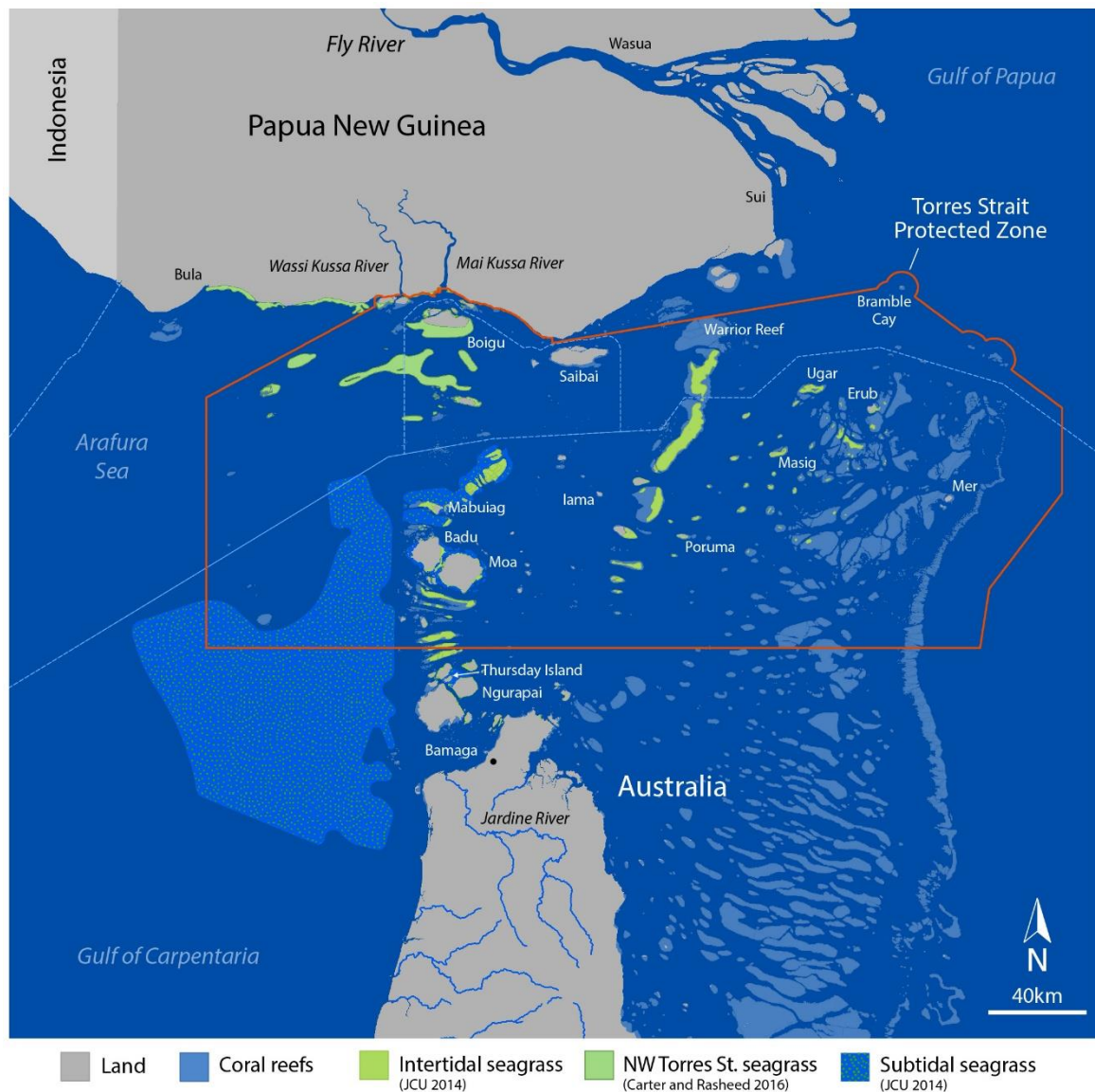
Figure 1–1: Map showing the Torres Strait region showing major rivers, islands, habitats and the boundary of the Torres Strait Protected Zone.

To enhance knowledge of the Fly River plume impacts on Torres Strait ecosystems and dependent islander communities, two partner projects were undertaken from 2015 to 2018 through the National Environmental Science Program (NESP) Tropical Water Quality Hub (TWQ Hub), building on previous work, to determine: (i) the spatial extent, temporal patterns and water and sediment quality of the Torres Strait region and (ii) which ecosystems in the

Torres Strait are exposed to the Fly River discharge. This work was subsequently extended in 2019 and 2020 to build on these findings with a follow-on project. The new findings are the focus of this report, and the preceding conclusions are highlighted for context.

The primary objectives of the extended project (2019-2020) were:
  i.   To quantify the concentrations of trace metals and sediments in the northern Torres Strait, with a focus on the marine areas around Boigu and Saibai Islands, the Warrior Reefs, Masig Island and Bramble Cay (locally known as Maizab Kaur).
  ii.   To identify the sources of trace metals in these areas and distinguish probable inputs from local sources or the Fly River.
  iii. To qualitatively assess the implications and potential risks of metals and sediments to marine ecosystems and local Torres Strait Islander communities.

This report presents the results of this extended project, supported by a synthesis of previous work in the region. A contextual overview of the Torres Strait study region is also provided, describing the Fly River, its ecological features and its potential threats (Section 0). The results of the extended study are presented in Sections 3.0 to 7.0:
  - Section 3: Weekly salinity monitoring conducted by TSRA Rangers;
  - Section 4: *In-situ* continuous monitoring of salinity and turbidity;
  - Section 5: Marine hydrodynamic modelling;
  - Section 6: Remote sensing of water quality conditions; and
  - Section 7: Field surveys of trace metals in waters, sediments and seagrasses.

The lines of evidence provide a basis for a summary assessment of the relative exposure of the Torres Strait region to Fly River contaminants of concern (Section 8.0).

Throughout the full study period, the work has been led by James Cook University (JCU; including TropWATER and the Centre of Excellence for Coral Reef Studies) and CSIRO in collaboration with scientists from the Australian Institute of Marine Science (AIMS), University of New South Wales, Macquarie University, University of Algarve, the Yantai Institute of Coastal Zone Research China and C_2O Consulting.

2.0 REGIONAL OVERVIEW

2.1 The Torres Strait and Gulf of Papua

The Torres Strait region covers an area of 48,000 km², of which only 2.6% is land mass, 6.2% is tidally inundated reef flats, and 91.2% open seas, most of which are relatively shallow (20–60 m). The region is located on the border between Australia (northern Queensland) and PNG and stretches 200 km from the tip of the Cape York Peninsula to the southwest coast of PNG (Figure 1-1). There are more than 300 islands and cays in the Torres Strait, 17 of which are inhabited, and which support an estimated 8,700 people (Torres Strait Regional Authority 2016a). The Torres Strait Protected Zone established under the Torres Strait Treaty protects the traditional way of life of Torres Strait Islanders between international boundaries (Figure 1-1).

The Torres Strait has the largest continuous area of seagrass meadows in the world, significant areas of high diversity coral reefs, extensive areas of coastal mangroves and productive fisheries. It is rich in biodiversity and cultural significance, with its ecosystems being amongst the most pristine in the world and retaining a high degree of natural and wilderness values. It has strong tidal currents and irregular bathymetry with a narrow continental shelf (Wolanski et al. 1999). The region's variety of habitats support highly diverse Indo-Pacific marine flora and fauna, including dugongs and marine turtles (Sobtzick et al. 2014; Hamann et al. 2015a, 2015b). The geographic location of the Torres Strait places it at risk from the impacts of shipping, downstream impacts of mining and land clearing in PNG (Waterhouse et al. 2013). Other major risks include climate change and local resource over-exploitation.

The catchment area of PNG rivers (e.g. Fly, Purari, Bamu, Kikori and Turama) draining into the Gulf of Papua is 1.42×10^5 km², and collectively its rivers deliver approximately 350 million ML of freshwater containing about 200 million tonnes of suspended sediments to the Gulf annually (Bolton 2008). The catchments of these rivers are largely undisturbed, except for two large mines, Ok Tedi Mining Ltd in the headwaters of the Fly River and Porgera in the headwaters of the Strickland River (Bolton 2008; Cresswell 2012).

2.2 The Fly River

The Fly River discharges into the Gulf of Papua to the northeast (NE) of the Torres Strait (Figure 1-1). It is a large river by world standards, with an estimated flow volume of 6,000 m³ sec⁻¹ (typically with ± 25% seasonal variations Wolanski et al. (1997)) and is ranked as the 17th largest river in the world in terms of sediment discharge (Galloway 1975; Milliman and Syvitski 1992).

Mining at the headwaters of the Ok Tedi River (the Ok Tedi copper mine) in PNG commenced in 1984 and in the headwaters of the Strickland River, which is the largest tributary of the Fly River (the Porgera mine), in 1990. Before the construction of the Ok Tedi mine, sediment discharge from the Fly River below the confluence with the Strickland River was estimated to be approximately 80 Mt/yr (Dietrich et al. 1999) and the mining operation is estimated to have caused a 40% increase in the sediment discharge of the river to approximately 120 Mt/yr (Wolanski et al. 1995; Canestrelli et al. 2010).

Various studies on the impacts of mine pollution in the Fly River system including the Fly River estuary have been completed over the last 25 years (Apte 2009). Recent data for the Fly River estuary indicate an increase in the copper content of waters and sediments has occurred over the operating lifetime of the Ok Tedi mine (Apte 2009; Angel et al. 2010a, 2014, 2020). These trends are illustrated in Figure 2–1a and Figure 2–1b. Based on a field survey conducted in 2013 (Angel et al. 2014), particulate copper concentrations in suspended sediments in the estuary have increased from pre-mine levels of around 40 µg/g to 83 µg/g. This increase was caused by the mixing of copper-rich mine-derived sediments (i.e. mine tailings and waste rock) with natural fine sediments. For further information on the impacts of the Ok Tedi mine on the Fly River system, readers are referred to the monograph edited by Bolton (Bolton 2008).

(a)   **(b)**
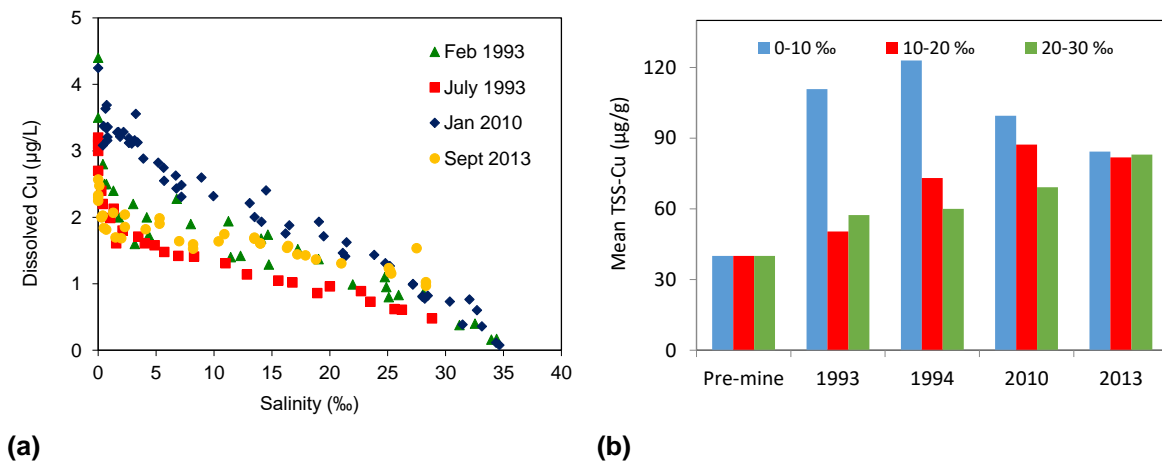
Figure 2–1: (a) Dissolved copper versus salinity profiles in the Fly River Estuary (1993 to 2013); (b) Increase in suspended sediment particulate copper concentrations by salinity zones in the Fly River Estuary over the period 1993 to 2013 (Angel et al. 2014).

2.3 Ecological features

2.3.1 Regional description

The Torres Strait region includes 247 islands and cays, large areas of coral reefs, seagrass meadows and mangroves. It is estimated that there are ~1,200 coral reefs in the Torres Strait which are part of the northern section of the Great Barrier Reef (GBR) and provide ecological functions that influence the broader GBR (Johnson et al. 2018). As encountered elsewhere, climate change, potential crown-of-thorns starfish (*Acanthaster* cf. *solaris*) outbreaks, coral diseases, potential increased frequency of severe storms, and pollution from river runoff and shipping are threatening the ecological integrity of Torres Strait reefs. Until recently, Torres Strait reefs were in good condition with high coral cover, presence of major taxonomic and functional groups, and minimal incidence of coral disease (Sweatman et al. 2015; Torres Strait Regional Authority 2016b); however, following mass bleaching and coral mortality in 2016 their status has significantly declined (Hughes et al. 2017, 2018a, 2018b).

The Torres Strait has some of the most extensive seagrass meadows in northern Australia and possibly the world, with an estimated area of 13,425 km^2 (Coles et al. 2002) to 17,500 km^2 (Poiner and Peterkin 1996). There are 13 species of tropical seagrasses in the region, mainly present in sub-tidal waters (McKenzie et al. 2010) and predominantly located in the western and central (Warrior Reefs) areas (Figure 2-2). The northern Warrior Reefs have a greater

diversity of seagrasses (*Halodule* spp*., Thalassia* spp*., Thalassodendron* spp. *and Cymodocea* spp.), while the south tends to be dominated by a single species of *Thalassia*. In the west, seagrass communities are more diverse to the north around the Orman Reefs (*Halodule* spp*., Thalassia* spp. *and Syringodium* spp.), (Haywood et al. 2007).

Torres Strait Seagrass Report Cards are prepared annually from the data collected as part of the Torres Strait Seagrass Monitoring Program incorporating data from a range of programs including local observations, TSRA Rangers, and data collected by TropWATER JCU in partnership with Queensland Ports and TSRA. The 2020 Report Card (Carter et al. 2020) indicated that seagrass status varied across the region. In the Western Cluster (Orman Reefs, Mabuyag, Badu, Mua) and Eastern Cluster (Dauar, Mer), seagrass condition declined from good to satisfactory between 2019 and 2020, mostly because of decreases in seagrass abundance (biomass/percent cover). Declines were particularly dramatic in the Orman Reefs-Mabuyag Island region. In the Central Cluster (Iama, Dungeness Reef, Poruma) overall condition remained good despite small declines in seagrass abundance. There is currently no monitoring in the top western areas such as Saibai and Boigu.
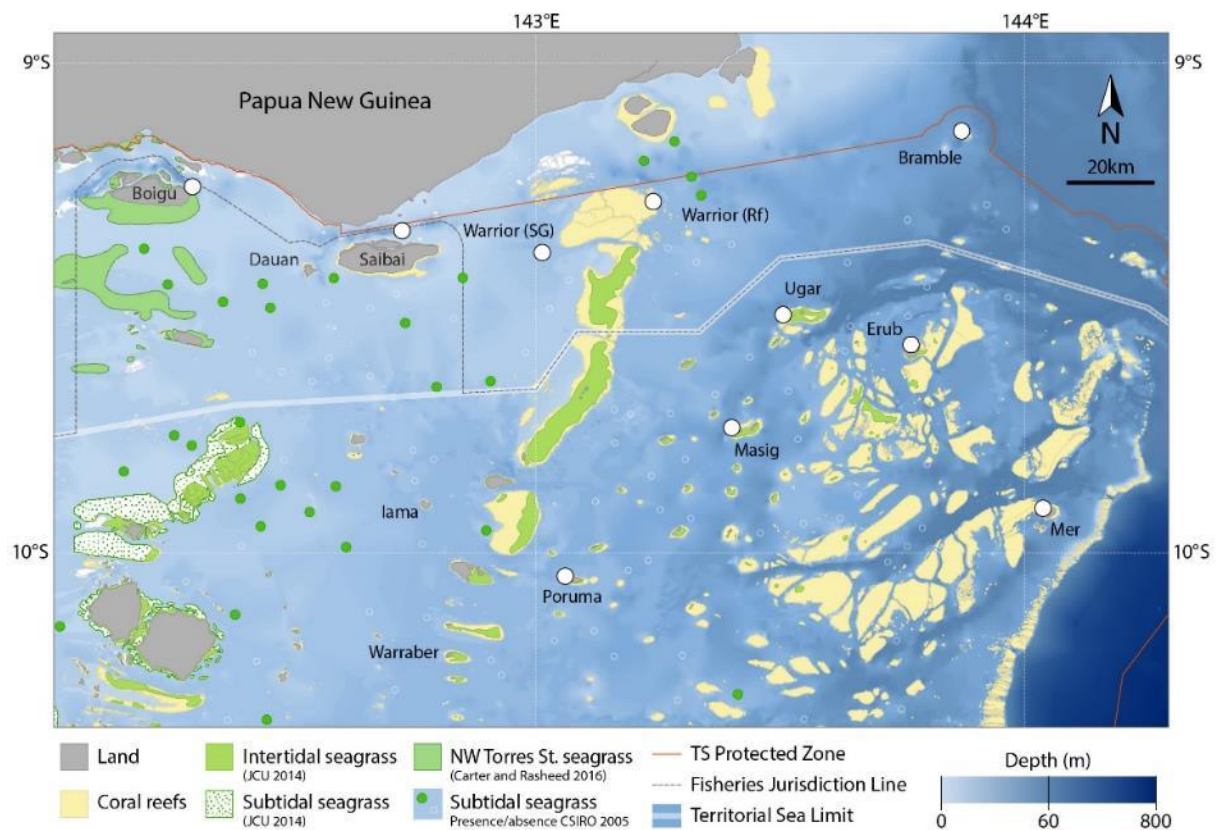
Figure 2-2: Spatial distribution of seagrasses in the Torres Strait region showing the mapped extent of intertidal and subtidal seagrass. Map prepared by D. Tracey, TropWATER JCU using datasets from GBRMPA, Carter et al. (2014), Hayward et al. (2008) and Carter and Rasheed (2016).

The wetlands comprising mangroves, salt marsh and freshwaters on the islands and cays in the Torres Strait region are ecologically important and support a diversity of biota. Whilst freshwater wetlands are rare, most Torres Strait islands have extensive mangrove areas and several islands (e.g. Saibai and Boigu Islands) are predominantly made up of intertidal wetlands (Duke et al. 2015). Many Torres Strait islands are low lying with large wetland areas

that are expected to be vulnerable to sea level rise and increased storm surge frequencies caused by climate change.

Torres Strait marine habitats support significant populations of dugongs (Sobtzick et al. 2014); hawksbill, green and flatback turtles (Hamann et al. 2015a, 2015b) - species of conservation concern - as well as fish and invertebrate species, many of which are important for local fisheries, such as tropical rock lobster and sea cucumbers (Welch and Johnson 2013). Aerial surveys show that the dugong population in the region has not changed significantly over time (Sobtzick et al. 2014). These aerial surveys also found a significant population of turtles (most likely greens; Fuentes et al. 2015) in the survey region, including within the Dugong Sanctuary in the western Torres Strait. Monitoring of nesting turtles since 2006 has identified the islands in the Mer group (Mer, Dauar and Waier) and Bramble Cay as the most significant green turtle rookeries in the Torres Strait and the main nesting sites for the Torres Strait/northern GBR genetic population (Hamann et al. 2015a).

The Torres Strait is under increasing pressure from a range of regional factors such as PNG population growth and resource demand, downstream mining and development impacts, and increased shipping, as well as local factors including resource exploitation, emerging tropical diseases and inadequate waste management. External drivers affect the entire region, namely climate change, mining discharges and shipping. Internal or local drivers show some differences between the Torres Strait Islands and the Western Province region and Treaty Villages in PNG partially due to differences in social factors (Butler et al. 2015). Natural resource extraction is escalating in Western Province, and related infrastructure is placing additional pressures on coastal and marine resources in southern PNG and the Torres Strait.

A study of potential water quality issues in the Torres Strait region identified regional pollution - discharge of metal (and other) contaminants from the Fly River associated with mining in the upper catchment, the port at Daru, other mines in PNG, land clearing and shipping - as well as local pollution from sewage and stormwater discharge, as key risks to the region (Waterhouse et al. 2013). Of these, the large-scale developments were considered to have the potential to pose the most consistent threat at the largest scale, although there was limited direct evidence to support this. The need to gain a better understanding of the likely patterns of influence of the Fly River discharge and mine-derived contaminants was identified, and the former NESP TWQ Hub research projects (Project 2.2.1 Waterhouse et al. 2018 and Project 2.2.2 Apte et al. 2018) designed to deliver this information.

More recently, the threat of increasing temperatures and rising sea level have become more evident in the region. There are concerns about the decline in seagrass extent in in the Western Cluster which has been linked to potential seagrass disease, however this is yet to be verified (Carter et al. 2020). The new knowledge presented in this report, coupled with previous studies, provides a solid foundation for improved understanding of the relative threat of the Fly River discharge to Torres Strait ecosystems.

2.3.2 Potential impacts of increased sediment and trace metal inputs

The extent and consequences of increased sediment inputs and trace metal concentrations in the Torres Strait region is not well quantified. The potential impacts of the exposure of Torres Strait marine ecosystems to the Fly River discharge can be estimated from knowledge derived

from other marine ecosystems including the GBR. Key points from the published literature were summarised in Waterhouse et al. (2018) and are included and updated here as relevant context for this report.

Increased sediment loads

The potential impacts of increased fine sediment inputs to reef ecosystems (based on GBR and international literature) include:

- Increased suspended particulate matter can cause light reduction, and disturbance by suspended particles and sedimentation (Jones et al. 2015; Duckworth et al. 2017). The impacts depend on the intensity and duration of exposure (e.g. Collier et al. 2016; Ferguson et al. 2017; O'Brien et al. 2018b; Statton et al. 2018; Chartrand et al. 2018).

- Light limitation is a primary driver of seagrass production in the GBR (Collier and Waycott 2009) and reductions in light availability have been directly linked to seagrass loss (Collier et al. 2012; Petus et al. 2014). This is reported to occur at suspended sediment concentrations >7mg/L, although this will vary with species and location (Collier et al. 2012). Under low light conditions photosynthetic carbon fixation is reduced in seagrass meadows which requires biochemical, physiological and morphological changes to minimise respiratory loss (O'Brien et al. 2018) and to enhance light capture (e.g. Collier et al. 2009; McMahon et al. 2013; Hedley et al. 2014). Mortality occurs if light levels fall below minimum light requirements (e.g. Chartrand et al. 2018). When benthic light is limiting, the time to mortality ranges from two weeks for small 'colonising' species (sensu Kilminster et al. 2015) to two years for 'persistent' species that can resist mortality by drawing on storage reserves in their large rhizomes (Collier et al. 2009; O'Brien et al. 2018b). As an example, Collier et al. (2016) defined a light threshold for seagrass at <6 mol photons m^{-2} day^{-1} for 42–100% days in the whole year, as seagrass loss is almost certainly expected if fine sediment loads increase in these habitats.

- Light reduction, elevated suspended sediments and sediment deposition can negatively affect the reproductive cycle and early life histories of corals (Jones et al. 2015). Some coral reef species are highly sensitive to reduction in photosynthesis caused by reduced water clarity (Erftemeijer et al. 2012, Bessell-Brown et al. 2017) while others can feed on the particulate matter, gaining energetic advantage over others as long as light is not limiting (Anthony 2000; Anthony and Fabricius 2000). Sensitivity also depends on the life stage, with young corals being particularly susceptible to damage caused by suspended sediment (i.e. without sedimentation or light reduction impacts). For example, fertilisation and subsequent settlement, and the growth and/or survival of coral juveniles can be negatively affected by suspended sediment (Humanes et al. 2017a, 2017b).

- Ecosystem-wide shifts can occur from species responses to increased turbidity. For example, studies of spatial gradients in coral reef communities have shown that in some locations the abundance, biomass and species diversity of corals, invertebrates and fish can be lower on turbid reefs than on non-turbid reefs or reefs adjacent to healthier river basins (Fabricius et al. 2005, Mallela et al. 2007; Bainbridge et al. 2018). Shifts from corals to macroalgae (De'ath and Fabricius 2010; Begin et al. 2016; de Bakker et al. 2017), and under more severe conditions of increased turbidity, shifts from macroalgae to heterotrophic filter feeders have been observed (Birkeland 1988).

- To provide context of the suspended sediment concentrations that may result in ecological effects, the Water Quality Guidelines for the Great Barrier Reef Marine Park (GBRMPA, 2010) define guideline trigger values for suspended sediments. These range from 5 to 15 mg/L in enclosed coastal waters, 2mg/L in open coastal and midshelf waters and 0.7mg/L in offshore waters. The effects on corals measured as a result of exposure to suspended sediment concentrations included increased macroalgal cover, decline in hard coral richness and phototrophic octocoral richness (GBRMPA, 2010).

Reef fish can be impacted by reduced water clarity and sedimentation indirectly (at suspended sediment concentrations >7mg/L or 5 nephelometric turbidity units (NTU), by changing their coral and seagrass habitats (Wenger and McCormick, 2013, or directly, as increased sediment loading can have direct behavioural, sub-lethal, and lethal impacts on fish (>10.5 mg/L or >7.5 NTU; Wenger et al. 2017). In some parts of the GBR, major seagrass losses have occurred following a series of large discharge events with large loads of fine sediment followed by prolonged resuspension of the fines in waters less than 15m deep (Collier et al. 2012; Petus et al. 2014) causing extended periods of reduced light (Fabricius et al. 2014, 2016). However, periods of reduced river discharge of fine sediment and hence disturbance have resulted in seagrass recovery (Wells and Rasheed 2017; Petus et al. 2014).

While evidence of the impacts of increased sediment loads in the GBR may be transferrable to the Torres Strait to some degree, there is one very important difference. The discharge patterns of the Fly River are much more consistent (and larger) than those in the GBR and Torres Strait ecosystems are likely to be exposed to both sediment plumes and resuspension events every year and throughout the year, unlike GBR ecosystems. Despite these differences, the ecosystem responses to increased sediment in the receiving environment of the Fly River discharge are expected to be similar to many inshore areas of the GBR. In addition, limited monitoring data exists to substantiate these potential impacts in the Torres Strait, or to compare current conditions to conditions prior to the commencement of Ok Tedi mining and the increased sediment discharge, highlighting that this information should be used as a guide only.

Elevated trace metal concentrations
Changes in trace metal concentrations in Torres Strait waters could have a direct impact on coral reef and seagrass meadow health as well as being a potential public health concern through consumption of contaminated seafood by Torres Strait Islander communities. Guideline values exist for a range of commonly encountered trace metals in Australia.

Water quality guideline values
The Australian and New Zealand guideline values for metals in surface waters (ANZG 2018) are toxicologically-based and derived from ecotoxicity testing using a species sensitivity distribution (referred to as 'SSD') of chronic toxicity data. Typically, metal default guideline values (DGVs) are set at concentrations that protect 80, 90, 95 or 99% of aquatic species. Separate guidelines apply to freshwater and marine systems. The DGV that is applicable for a water body depends on the current or desired condition of the ecosystem and the associated level of protection that is assigned. The following DGVs are recommended:

- high ecological/conservation value system - 99% species protection DGV
- slightly to moderately disturbed system - 95% species protection DGV

- highly disturbed system - 90 or 80% species protection DGV.

The current DGVs for marine waters are summarised in Table 2–1. Note that for some metals DGVs are not available due to lack of ecotoxicity data. The 95% DGVs are typically the guidelines most frequently applied by regulators as most systems have some degree of moderate disturbance. However, application of the 99% species protection guidelines is appropriate for the Torres Strait which is a system of high ecological/conservation value.

Table 2–1: Summary of current marine water quality default guideline values (DGV) that apply in Australia and New Zealand (ANZG 2018).

Metal	95% protection DGV	99% protection DGV
	(µg/L)	(µg/L)
Cadmium	5.5	0.7
Cobalt	1	-
Copper	1.3	0.3
Mercury	0.4	0.1
Nickel	70	7
Lead	4.4	2.2
Zinc	15	7

Note that the DGVs are not applicable in situations where metal concentrations are naturally elevated (e.g. as a consequence of local metalliferous geology). In this situation, some investigation first need to be conducted to confirm there is a natural source of metals.

The guideline values are part of a decision framework that is recommended for water quality management in Australia and New Zealand (ANZG 2018). As a first step, dissolved metal concentrations are compared against DGVs. Where there is an exceedance, the framework leads to an examination of the speciation and bioavailability of the metals in question (ANZG 2018). This can involve measurements of the chemical speciation (form) of the metals and toxicity testing using appropriate test organisms. These specialist investigations lead to the determination of the bioavailable concentration of metals, which are then compared to the DGV. If the bioavailable metal concentrations are below the DGV then no further action is required.

Sediment quality guidelines
In Australia and New Zealand sediment quality guidelines are available for 8 metals and two metalloids (arsenic and antimony). The total particulate metal concentrations measured in the <2 mm sediment fraction of a sediment sample are compared to the guideline values listed in Table 2–2. Two values are specified, the DGV and the guideline value-high (GV-high). There is a low risk of unacceptable effects occurring at concentrations below the DGV. The GV-high values provide an indication of concentrations at which toxicity-related adverse effects may be observed. A concentration that exceeds the DGV does not necessarily mean that adverse biological effects will occur in the sediments but indicates that further investigations should be undertaken to confirm the likely effects. Such investigations usually involve determination of the bioavailable metal concentration (e.g. by measuring weak-acid extractable metal concentrations) and, if this still exceeds the DGV, further lines of investigation are pursued such as toxicity testing. Further lines of evidence might include bioaccumulation and sediment

ecology (Simpson and Batley 2016). Similar to water quality guidelines, provision is also made for naturally elevated metal concentrations by comparison against background sediment metal concentrations for the region.

Table 2–2: Australia and New Zealand sediment quality guideline values (ANZG 2018).

Toxicant	DGV (µg/g)	GV-high (µg/g)
Antimony	2.0	25
Cadmium	1.5	10
Chromium	80	370
Copper	65	270
Lead	50	220
Mercury	0.15	1.0
Nickel	21	52
Silver	1.0	4.0
Zinc	200	410
Arsenic	20	70

Examples of documented impacts

Examples of the potential impacts of trace metals on marine species are provided below. It is important to note that the concentrations of metals required to cause toxic effects to aquatic biota are generally orders of magnitude higher than what are measured in typically unpolluted environments including the Torres Strait (refer to Section 7 and 8).

Specific stress responses of corals and reef organisms to elevated levels of toxic metals (and specifically possibly to copper) include:

- inhibition of coral fertilisation and reduced reproductive success (Reichelt-Brushett and Harrison 2005; Richmond et al. 2018; Gissi et al. 2017);
- decreased settlement and survival of coral larvae (Reichelt-Brushett and Harrison 2000; Woods et al. 2016);
- changes in the population and growth of zooxanthellae (endosymbiotic algae) (e.g. Rodriguez et al. 2016);
- changes in the rate of photosynthesis resulting in a decrease in coral calcification and growth rates during the juvenile polyp stage (e.g. Biscéré et al. 2017; Ferrier-Pages et al. 2001);
- increased coral bleaching (e.g. Reichelt-Brushett and Hudspith 2016; Sabdono 2009);
- reduced thermal tolerance in some corals specifically associated with copper enrichment (Banc-Prandi and Fine 2019);
- enhanced coral mortality especially at the juvenile stage (e.g. Sabdono 2009); and
- mortality in invertebrates and fishes (Peters et al. 1997; Wenger et al. 2015).

The concentrations of trace metals required to induce these responses range between responses and species, but for examples for copper, are in the order of 15 to 40 µg/L to impact coral fertilisation and reproductive success (Reichelt-Brushett and Harrison 2000, 2005).

For fish, exposure to elevated metal concentrations (Wenger et al. 2015) can result in: immuno-suppression, leading to increased susceptibility to disease; impaired olfactory ability; disruption of critical behaviours such as predator avoidance, social interactions and reproduction; disruption of the metabolism of sex hormones; and adverse effects on embryonic development

in the egg by changing development rates and causing malformations, and reduction in hatching success.

It is well documented that marine and estuarine macroalgae and angiosperms concentrate metals from surrounding waters (Bonanno and Orlando-Bonaca 2017, 2018; Ward et al. 1986; Phillips 1994). Seagrasses and macroalgae can accumulate high concentrations of trace elements and accumulation is mainly element- and organ-specific (Bonanno and Orlando-Bonaca 2017, 2018). Most metals are not significantly toxic to algae or seagrass at concentrations likely to be present in coastal seawaters (Ward 1989; Phillips 1994). However, there is little documented evidence of the main stress responses of seagrasses to elevated concentrations of trace metals and field studies reporting cases of severe decline or disappearance of seagrasses and macroalgae under trace element pollution are relatively scarce (Bonanno and Orlando-Bonaca 2017, 2018). Although numerous studies have been conducted in highly contaminated sites globally (e.g. industrial ports, smelting plants), seagrass and macroalgal populations have not shown significant adverse effects on their vitality (Benfares et al. 2015). For most trace elements, phytotoxic levels in seagrasses are unknown (Bonanno and Orlando-Bonaca 2018). However, the sublethal toxicity of elevated concentrations of copper and zinc to seagrass species *Halophila ovalis* has been demonstrated at trace metal concentrations of 1 to 10 mg/L (Ralph and Burchett 1998), and laboratory studies have demonstrated that zinc, iron, and copper may inhibit growth of bacteria associated with *Zostera marina* and *Halodule wrightii* rhizomes (Smith et al. 1982). Mercury, nickel and lead will also significantly reduce nitrogen fixation (acetylene reduction) by symbiotic nitrogen fixing bacteria associated with the roots and rhizomes of *Z. marina*, potentially affecting the supply of nutrients to seagrass (Brackup and Capone 1985).

Globally, Govers et al. (2014) and Vonk et al. (2018) summarised concentrations of metals in seagrass and the importance of metals to seagrass functioning. Govers et al. (2014) concluded that trace metal concentrations in seagrass leaves, regardless of the species, can vary over a 100 to 1000-fold range, and are related to the level of anthropogenic pressure, making seagrasses highly valuable indicators. While there is only limited data on trace metals in seagrass leaves in the Torres Strait or the GBR, Haynes (2001) and Thomas et al. (2020) do provide useful comparative data relevant to the current study (see Section 7). Whilst seagrass is generally reported as being in good condition in the Torres Strait (Carter and Rasheed 2018; Carter et al. 2018, 2020), further work is required both locally and globally to understand the importance of various metals to seagrass health and productivity.

Overall, seagrasses are not particularly susceptible to trace metal pollution in comparison to animals. However, pollutants present in intertidal (and subtidal) seagrass environments can be bioaccumulated by seagrass grazing organisms such as dugongs and turtles, and this may have the potential to impact dugong populations directly following bioaccumulation of contaminants via seagrass consumption, or, indirectly by impacting on seagrass health to reduce the availability of the animals food resource (Haynes, 2001). In addition, a potentially more important threat is present when dugong or turtle may be consumed by Torres Strait Islander communities (Gladstone 1996), where dietary intake may cause human health issues (Nunez-Nogueira et al. 2019). In the Torres Strait Baseline Study (Dight and Gladstone 1993), the metals identified at elevated concentrations were not believed to be associated with mine-derived runoff. No further documented studies of trace metal concentrations in marine mammals have been undertaken in the Torres Strait region since this time.

PART B: SUPPORTING EVIDENCE

3.0   SALINITY MONITORING

3.1 Previous findings

The salinity monitoring in NESP TWQ Hub Project 2.2.1 collected salinity data to assess the potential influence of the Fly River into the Torres Strait (in addition to the remote sensing and hydrodynamic modelling data) and engaged local communities in making this assessment.

Rangers from the TSRA were trained through the project in 2016 to undertake a weekly salinity monitoring programme using salinity and temperature meters. Data were collected at Boigu, Saibai, Erub, Masig, Iama, Poruma and Warraber Islands, commencing at different times in 2017 (Figure 3-1). This involved:

- July 2016—Introduction to the use of the handheld salinity and temperature meters to 'validate' the salinity modelling for the dispersion of the Fly River plume into the Torres Strait.
- December 2016—Delivery of the meters, instruction sheets and standards to the Rangers. The Rangers were provided with two handheld salinity-temperature meters (AZ Instrument Corp. Water Quality Meter–Salinity meter, Model #8371). The meters were calibrated in the TropWATER JCU laboratory prior to dispatch. Attempted visits to Warraber, Masig and Erub Islands were unsuccessful due to weather conditions but provided direct training to the Ranger in Charge (Troy Stow) on Thursday Island and all the equipment and training manuals were provided. Conducted training at Saibai and Boigu Islands.
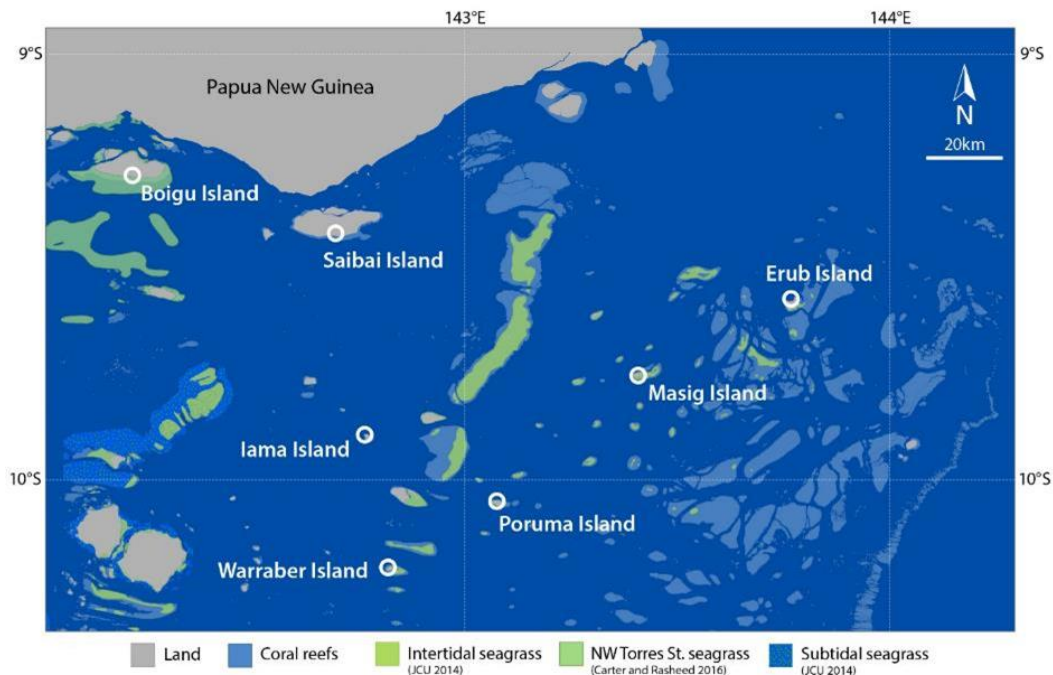
Figure 3–1: Location of islands where weekly salinity measurements have been taken since 2016–2017 by TSRA Ranger teams.

- Analysis of collected data showed that the northern sampling sites were exposed to lower salinity waters and were exposed to greater salinity ranges than sites located in the mid and southern regions of the Torres Strait.
- Recorded salinity values fell into three areas that measured similar values:
  i. The islands north west (NW) of Masig Island—Saibai and Boigu: mean salinity of 29 and 26 PSU, respectively, with the highest salinity range of 10.7 and 8.4 PSU, respectively; however, only four samples were collected at Boigu Island at the time of reporting;
  ii. The islands south of Masig Island—Iama, Poruma and Warraber: mean salinity 35.3, 34.8 and 35.0 PSU respectively and salinity range all < 5 PSU; and
  iii. Masig Island: transitional area with a mean salinity of 33.3 PSU and a salinity range of 6.3 PSU.
- The salinity monitoring provided useful *in-situ* data that could ultimately be used to support further hydrodynamic modelling and validate the remote sensing analysis.
- Satellite images corresponding with the same time period of collected field data were used to help illustrate potential links to specific causes of salinity variability such as river plumes.

3.2 Additional work: Scope and methods

3.2.1 Purpose

To continue weekly salinity monitoring by TSRA Rangers at northern locations to link results to the logger data where applicable and provide local data from additional locations. Analyse salinity monitoring data collected from Boigu, Saibai, Erub, Masig, Iama, Poruma and Warraber.

3.2.2 Methods

Sampling continued at Boigu, Saibai, Erub, Masig, Iama, Poruma and Warraber islands at varying frequencies, with monitoring at some islands more regular than others (see Table 3–1). The monitoring sites were located in at least 1 metre of water, and were either located at the end of a jetty or off the beach. The Rangers were advised not to locate the sites close to any land based freshwater influence such as a stream or discharge area, and to avoid periods of heavy rainfall.The position of the sampling site was recorded using a GPS. Additional information including the date, time, estimate of the tide and the wind, and the collector's name and contact details was captured on the sample recording sheet.

Data was entered directly to the TSRA automated Fulcrum system, with notification of the sample collection to the project team. This enabled all entered data to be downloaded in a collated spreadsheet.

Outliers (N = 16) were removed from the salinity database and the time series of corrected data were plotted and summarised.

3.3 New results

The time series of data collected is presented in Figure 3–2 and summarised in Table 3–1. As shown in Table 3–1, the greatest number of valid salinity measurements were collected at Warraber and Masig islands (128 and 117 respectively) and were collected consistently throughout the monitoring period. Sampling at Poruma (69) and Iama (71) was also relatively consistent but not as frequent. Sampling at Saibai (51) and Boigu (28) islands increased in 2019 and 2020. The lowest number of measurements were collected at Erub island (20).

Table 3–1: Summary statistics of the corrected salinity time series. SD: standard deviation, range: maximum − minimum, Q1/Q3: first/third quartile, N outliers: number of outliers removed. Statistics are calculated without the outliers

Location	Saibai	Boigu	Erub	Masig	Iama	Poruma	Warraber
n	51	28	20	116	71	69	124
Mean	29.8	30.1	34.2	33.4	35.2	34.7	35.3
Median	30.4	30.2	34.5	33.4	35.2	34.9	35.5
SD	2.2	2.6	1.5	1.3	1.0	1.0	1.2
Min	24.7	21.7	30.8	29.8	31.7	31.1	32.1
Max	35.3	34.1	36.6	36.4	37.3	36.0	37.9
Range	10.7	12.4	5.7	6.7	5.7	4.8	5.9
Q1	29.4	29.1	33.0	32.8	34.6	34.3	34.4
Q3	31.6	32.3	35.2	34.1	36.0	35.5	36.1
N outliers	1	7	4	5	1	0	4

The lower mean salinities were measured at the most northern sites, Saibai Island (29.8 ± 2.2 PSU) and Boigu (30.1 ± 2.6 PSU), and the highest mean salinities were measured at the more southern sites, Warraber (35.3 ± 1.2 PSU), Iama (35.2 ± 1.0 PSU), and Poruma Islands (34.9 ± 1.0 PSU). The mean salinity measurement at Masig Island continued to be lower than expected for an open ocean site with 33.4 ± 1.3 PSU, but the range was relatively high (6.7 PSU) in the 117 samples collected between June 2017 and January 2021. The greatest salinity ranges were measured at Boigu Island (12.4 PSU) and Saibai Island (10.7 PSU), with the lowest ranges at Poruma (4.8 PSU), Iama and Erub (both 5.7 PSU). There is insufficient data to allow detailed statistical analysis including time series analysis, analysis of seasonal variation or correlations between sites.

Figure 3–3 shows a box plot of salinity measured at Boigu, Saibai, Masig, Erub, Poruma, Iama and Warraber Islands. This shows the gradient in salinity values from north to south, and the relatively low values recorded at Boigu and Saibai. It also highlights the changing variability in the range from north (greatest) to south (least). In the previous study (Waterhouse et al. 2018), the locations were grouped into zones of similar values along with the turbidity results obtained from remote sensing data, grouping them into areas of highest potential exposure to freshwater discharge (Boigu and Saibai), moderate (Masig and Erub) and lowest (Iama, Poruma and Warraber). As shown in this figure, these groupings are still relevant.
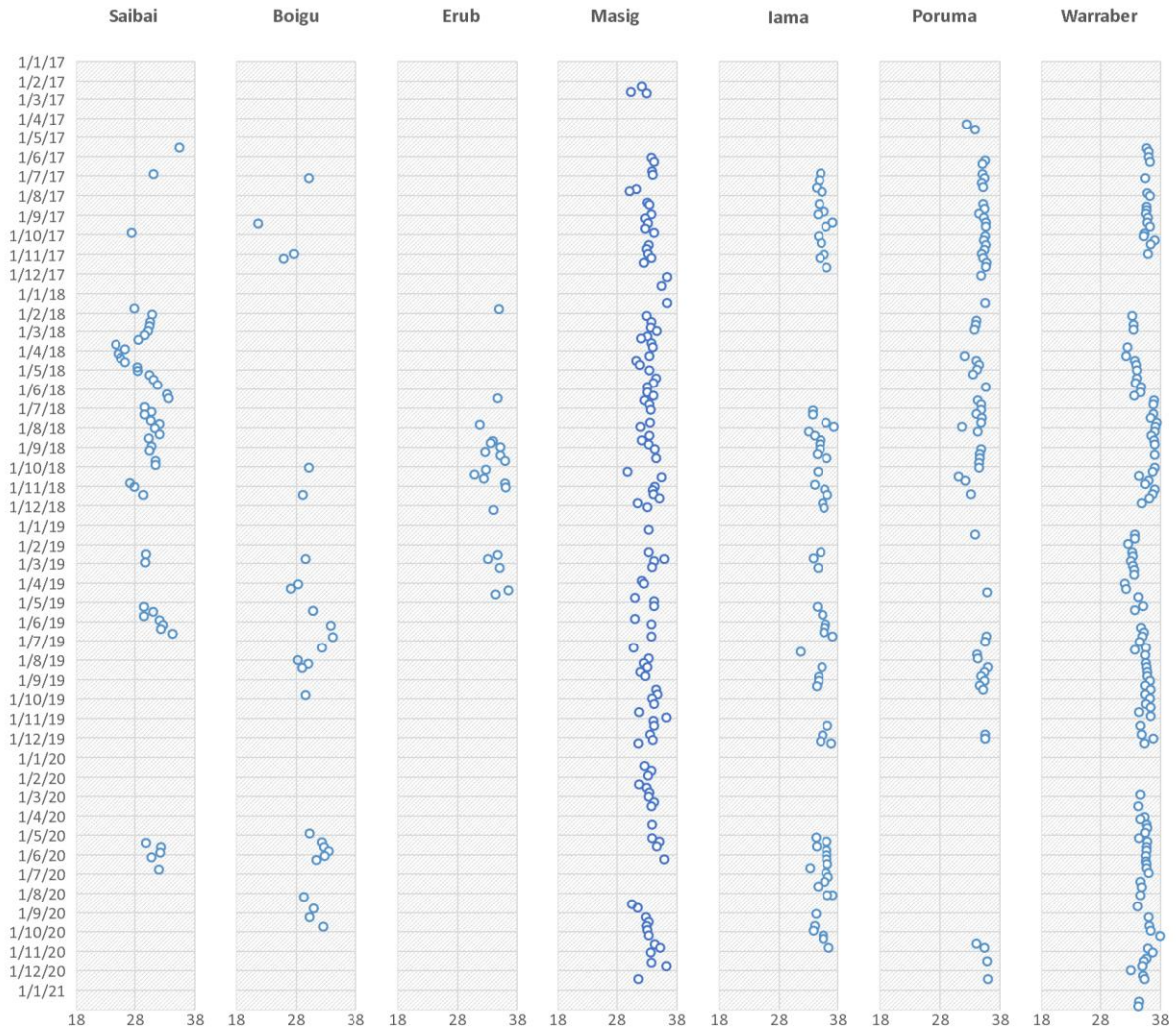
Figure 3–2: Time series of salinity measured at Saibai, Boigu, Erub, Masig, Iama, Poruma and Warraber Islands corrected salinity values.

Examples of Moderate Resolution Imaging Spectroradiometer (MODIS) true colour satellite images showing periods where there was possible influence of Fly River discharge resulting in lower salinity measurements are presented in Figure 3–44 (March-April 2018) and Figure 3–5 (July 2019). The descriptions and possible explanations are explained in the figure. It is noted that these images are examples by observation only and do not necessarily describe typical/systematic trends in water composition associated with low/high salinity values specifically linked to the Fly River discharge in these locations.
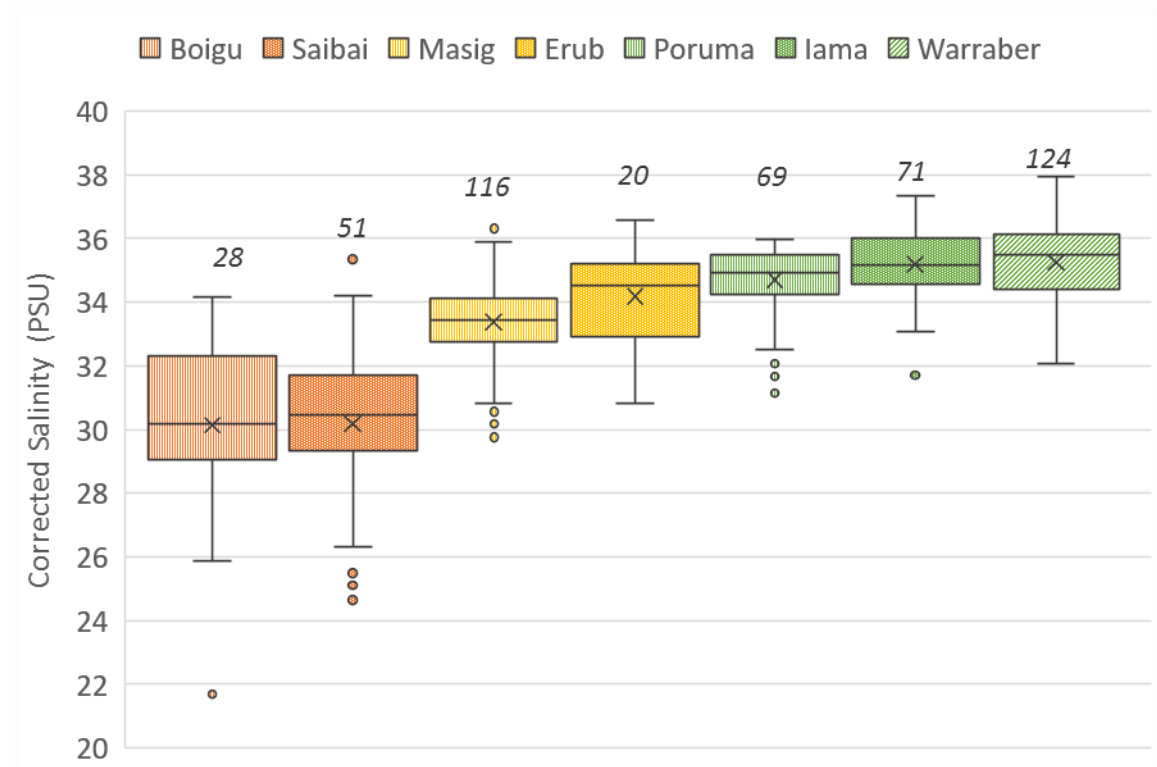
Figure 3–3: Blox plots of the salinity measured at Boigu, Saibai, Masig, Erub, Poruma, Iama and Warraber Islands. Colour code denotes zones of relative influence from Fly River discharge, as defined in Waterhouse et al. (2018): orange > yellow > green. Number of data collected at each site is indicated (italic font).

3.4 Conclusions and recommendations

These results continued to demonstrate that northern areas in the Torres Strait region were exposed to lower salinity waters and greater salinity ranges than those located in the mid and southern region of the Torres Strait. This is in agreement with the results of the hydrodynamic modelling and remote sensing, and historic salinity studies (discussed in Section 8.1.3).

The project team encourages the TSRA to continue the weekly salinity monitoring programme around the northern islands in the Torres Strait. When this programme has been implemented for an extended time with consistent sampling it will be possible to define any statistically significant trends and seasonal patterns in water salinity. It will also be possible to define 'alert' salinity thresholds at each island under which satellite images can be downloaded and reviewed. This will support more accurate tracking of the Fly River plume and the evaluation of its potential threat in real time.

The series of True Colour images on the right between 28 March and 25 April 2018 (end of monsoon) show the influence of turbid waters from the Fly River extending as far west as Saibai and Boigu islands and beyond. The plume also appears to influence the northern Warrior Reefs. There is also possible local influence from the Wassi Kussa and Mai Kussa rivers, particularly around Boigu Island, as well as sediment resuspension and calcareous sediments in the middle of the Torres Strait.

Salinity measurements were undertaken at Saibai on a weekly basis during this period (see figure above). The salinity measurements ranged between 24.6 and 30.4 PSU indicating the presence of a freshwater plume.

Measurements were not undertaken at Boigu during this period.

The salinity measurements at Masig on 16 and 23 April 2018 were below the average reading of 33.3, at 31.3 and 31.7 PSU respectively; the edge of the plume waters appear to extend to this area on the image of 25 April 2018.

MODIS Terra 28 March 2018

MODIS Terra, 1 April 2018

MODIS Terra 25 April 2018

Figure 3–4: Example of MODIS true colour satellite images and salinity data collected around March and April 2018

MODIS Terra 1 July 2019

The True Colour image on the right from 1 July 2019 (during south east [SE] trade wind season) show the influence of turbid waters from the Fly River extending as far west as Saibai and Boigu islands and beyond. The plume also appears to influence the northern Warrior Reefs. There is also possible local influence from the Wassi Kussa and Mai Kussa rivers, particularly around Boigu Island, as well as sediment resuspension and calcareous sediments in the middle of the Torres Strait.

Salinity measurements were undertaken at Boigu on a weekly basis around this time (see figure above). The lowest salinity measurements ranged between 28.3 and 32.3 PSU indicating the presence of a freshwater plume.

Measurements were not undertaken at Saibai during this period.

The closest salinity measurements at Masig was on 12 July 2019 and was below the average reading of 33.3, at 30.8 PSU although there is not an image available from this date to assess the likely influence of the Fly River discharge on this measurement.

Figure 3–5: Example of MODIS true colour satellite images and salinity data collected around July 2019.

4.0 *IN-SITU* CONTINUOUS LOGGERS

4.1 Previous findings

NESP TWQ Hub Project 2.2.1 maintained real-time weather (wind, precipitation, humidity, barometric pressure, air temperature), water temperature, salinity and turbidity measurements from monitoring stations at Masig Island and Bramble Cay to record local weather and water quality data to assist in analysis of water quality variability patterns (Waterhouse et al. 2018).

- Bramble Cay had higher than expected levels of turbidity (average of 10.7 NTU) for a remote offshore reef (as compared to offshore reefs in the GBR that average 0–3 NTU and near-shore reefs that average 3-5 NTU in the dry season and a maximum of 10-15 NTU in the wet season) reflecting its location in a shallow system directly south of the Fly River.
- The observed patterns of turbidity at Bramble Cay were most strongly correlated with wind speed and were likely to be a consequence of local wind driven resuspension of *in-situ* material and not episodic movement of material from the north. The exception was a peak observed in June 2017 that could not be explained by local environmental conditions.
- The presence of fine terrestrial material at Bramble Cay, which seems to make up much of the resuspension material, indicated that there is transport of material from PNG as the nearest source. However, this may be via more complex long-term transport mechanisms rather than short-term episodic events, which in turn will have implications for the potential transport of contaminants into the area.
- Logger data and weather stations recorded anomalously high sea temperatures over the 2015–2016 summer related to a period of high air temperatures and low wind speed. The station at Thursday Island recorded a new record maximum above the empirical bleaching threshold and coral bleaching was subsequently observed in the region.
- The logger data confirmed previous data and modelling work that showed that the eastern part of the Torres Strait is cooled by off-shelf upwelling making this part of the Torres Strait less likely to be affected by coral bleaching, as was the case during the 2015–2016 and 2016–2017 bleaching events where the most severe bleaching occurred in the southern and western reefs.

4.2 Additional work: Scope and methods

4.2.1 Purpose

The *in-situ* loggers allow for the collection of environmental data over long time periods and large geographic areas to record environmental parameters that influence the biological systems under study. For this project, *in-situ* wind data from weather stations was used to develop and drive the oceanographic models of water movement to ensure that they reflected actual conditions. The *in-situ* turbidity loggers provided localised turbidity data and allowed the calibration of satellite images to elucidate the large-scale patterns of water movement. Finally, the deployment of small, inexpensive temperature loggers collected water temperature data across the deployment sites which provided information on general water movement patterns as well as temperature anomaly events which may be linked to coral bleaching.

The current study involved deployment of a new set of instruments on the northern Warrior Reef complex with turbidity, salinity and depth sensors deployed in February 2020 and retrieved in November 2020. The deployment was designed to collect data on the south west extent of turbidity plumes in central Torres Strait. The Warrior Reef is an area of local concern as recent bleaching and seagrass dieback events have been observed in the region (observations from local TSRA Rangers). The reefs also form an east-west barrier for the central Torres Strait and may act as a boundary to ocean borne particles.

4.2.2 Methods

Weather stations were installed and maintained at Thursday Island, Masig Island and Bramble Cay (Bainbridge et al. 2015; Waterhouse et al. 2018). These provided 10-minute interval data on wind speeds, air temperature, barometric pressure, humidity and rainfall as well as water temperatures. The network supported by NESP is more extensive than that maintained by the Bureau of Meteorology in the region. The new station at Warrior Reef was installed at Kokope Reef (9°15'35.67"S, 143°12'3.27"E) (see Figure 4–1). Figure 4–2 provides an example of the land-based component of the weather stations.
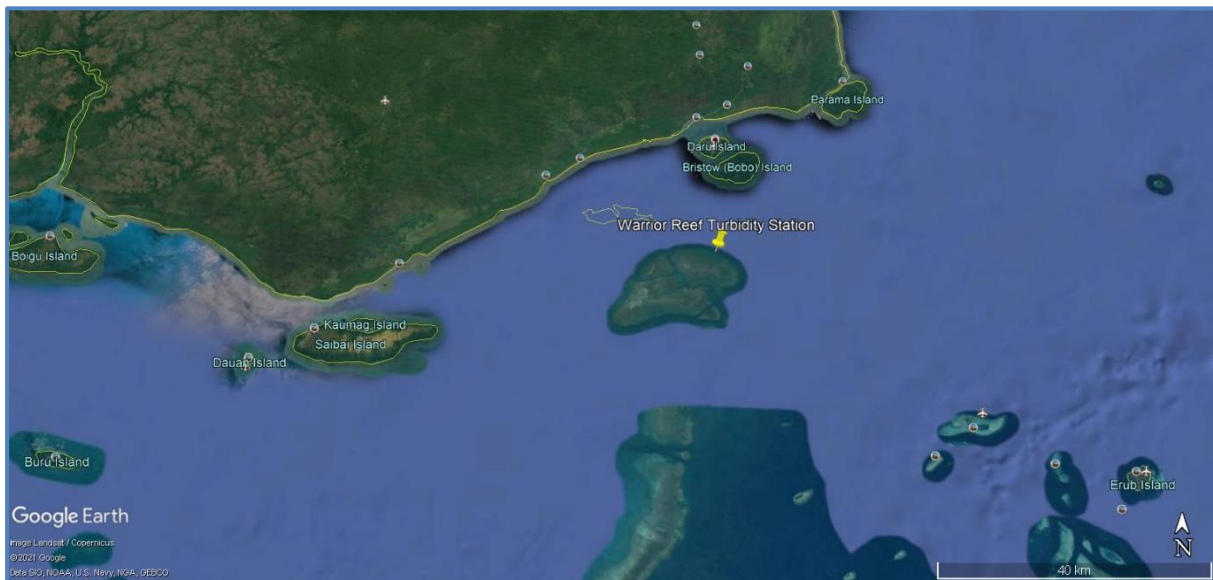
Figure 4–1: Location of the turbidity monitoring station at the northern end of Warrior Reef.

Figure 4–2: Land based component of the Bramble Cay weather station

Cyclones are rare in the Torres Strait but the wind data shows that storms do occur, and it is expected these will be important in driving water movement. One by-product of storms is the movement of sand cays such as Bramble Cay. Drones were used to survey the cay over the course of two years as a proxy measure of the impact of storms and other events that re-shape sand cays.

4.3 New results

4.3.1 Weather Stations

The three existing weather stations near Thursday Island (at Tuesday Islet to the east of Thursday Island), Masig Island and Bramble Cay (Bramble Cay) were maintained for the period of the study although COVID19 travel restrictions in place for most of 2020 increased service intervals, and resulted in some data losses. The availability of the data is detailed in Table 4–1.

Table 4–1: Data availability for the three weather stations

Station	Variable	Data Availability
Thursday Island [est. Feb 2012]	Wind Data	Feb12-Aug14 | Dec14-Nov16 | May17-Jun20 | Nov20 - Present
	Atmospheric Data [pressure, humidity, temperature]	Feb12-Aug14 | Dec14-Nov16 | May17-Jun20 | Nov20 - Present
	Water Temperature Data	Feb12-Jan13 | Jul13-Aug14 | Dec14-Nov16 | Dec17 - Present
Masig Island [est. Jun 2013]	Wind Data	Jun13-Jan19 | Feb20 - Present
	Atmospheric Data [pressure, humidity, temperature]	Jun13-Jan19 | Feb20 - Present
	Water Temperature Data	Jun13-Sep14 | Jul15-Jan18 | Mar18-Mar19 | Mar20 - Present
Bramble Cay [est. Jun 2015]	Wind Data	Jun15-Dec16 | Jun17-Oct17 | Dec17-Present
	Atmospheric Data [pressure, humidity, temperature]	Jun15-Dec16 | Jun17-Oct17 | Dec17-Present
	Water Temperature Data	Jun15-Oct17 | Nov19-*

Station	Variable	Data Availability
	Salinity and Turbidity	Jan16-Jan18 | Nov19-* *The loggers were not able to be serviced due to COVID access restrictions and so it is uncertain what data has been collected.
Warrior Reef [est. Feb 2020]	Water Temperature, Salinity and Turbidity Data	Feb20-Dec20

Water Temperature

The data show that, using average daily water temperature values, the site at Thursday Island did not exceed the empirical bleaching threshold for daily values and that water temperatures have been relatively stable since the 2015-16 bleaching event (Figure 4–3). While the logger data shows short term exceedances of the bleaching threshold, the daily average data (which includes the night-time values) shows temperatures approaching, but not exceeding the threshold. The data from the other sites (which is only partial due to technical difficulties) shows the same pattern of daily averages below the bleaching thresholds and within long-term values.
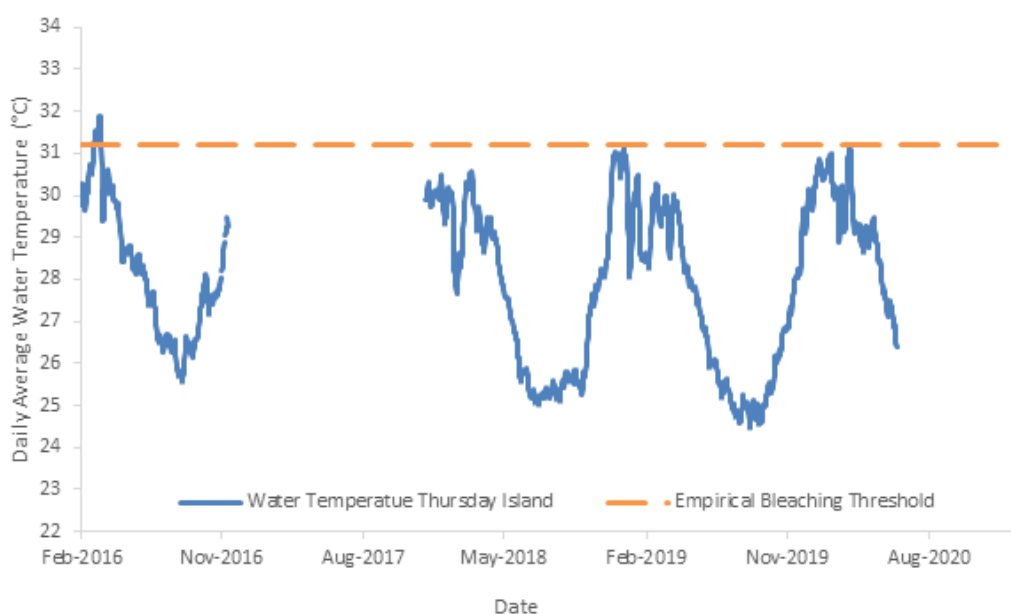
Figure 4–3: Temperature data from the Thursday Island weather station as daily average values contextualised by the empirical bleaching threshold showing that temperatures since 2016 have stayed below the bleaching threshold for this site.

Wind Data

The wind data shows typically monsoonal patterns across the region and the study period with strong consistent south-east trade winds present for most of the winter months followed by more variable winds during the summer monsoonal period (Figure 4-3). The data shows that for Bramble Cay, there were no events with winds at or above gale force (defined as 34 knots or 63 km per hour) although there were a number of short-lived gusts at or near this limit, but no significant wind events that would impact the region.
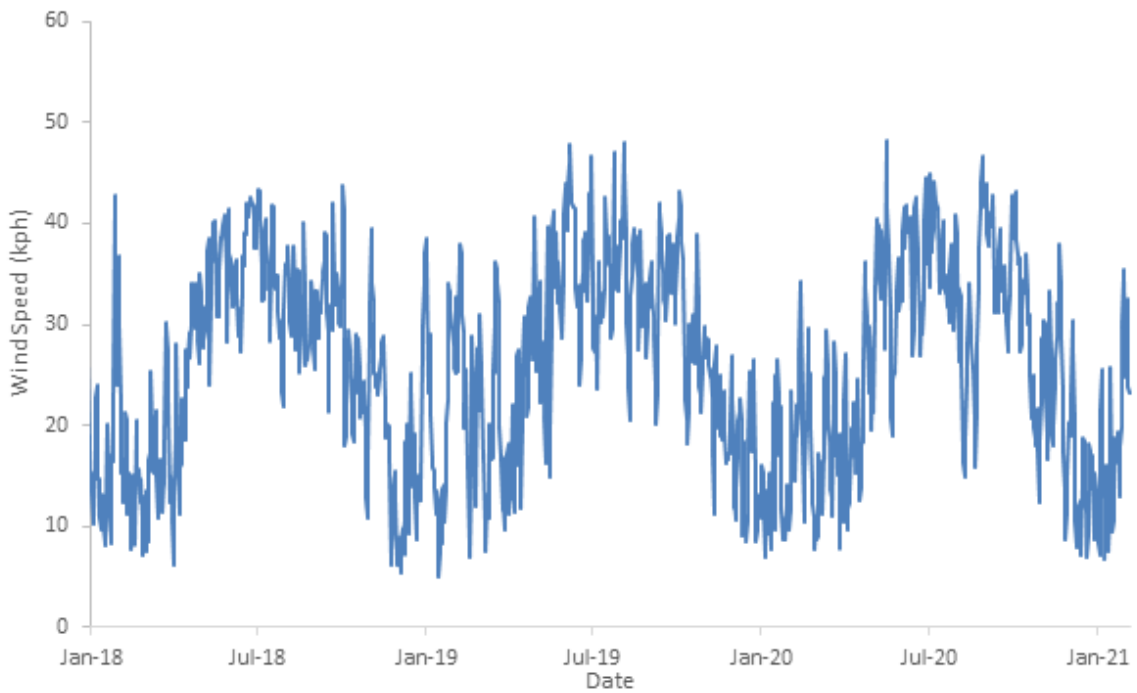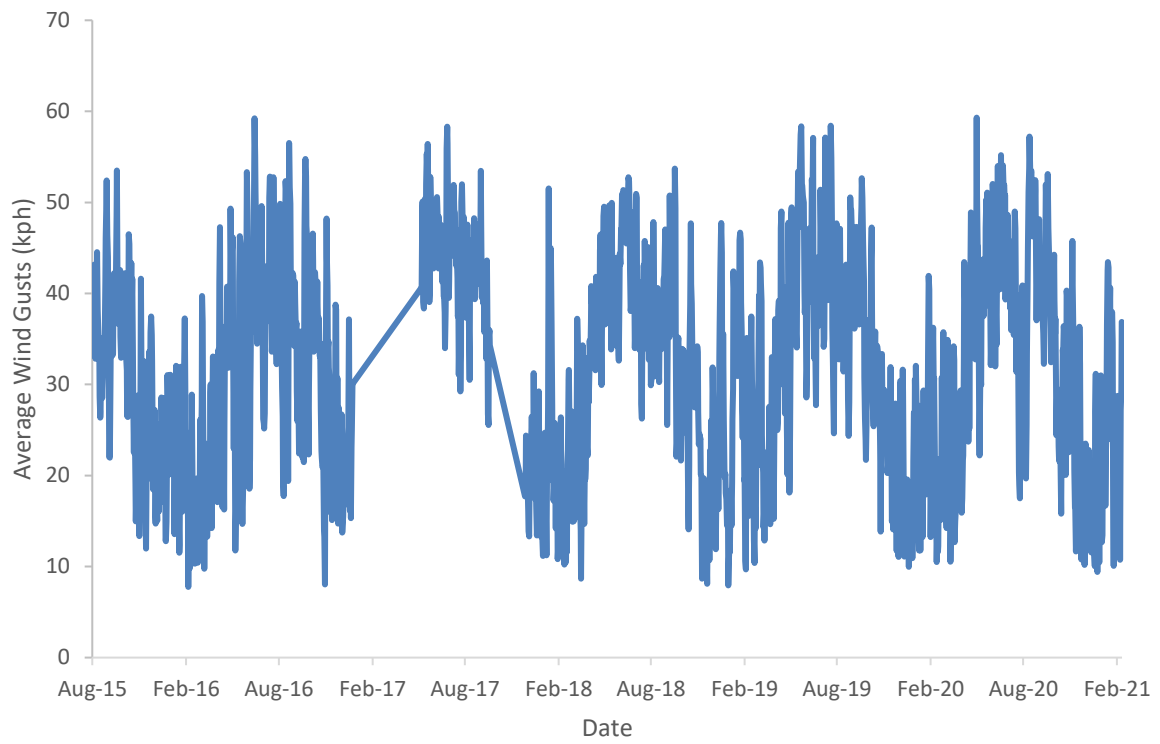
Figure 4–4: Average wind gusts (top) and daily average wind speed (bottom) for Bramble Cay indicating that there were no severe wind events (defined as gale force winds in excess of 63 kph) in the region during this period.

Rainfall (Figure 4–5) follows a pattern of a wet monsoon period followed by a dry winter period dominated by trade winds. The rainfall graphs show no significant winter rainfall for any of the three stations with the exception of 30mm rainfall recorded in May 2020 at Bramble Cay.
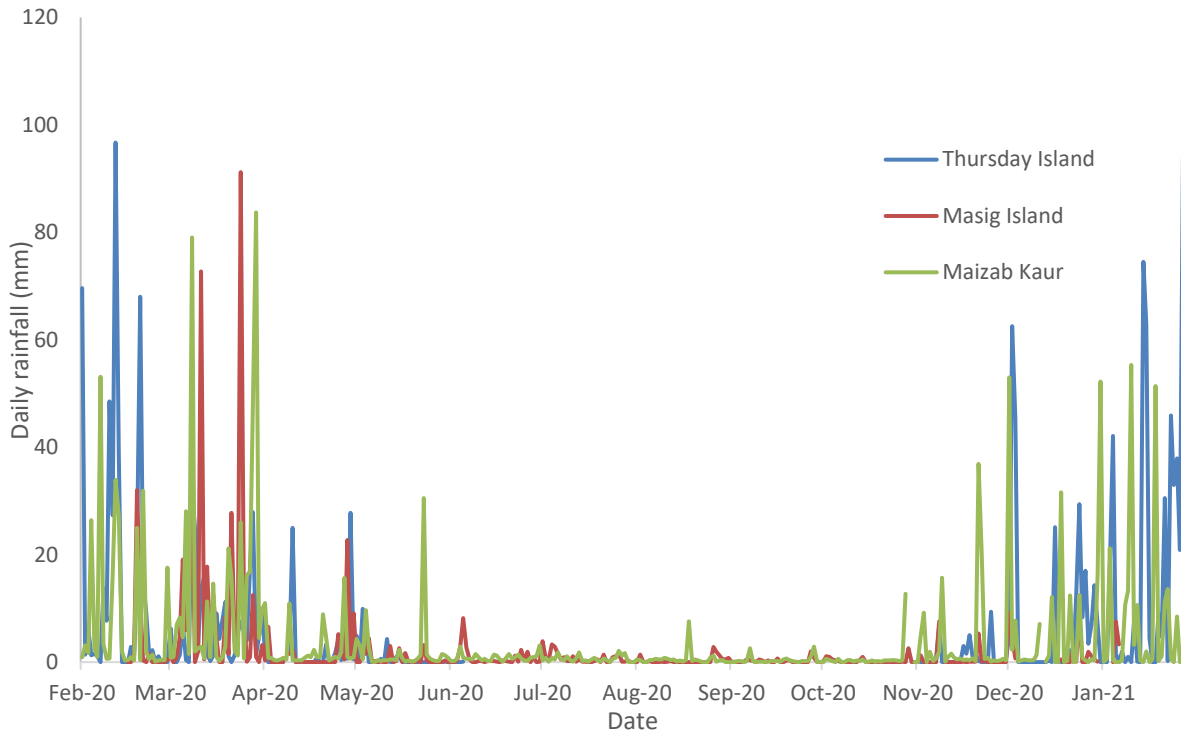
Figure 4–5: Daily rainfall totals (mm) for the three stations for the period of the Warrior Reef turbidity measurements.

4.3.2 Turbidity Monitoring

A turbidity instrument was deployed at the northern Warrior Reefs in February 2020 to identify any highly turbid waters flowing westward and potentially from Fly River or coastal PNG sources. The data was also used to ground truth the satellite images documenting the same phenomena.

Collected turbidity data for the period is shown in Figure 4-6. The average turbidity is 2.8 NTU which is similar to clear water reefs with the highest being 33 NTU which is again not unusually high. Note that the average of 2.8 NTU is half the average previously observed at Bramble Cay (around 5 NTU, see Waterhouse et al. 2018) and while the maximum is similar (over 30 NTU) the Warrior Reefs values are skewed to lower values than the previous Bramble Cay data.

A comparison with the wind data from Masig Island as the closest weather station (approximately 60km south-SE) (Figure 4-7) shows a relationship with turbidity being higher in the winter when wind speeds are greater (r=0.52, n=37985, p<0.005), but wind speeds alone do not account for the spikes in turbidity seen between May and July 2020 and so there are other factors that are impacting turbidity during these events. Observations from the divers that deployed the equipment indicate that the sea floor where the instrument was located is

regularly swept clean by the high currents that flow through the area. This means that turbidity is unlikely to be from simple local re-suspension and reflects sediment sources from elsewhere.
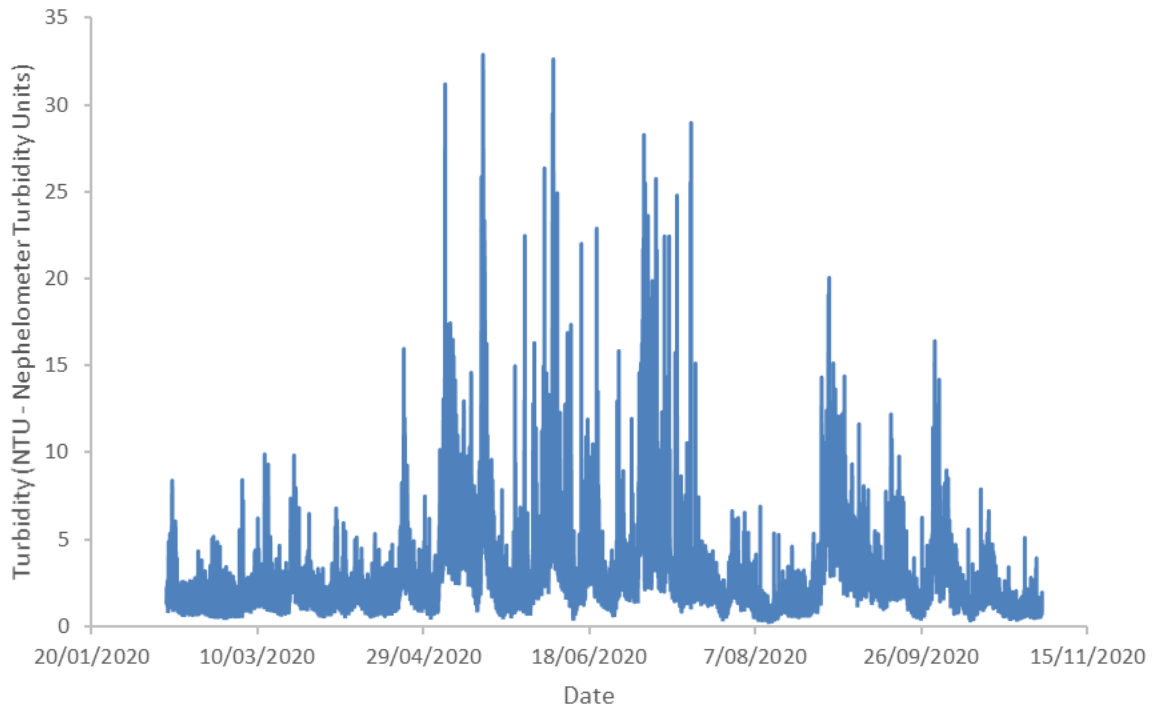
Figure 4–6: Turbidity data for the Warrior Reef station
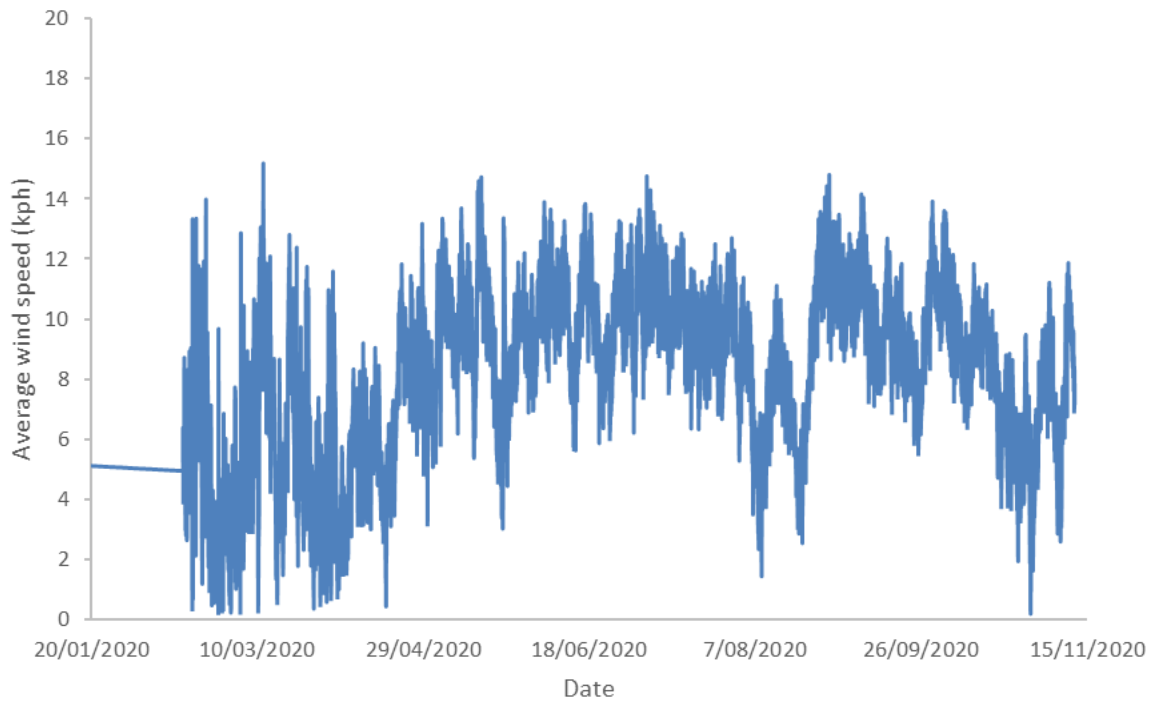
Figure 4–7: Wind speed data from the Masig Island station

4.3.3 Salinity monitoring

The salinity data from the station is shown in Figure 4–8. The data shows a marked periodic deviation away from 'standard' ocean values of 33 PSU with a series of low salinity events occurring on a monthly basis aligned somewhat to the spring tides (Table 4–2). The decrease in salinity cannot be explained by local rainfall (see Figure 4–5) or localised run off and probably reflects tidally driven movement of water from other sources (such as PNG mainland). The logger site at Kokope Reef (northern Warrior Reefs) is only approximately 20 km from mainland PNG (directly north), and for context, the Fly River mouth is approximately 60 km to the east, and Wassi Kussa River is approximately 110km to the east. The links between these potential freshwater sources and the low salinity values recorded at the northern Warrior Reefs requires further investigation.
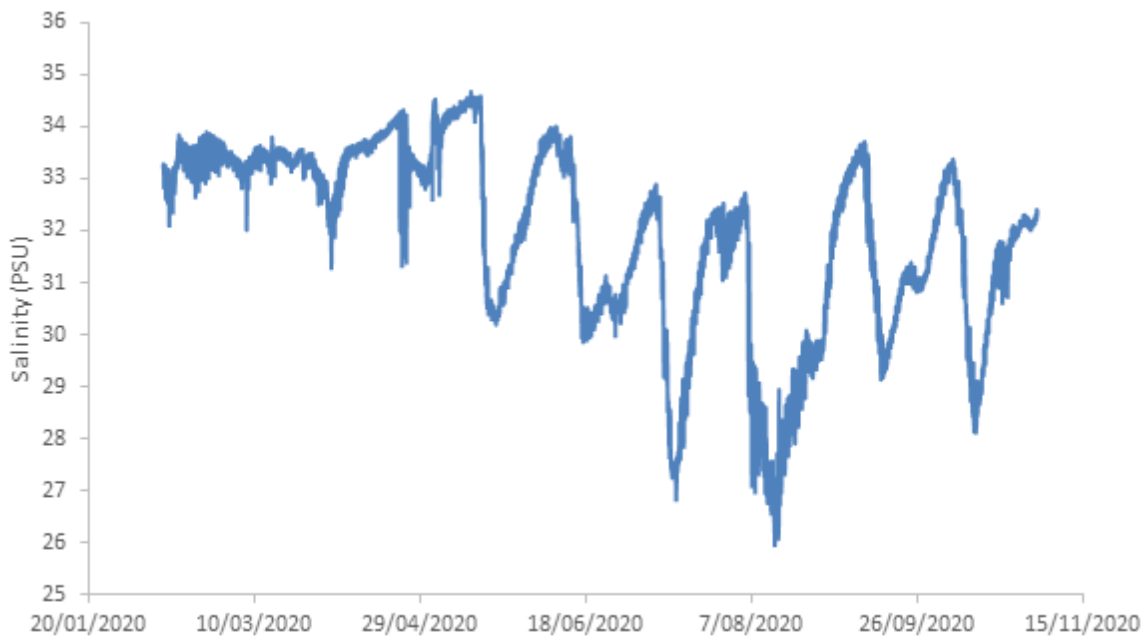
Figure 4–8: Salinity data from Warrior Reef station

Table 4–2: Timing of the low salinity events against the new moon

Low Salinity Event	New Moon (Spring Tide)
22-May	22-May
17-Jun	21-Jun
15-Jul	20-Jul
15-Aug	19-Aug
15-Sep	17-Sep
13-Oct	16-Oct

4.3.4 Additional observations

Drone surveys of Bramble Cay were completed in October 2019 and again in November 2020 (Figure 4–9). The resulting images show a large change in the shape and size of the Cay over a single year when the weather data shows no significant weather events. The change demonstrates that significant ocean events occur that are driven by factors that are not

recorded by standard weather monitoring and other observations such as currents and tidal influences. This indicates there are mechanisms that provide wave energy significant enough to alter the shape and geomorphology of the Cay over the period of a year (the cay area to the high-tide mark was 4.04Ha in 2019 and 3.43Ha in 2020 or a 15% change). This wind/wave energy represents a potential mechanism for coastal PNG water to move into the Torres Strait, as shown by proxies such as the movement of sand cays.
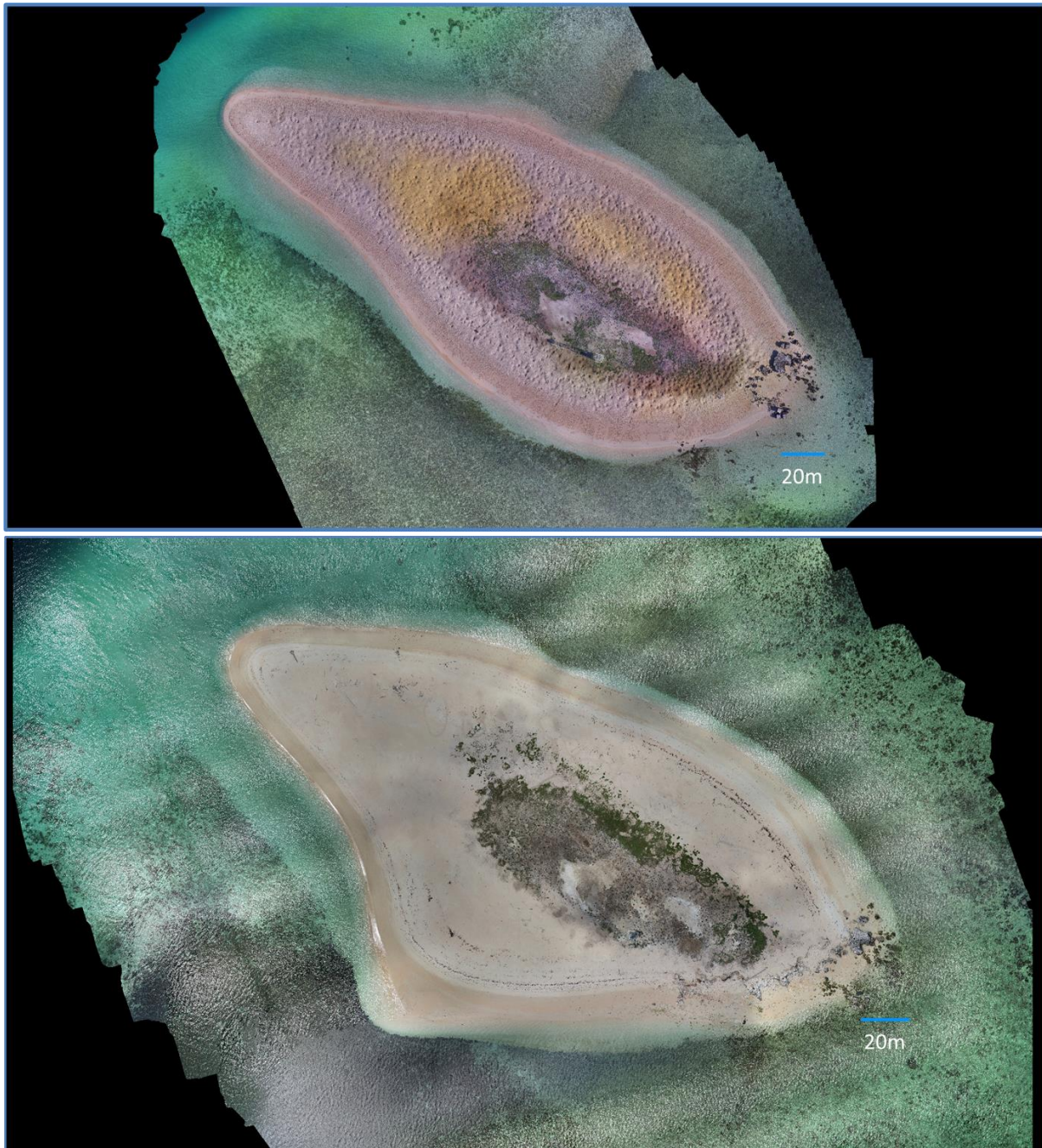
Figure 4–9: Drone surveys of Bramble Cay from November 2019 (top image) and October 2020 (bottom image) (images collected by Shaun Hahn, AIMS).

4.4 Conclusions

The weather station and temperature logger data show that the last few years had lower ocean temperatures than the extreme events recorded in 2015/16 and so the risk of coral bleaching and other events was reduced over this time. Wind patterns and atmospheric data show relatively normal conditions with variable monsoonal conditions transitioning to more stable winter conditions driven mostly by the southeasterly trade winds.

The turbidity data showed that the northern Warrior Reefs experienced relatively clear water and, while there were a few short-lived turbidity spikes, in general the turbidity levels were low with a correlation between winter wind driven higher levels and lower levels during the summer monsoonal period. The patterns of salinity, however, did show a strong monthly cycle with low salinity events that cannot be explained by localised rainfall or run-off. These may represent tidal driven waters from coastal PNG flowing into the northern Warrior Reefs. The correlation between the low salinity events and spring tides may provide a mechanism for explaining the observed periodic low salinity events.

The work highlights the utility of long-term observations in understanding the observed patterns and so there is ongoing value in continuing these observations. The unexpected low salinity events observed at the northern Warrior Reefs shows that the understanding of the systems is still incomplete reflecting the complex nature of the oceanography in this region. Improved understanding of this remains a priority to better understand the functioning of the biological systems of Torres Strait.

5.0 HYDRODYNAMIC AND SEDIMENT TRANSPORT MODELLING

5.1 Previous findings

NESP TWQ Hub Project 2.2.1 evaluated wind and current intensities that result in freshwater intrusions into the Torres Strait. Used MOHID 3D coastal model of Gulf of Papua with 2D-SLIM high-resolution model for the Torres Strait[1]; calibrated and validated using observational data and tracing studies (Li et al. 2013; Waterhouse et al. 2019).

- The modelling suggested that the plume of potentially polluted river water from the Fly River is probably mostly of concern in the Torres Strait region during the SE trade wind season. During that season the plume is permanent, although variable in characteristics following fluctuations of the wind and differences in mean sea level (ΔMSL[2]) across the Torres Strait.
- The study also reviewed the historical field data from ship-borne observations and oceanographic moorings, which showed:
  - a permanent intrusion into the northern top third of the Torres Strait of brackish, river plume waters from the Gulf of Papua;
  - lower salinity in the east than in the west; and
  - strong seasonal variation with the largest and most intense intrusions during the SE trade wind season, and the smallest and least intense intrusions during the monsoon season.
- Analysis of the field data describing the physical oceanographic processes that control this intrusion showed that the key influencing factors are freshwater discharge in the Gulf of Papua; the wind; the MSL in the Gulf of Carpentaria, the Gulf of Papua and the northern Coral Sea; and tidal mixing.
- Field data was used to drive oceanographic models to describe the behaviour of the freshwater plumes over the Gulf of Papua and their intrusion in the Torres Strait using the 3D MOHID oceanographic model. The model predictions were successfully verified against field data. The river plume intrusion was largely limited to the northern third of the Torres Strait and was more intense in the east than in the west. The plume was vertically well-mixed throughout the Torres Strait. Tidal influences have a lower influence than other physical oceanographic influences.
- The MOHID model results were used at the open boundaries to drive the high resolution, 2D-SLIM model. The SLIM model demonstrated the high variability of the extent and dilution of the Fly River plume in the Torres Strait.
- This study was limited to understanding the intrusion of the Fly River plume (water) in the Torres Strait. It did not address the intrusion of Fly River fine sediment and its particle-bound contaminants.

The large-scale patterns identified in the modelling were consistent with the key findings from the remote sensing analysis; however, the modelling of salinity and remote sensing of turbidity

---

[1] Wolanski et al. (2013) and Martins and Wolanski (2015).
[2] Difference in mean sea level (MSL) across the Strait. ΔMSL is > 0 when the MSL in the Gulf of Papua is greater than the MSL in the Gulf of Carpentaria.

were not directly comparable due to alternative sources of sediment and turbidity in the region including the dominant processes of resuspension.

5.2 Additional work: Scope and methods

5.2.1 Purpose

Previous studies showed that the Fly River plume commonly moves into the northern Torres Strait and along the PNG coast, particularly affecting the northern and north western islands (Daru, Saibai and Boigu Islands) and reefs (Warrior Reef) during the six months of the SE trade wind season (May to October). Modelling studies have focused on describing the intrusion of the Fly River plume in Torres Strait (Li et al. 2017, Waterhouse et al. 2018). However, most of the mine-derived contaminants, including copper, discharged by the Fly River are in particulate form and absorbed[3] onto the cohesive fine sediment (Wolanski et al. 1992; Angel et al. 2010a; Apte et al. 2018). These previous studies did not assess the transport of polluted fine sediment, or 'mud', in Torres Strait. For the first time, a model was developed to assess the transport of Fly River mud and its particulate metals in the Torres Strait region. This was linked to other components in this project including field data from the *in-situ* loggers, water quality sampling (recent plus Wolanski's 1990s studies) and remote-sensing. The model was also used to predict changes in the distribution of particulate material from the Fly River over time.

5.2.2 Methods

The modelling methods are built on several aspects of a pre-existing understanding of mud distribution and movement in the Torres Strait region. The map in Figure 5–1 includes several locations that are referred to in the description of these methods. The Fly River mud is diluted by two mud baths before it can enter the Torres Strait, and mix with its mud bath (Area 3); they are located (i) in the estuary itself (hereafter 'estuarine mud bath': Area 1) and (ii) in coastal waters of the Gulf of Papua (hereafter 'Gulf of Papua: Area 2'). Each 'mud bath' is a pool of resuspendable, non-consolidated mud that was originally non-polluted (i.e. before mining - note that our study refers to additional metals above those that may have occurred before mining commenced). The model does not include the fate of metals, only the mud dynamics. Mud in the mud baths is resuspended by swift tidal currents and waves and while in suspension it is transported by the water currents; it settles during calm weather and during slack tides (Ayukai and Wolanski 1997; Harris et al. 2004). Note that the sediment transport model does not extend far enough eastward to include Bramble Cay, but this was included in the salinity model (Li et al. 2017).

---

[3] Note that the metals are absorbed in the mud flocs (i.e. the marine snow studied by Ayukai and Wolanski, 1997), and they are presumably adsorbed on the solid mud particles in the flocs.
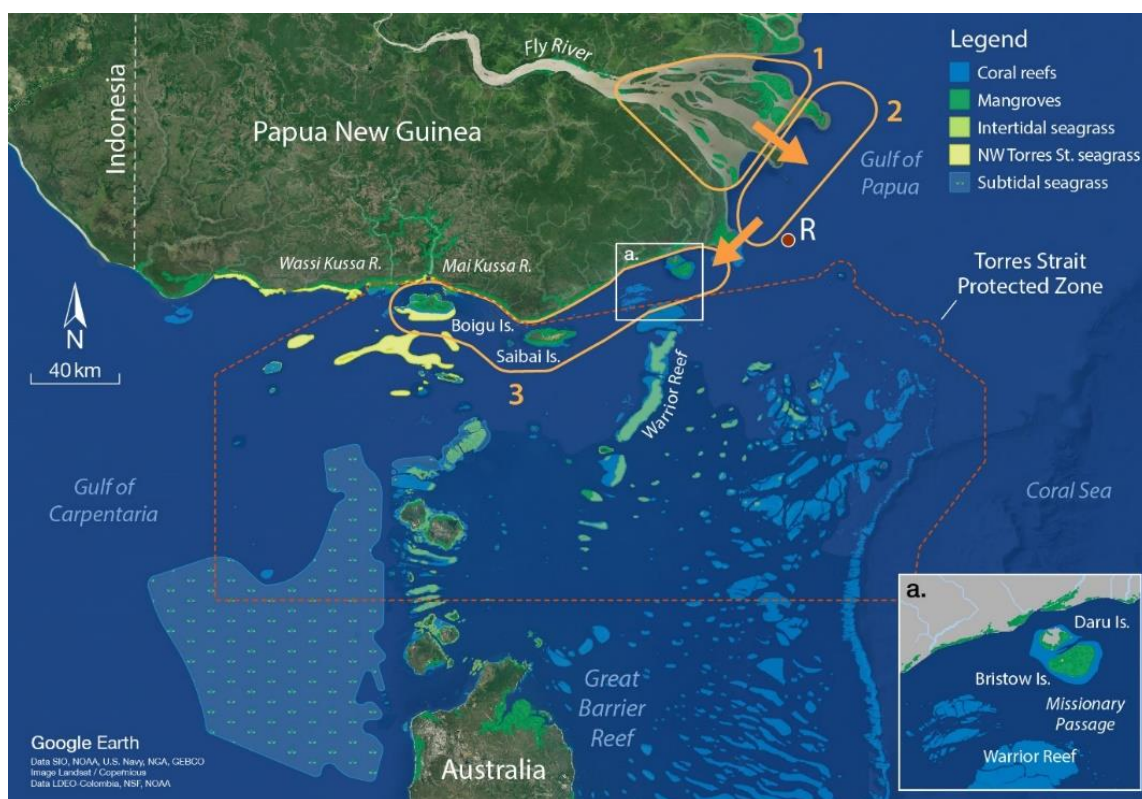
Figure 5–1: Map of the Torres Strait region showing the major rivers, islands, habitats and the boundary of the Torres Strait Protected Zone as well as the major locations in the Torres Strait referred to in this study. Area 1 = estuarine mud bath; Area 2 = inshore Gulf of Papua mud bath; Area 3 = Torres Strait mud wedge. The arrows indicate the general direction of movement of the Fly River mud. Sampling site R is located at -9.01 °S, 143.68 °E. Modified from Carter et al. (2014).

The thickness of the estuarine mud bath is about 0.5 m (Wolanski et al. 1992), but the thickness of the Gulf of Papua and the Torres Strait mud baths are unknown (Crockett et al. 2008, 2009; Harris et al. 2004; Heap et al. 2005; Hemer et al. 2004). Most of the mud transported out of the inshore Gulf of Papua mud bath (Area 2) is transported to the SE into the outer Gulf, but a fraction (3 - 11% according to the wind speed and direction; Harris et al. 2004) enters the Torres Strait to mix with mud in the Torres Strait mud bath (Area 3). This mud (hereafter called 'new mud') is potentially polluted by mine-derived contaminants. This new mud intrudes as suspended sediment into the Torres Strait when the prevailing current is westward, i.e. during the SE trade wind season (April to October; Waterhouse et al. 2018). The new mud entering Torres Strait is diluted by the original, old, ('non-polluted') mud present in the Torres Strait (hereafter 'old mud'). The old mud is present because Fly River mud has intruded the Torres Strait region over thousands of years where it has formed a 'non-polluted' mud bath (hereafter 'the Torres Strait mud wedge') along the PNG coast (Area 3) (Heap et al. 2005).

Mud resuspension by strong tidal currents and waves creates a turbid coastal boundary layer north of the Warrior Reefs all along the southern PNG coast including around Saibai and Boigu Islands (e.g. Heap et al. 2005; Waterhouse et al. 2018) (Area 3). This turbid coastal boundary layer is visible on GoogleEarth and MODIS satellite images (see example in Figure 5–2) and aerial observations. It is possible to distinguish the terrigenous mud (i.e. originating from rivers; brownish colour) from the calcareous mud (i.e. originating from coral reefs; greyish colour).
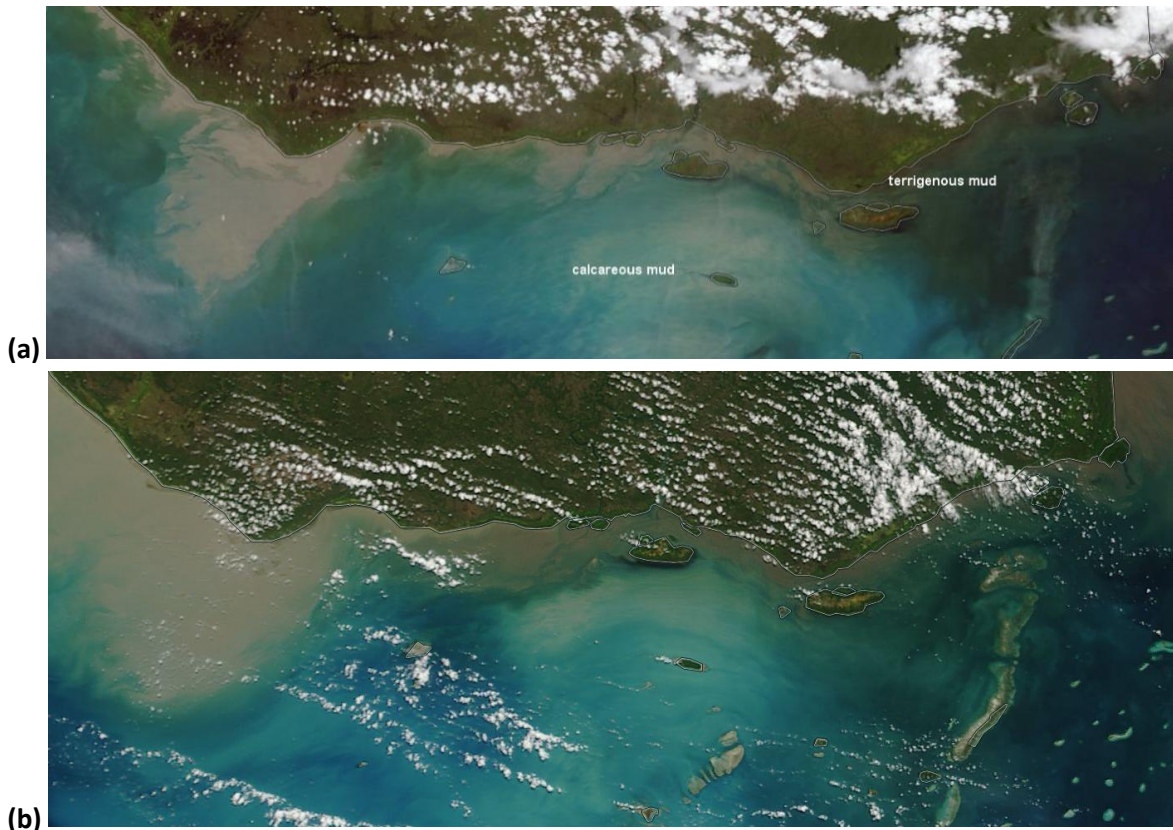
Figure 5–2: Examples of the MODIS true colour satellite images showing the turbidity in the Torres Strait (a) during the monsoon season (2 February 2014) and (b) during the SE trade wind season (23 August 2009). Source: NASA Worldview

The area has been sampled by moored nephelometers and ship-borne turbidity meters in the 1990s (Wolanski et al., 1992, 1995, 1999) and with water samples collected in October 2016 (Apte et al. 2018) and 2018 and 2019 (see Section 7.0). The modelling in this study builds on this knowledge to predict the distribution and timing of new mud transport into the Torres Strait.

Modelling the hydrodynamics

The spread of new mud into the Torres Strait, both in suspension and on the ocean floor, was modelled using the 2D vertical integrated SLIM model. The model had two 'sub' models: 1) an oceanography sub-model (developed in the previous NESP study by Wolanski et al. 2013a, 2013b; Li et al. 2017); and 2) a mud dynamics sub-model in which the mud is one-way coupled to the hydrodynamics model. The model domain covered the whole of the Torres Strait and the model mesh was highly refined along the PNG coast (Figure 5-3). The open boundaries in the Gulf of Papua, the Coral Sea and the Gulf of Carpentaria were forced by sea level, defined as the sum of the tides and the mean sea level, which was taken from satellite altimetry data following Li et al. (2017). The open boundary conditions for the hydrodynamic model were already established (Li et al. 2017). However, the more complicated mud conditions were more challenging to model, requiring the exclusion of coastal regions adjacent to the Fly River mouth from the model domain (i.e. Area 2 in Figure 3-1). Instead the model domain is the north east (NE) boundary of Torres Strait where the open boundary condition was the suspended sediment concentration along the NE open boundary of the model - i.e. the mud in suspension in the Fly River plume calculated using historic field data (Wolanski et al. 1995a, 1995b, 1999).
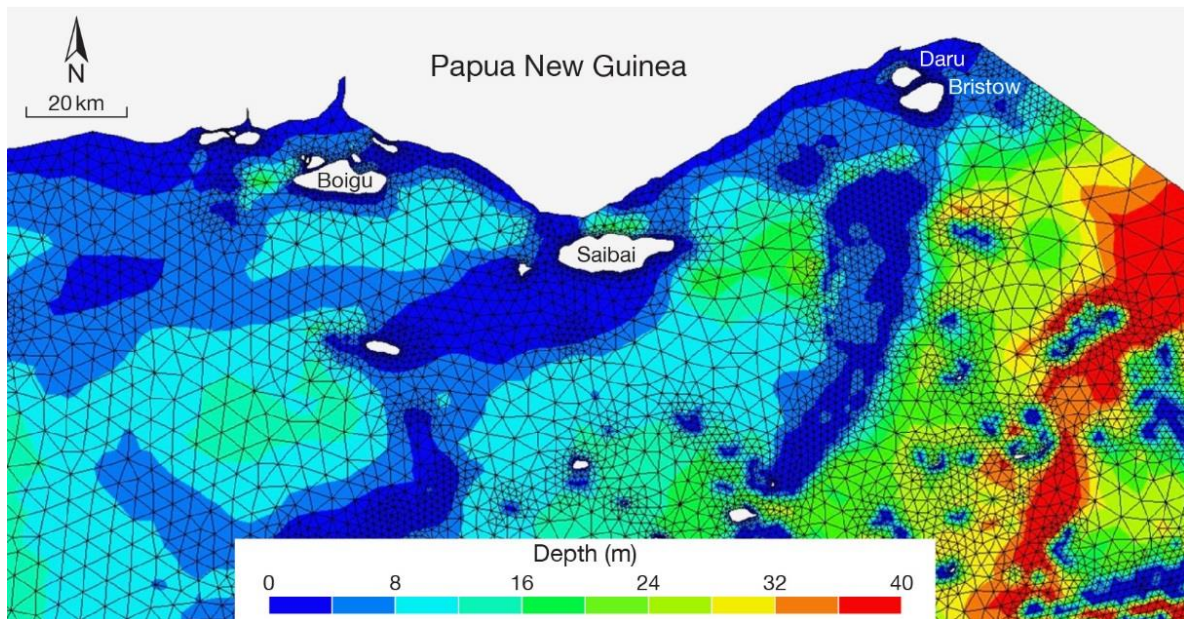
Figure 5–3: A zoom-in view of the model domain in the northern Torres Strait, showing the mesh; the colour bar shows the depth ranging from 0 to 40 m.

Wind data was sourced at 30-minute intervals from the weather stations managed by AIMS and TSRA at Bramble Cay (in the north of the domain) and Tuesday Island (near Thursday Island in the south of the model domain). Due to their comparability, it was assumed that the wind was spatially homogeneous. The frequency of occurrence of the dominant wind was calculated from the Bramble Cay wind data. Strong SE winds occurred 5.7% of the time and strong NW winds occurred 60.7% of the time. The hydrodynamics were modelled for 8 scenarios of wind (SE/north west, strong and light) and tides (spring/neap) to represent the dominant hydrodynamic processes over a year.

Modelling the mud dynamics

A conceptual illustration of the model is shown in Figure 5-4. As illustrated in Figure 5–4a, the model starts with a non-polluted mud wedge along the PNG coast. The bottom mud is resuspended by the water currents as well as fluidised by the wind waves; the fluidised mud is readily resuspended by currents.

Mud also exists further below this readily resuspendable mud layer, but is consolidated and thus much harder to resuspend (e.g. Mehta 2013) (Figure 5–4b). The open boundary condition was the suspended sediment concentration along the NE open boundary of the model - the mud in suspension in the Fly River plume. The depth-averaged polluted suspended sediment concentration (in g/L) along that open boundary during SE trade winds, and the mud settling velocity in the model was calculated using historic field data (Wolanski et al. 1995b, 1999).

The width of the Torres Strait mud wedge (i.e. the active mud layer) is about 20 km but its thickness is not known. The thickness of the Torres Strait mud wedge was assumed to be smaller than that in the estuary (~ 0.5 m, i.e. ~ 865 kg/m^2; Wolanski et al. 1992) because the currents are smaller than in the Fly River estuary and thus the mud would be less disturbed and more consolidated. Thickness values of 0.12, 0.25 and 0.5 m were used, decreasing

linearly with distance seaward to be zero at 20 km from the PNG coast (Heap et al. 2005) (Figure 5–4c).

The old mud and the new mud in suspension are present together and together they determine the suspended sediment concentration. This in turn determines the settling velocity. When settling occurs, both the new and the old mud in suspension settle together and they mix in the Torres Strait mud wedge, progressively polluting the originally un-polluted mud wedge (Figure 5–4a). The compacted, non-polluted mud layer underneath the active mud layer has an erosion rate typically 1/10th that of the mud in the mud wedge. It is only eroded when the active mud layer is removed (Figure 5–4b; Mehta 2013). The model did not consider the bed load, which applies for coarse sediment (e.g. sand, which is not cohesive and thus not polluted by metals) (Salomons and Eagle 1990).

The mud model was used to calculate the mud transport for eight scenarios of varying wind and tide characteristics. The total net longshore mud flux (in ton/s) of sediment in coastal waters of the PNG coast was calculated from the model output at eight cross-sections from Daru to the PNG border, allowing estimation of the yearly-averaged and spatially-averaged westward mud flux along the PNG coast. From this, the residence time of the active non-polluted mud layer along the PNG coast was estimated.

To estimate a spatially-averaged net mud flux, the scenario outputs were used to calculate the averaged mud flux between spring tides and that at neap tides across 7 cross-sections perpendicular to the coast west of Daru Island. Sensitivity tests were carried out by varying the various parameters in the mud model within a reasonable range to estimate the likely 'error bars' (see Wolanski et al. 2021).
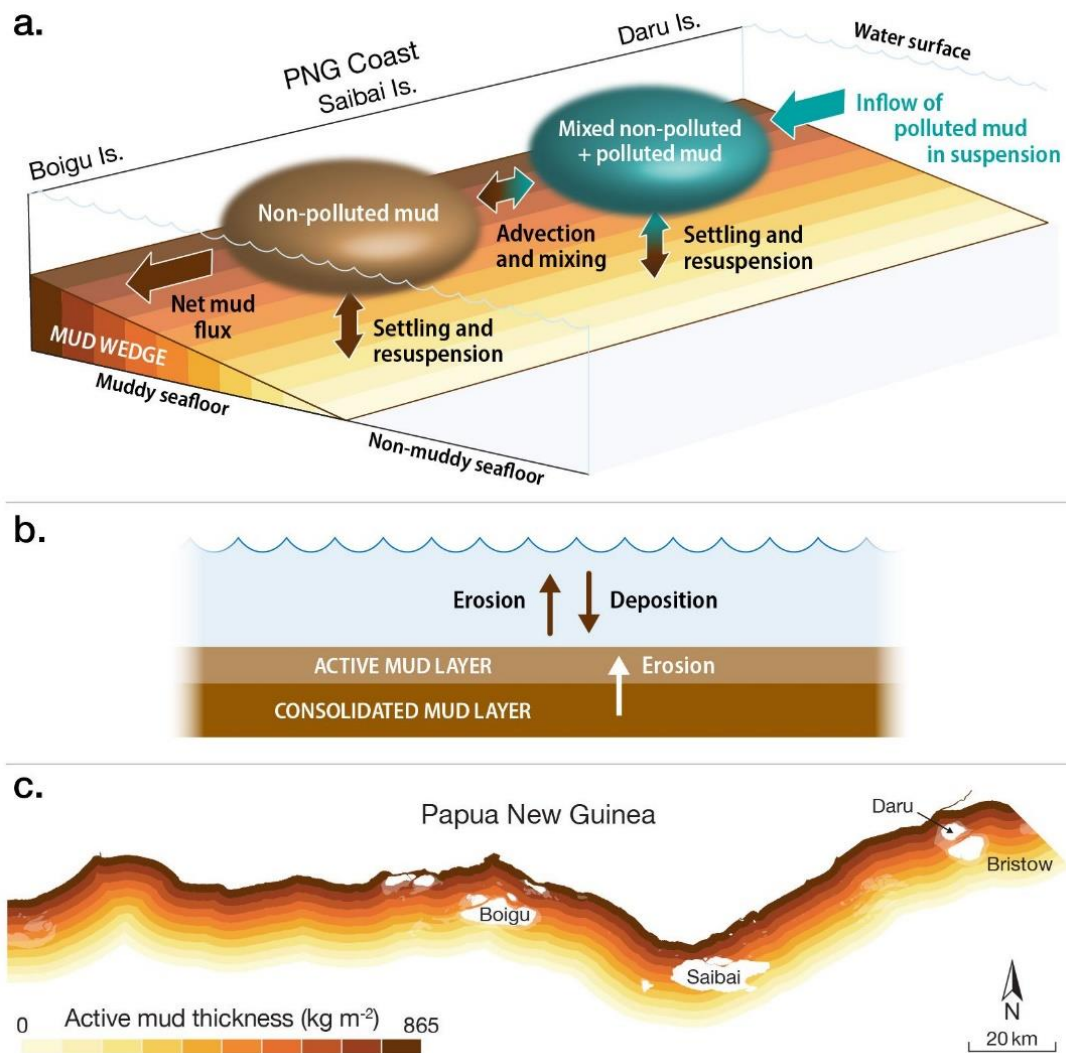
Figure 5–4: A conceptual illustration of the mud model developed for the Torres Strait. (a) calculating the spread of new, potentially polluted mud in Torres Strait, starting from the original, non-polluted mud. (b) Erosion of the consolidated mud layer occurs only when the active mud layer is eroded out. (c) The original, non-polluted mud wedge for the maximum water depth that mud can be resuspended by waves and a maximum distance from the PNG coast of 20 km. The colour bar shows the modelled thickness of the mud wedge.

Suspended sediment concentration data for model validation

The method for generating suspended sediment concentration maps is described in the Remote Sensing methods, Section 6.2. Field suspended sediment concentration (SSC) data were extremely limited due to the remoteness of the study area.

A selection of MODIS satellite images was thus used to preliminarily compare (qualitative assessment) large scale and seasonal SSC patterns between the model and satellite data. Twenty-eight MODIS SSC images in 2016 and 2017, selected to be relatively cloud-free, were produced for the study area. This limited selection of MODIS SSC maps was used to map low/high trends in SSC distribution and visually assess similarity between satellite and model patterns in SSC distribution. Note that the modelled SSC only considered the terrigenous mud while the SSC maps also show suspended calcareous sediments (particularly in the middle of

the Torres Strait) but cannot separate them. It is therefore likely that the suspended terrigenous sediments concentrations were overestimated in the satellite maps.

The range of SSC retrieved by the MODIS maps was compared against *in-situ* SSC range using limited published field datasets to provide preliminary confidence in the satellite maps. Field data included SSC data collected (i) in and near the Fly River (ii) in the 1990's between slightly east of the Warrior Reef (Wolanski et al. 1999) and (iii) SSC measurements collected in calm weather around Saibai and Boigu Islands in October 2016 (Apte et al. 2018 and URL: https://eatlas.org.au/node/45552) and in June 2018 (see Section 7.0).

5.3 New results

5.3.1 Hydrodynamic modelling and mud dynamics

The model successfully provided a prediction of the movement of mud from the Fly River into the Torres Strait (see model verification steps below). During strong SE wind and spring tides, the spatially-averaged westward mud flux along the PNG coast of Torres Strait west of Daru was calculated to be 0.36 ton/s, i.e. 5.4 % of the Fly River estuary mud discharge estimated to be 6.7 ton/s (Wolanski et al. 1995a). This westward mud flux is equal to 9 % of the mud discharge (4 ton/s) through the southern channel of the Fly River estuary, which is located closest to Torres Strait. The model suggested that the net (tidally averaged) transport of mud along the PNG coast was highly dependent on both the wind and the tides (see example in Figure 5–5a). The system is patchy, with zones of high net transport and other zones of small net transport. As shown in Figure 5–5a, for Fly River mud to enter the Torres Strait it was either forced through the small passages between Daru Island and the PNG coast and between Daru and Bristow Islands, or flowed seaward around these islands to enter Torres Strait through Missionary Passage. Because of that bottleneck, the net mud flux west of Daru Island was insensitive to the inflow of Fly River mud at the open boundary of Torres Strait facing the Gulf of Papua.

Figure 5–5b compares the mud transport under strong SE winds and spring tides during normal Fly River conditions and during a drought. Linked with the El Nino- La Nina phenomenon, there are occasional droughts of the Fly River (Bolton 2008). They last several months; for instance, Ok Tedi Mining declared a force majeure on 17 August 2015 after the El Nino weather pattern sank river water levels and the mine was put on care and maintenance when the drought cut off its transport links. Modelled as a 50% decrease in the inflowing mud, the mud transport during the drought west of Daru was not changed, i.e. local mud was resuspended, while the mud transport east of Daru was substantially changed. This was due to the bottleneck that is formed by Daru and Bristow Islands.
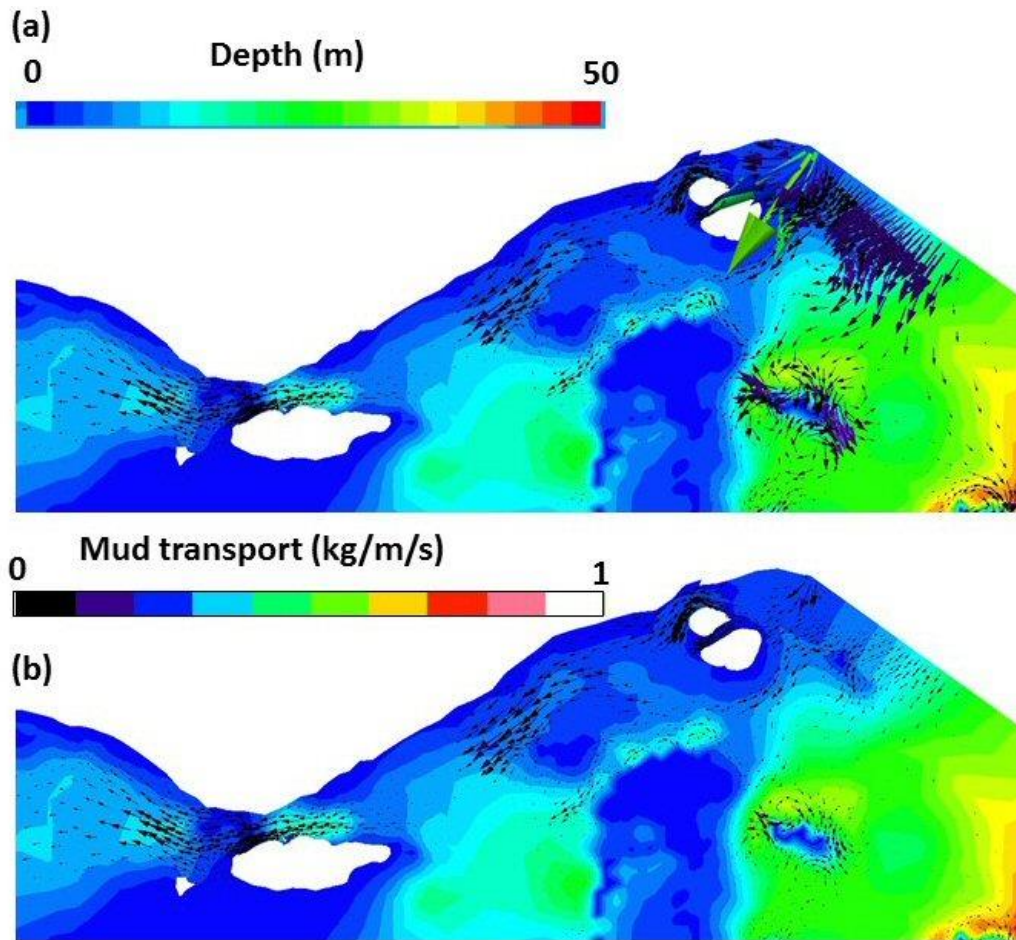
Figure 5–5: The predicted net (tidally averaged) mud transport under strong SE trade wind conditions and spring tides during (a) normal Fly River flows (scenario 1), and (b) a Fly River drought. The top scale bars indicate the meaning of the colours and the size of the arrows represents the magnitude of the response. Note that there is little difference west of Daru Island but a large difference east of Daru Island.

From such data the longshore mud flux was calculated at cross-sections along the PNG coast. Figure 5–6 shows scenarios for a strong SE trade winds, and strong monsoonal winds. The direction of the mud movement generally followed the direction of the longshore wind component with mud transported eastward and along the PNG coast by strong SE winds; the mud was transported westward by strong monsoonal winds (not shown) and there was negligible net transport in calm weather conditions both for spring tides and neap tides (not shown). From these data the yearly-averaged, spatially-averaged (i.e. the net) mud flux was calculated to be 0.14 ton/s westward (Table 5–1).
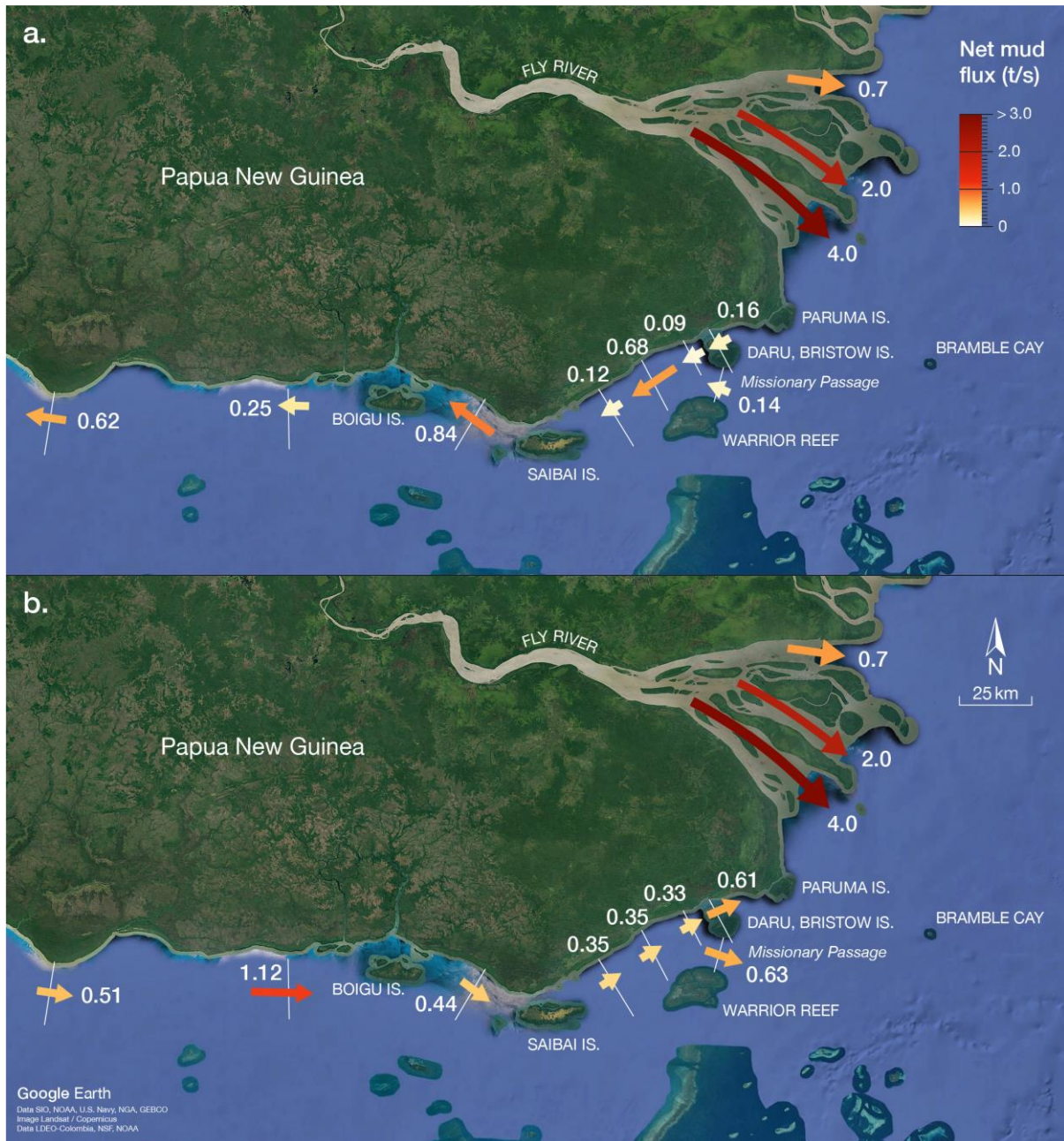
Figure 5–6: Net mud fluxes in tons/s along the PNG coast during spring tides and (a) strong SE tradewinds and (b) strong monsoonal winds. The values of the mud fluxes in the Fly River estuary are reproduced from Wolanski et al. (1995a).

From Table 5–1 the yearly and spatially averaged net mud flux was ~ 0.14 ton/s, or 0.252 m³/s for a wet mud density of 1,800 kg/m³. The length of the PNG coastal mud wedge is about 210 km; its width is about 20 km. For a depth of the active mud layer at the PNG coast of 0.5 m and zero at 20 km offshore, the volume of the active mud layer was estimated around 1.05 X 10^9 m³. This volume divided by the volumetric flux is the e-fold residence time, which was about 132 years. This long residence time was driven by the large size of the Torres Strait mud wedge, and also because the mud flux is eastward during monsoonal winds and brings non-polluted mud from Indonesia that dilutes pollution from the Fly River. The area of higher turbidity to the west of Boigu Island is also identified in the satellite images (see Section 6.3).

The time scales for Fly River discharge to reach Boigu Island are much larger. By contrast the intrusion of new mud to Daru Island in PNG Torres Strait should occur much more swiftly as it does not depend on the Torres Strait mud wedge.

Table 5–1: Estimate of the net mud flux (ton/s) along the Torres Strait PNG coast. U is the wind velocity in m s^{-1} (>0 if northwestward) along a NW-SE axis. The net mud flux is >0 if westward

	Wind velocity (*m s^{-1}*)				
	U<-6	-6<U<-3	U>-3,U<3	3<U<6	U>6
Frequency (%)	5.67	4.92	15.05	13.61	60.74
Net mud flux (ton/s)	-0.26	-0.25	-0.11	0.063	0.29
Flux X frequency	-0.0147	-0.0123	-0.0166	0.0086	0.1761

Note: Yearly-averaged net flux (ton/s): 0.14

A second estimate of the residence time was provided by the model showing slow propagation of new mud in Torres Strait. This is detailed in Wolanski et al. (2021). A number of numerical tests were also carried out to evaluate the sensitivity of the predictions to various parameters and assumptions and reported in Wolanski et al. (2021).

It is important to note that the movement of mud waves may be a major process contributing to the events of high turbidity observed near Boigu Island (Wolanski et al. 2021). These mud waves are typically 1 m high and several km to a few tens of km in wave length, and they move slowly longshore (it can take several years for a mud wave to pass from a wave crest to a wave trough). Evidence of such mud waves were identified in Google Earth images, with erosion at one site north of Saibai Island and progradation at another site 9 km away and also north of Saibai Island (refer to Wolanski et al. 2021). The mud waves result in local erosion and sedimentation hotspots which are expected to move in time with the moving mud waves. This implies that spatial patterns in shoreline erosion and sedimentation are not due to the intrusion of polluted mud in the far northern Torres Strait. This is a natural variability that should be taken into account in future studies.

5.3.2 Model verification

The model was verified using historical field data and MODIS SSC data. Historical field data inside and near the Fly River estuary suggested that the MODIS data were likely to underestimate SSC concentrations in the very turbid waters by an order of magnitude, most probably due to saturation of the reflectance in the MODIS band 1. This saturation has been widely documented (e.g., Doxaran et al. 2003, Petus et al. 2010, Dorji et al. 2016) and is partly taken into account by using an empirical algorithm with a polynomial form (Petus et al. 2010). SSC values decreased rapidly with distance from the PNG coast. Indeed, field data collected in August-September 1994 by Wolanski et al. (1995a) at sites slightly east of the Warrior Reef showed SSC values always < 30 mg l^{-1} and commonly < 20 mg l^{-1}, which agreed with the range of SSC concentrations derived from the selected MODIS data. Similar SSC values were also recently measured south of the Torres Strait mud wedge in calm weather (Apte et al. 2018; Section 7.0) and were also well predicted by the model. It was assumed that during strong winds and/or spring tides, the PNG coastal waters in Torres Strait were likely to be as turbid as the waters in the Fly River estuary and a SSC x 10 adjustment factor was applied to better illustrate SSC concentrations in the Torres Strait mud wedge (Figure 5–7).
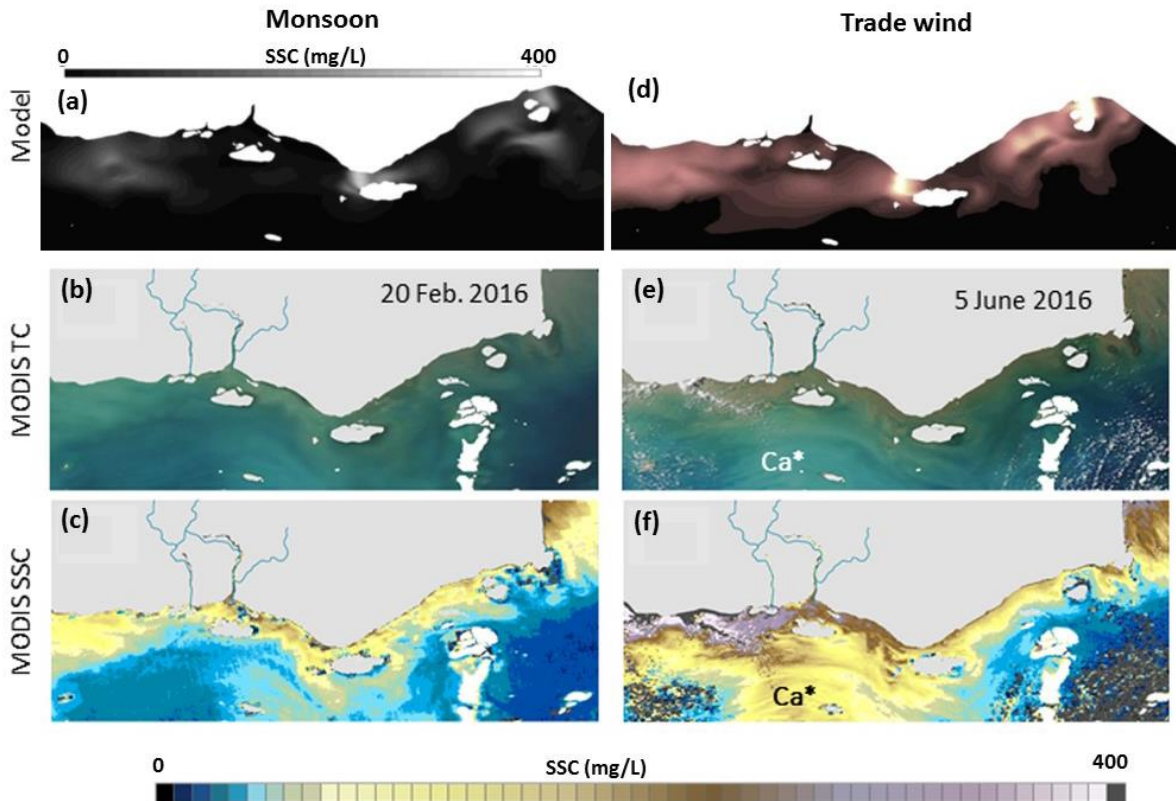
Figure 5–7: A sample from several images comparing the (a, d) model SSC, (b, e) MODIS true colour (Source: NASA Worldview) and (c, f) MODIS SSC data during the SE tradewind season (right) and the monsoon season (left). The MODIS SSC have been estimated using a simple polynomial algorithm using the MODIS band 1 (Petus et al. 2010) and SSC retrieved from the MODIS satellite images have been multiplied by 10 to account for saturation of the MODIS band 1 at high SSC values (i.e. in the range of SSC typically found in the Fly river estuary). They are used to illustrate high/low SSC, but SSC values per se. should be taken with caution. Ca*: calcareous sediment.

Visually, the predicted and observed SSC distribution compared favourably with each other during the SE trade wind season and during the monsoon season (Figure 5–7). These images showed a turbid coastal boundary layer with highest SSC values inshore. However, because of the conversion factor applied and the inability to distinguish between calcareous and terrigenous mud, the MODIS SSC are likely overestimated at distance > 20 km from the PNG coast. Within this coastal boundary layer, the SSC distribution was sometimes patchy, with quite often a patch of high SSC west of Saibai Island and a zone of relatively lower SSC present half way between Saibai and Daru Islands. Such patterns were observed in both the model outputs and the MODIS images and the width of the turbid coastal boundary in the satellite images was similar to the predicted one. Occasionally a patch of high SSC was found in both observations and predictions to the SE of Saibai Island and reaching the Warrior Reefs, often during the monsoon season. Both the model outputs and the MODIS images showed that the width of the turbid coastal boundary layer (a) is the largest in the western part of the northern Torres Strait during the SE trade wind season, and (b) it is the largest in the eastern parts of the northern Torres Strait during the monsoon season, in agreement with the earlier results of Waterhouse et al. (2018). While these preliminary match-ups are encouraging, moored nephelometer data would be needed to obtain time-series of SSC data and verify the model as was done for the Fly River estuary by Wolanski et al. (1995a). The remoteness of the study areas, however, limits the ability to easily collect such field data and there is thus some uncertainty here. In the absence of adequate field data, the mud transport parameters were

chosen to be those of the Fly River estuary mud. This assumption is expected to be reasonable, as it is likely that it is the same mud and, thus, that the mud physical properties are the same in the estuary and in the far northern Torres Strait. Further investigation of the contributions of smaller PNG mainland rivers to the coastal turbidity would also be warranted.

5.4 Conclusions

The study reinforced that there is a turbid coastal boundary layer along the PNG coast of the Torres Strait with maximum turbidity found inshore and decreasing seaward. The turbid coastal boundary layer is patchy due to the existence of a persistent mud wedge along the PNG coast which is resuspended by tidal currents, wind and waves, especially during strong wind events. The model demonstrated that polluted new mud intrudes Torres Strait from the Fly River discharge and is diluted by the non-polluted mud of the mud wedge. Daru and Bristow Islands, located close to the PNG coast, form a hydrodynamic barrier that restricts the circulation pattern and slows down the intrusion of Fly River contaminated material further west into the Torres Strait. The time scales for the pollution spread in Torres Strait are probably of the order of 100 years.

The model appears to produce realistic results for the SSC distribution and also for the SSC fluxes. For the latter, the prediction that about 9% of the Fly River mud flux enters the Torres Strait through the Southern Channel of the Fly River estuary, the closest channel to Torres Strait, is consistent with the estimate of 11% of previous studies (Harris et al. 2004). The model predictions must be seen as qualitative in the absence of field data of mud dynamics in Torres Strait; however there is some confidence in the results as long as the main assumption – that the physical properties of erosion and settling of the mud in Torres Strait are the same as those in the Fly River estuary – is valid.

The results of the modelling need to be refined and validated through ongoing modelling and assessment. In particular, future work should focus on collecting *in-situ* SSC measurements across turbidity gradients and moored nephelometer data to further verify the mud model and the results described above. These data would help to improve the accuracy of the satellite SSC retrieval in the higher SSC range, and would allow development of more complex satellite retrieval models. Acquisition of field SSC measurements will be fundamental to progress understanding of mud dynamic in the study area. Despite these limitations and the complexity of this remote study area, this study is probably the first attempt in the world at modelling the dynamics of a polluted mud plume in open coastal waters.

6.0 REMOTE SENSING ANALYSIS

6.1 Previous findings

NESP TWQ Hub Project 2.2.1 involved acquisition and analysis of daily true-colour satellite data to identify instances of likely Fly River plume intrusion, linking to coincident oceanographic and meteorological conditions to refine modelling (Petus et al. 2018; Waterhouse et al. 2018).

- The study used medium resolution satellite data to: (i) provide a large-scale baseline of the composition of coastal waters around the Gulf of Papua–Torres Strait region, (ii) investigate the spatial and temporal variability of the Fly River turbid plume, and (iii) identify instances and areas with likely plume intrusion into the Torres Strait Protected Zone.

- Nine years of daily MODIS true colour data (2008–2016) were processed using a semi-automated colour classification method developed for the GBR. This method classifies the coastal waters into six different colour classes (CCs). It is particularly useful in remote areas where *in-situ* water quality data are scarce or unavailable, such as the Gulf of Papua–Torres Strait region, as it relies only on the apparent colour of the seawater.

- The brownish to brownish-green Colour Classes (CC1–4) represent very turbid, sediment dominated waters with high coloured dissolved organic matter (CDOM) concentrations and are classified as 'Primary' waters; the greenish to greenish-blue CC (5) represents turbid waters with dominant to moderate concentrations of Chlorophyll-a (Chl-a, phytoplankton algae) and finer sediments and are classified as 'Secondary' waters; and the blueish-green CC (6) represents waters with slightly elevated ambient turbidity and Chl-a concentrations and are classified as 'Tertiary' waters.

Long-term water quality conditions in the study area
- In the estuarine area of the Fly River, brownish-green (Primary) waters were mapped inside the Fly River delta (< 5 m depth) with the most brownish, turbid waters located inside the very shallow delta plains. This suggested that a large proportion of sediment is generally retained in the Fly River estuary through flocculation, in agreement with previous studies.

- The study showed the regular intrusion of greenish-blue (Secondary) waters from the Gulf of Papua in the NE corner of the Torres Strait Protected Zone (including Daru), the north of Warrior Reefs and north and south of Sabai Island. The presence of these turbid waters is likely the result of the complex physico-chemical transformation occurring across the Fly River plume, local resuspension of sediments and the water circulation in this area.

- Brownish-green (Primary) and greenish-blue (Secondary) waters were also mapped around Boigu Island. The presence of these turbid waters is likely the result of the local resuspension of sediments and the water circulation in this area, as well as sediments discharged by the Wassi Kussa and Mai Kussa Rivers and potentially transported from the Fly River.

Annual and seasonal dynamics in the Southwest Fly District

- The Southwest Fly District was defined in this study as the area extending from the central Fly River mouth and as far west and south as the northern Warrior Reef. The spatial extent of the Primary and Secondary waters in this area varied seasonally and larger turbid areas (km^2) were mapped during the SE trade wind season.

- The spatial extent of Primary waters was also correlated with ENSO events and smaller areas (km^2) were mapped during El Niño years. El Niño creates a large negative perturbation (i.e. low flow) to the relatively constant sediment discharge and limits the transport of sediment from the tributaries to the nearshore zone.

6.2 Additional work: Scope and methods

6.2.1 Purpose

To extend the 10-year dataset of satellite remote sensing data of plume movement, turbidity and frequency of the exposure of turbid waters in the northern Torres Strait. This enables analysis of regional multi-annual patterns, and assessment of variability. The assessment included further investigation of several areas identified as priorities in the previous study, including the Wassi Kussa and Mai Kussa rivers contributions and observations for the Warrior Reefs and Bramble Cay. Analysis of the remote sensing data with other data sources including the salinity measurements (Section 3.0), logger data (Section 0), new sediment modelling (Section 0) and *in-situ* metals data (Section 7.0) enhances the value of this dataset. The detailed results of this component are reported separately in Petus et al. (manuscript in preparation).

6.2.2 Methods

Satellite datasets and monitoring products

A combination of freely available satellite datasets were downloaded and analysed using ARCGIS 10.6 (Figure 6–1 and Table 6–1). Daily MODIS-Aqua (MA) true colour images of the Gulf of Papua-Torres Strait region were downloaded from the EOSDIS website from mid-2018 to mid-2019 and added to the existing multi-year satellite databases of the study area (2008 - 2018) (Figure 6–1). Sentinel-3 (S3) Ocean and Land Colour Instrument (OLCI) Level-2 datasets of the study area (2019) were downloaded on the EUMETSAT Copernicus Online Data website.
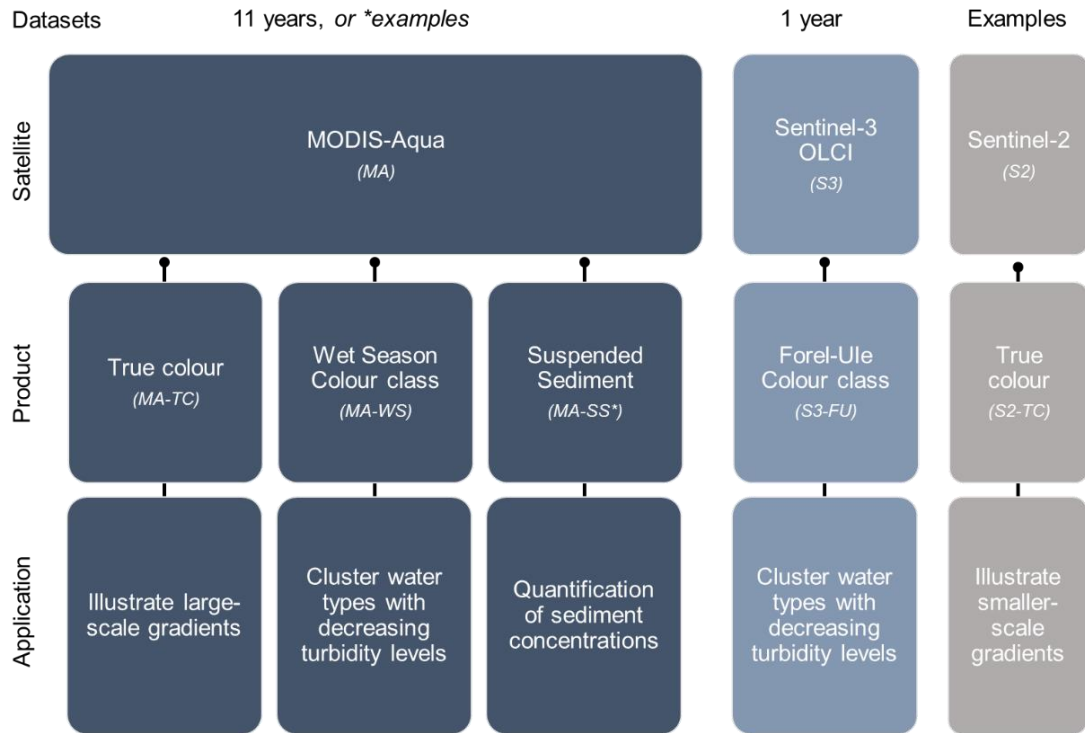
Figure 6–1: Satellite images and products used in this study. Satellites: MA - MODIS-Aqua data, available since 2002; S3 - Sentinel 3 OLCI, available since 2016; S2 - Sentinel-2 data available since 2015. Products: MA-TC - MODIS-Aqua true colour images (250 m resolution), MA-WS: MODIS-Aqua wet season colour scale maps (500-m resolution); MA-SSC: MODIS-Aqua Suspended sediment concentration maps (250 m resolution); S3-FU - S3 Forel Ule colour scale maps (330-m resolution); S2-TC: S2 true colour images (10-m resolution).

Table 6–1: Satellite products used to describe turbid waters and habitat exposure in the Gulf of Papua-Torres Strait region.

Product	Objective	Time scales	Production
a) composite Colour class map	Illustrate large scale trends in turbidity levels at different time scales	(ii) Decadal (2009 – 2018), (iii) Decadal seasonal and decadal monthly	Decadal median maps are produced by calculating the median long-term colour class category value for each pixel of our study area using (i) all daily MA-WS data using data from 2009 to 2018, or using data collected in the (ii) monsoon and trade wind seasons or (iv) in each month of the 2009 – 2018 period
b) Frequency maps	Evaluate the long-term and annual frequency of exposure of Torres Strait coral reefs and seagrass habitats to Primary, secondary and Tertiary water types	Annual and decadal average	The annual water type frequency was defined as the total number of days per year exposed to a given water type divided by the number of data days (non-cloud) recorded per year, resulting in a normalised frequency on a scale from 0 to 1. Decadal average were calculated as the average of all annual maps.

c) Difference maps	Illustrate areas with an increase (positive anomaly) or decrease (negative anomaly) in turbidity: (i) in the trade wind season against the monsoonal trends; or (ii) in each month against long-term trends	(i) Decadal seasonal or (ii) Decadal monthly	(i) The seasonal difference map is calculated by subtracting the median decadal monsoonal and the median decadal trade wind maps. (ii) The monthly difference maps are calculated by subtracting the mean decadal monthly median maps and the decadal median map.

Daily coastal water types within the Torres Strait region were mapped using the MODIS Aqua (mid 2018–mid 2019) and Sentinel 3 data (2019) processed using two respective colour classification scales; the wet season (described in detail in Waterhouse et al. 2018) and Forel-Ule (Ule) colour scales (Petus et al. 2019 and in prep). Both colour classification scales are implemented into automated toolboxes developed originally for the Reef 2050 Marine Monitoring Program (see for example, Gruber et al. 2020) and that have been adapted for the study area through this and the previous NESP TWQ Hub Projects (2.2.1 and 5.14). These toolboxes allow the classification of large areas and multi-year datasets.

In the FU colour scale, 21 water types (FU1-21) are defined by their colour properties across a Hue gradient (e.g., Van der Woerd and Wernand 2015, 2018). A first comparative study in the GBR suggested that FU4-5, FU6-9 and FU ≥ 10 were similar to the Tertiary, Secondary and Primary water types in the wet season colour scale, respectively (Table 2, Petus et al. 2019). Methods used to produce the Sentinel 2-FU maps are described in further detail in Petus et al. (in prep) (Supplementary Material A).

A selection of daily MODIS-Aqua Surface Reflectance band 1 product (MYD09GQ, 250 m resolution) was downloaded from the AppEEARS website between January 2016 and March 2017. This MODIS dataset was used to map total suspended sediment concentration (SSC, in mg.L^{-1}) in the Gulf of Papua-Torres Strait region. Clouds were masked and SSC concentrations were mapped using the empirical bio-optical algorithm of Petus et al. (2010). This algorithm has been successfully used to map SSC concentrations in French turbid plume waters (Petus et al. 2010, 2014), showed good results in Australia (Queensland, Port Curtis) and is currently used to estimate total suspended matter in the Environmental Modelling Suite for the GBR (Baird et al. 2017, 2020a, b). The SSC maps are preliminary results and there is a high uncertainty in the satellite SSC concentrations at this stage, more specifically for the higher range of SSC concentrations as this bio-optical algorithm was not developed specifically for the study area. Field data are needed to validate the satellite retrievals and progress this work (see preliminary comparisons below). Preliminary SSC maps were nevertheless compared (qualitative comparison) with outputs from the model and results of this comparison are presented in Wolanski et al. (2021) and in Section 5.3 of this report.

MODIS-Aqua wet season composite maps produced as part of the previous NESP study (Waterhouse et al. 2018), including median (Table 6–1a) and frequency (Table 6–1b) maps, were updated[4] with the new MODIS-Aqua wet season maps to produce decadal (2009-2018) maps of colour and turbidity gradients in the study area. Mean decadal frequency of exposure

---

[4] *Data from 2 Feb. 2011 to 8 May 2012 were previously missing from the NASA websites due to a hardware failure of a NASA disk array that contained the MODIS images and have now been included in the analyses.*

to the Primary, Secondary and Tertiary water types were extracted at a selection of coral reef and seagrass habitats in the northern Torres Strait and the updated results were used to describe the frequency of exposure of local ecosystems to turbid waters. These results are presented in Petus et al. (in prep.) and briefly described below.

Difference maps were processed and used to illustrate areas with an increase (positive anomaly) or decrease (negative anomaly) in turbidity: (i) in the trade wind season against the monsoonal trends; or (ii) in each month against long-term trends (Table 6–1c). Finally, a selection of Sentinel-2 high resolution true colour images were presented and used to illustrate sediment transport at a finer scale. Observations were discussed against recent modelling results from Wolanski et al. (2021) and other recent studies (Waterhouse et al. 2018, 2019).

Verification of the MODIS datasets

Verification of the products was necessary prior to further analysis of the processed satellite products. In order to verify the MODIS maps, a selection of MODIS-Aqua wet season colour class maps was compared with Sentinel-3 Forel-Ule colour class maps. To support this comparison, field water quality (SSC, Secchi Disk Depth and FU ocean colour datasets were collected in November 2020 around Saibai Island as part of a field campaign aiming to collect water, sediment and seagrass for trace metal analyses (Section 7.0). Field FU colour class were measured with the Eye on the Water phone application (Petus et al. in prep., Supplementary Material A) and were matched-up to the SSC and Secchi Disk Depth data to test the assumption that SSC and turbidity levels decrease with the FU colour class categories.

Boat-based SSC measurements collected in October 2016, June 2018, December 2019 and November 2020 (Apte et al. 2018 and Section 7.0) were matched up, when possible (pending on cloud cover), with the MODIS-Aqua-SSC and MODIS-Aqua maps to further verify the satellite data. Salinity and SSC field data collected between 2016 and 2020 were further analysed in salinity-SSC plots. Continuous measurements of temperature, salinity and turbidity were collected from a mooring station at Warrior Reef between February and October 2020 (Section 0). Monthly average temperature, salinity and turbidity values were calculated and visualised in salinity-temperature and salinity-turbidity plots. These results were interpreted against seasonal patterns retrieved from the MODIS-Aqua wet season maps.

6.3 New results

6.3.1 Verification of the MA-WS and MA-SSC maps

The Sentinel water type maps (S3-FU) showed patterns very similar to the MODIS water type maps (Figure 6–2).
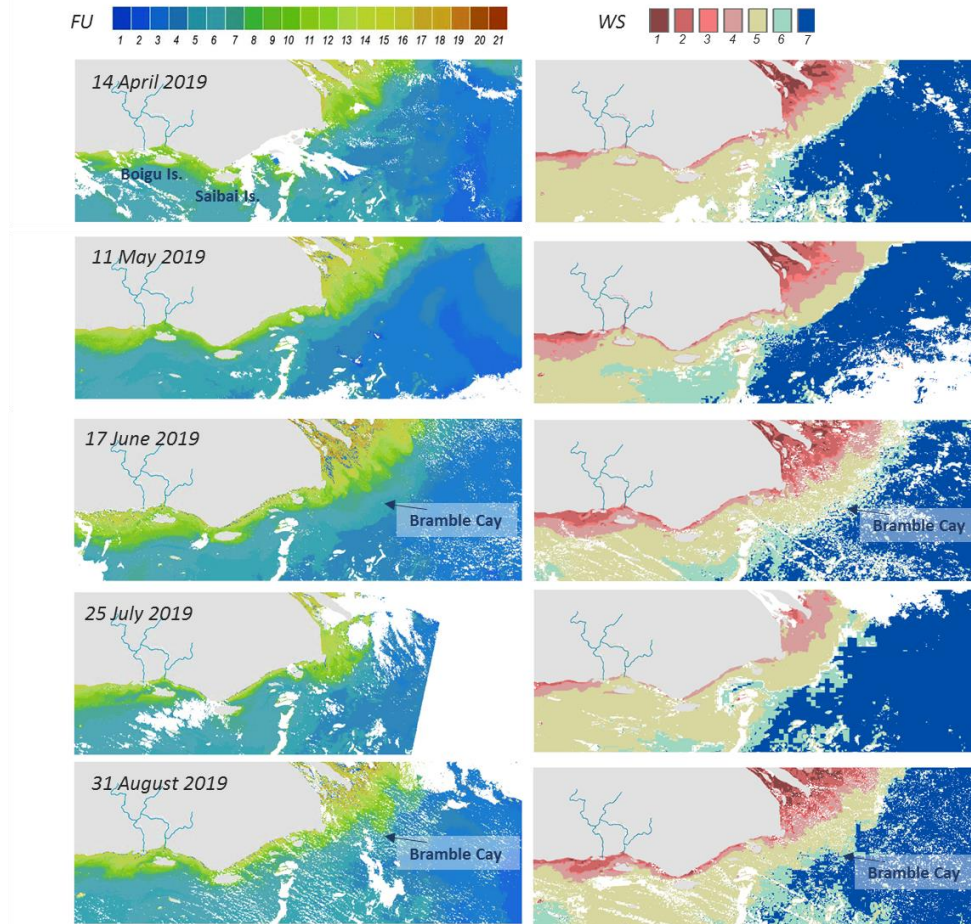
Figure 6–2: Example MA-WS (left) and S3-FU (right) maps showing the Fly River plume, and southern PNG coastal waters.

MODIS Primary water type corresponded to higher colour class categories in the FU scale (> 8 to 10 FU). Large river plumes off the Fly River estuary, and smaller plumes off the Wassi Kussa and Mai Kussa rivers were well captured and showed the same shapes, spatial areas and orientation in all example images. During the trade wind season both satellites captured intermittent influence of the Fly River plume on Bramble Cay, the most north-eastern island of Australia located 55 kilometres SE of the mouth of the Fly River (Figure 6–2: 17 June and 31 August 2019).

This study assumed that SSC and turbidity levels decreased from the Primary to Tertiary waters types, as observed in the GBR (e.g., Alvarez-Romero et al. 2013; Devlin et al. 2015; Petus et al. 2019). The spatial agreement observed between the S3-FU and MODIS-Aqua wet season composites provided confidence in this assumption as water turbidity has been shown to increase with FU in global oceanic waters (measured as decreased Secchi Disk Depths and increased diffuse attenuation coefficient; Pitarch et al. 2019). It was further validated by the

field data collected around Saibai Island in November 2020. Indeed, field SSC, Secchi Disc Depth and FU measurements showed the expected trends, i.e. SSC values increasing, and inversely, and Secchi Disc Depth decreasing with the FU number (Figure 6–3).
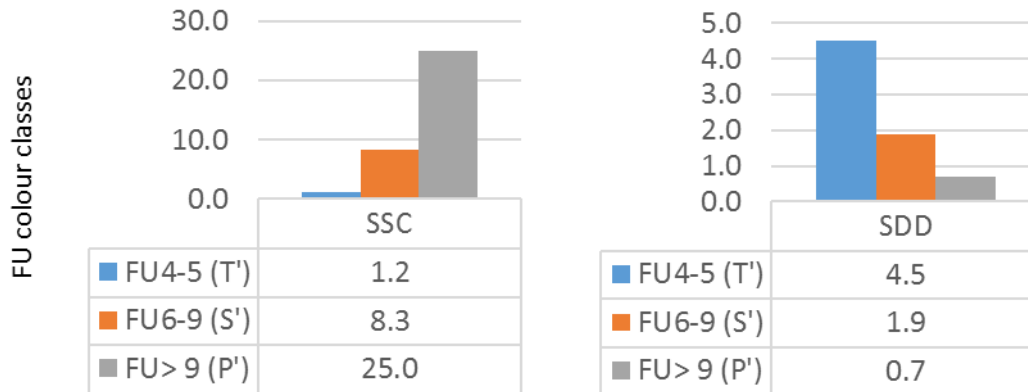
Figure 6–3: Mean SSC and Secchi disk depth (SDD) values collected across FU colour categories. A first comparative study in the GBR suggested that FU4-5, FU6-9 and FU ≥ 10 are similar to the Tertiary (T'), Secondary (S') and Primary (P') water types in the wet season colour scale, respectively (Petus et al. 2019).

The assumption was further supported by the available field datasets and preliminary match-ups with the satellite data. Except for 12 October 2016 (Figure 6–4a), MODIS-Aqua satellite images were largely cloudy between 3 and 16 October and did not allow formally matching-up the field and satellite datasets to validate the MODIS-Aqua-SSC and MODIS-Aqua-wet season maps. Field SSC data collected in October, however, agreed with the range and trends in SSC concentrations derived from the cloud-free MODIS-Aqua -SSC map of 12 October 2016 (Figure 6–4b). The SSC ranged from 0.6 to 12.0 mg/L in the field and from 0.5 to 17 mg/L in the satellite map at the different sites, and both datasets showed decreasing SSC trends with greater distance south. The higher field SSC concentrations (site A and 8, > 10 mg/L) were measured in the Secondary water type (Figure 6–4c). MODIS-Aqua satellite images were also largely cloudy between the 28 October and 2 November 2020 and did not allow formally matching-up the field and satellite datasets. Field SSC data collected in October, however, agreed with the range and trends in SSC concentrations derived from the relatively less cloudy MODIS SSC map of the 30 and 31 October 2020 (Figure 6–5). Calcareous sediments south of Boigu were however likely overestimated in the SSC map of 31 October 2020.

A similar range of concentrations (SSC < 30 mg/L) were measured from 18 to 21 June 2018 (Section 0) and in the past (Wolanski et al. 1995a, east of Warrior Reef); but unfortunately the MODIS-Aqua images were cloud obstructed or not available for these dates. This, however, suggested that the empirical SSC algorithm is likely to estimate the right order of magnitudes for the moderate to low SSC ranges (Secondary and Tertiary water types). Unfortunately, no field data were collected in colour/turbidity gradients off the Fly River estuary mouth due to logistical constraints.
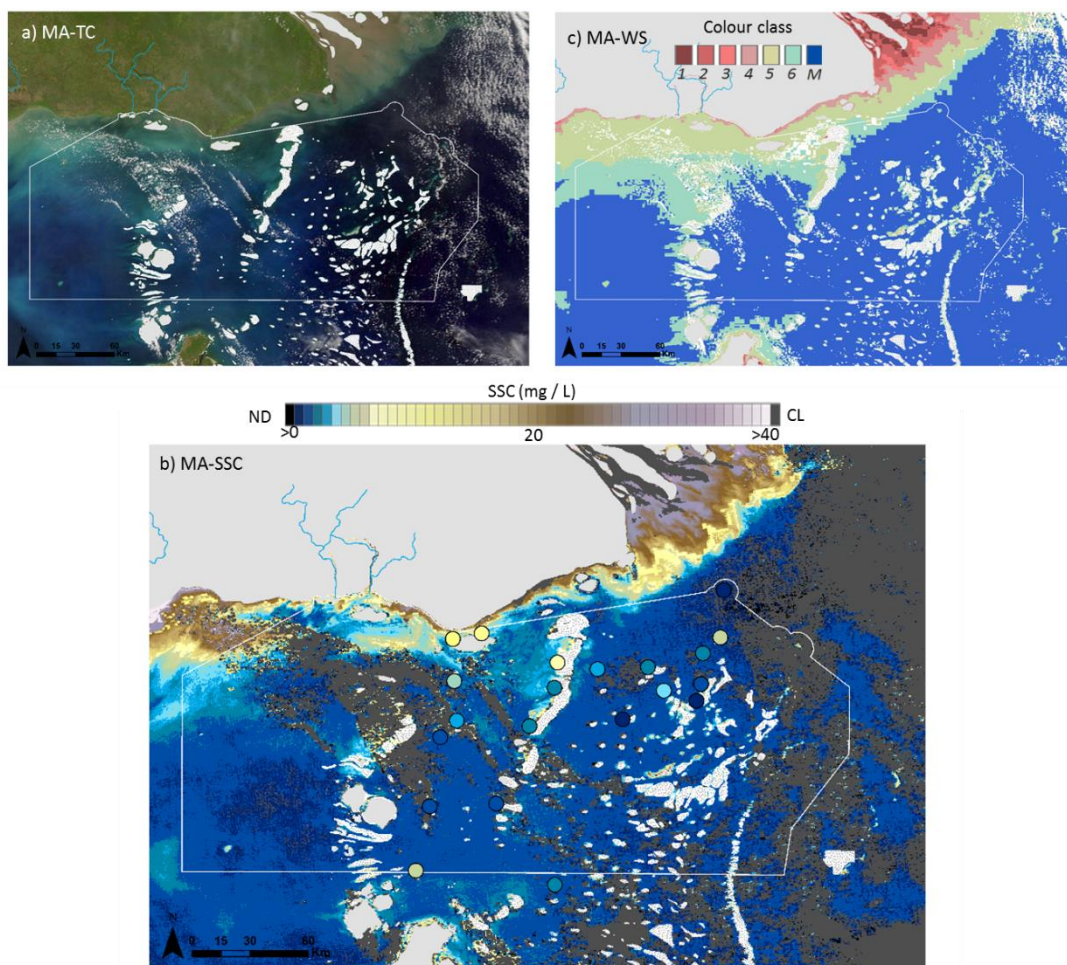
Figure 6–4: MODIS-Aqua images of 12 October 2016:a) True colour (MA-TC), b) Suspended sediment concentrations (MA-SSC) in mg/L c) wet season colour class (MA-WS) maps. SSC field data collected from 3 to 16 October 2016 at 21 sites across the Torres Strait Protected Zone are overlayed with dots onto the MODIS SSC map and coloured using the same SSC colour scale (Apte et al. 2018). In the MA-SSC map, dark grey areas represent clouds, and black areas no data.
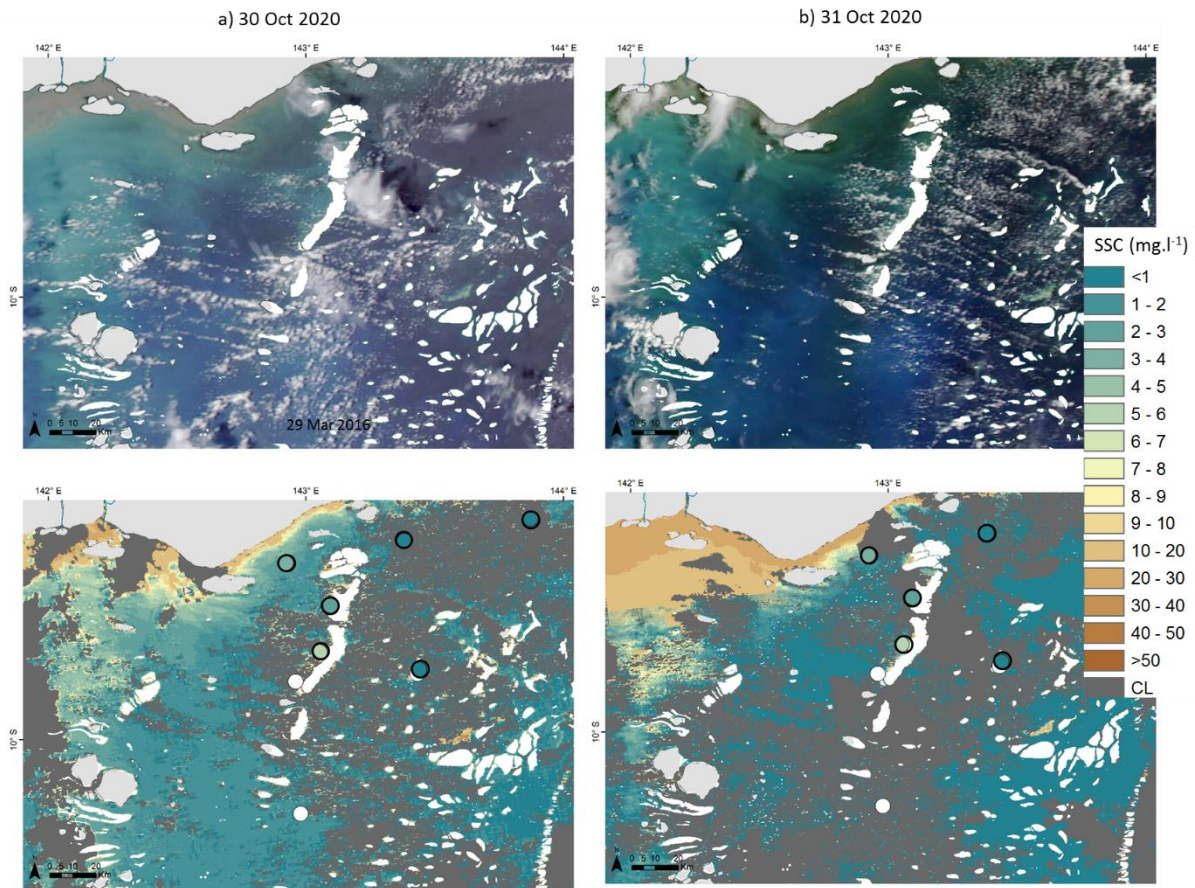
Figure 6–5: MODIS-Aqua images of 30 October 2020:a) True colour (MA-TC), b) Suspended sediment concentrations (MA-SSC) in mg/L c) wet season colour class (MA-WS) maps. SSC field data collected from 3 to 16 October 2020 at sites across the Torres Strait Protected Zone are overlayed with dots onto the MODIS SSC map and coloured using the same SSC colour scale (Apte et al. 2018). In the MA-SSC map, dark grey areas represent clouds, and black areas no data.

6.3.2 Decadal patterns in water composition

The updated median decadal MODIS-Aqua-wet season map (Figure 6–6) and decadal frequency maps (Figure 6–7) showed colour and turbidity trends similar to those described in Waterhouse et al. (2018). Maps and analyses are presented in detail in Petus et al. (in prep) and are summarised below:

- Most turbid water masses were mapped off small local streams and inside and off the Fly River delta. The Wassi Kussa and Mai Kussa Rivers were also important contributors to the turbidity levels in the northern Torres Strait, particularly around Boigu Island.

- The waters in the NE corner of the Torres Strait Protected Area including Daru Island, the north of Warrior Reefs, and Saibai Island, were classified as Secondary water type in the decadal colour class analyses, which indicated a regular occurrence of moderately turbid waters in this area. The source cannot, however, be fully attributed to the Fly River and is likely to include other sources of sediments associated with the smaller streams as well as resuspension of sediment deposited in the Torres Strait mud wedge via currents, wind and wave action (Ayukai and Wolanski 1997; Harris et al. 2004; Heap et al. 2005; Waterhouse et al. 2018). The greatest frequency of exposure to Primary and Secondary waters was measured at Saibai and Boigu Islands (> 10% and >80 % of the time, respectively).
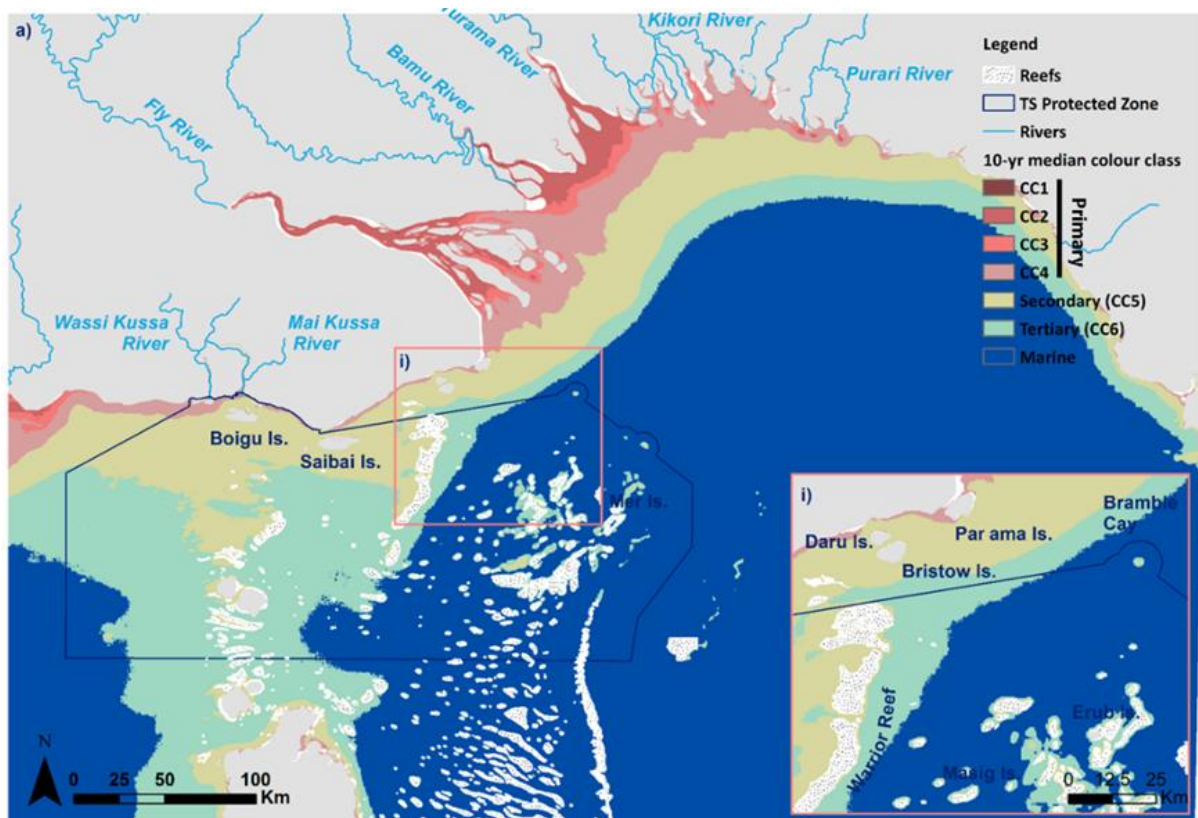
Figure 6–6: Decadal median (2009–2018) colour class map illustrating long-term trends in turbidity levels in the study area.

- In the middle of the Torres Strait, between the south of Boigu Island and Cape York, suspended calcareous sediments originating from Torres Strait reefs and carbonate platforms (e.g., Harris 1988) were largely classified as the Tertiary water type. These calcareous sediments were stirred by currents and flowed through the Warrior Reef. They sometimes mixed with the terrigenous sediments originating from the Fly River and/or resuspended from the Torres Strait mud wedge; complicating the optical and colour signature of coastal waters around Boigu, Saibai and the northern Warrior Reef (for example Figure 6–12b). On the Eastern side, the Ugar, Masig and Poruma Island sites were predominantly exposed to Tertiary waters (CC6, ≥ 50% of the time).

- Bramble Cay was exposed 26%, 38% and 34% of the time to Secondary, Tertiary and marine waters, respectively. While waters around Bramble Cay were largely classified as Tertiary or marine waters; several satellite images showed the Fly River plume reaching the Cay (Figure 6–11 and Figure 6–12d), and this seemed to be enhanced by trade wind environmental conditions (see section below: Figure 6–8 and Figure 6-9. Luminescent lines have been previously observed in corals from Bramble Cay back to 1781 (Lough 2016), which along with older observations (Wolanski et al. 2013a, 2013b) confirmed a plume influence at this site.
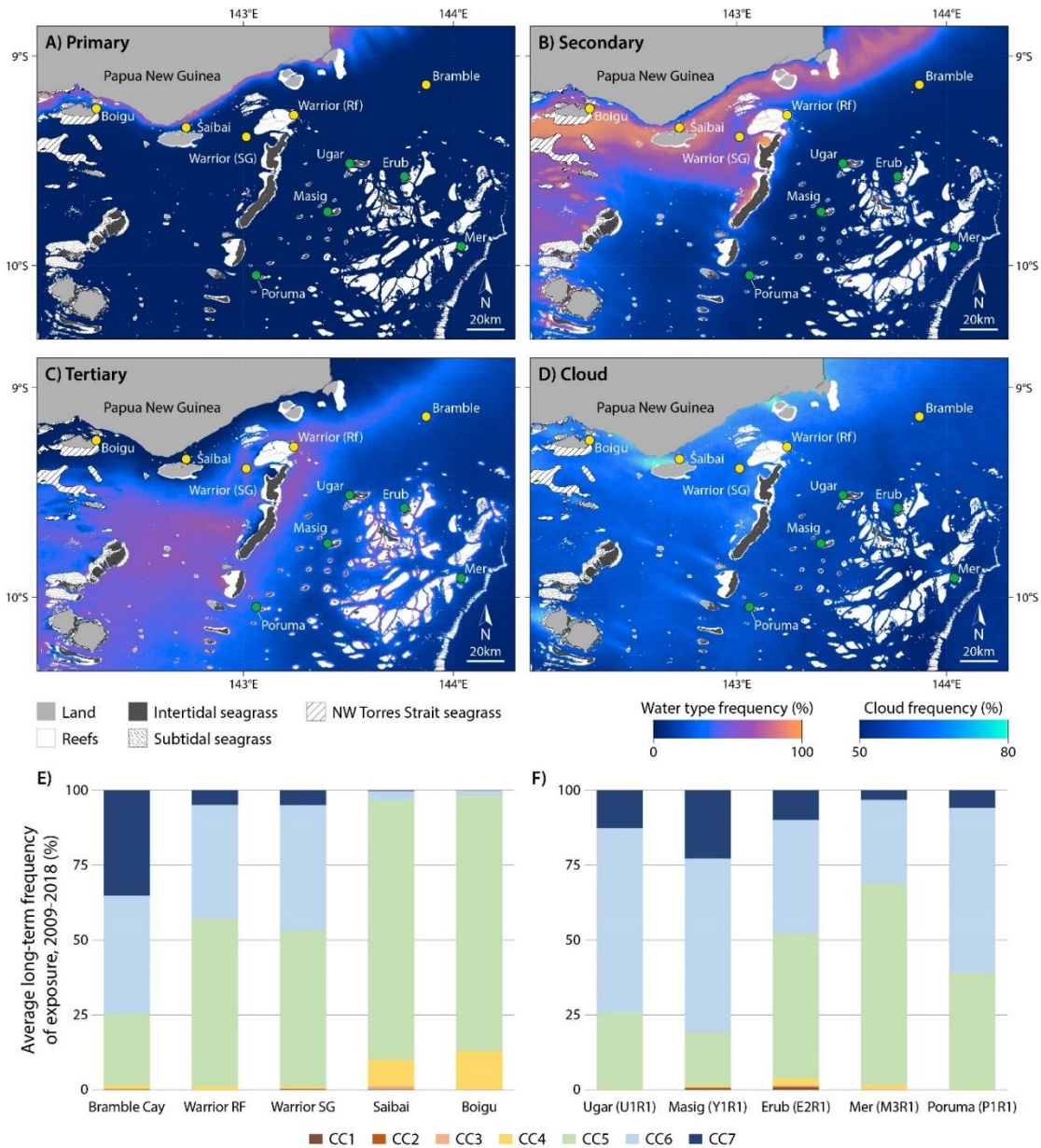
Figure 6–7: Maps showing the decadal (2009–2018) normalised frequency (0-100%) of water types and cloud frequency. a) Primary water type (CC1–4), b) Secondary water type (CC5) and c) Tertiary water type (CC6), where the highest frequency is shown in orange and the lowest frequency is shown in dark blue. d) Cloud frequency occurrence where the highest frequency is shown in light blue and the lowest frequency is shown in dark blue. Bottom plots show the long-term frequency (% of exposure) extracted at a selection of coral reef and seagrass monitoring sites in the Torres Strait: e) northern sites (yellow dots), f) southern sites (green dot points). Datasets from GBRMPA, Carter et al. (2014), Hayward et al. (2008) and Carter and Rasheed (2016).

6.3.3 Seasonal patterns

The decadal seasonal difference map supported previous findings (e.g., Waterhouse et al. 2018) and showed the Fly River influence in the Torres Strait region is largely limited to the NE corner of the Torres Strait and is greater during the SE trade wind season than during the monsoon season (Figure 6–8). Indeed, higher relative turbidity levels were measured in the trade wind season than during the monsoon season between Daru Island and Bramble Cay and along the southern PNG coast between Panama and Saibai Island (the band of higher turbidity was patchy and restricted close to the coast). Higher relative turbidity levels were also

measured west of Boigu Island in a large band along the southern PNG coast originating at the Mai Kussa and Wassi Kussa rivers. Inversely, the central Torres Strait was globally less turbid during the trade wind than during the monsoon season in the decadal satellite database. Median decadal changes between the monsoons and trade wind were often of one colour class category (see ΔCC in Figure 6–8); but the significance in terms of change in turbidity or SSC concentration is unknown.
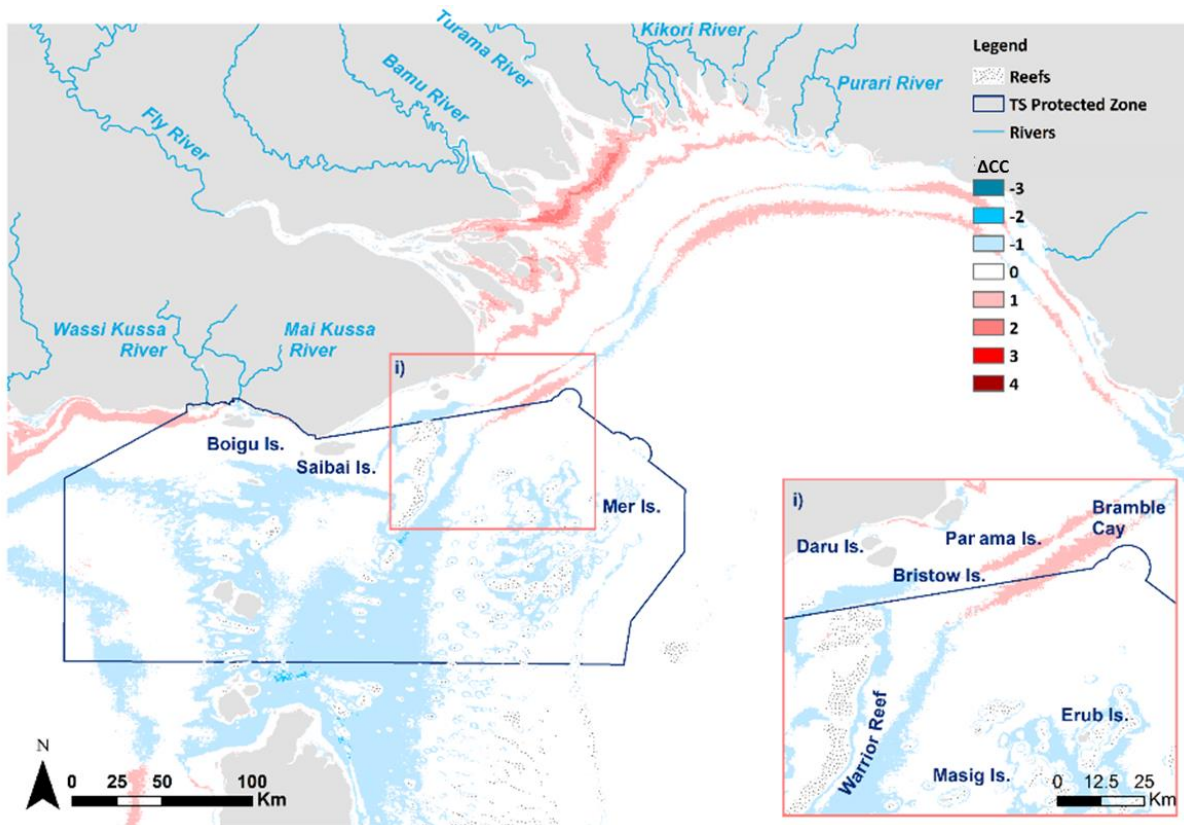
Figure 6–8: Decadal seasonal difference map illustrating areas with an increase (red) or decrease (blue) in turbidity in the trade wind season against the monsoonal trends. Reddish colours show areas with higher turbidity levels, bluish colour areas with lower turbidity levels. The seasonal difference map is calculated by subtracting the decadal median SE trade wind map to the decadal median monsoonal map.

Positive turbidity anomalies in Figure 6-9 illustrated, for each month, areas with greater turbidity (lower colour class) categories relative to the median decadal values. During the trade wind season, positive turbidity anomalies were mapped in the NE corner of the Torres Strait Protected Zone with the largest positive areas mapped between June and September (Figure 6-9c and Petus et al. in prep., Supplementary Material C).
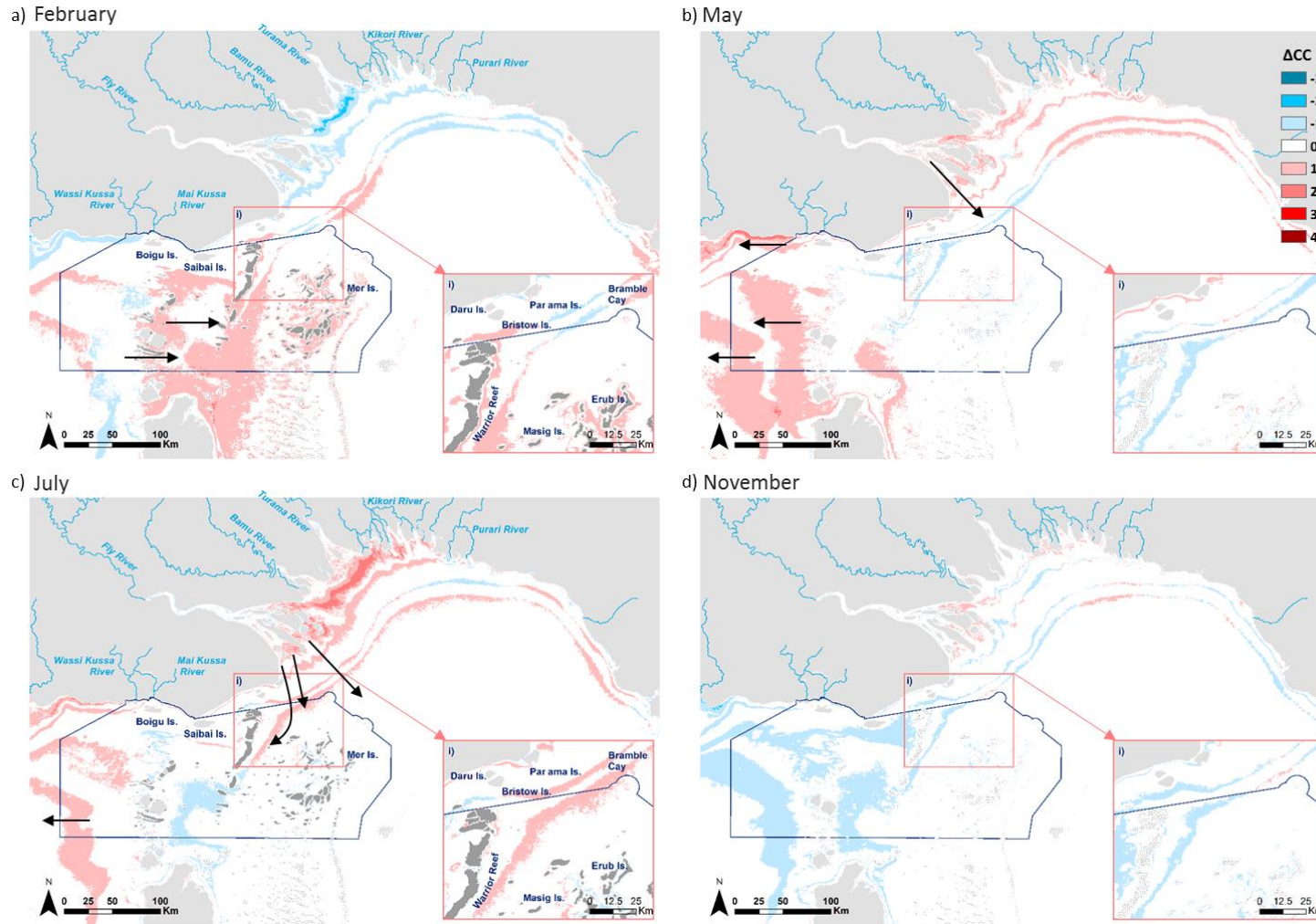
Figure 6–9: Selection of decadal monthly difference maps illustrating areas with an increase (positive turbidity anomaly) or decrease (negative turbidity anomaly) in turbidity in each months relative to long-term trends: a) February, b) May, c) July and d) November. Reddish colours show areas with higher turbidity levels, blueish colour areas with lower turbidity levels against the long-term trends. The monthly difference maps are calculated by subtracting the decadal median map (Figure 6–6) from the decadal median monthly maps (Table 6–1). Black arrows indicate tentative water circulation orientation inferred from the water type movements

This observation was supported by the mean monthly mooring data collected at Warrior Reef (Figure 6–10a). These datasets indicated an increase in turbidity and a decrease in salinity (typical of a turbid plume influence), as well as lower temperature and salinity from around May to September (Figure 6–10b). Maximum turbidity and lower temperature and salinity were measured in August, then July (Figure 6–10a and Figure 6–10b). Despite the increase in turbidity and decrease in salinity observed during the trade wind months, turbidity levels stayed relatively low (see Section 4 and Figure 6–10). The patterns of salinity could not be explained by localised rainfall or run-off (Section 3.3) and may indicate the influence of diluted plume waters.
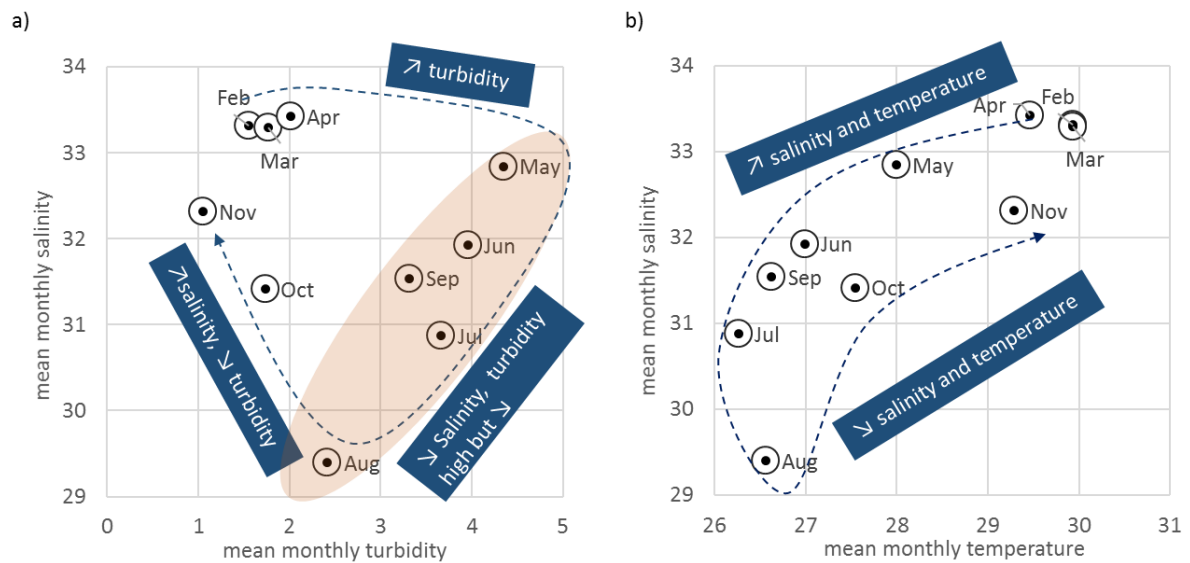
Figure 6–10: (a) Salinity-turbidity and (b) salinity-temperature plots using mean monthly data mooring collected at Warrior Reef in 2020. The red area highlights months with increased turbidity and decreased salinity levels (typical of a turbid plume influence).

The contribution of the Wassi Kussa and Mai Kussa Rivers also varied seasonally and is expected to peak around May to August (Figure 6-9c). In the middle of Torres Strait, positive turbidity anomalies were measured east of the central islands in January and February (Figure 6-9a), in the middle of the Torres Strait in May and April (Figure 6-9b) and then west of the central Islands in April to August (Figure 6-9c). Currents in the Torres Strait have been observed to reverse seasonally, with flow being predominantly westwards during the SE trade wind season (negative mean sea level) and eastwards during the NW monsoon (positive mean sea level, Harris 1994, Li et al. 2017, Wolanski et al. 2013a, 2013b). This is supported by the satellite observations which suggested reversing turbid-water movement in the middle of the Torres Strait across seasons (Figure 6-9, black arrows). The turbidity levels were globally lower during the transition period (November and December, Figure 6-9d).

6.3.4 Further examples

While large spatio-temporal and seasonal trends were well defined by the above analyses, daily MODIS-Aqua true colour and MODIS-Aqua-SSC examples further illustrated the complex sediment transport patterns and high spatio-temporal variability in the study area (Figure 6–11 and Figure 6–12). During the monsoon season the Torres Strait mud wedge was regularly larger and more turbid east than west of Saibai Island (Figure 6–11a and Figure 6–12a) and

suspended calcareous sediments were visible on the true colour images in the middle of the region. As discussed in Section 0, calcareous sediments are distinguishable from the riverine terrigenous sediments by their bright colour, as carbonate sediments are highly reflective in the visible bands, and it is likely that their concentrations was overestimated in the MODIS-Aqua-SSC maps (Figure 6–11 right).
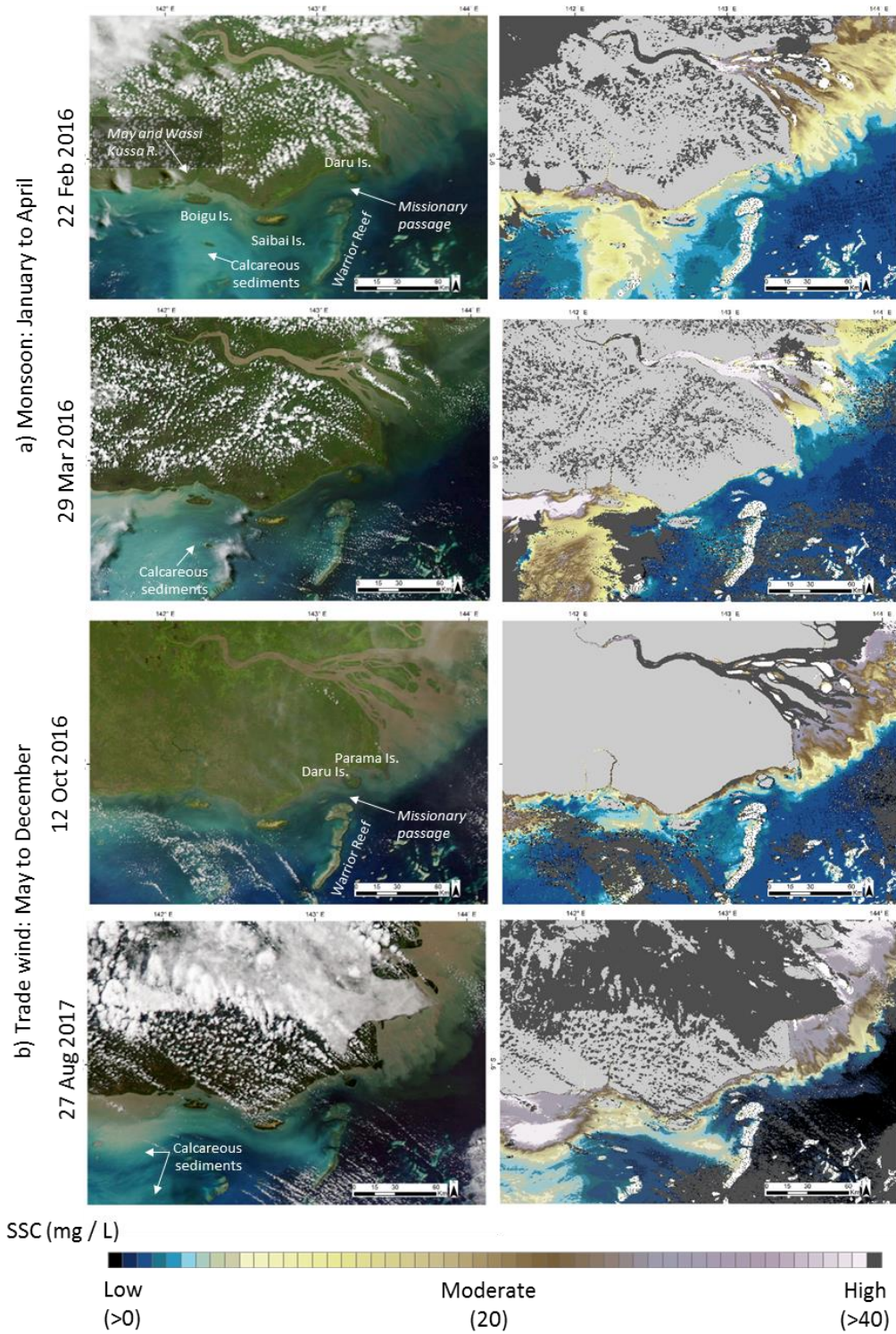
Figure 6–11: Example of (left) MODIS-Aqua true colour and (right) MODIS-Aqua-SSC showing turbid water circulation in the Gulf of Papua-Torres Strait region. Maps are used to illustrate turbidity gradients in the Gulf of Papua-Torres Strait region during the (a) monsoon and (b) trade wind season; however, SSC values *per se.* must be taken with caution and are indicated in bracket.
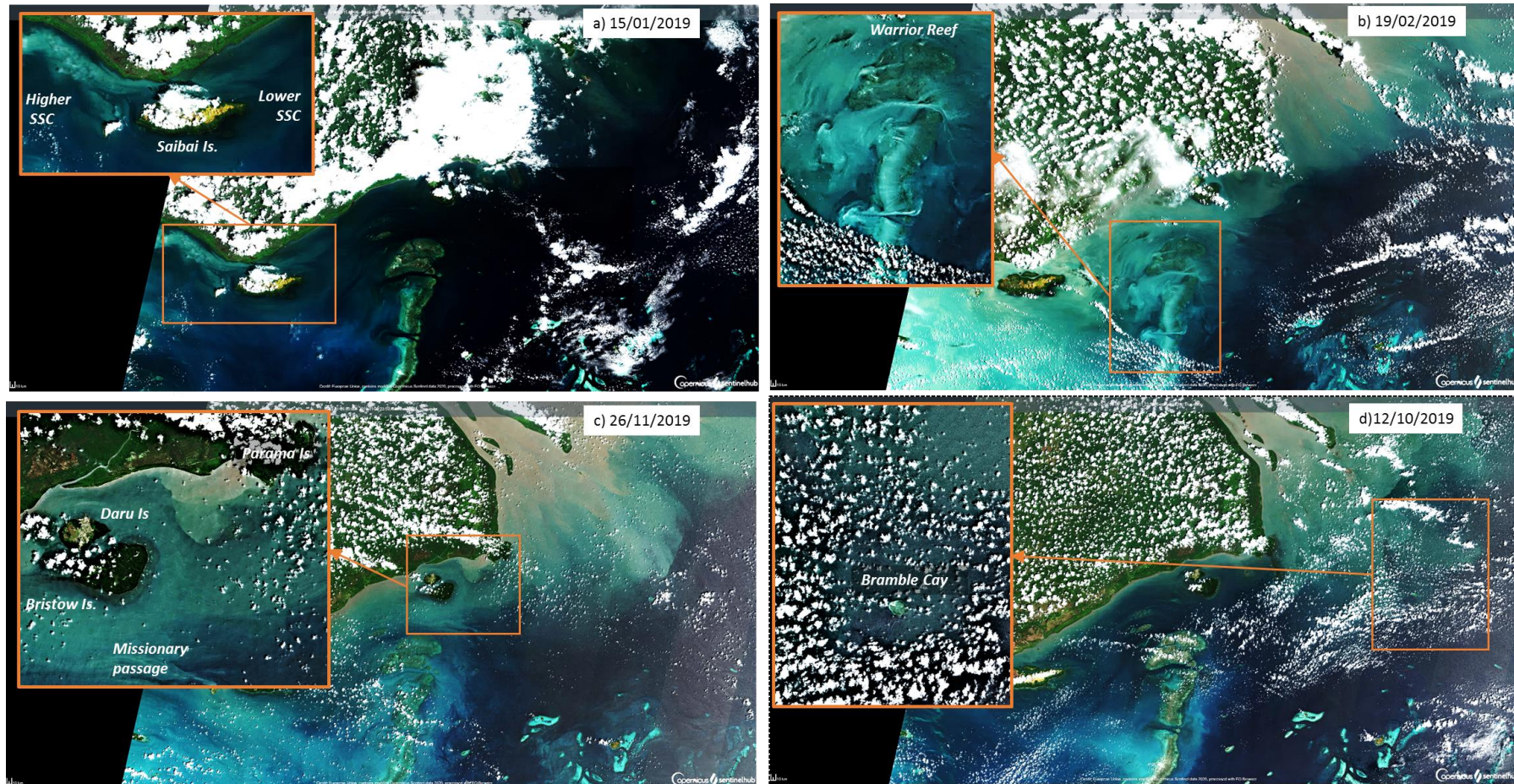
Figure 6–12: High resolution (10-m) Sentinel 2 true colour images captured during the (top) monsoon and (bottom) trade wind seasons illustrating the very complex sediment circulation in the study area. a) Typical monsoonal pattern with no sediment import from the Fly River and higher SSC concentrations west of Saibai Island. Inversely, b) shows high turbid levels all along the PNG coast and in the middle of Torres Strait, and is a great illustration of flow channelisation in passages among the Warrior Reefs. Trade wind image c) illustrates complex sediment transport patterns near the coast and Fly River sediments flowing westward through passages between Parama and Daru Island and the PNG coast and through Missionary Passage. d) shows a large Fly River plume reaching Bramble Cay, 55 kilometres SE of the mouth of the Fly River. Images are from the Sentinel-hub website and have been enhanced by +40% (brightness and contrast). Enlargement are sharpened by 50%.

One notable exception to this 'typical' monsoonal pattern was the Sentinel 2 true colour image retrieved for 19 February 2019 (Figure 6–12b), where very large turbid areas, likely related to wind induced resuspension, were mapped all along the PNG coast and in the middle of Torres Strait. The colour suggested a mixture of terrigenous and carbonate suspended sediments near the coast, while sediment in the middle of the region were most likely to be calcareous. In this image, suspended carbonate sediments were flowing through passages among the Warrior Reefs and were also observed around the eastern reefs (near Ugar, Masig and Erub islands).

During the SE trade wind season, the Torres Strait mud wedge was often larger west of Saibai Island and higher SSC concentrations were observed to the east around Parama, Daru and Bristow Islands and along the coast between Daru and Saibai Island (Figure 6–11b). Waters were still turbid on some images east of Boigu Island, but turbid areas were often smaller between Saibai and Boigu in the SE trade winds than during the monsoon season. These observations were in agreement with model outputs (Wolanski et al. 2021 and Section 0). Near the Fly River estuary, transport of PNG sediment to the Torres Strait was particularly well illustrated by the Sentinel 2 true colour image of 26 November 2019 (Figure 6–12c). In this image, terrigeneous sediments from the Fly River were observed flowing westward through small passages between Parama/Daru Islands and the PNG coast, between Daru Island and Bristow Islands and through Missionary Passage. Figure 6–12d on 12 October 2019 shows an example of when the Fly River plume was large and extended well offshore in the Gulf of Papua, reaching Bramble Cay.

Finally, there was a good spatial match between the 2019-2020 SSC-salinity plots (Figure 6-13c-d) and satellite plumes boundaries (Figure 6-14). The field datasets collected between 2016 and 2020 (Figure 6-13) provided further evidence of the spatial patterns defined above:

In the North-West region:
- The very likely influence of turbid plume waters around Boigu Island was indicated by the low salinity levels (< 32 PSU) and higher SSC (> 10 mg/L). The influence of the Wassi Kussa and Mai Kussa rivers was very likely around Boigu Island, as observed on the MA-TC image of the 10 December 2019 (Figure 6–14a).
- The very likely influence of diluted plume waters around Saibai Islands was measured by the low salinity levels (often under standard ocean values) and moderate turbidity levels (< 10 mg/L). At this site, influence of both the Wassi Kussa and Mai Kussa river plumes and the Fly river plume is possible, as observed on the MA-TC image of the 10 December 2019 (Figure 6–14d) and 31 October 2020 (Figure 6–14b).
- SSC concentrations were in the 0 - 50 mg/L range around Boigu and Saibai (Figure 6-13b and c) i.e., in the range of the MA-SSC maps produced above (Figure 6–4, Figure 6–5 and Figure 6–11).

In the North central region (Warrior Reef) and North east (Bramble Cay):
- The likely influence of diluted Fly River plume waters at both sites as illustrated, for example by the October 2020 field and satellite data (Figure 6-13c and Figure 6–14b).
- At the Warrior Reef less saline but slightly more turbid waters where also measured in Dec 2020 (yellow dots, Figure 6–14d). This may also indicate presence of other turbidity sources, for example due to the transport of calcareous sediments (see bright sediments left of warrior on S2-TC image of Dec 2019 and Oct 2020).
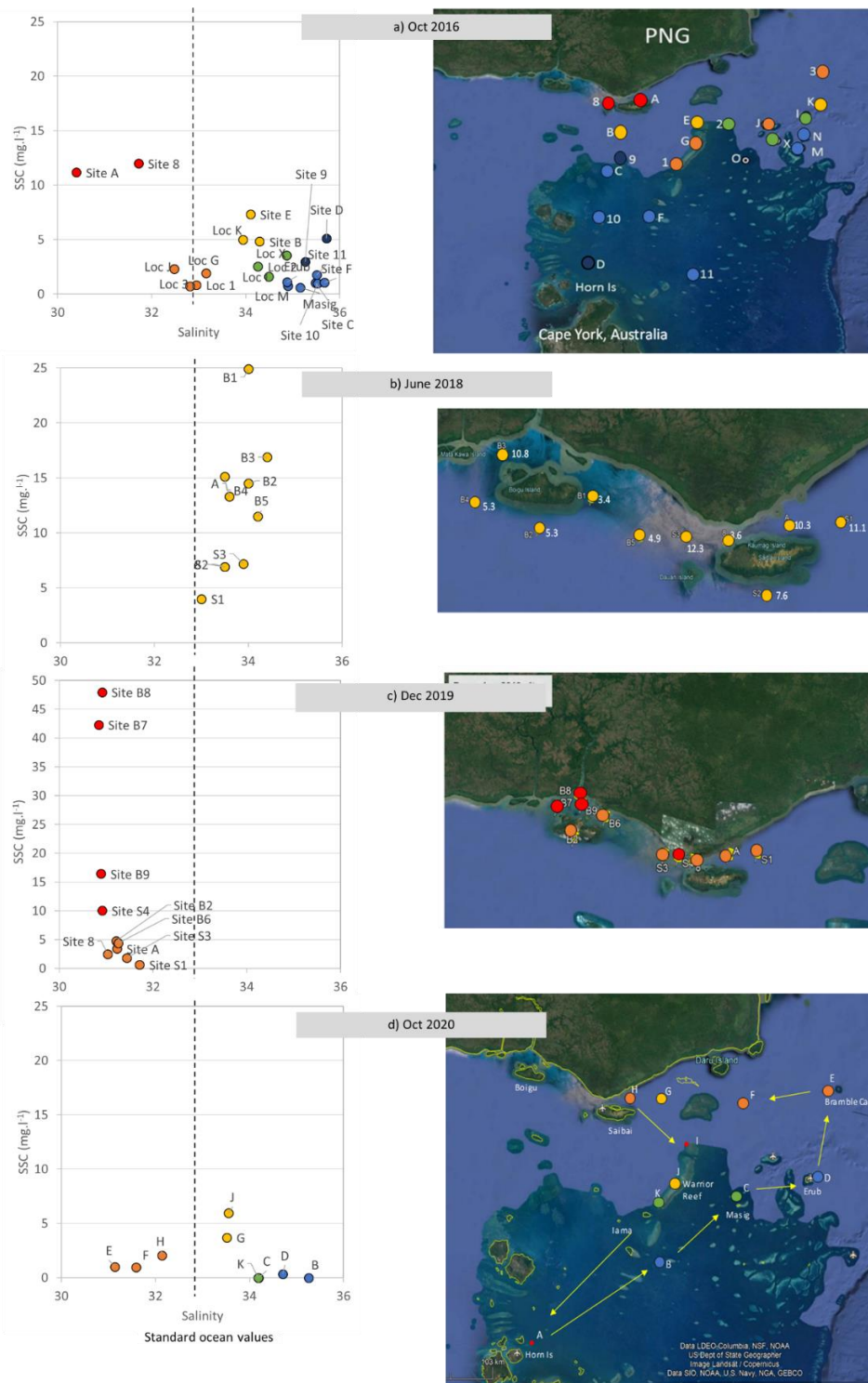
Figure 6–13: (left) SSC-salinity plots and (right) location of SSC field samples collected in: a) Oct 2016, b) June 2018, c) Dec 2019 and d) Oct/Nov 2020 (Section 7.0). Samples are colour coded based on salinity and SSC: 🔴 **Low salinity (< 32 PSU) - SSC > 10 mg/L indicating a likely Turbid plume influence,** 🟠 **Low salinity (≤ 33 PSU), SSC < 5 mg/L indicating a likely diluted riverine influence,** 🟡 **Higher salinity (33 - 34.5 PSU) and SSC ≥ 4 mg/L likely indicate presence of a diluted plume influence (less saline but slightly more turbid) / or other turbidity sources e.,g. calcareous sediments.** 🟢 **High salinity (34.5 - 35 PSU) and SSC < 5 mg/L likely indicating transitional waters with slightly over marine conditions and** 🔵 **> 35 PSU, negligible SSC likely indicating marine waters.**
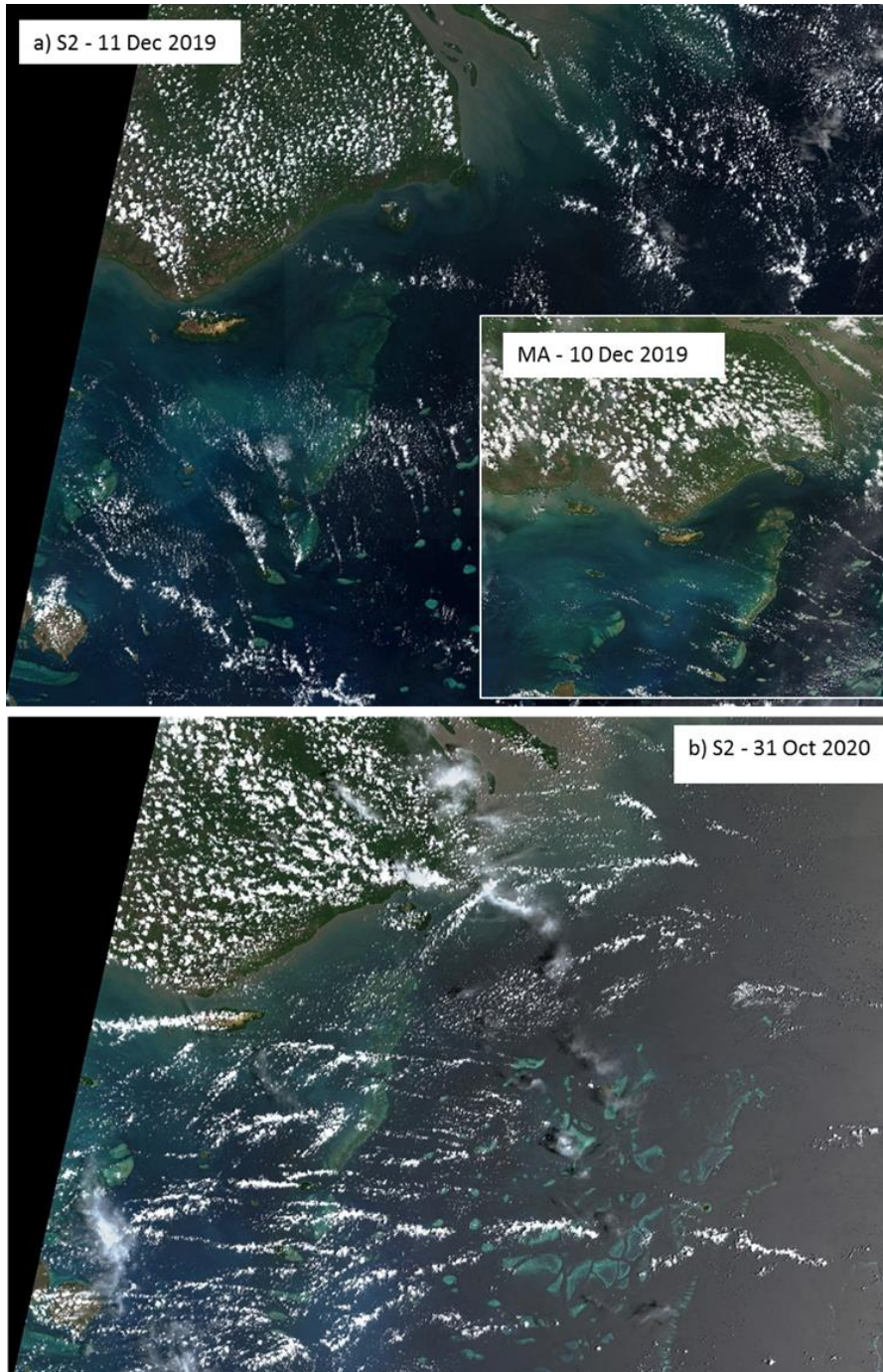
Figure 6–14: MODIS-Aqua (MA) and/or high-resolution Sentinel-2 (S2) and satellite images of the a) 11 December 2019 and of the b) 31 October 2020.

In the north central (Ugar and Masig) and south-west regions (Erub, Mer) the field salinity (> 34.5 PSU and low to negligible SSC (< 5 mg/L) and example satellite data field data indicated a likely very diluted or negligible influence of the Fly River plume (green or blue dots, Figure 6-13a and d). In the central region (Iama, Warraber, Poruma) data indicated that the Fly River was unlikely to have any influence (salinity > 35 PSU, Figure 6-13a and d).

6.4 Conclusions and recommendations

The remote sensing data analysis showed similar patterns to the previous years and provided further information on the distribution of sediment and spatio-temporal dynamic in the study area. This study reaffirmed that habitats located in the NE corner of the Torres Strait Protected Zone, including the northern Warrior Reef, as far west as Saibai Island and as far east as Bramble Cay are located in a higher potential risk area of exposure to sediments from, or derived from, the Fly River. The influence of the Fly River on Bramble Cay seemed enhanced by trade wind environmental conditions and several satellites images captured intermittent influence of the Fly River plume on Bramble Cay during the SE trade wind season. The Fly River signature is likely to be diminished around Boigu Island (e.g., Wolanski et al. 2021), and the high turbidity levels measured there are largely influenced by the Mai Kussa and Wassi Kussa rivers, but this needs to be confirmed by further data. In the middle of the Torres Strait, the presence of moderately turbidity water masses was most likely associated with calcareous sediments flowing through the Warrior Reef or a mixture of terrigenous and carbonate suspended sediments closer to the coast.

The Fly River plume intruded the Torres Strait the greatest during the SE trade wind season and less during the monsoon season, in agreement with hydrodynamic and sediment modelling results in the region (Li et al. 2017; Martins and Wolanski 2015; Wolanski et al. 2013, 2021; and Section 0 in this report), field salinity records (Waterhouse et al. 2018 and Section 3.0 in this report) and other field observations (Harris et al. 1993 and Sections 0 and 7.0 of this report). The new satellite analyses supported previous studies and hypotheses suggesting that currents in the Torres Strait reverse seasonally, with flow being predominantly westwards during the SE trade wind season (negative mean sea level) and driving PNG turbid river into the Torres Strait (Harris 1994; Li et al. 2017; Wolanski et al. 2013). Satellite and mooring data collected as part of this study suggested that, during the trade wind period, the intrusion in the Torres Strait Protected Area is greater between June and September and is likely to be maximum in July to August.

Preliminary validation exercises conducted as part of this study provided confidence in the colour and turbidity trends described. The limitations of these studies and recommendations for future work are included in Section 8.5.

This study provides a long-term and large-scale view of turbidity patterns in the Gulf of Papua-Torres Strait region and spatially explicit information that can help identifying areas which need further investigation and/or where management effort should be focused. Finally, the water colour is a simple optical indicator and a very intuitive measure that has been previously used in Torres Strait community surveys to describe change in water 'muddiness' (Waterhouse et al. 2018). Such information could be combined in the future with the satellite data and provide local community members with the opportunity to share their knowledge.

7.0 FIELD SURVEYS OF TRACE METALS IN WATERS, SEDIMENTS AND SEAGRASS

7.1 Previous findings

NESP TWQ Hub Project 2.2.2 involved collection of water, suspended sediment and benthic sediment samples for trace metal analysis to assess the potential link to the intrusion of contaminated mine-derived sediments into the Torres Strait region (Apte et al. 2018; Waterhouse et al. 2019).

- High quality data on trace metal concentrations in waters, suspended sediments and benthic sediments was generated for 29 sites across the Torres Strait. The measured trace element concentrations were generally very low and consistent with uncontaminated marine waters and sediments from other regions of the world. Trace metal concentrations in waters and sediments were highest in the northern Torres Strait, around Saibai and Boigu islands. Slightly elevated concentrations of copper in waters and sediment were also detected at Bramble Cay which is likely to be a consequence of periodic intrusions of the Fly River plume.
- The concentrations of dissolved metals were below the 95% species protection guideline values of the Australian and New Zealand water quality guidelines (ANZG 2018) which are used by regulators in most areas of Australia as default benchmarks. Dissolved copper concentrations exceeded the 99% species protection guideline values which are applicable to pristine water bodies in ten water samples collected in the vicinity of Boigu and Saibai Islands. Dissolved cobalt concentrations exceeded the 99% protection guideline value in five water samples collected in the vicinity of Boigu and Saibai islands. However, a subsequent investigation of the cobalt marine guidelines indicated that they are based on inappropriate data and overestimate the risks posed by cobalt in marine systems. Exceedance of the 99% protection guideline value can therefore be disregarded. Metal concentrations in benthic sediments were generally very low and below ANZ guideline values, apart from particulate arsenic and nickel concentrations detected in two sediment cores collected close to Saibai Island. These elevated arsenic and nickel concentrations are most likely due to natural background mineral enrichment in the area rather than any anthropogenic contamination.
- The sources of the higher metal concentrations around Boigu and Saibai was not identified. The most likely source of metals are inputs of sediments and waters from PNG comprising local riverine inputs and direct runoff from the PNG mainland. However, contributions from the Fly River plume could not be discounted.

It was recommended that further work was required to understand the sources and distributions of trace metals in the northern Torres Strait, particularly around Bramble Cay, Boigu and Saibai islands and how they vary with time. To assist in this endeavour, tracing techniques that allow the differentiation of mine-derived sediments from natural sediment should be developed and applied to sediment samples from the Torres Strait.

7.2 Additional work: Scope and methods

7.2.1 Purpose

Building on the recommendations above, the purpose of the two-year follow-up study was to:

i.   Develop methods for tracing mine-derived sediments in the Torres Strait and apply these to benthic and suspended sediment samples collected in the field campaigns described above and to archived sediment cores collected during the first NESP project.

ii.   Obtain further data on trace metals distributions in the northern Torres Strait, with a focus on the marine areas around Boigu and Saibai Islands, the Warrior Reefs, Masig Island and Bramble Cay.

iii. Identify the sources of trace metals to the northern Torres Strait including Boigu and Saibai and distinguish local inputs from those originating from the Fly River, including mine-derived inputs.

It should be noted that the COVID-19 pandemic severely impacted on field work planned for the latter half of the project. It was not possible conduct an extensive survey of the northwest Torres Strait and collect additional samples for analysis of dissolved metal concentrations and also collect additional sediment samples as had originally been intended. Subsequent modifications to the program of work are described in ensuing sections of this report.

7.2.2 Methods

Field campaigns

Table 7-1 summarises the three field campaigns were conducted over the duration of the project, and the activities undertaken during each sampling campaign.

Owing to COVID-19 restrictions CSIRO staff based in Sydney were not able to participate in field work from March 2020 onwards. A major cruise organised for late March 2020 had to be cancelled and because of ongoing travel restrictions, could not be rescheduled. In its place, samples were collected by AIMS staff under the direction of CSIRO during an AIMS organised cruise of the Torres Strait in October/November 2020. This allowed some sampling of sediments, and water samples for suspended sediments at sites across the Torres Strait. It was not feasible to collect samples for dissolved metals analysis as this required specialist ultra-trace sampling expertise which was not available in the absence of CSIRO staff. The last field campaign was conducted by JCU staff during November 2020 and involved benthic sediment and water sampling around Boigu and Saibai Islands. Seagrass samples for trace metals analysis were also taken during the AIMS and JCU field trips.

Details of field sampling procedures, processing (e.g. filtrations) and storage protocols for waters, sediment and seagrass can be found in Appendix A.

Table 7–1: Summary of field surveys undertaken for the trace metal analysis

Survey	Activities
Saibai and Boigu Islands, December 2019 (CSIRO)	Water quality sampling – general parameters, dissolved trace metals
Torres Strait Regional survey, October/November 2020 (AIMS)	General water quality sampling, suspended sediments, benthic sediment cores, seagrass samples.
Saibai and Boigu Islands, November 2020 (JCU)	General water quality sampling, suspended sediments, benthic sediment cores, seagrass samples

Saibai and Boigu Islands Survey, December 2019

Water samples were collected from five sites around Saibai Island and five sites around Boigu Island (Table 7-2, Figure 7-1) on 10 -11 December 2020. Two of the sites (A and 8, located north of Saibai; Figure 7–1) had previously been sampled during the 2016 field survey (Apte et al. 2018). Duplicate water samples were collected at Sites B7. Sampling was conducted at Saibai with the assistance of TSRA staff from on-board the TSRA patrol vessel. At Boigu, sampling was conducted from a locally chartered boat with the assistance of TSRA staff. A field blank was also prepared during the Saibai leg of the survey.

Water samples were transported by air charter to Horn Island and were processed within 24 hours of collection in a clean laboratory area which was free of dust and other potential sources of metal contamination. The processed water and sediment samples were stored chilled and transported back to the CSIRO laboratories in Sydney for analysis of dissolved metals.

Figure 7–1: Location of sampling sites around Boigu and Saibai Islands (December 2019).

Table 7–2: Location of sites sampled during the December 2019 survey

Site	Date	Depth (m)	Coordinates	
			Latitude	Longitude
Saibai sites				
Site 8	10/12/19	5.6	9°22'16.86"S	142°36'26.62"E
Site A	10/12/19	4.3	9°20'44.19"S	142°44'14.31"E
Site S1	10/12/19	12.0	9°20'1.01"S	142°50'3.11"E
Site S3	10/12/19	11.9	9°21'31.65"S	142°30'37.80"E
Site S4	10/12/19	26.2	9°21'41.55"S	142°33'38.39"E
Boigu sites				
Site B2	11/12/19	2.8	9°19'26.58"S	142°11'40.98"E
Site B6	10/12/19	7.2	9°15'3.90"S	142°17'53.40"E
Site B7	10/12/19	18.8	9°13'45.60"S	142° 7'37.62"E
Site B8	10/12/19	10.0	9°11'11.70"S	142°12'1.50"E
Site B9	10/12/19	32.5	9°12'55.32"S	142°12'50.76"E

Torres Strait Regional survey, October and November 2020

The sampling program was carried by a team of scientists from AIMS between 27 October to 2 November 2020. The team were instructed on sampling techniques by JCU and CSIRO staff and were supplied written standard operating procedures.

The MV Free Spirit, a charter vessel equipped for conducting surveys in marine waters, was used for the sampling campaign. The sampling activities conducted at each site are summarised in Table 7-1. A total of 11 sites were identified for water seagrass and benthic sediment sampling. The sampling locations are listed in Table 7–3 and shown in Figure 7–2.

Sediment samples were collected using a gravity core sampler (Uwitec, Austria) deployed from hand-held line or winch fitted with pre-loaded plastic core tubes. Sediment cores were sliced into 2cm sections on-board boat (Apte et al. 2018) and stored frozen. Water samples were collected in 5L polyethylene container and stored refrigerated. Seagrass samples were taken by hand (5 replicates), transferred to ziplock plastic bags and stored frozen. At the end of the cruise, all samples were freighted from Horn Island to Sydney by refrigerated transport.
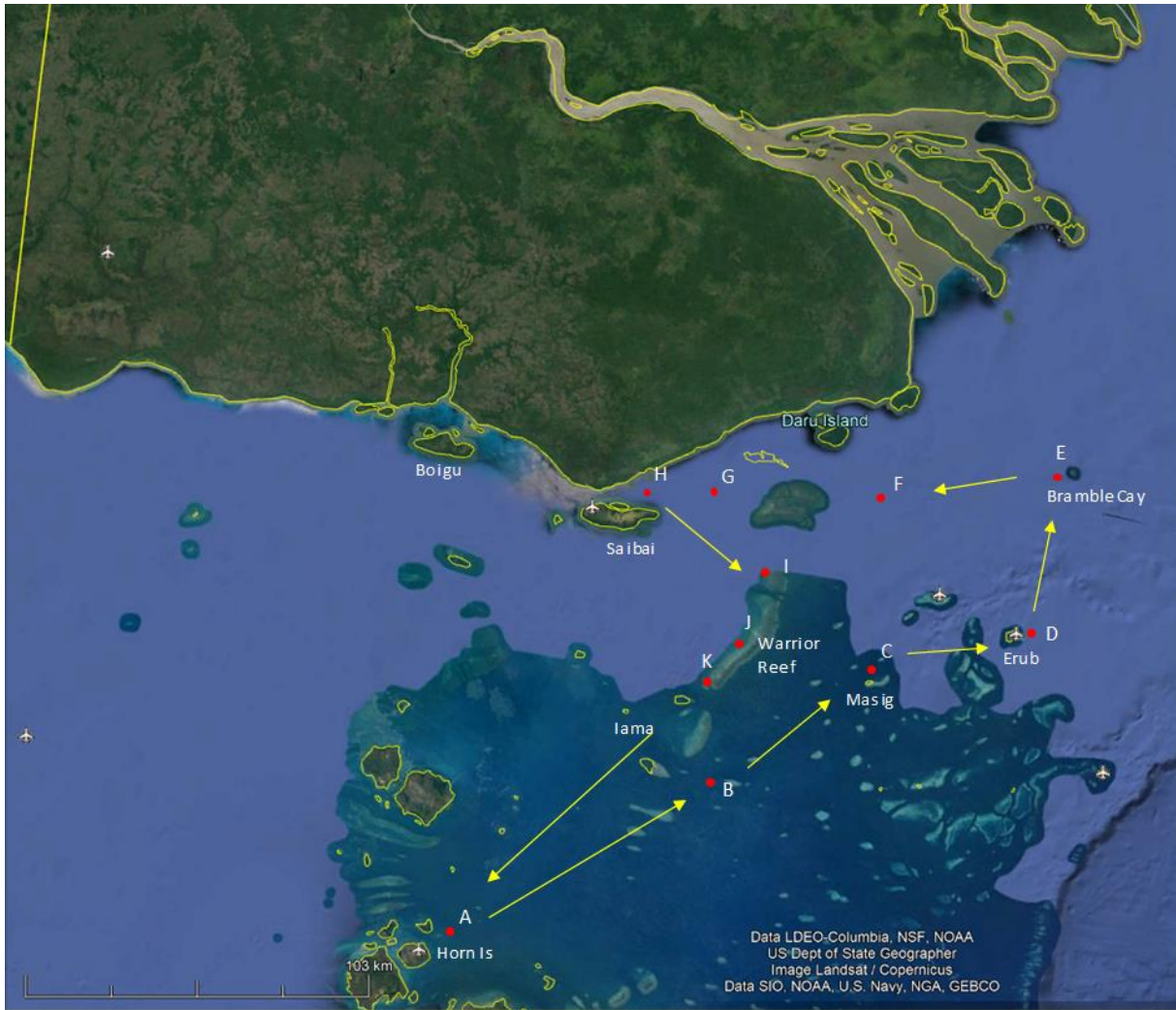
Figure 7–2: Map showing the location of the October and November 2020 sampling sites. Note that Site A was added for temperature logger maintenance and not sampled

Table 7–3: Location of the sites sampled during the October and November 2020 survey

Location	Site	GPS coordinates	
		Latitude	Longitude
SE of Iama	B	10.28725°	142.97931°
Masig	C	9.74439°	143.43256°
Masig	C1	9.74439°	143.43256°
Masig	C2	9.74613°	143.43320°
Erub	D	9.58792°	143.78841°
Erub	D1	9.72797°	143.44038°
Bramble Cay	E	9.14159°	143.87248°
South of Daru	F	9.22750°	143.38278°
East of Saibai	G	9.25969°	142.20375°
North Warrior Reef	I	9.478533°	143.09518°
Middle Warrior Reef	J	9.659467°	143.053064°
South Warrior Reef	K	9.773701°	142.959670°

Saibai and Boigu Islands survey, November 2020

This survey was conducted by staff from JCU with assistance from TSRA staff based at Saibai and Boigu on 10 and 12 November 2020. Field sampling of waters, seagrasses and benthic sediments (see Table 7-1) was conducted from on-board a TSRA patrol vessel at the sites shown Figure 7–3 and Figure 7-4, and listed in Table 7-4. Samples were subsequently hand carried to Townsville and then transferred by express courier to CSIRO Land and Water, Sydney where analyses were conducted.

Figure 7–3: Map showing the location of sampling sites (red markers) around Boigu Island November 2020 survey.

Figure 7–4: Map showing the location of sampling sites around Saibai Island November 2020 survey.

Table 7–4: Sampling locations and details of the Saibai and Boigu Islands survey, November 2020.

Site	Location	Date	Time	GPS Coordinates		Water depth (m)
				Latitude	Longitude	
Site 1	Boigu	10/11/20	13:15	9.21136	142.23433	50
Site 2	Boigu	10/11/20	13:45	9.22688	142.19263	3.5
Site 3	Boigu	10/11/20	14:35	9.24005	142.14672	2.1
S3	Saibai	12/11/20	10:20	9.3661	142.5203	11.8
8	Saibai	12/11/20	11:20	9.37476	142.60606	4.8
A	Saibai	12/11/20	12:10	9.3489	142.73984	9.6
S1	Saibai	12/11/20	13:25	9.34262	142.85787	11.7
S2	Saibai	12/11/20	14:42	9.47563	142.69138	7.6
Additional Sediment samples						
Site1 Boigu sediment	Boigu	10/11/20	13:30	9.21731	142.23398	3
Site 8 Sediment	Saibai	12/11/20	11:38	9.37685	142.59624	-
Seagrass samples						
SG1	Saibai	12/11/20	12:53	9.36589	142.7511	2.0
SG2	Saibai	12/11/20	16:00	9.37693	142.61601	1.6
Intertidal Boigu	Boigu	10/11/20	11:30	9.21731	142.23398	0

Chemical analysis

The CSIRO laboratories at Lucas Heights are accredited by the National Association of Testing Authorities (NATA) for the chemical analyses performed as part of this project. The analysis of trace metals at sub-µg/L concentrations is acknowledged to be technically challenging and necessitates the application of rigorous protocols for container preparation, sample collection and analysis (conducted in a clean room environment), in order to minimise the risk of sample contamination.

Rigorous quality control procedures are employed in the laboratory. These comprise the following steps:
- Field blanks for water samples (trace metals)
- Replicate field samples
- Laboratory replicates (at least one in each batch)
- Laboratory blanks in each batch of samples (at least 3 in each batch)
- Where available, analysis of a certified reference material in each batch of samples
- Spike recovery tests (at least one in each batch)

The limits of detection for the trace metal analyses are calculated based on the actual blank measurements made during the analyses conducted (three times the standard deviation of the blank measurements). This provides a more realistic assessment of actual detection limits rather than the generalised detection limits based on historical data that are quoted by general commercial laboratories.

Details of the analytical methods employed are presented in Appendix A.

Spreadsheet reports containing full analytical data, including quality control may be accessed via the e-Atlas portal. For the sake of brevity, summary information only is included in this report. In this report, for the sake of brevity, the term trace metal also includes arsenic which is a metalloid element.

Mine tracer analysis

A newly developed procedure for identifying mine-derived minerals in natural sediments applied to selected sediment samples in order to gain additional information in support of data derived from conventional chemical analyses of particulate and dissolved metal concentrations. Previous work by CSIRO (CSIRO unpublished) has shown that tailings samples from copper mines such as the Ok Tedi mine invariably contain fragments of sulphide minerals such as chalcopyrite and pyrite. These mineral particles are clearly distinguishable by scanning electron microscopy (SEM) as they have a lighter colour contrast compared to aquatic sediments due to their higher density. This newly developed procedure for identifying mine-derived minerals in natural sediments was applied to selected sediment samples to provide additional information to support of data derived from conventional chemical analyses of particulate and dissolved metal concentrations.

The tracing procedure is based on the combination of a number of standard sediment fractionation procedures followed by examination of the concentrated solids fractions by SEM and energy dispersive X Ray analysis (EDS), which allows qualitative elemental analysis. The procedure was used to target minerals that are likely present in mine tailings and waste rock

originating from the Ok Tedi mine, such as chalcopyrite and pyrite. Samples were also scanned for other dense minerals which may also have a mine-related origin.

A flowchart summarising the overall procedure is shown in Figure 7–5. Details of method validation are provided later in this section. Sample preparation is described below.

```
┌──────────┐                          ┌──────────┐
│   TSS    │                          │ Benthic  │
│          │                          │ sediment │
└────┬─────┘                          └────┬─────┘
     │                                     │
     └──────────────┐      ┌───────────────┘
                  ┌─▼──────▼─┐
                  │ Wet sieving│
                  │   <2 mm    │
                  │ <210 micron│
                  └─────┬──────┘
                        │
                 ┌──────▼──────┐
                 │ Clay removal │
                 └──────┬──────┘
                        │
              ┌─────────▼─────────┐
              │ Carbonate removal │
              └─────────┬─────────┘
                        │
             ┌──────────▼──────────┐
             │ SEM screening and   │
             │   identification of │
             │   possible mineral  │
             │      particles      │
             └──────────┬──────────┘
                        │
            ┌───────────▼───────────┐
            │ Elemental analysis    │
            │    (EDS) of suspected │
            │   mineral particles   │
            └───────────────────────┘
```
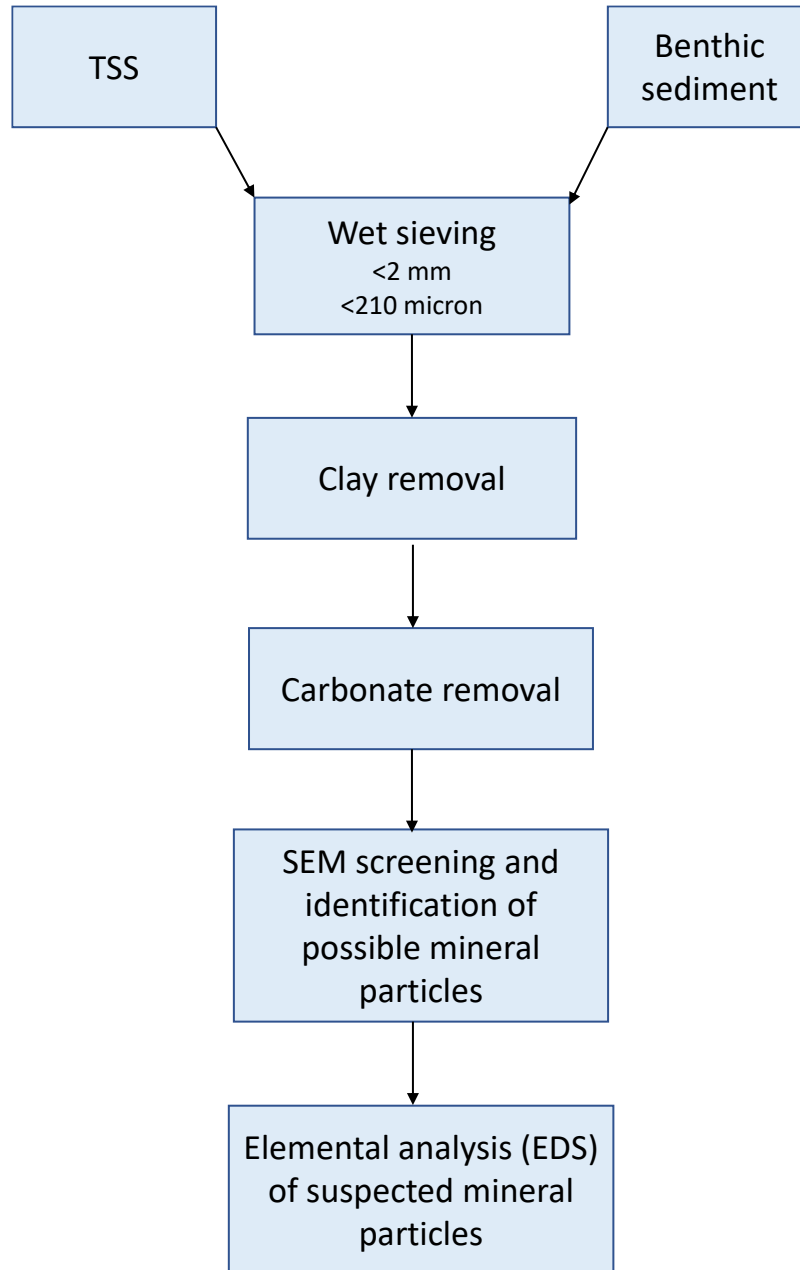
Figure 7–5: Flow chart of the method for identifying mineral particles that are potentially mine-derived.

Isolation of suspended sediments: Unfiltered water samples (5 L) were stored refrigerated and sediment allowed to settle for a period of several days or longer. The overlying water was then removed by positioning a silicone tube above the sediment layer and slowly pumping out the water using a peristaltic pump. The final slurry volume was around 200 ml which was

decanted to a smaller container and allowed to settle refrigerated for a further time period (typically 2 days).

Preparation of benthic sediments: Frozen core slices were thawed to room temperature, homogenised and a sub-sample (typically 10 to 20 g) removed and placed in a polycarbonate vial. One hundred 100 ml of MQ water was then added and the mixture thoroughly shaken by hand in order to disperse the sediment particles.

Sediment fractionation: Sample fractionation involved a number of stages which are detailed below.

(i) Wet Sieving: Samples were wet sieved first through a coarse plastic mesh sieve (2 mm diameter) and unless otherwise stated, then through a 210 micron plastic mesh sieve into a polycarbonate vial. A minimum quantity of deionised water was used to flush the sediments through the sieves.

(ii) Clay removal: The clay fraction (<2 micron diameter particles) of each sample was removed using a well-established settling procedure based on Stokes' Law (Poppe et al. 2001). The method assumes a density of 2.7 g/cm^3 for clay mineral particles which is much lower than the typical densities of sulphide minerals (Table 7–5). Sieved samples were transferred to 110 ml polycarbonate vials and MQ water added to give a final volume of 100 ml. The distance from the meniscus to 5 cm below this level was measured and marked with a marker pen. The vials were shaken for around 60 seconds to suspend and disperse particles and then allowed to settle at room temperature for 4 hours. The suspension above the 5 cm mark was then carefully removed by pipette. The procedure repeated at least two times or until the overlying water layer after the settling period was clear of visible sediments.

(iii) Carbonate mineral removal: Carbonate-based minerals were removed by dissolution under mildly acidic conditions (Poppe et al. 2001). Sediment suspensions were allowed to settle overnight and the overlying water fraction removed by pipette to form a concentrated slurry. Fifty ml of acetic acid (20 % v/v) solution was then added to the slurry. The solutions were shaken and allowed to react, with occasional agitation, for at least 8 hours or until effervescence ceased. The overlying acetic acid solution was removed by pipette and replaced with MQ water, the solutions were then shaken and allowed to settle. This washing procedure was conducted three times in order to remove traces of acetic acid.

(iv) Drying: Overlying water was removed from settled samples using a plastic pipette. The resulting concentrates were quantitatively transferred to a Petri dish with a minimum amount of MQ water washings and dried in a drying oven at 40°C overnight. The dried samples were allowed to cool to room temperature and removed from the Petri dishes using a plastic scraper, followed by gentle disaggregation in an agate mortar and pestle. The resulting powders were transferred to plastic vials which were stored at room temperature.

SEM analysis: A small amount of dried powder was placed onto a standard SEM stub with double sided conductive carbon adhesive. Approximately 50 Å of carbon was evaporated onto the surfaces under vacuum to prevent charging. The SEM was a Zeiss Ultra Plus with an attached Oxford Instruments X-Max 80mm^2 SDD X-ray microanalysis system with Oxford

Aztec software. The SEM was operated at an accelerating voltage of 15 kV, all results are qualitative only. Images were recorded at x50, x100, x200 and x400 magnifications.

The SEM field of view was scanned by eye and any lightly contrasting particles (indicative of dense minerals such as sulphides) selected for EDS analysis. Typically between 3 and 10 EDS spectra were recorded per powder sample.

The fractionation procedure and SEM analysis protocol was applied to range of samples benthic and suspended sediment samples. Full details are given in Section 0.

Table 7–5: Examples of mineral densities relevant to this study.

Mineral	Specific gravity
Sulphide minerals	
Chalcopyrite	*4.1 – 4.3*
Chalcocite	*5.5 – 5.8*
Covellite	*4.6 – 4.8*
Digenite	*5.5 – 5.7*
Pyrite	*5.0 – 5.1*
Typical marine sediment components	
Calcite	*2.71*
Aragonite	*2.95*
Vaterite	*2.54*
Dolomite	*2.84-2.86*
Inorganic clays	*2.7-2.8*
Quartz Sand	*2.7*

Mine tracer validation experiment

A preliminary experiment was performed to demonstrate the ability of the tracing procedure to detect sulphide mineral particles in natural sediments. Mineral specimen samples of pyrite (Victoria Mine, Navajun, Spain) and chalcopyrite (Mt Lyell, Tasmania) were obtained from a mineral supplier (The Mineral Store, QLD). The minerals were cleaned by successive rinsing (1 to 2 minutes contact time) with acetone, deionised water, 0.01 M HCl solution and deionised water. The samples were then allowed to dry in a nitrogen glove box. The minerals were then crushed manually with a hammer, ground in a ring mill and then sieved to <180 µm. Weighed amounts of the mineral were then added to 10 g portions of homogenised natural sediment (Site 3, 4-6 cm core slice from Boigu, December 2020 survey) and mixed using a plastic spatula to produce mixtures containing 10%, 1% and 0.1% (m/m) of the added mineral. A control sediment sample (no mineral added) was also prepared. The sediment-mineral mixtures were then put through the fractionation procedures shown in Figure 7–5. SEM images were recorded for each sample and EDS overlay maps of iron, sulphur and copper distributions in the observed particles present in the field of view were generated.

7.3 New results

7.3.1 Water and sediment surveys

2019: Saibai and Boigu Islands survey (December 2019)

General water quality parameters

The general water quality parameters measured in waters during the survey are shown in Table 7-6. Water pH was relatively constant and ranged from 8.07 to 8.20 with no obvious spatial trends. Salinity was reasonably uniform across the sites and ranged from 30.8 to 31.7 PSU This compares to an expected value of around 35PSU for seawater. The lower salinity values around Boigu and Saibai are consistent with the salinity monitoring results presented in Section 3.3 and are a consequence of freshwater inputs from the PNG mainland including the smaller coastal rivers, and potentially, the Fly River.

Total suspended solid concentrations ranged from 0.6 to 48.0 mg/L with the highest concentrations observed at the three sites (B7, B8, B9) to the north of Boigu (Figure 7–6). The lowest salinity values were also found at these sites. The observations are consistent with the input of sediment-laden freshwaters from the Mai and Wassi Kussa rivers adjacent to Boigu on the PNG mainland.

Dissolved metal concentrations

Dissolved metal concentration data are summarised in Table 7–7. Maps showing the spatial distribution of dissolved copper and lead are presented in Figure 7–7 and Figure 7–8 respectively. Dissolved zinc data was deemed unreliable owing to possible contamination from the sacrificial zinc anodes on the survey boats and is not reported. Strong spatial trends in dissolved metal concentrations were not evident in the collected data.

None of the dissolved metal concentrations exceeded the ANZG (2018) 95% species protection marine water quality guideline values (WQGVs), however all 10 samples exceeded the 99% species protection marine WQGV for copper (0.3 µg/L). Overall, the data from the survey confirmed the previous observations of the presence of elevated dissolved metal concentrations in this part of the Torres Strait. A synthesis of dissolved metals data is presented in Section 8.2.1.

Table 7–6: General water quality parameters Saibai and Boigu Islands survey, December 2019. Refer to Figure 7-1 and Table 7-2 for site locations.

Sample name	TSS (mg/L)	pH	Salinity (PSU)
Saibai sites			
Site 8	2.5	8.13	31.0
Site A	3.4	8.16	31.2
Site S1	0.6	8.18	31.7
Site S3	1.8	8.16	31.4
Site S4	10.0	8.08	30.9
Boigu sites			
Site B2	4.8	8.20	31.2
Site B6	4.4	8.16	31.3
Site B7	42.3	8.15	30.8
Site B7 duplicate	36.7	8.16	30.9
Site B7 mean	39.5	8.16	30.9
Site B8	48.0	8.07	30.9
Site B9	16.4	8.08	30.9

Table 7–7: Dissolved metals data Saibai and Boigu Islands survey, December 2019. Figures in orange exceed the ANZ marine guideline value for 99% species protection.

Sample Name	Aluminium	Cadmium	Cobalt	Copper	Iron	Manganese	Nickel	Lead
	(µg/L)							
Saibai sites								
Site 8 mean	3.1	0.005	0.010	0.47	<0.07	0.4	0.16	0.0038
Site A mean	4.1	0.005	0.010	0.50	<0.07	<0.1	0.20	0.0047
Site S1	<1.4	0.003	0.005	0.33	<0.07	0.2	0.14	0.0043
Site S3	3.2	0.005	0.009	0.40	<0.07	<0.1	0.16	0.0060
Site S4	4	0.006	0.006	0.48	<0.07	<0.1	0.16	0.0041
Saibai mean	**3.6**	**0.0048**	**0.008**	**0.436**	**<007**	**0.3**	**0.164**	**0.00458**
Boigu sites								
Site B2	1.6	0.003	0.006	0.37	<0.07	<0.1	0.14	0.0041
Site B6	3.1	0.005	0.009	0.44	<0.07	0.2	0.15	0.0035
Site B7	4.5	0.006	0.005	0.47	<0.07	<0.1	0.17	0.0023
Site B8	5.1	0.005	0.008	0.47	<0.07	<0.1	0.18	0.0035
Site B9	3.6	0.005	0.005	0.49	<0.07	<0.1	0.18	0.0024
Boigu mean	**3.6**	**0.0048**	**0.0066**	**0.448**	**<0.07**	**0.2**	**0.164**	**0.00316**
Saibai/Boigu ratio	**1.01**	**1.00**	**1.21**	**0.97**	**-**	**1.50**	**1.00**	**1.45**
Marine DGV (95%)	-	5.5	1	1.3	-	-	70	4.4
Marine DGV (99%)	-	0.7	-	0.3	-	-	7	2.2

Figure 7–6: Map showing the distributions of suspended sediments (TSS mg/L) around Boigu and Saibai Islands, December 2019 survey.

Figure 7–7: Map showing the distributions of dissolved copper concentrations (µg/L) around Boigu and Saibai Islands, December 2019 survey.

Figure 7–8: Map showing the distributions of dissolved lead concentrations (ng/L) around Boigu and Saibai Islands, December 2019 survey.

2020: Torres Strait Regional survey (October/November 2020) and Saibai and Boigu Islands survey (November 2020)

General water quality parameters

The physico-chemical parameters measured in waters and details of the samples collected during the Torres Strait Regional survey in October/November 2020 are shown in Table 7-8. Water pH ranged from 8.24 to 8.35 and was relatively constant throughout the region with no obvious trends. Salinity ranged from 31.1 to 35.3 PSU with the lowest salinities being measured at Bramble Cay (E) and South of Daru (F) which were closest to the Fly River Estuary. This suggests likely freshwater contributions by the Fly River plume at these sites. Total suspended solids concentrations were generally low and ranged from <0.3 to 6.0 mg/L. The highest TSS concentrations were measured at the Saibai (G) and Middle Warrior Reef (J) sites (Figure 7–2).

Table 7–8: Sampling details and physico-chemical data, Torres Strait Regional survey, October/November 2020. Site locations are presented in Table 7–3

Site	Location	Date	Time	Depth (m)	Sediments	Waters	Seagrasses	pH	Salinity (PSU)	TSS (mg/L)
B	SE of Iama	28/10/2020	7:30	20		✓		8.25	35.3	<0.3
C	Masig	28/10/2020	17:00	15	✓		✓			<0.3
C1	Masig	29/10/2020	9:45	5		✓		8.29	34.2	-
C2	Masig	29/10/2020	11:00	3	✓	✓		8.3	34.3	-
D1	Erub	29/10/2020	15:30	15		✓		8.29	34.7	0.3
D	Erub	30/10/2020	7:30	5	✓	✓	✓			-
E	Bramble Cay	30/10/2020	11:45	7	✓	✓	✓	8.28	31.1	1.0
F	South of Daru	1/11/2020	7:00	22		✓		8.28	31.6	1.0
G	East of Saibai	1/11/2020	9:00	6		✓	✓	8.31	33.5	3.7
I	North Warrior Reef	1/11/2020	13:20	3	✓	✓	✓	8.24	32.1	2.0
J	Middle Warrior Reef	1/11/2020	15:30	3	✓	✓	✓	8.35	33.6	6.0
K	South Warrior Reef	2/11/2020		3	✓	✓	✓	8.3	34.2	<0.3

The results for the general water quality parameters measured in waters during the Boigu and Saibai November 2020 survey are shown in Table 7–9. Water pH was relatively constant and ranged from 8.17 to 8.29 with no obvious spatial trends. Salinity was reasonably uniform across the sites and ranged from 28.9 to 31.5 PSU. This compares to an expected value of around 35 PSU for seawater. The lower salinity values around Boigu and Saibai are consistent with the salinity monitoring results in Section 3 and likely to be linked to the diluting effects of freshwater inputs from the PNG mainland including the Mai and Wassi Kussa Rivers and potentially the Fly River. Total suspended solids ranged from 1.2 to 25 mg/L with the lowest concentrations observed at the open water sampling sites (S1 and S2; Figure 7-4).

Table 7–9: Water quality results from Saibai and Boigu Islands survey, November 2020.

Site	Location	Water depth (m)	pH	Salinity (PSU)	TSS (mg/L)
Site 1	Boigu	50	8.29	28.9	9.3
Site 2	Boigu	3.5	8.29	29.4	13.0
Site 3	Boigu	2.1	8.25	30.2	14.0
S1	Saibai	11.7	8.28	30.9	2.3
S2	Saibai	7.6	8.29	31.5	1.2
S3	Saibai	11.8	8.25	29.9	15
Site 8	Saibai	4.8	8.17	29.5	25
Site A	Saibai	9.6	8.28	30.2	7.7

Metals associated with benthic sediments

The concentrations of 65 trace elements were measured in the benthic sediment samples in the 2020 surveys. Data for the 17 most commonly monitored elements are shown in Table 7–10 and Table 7–11. The data for all elements and associated laboratory quality control data are available in the eAtlas data repository.

Photographs illustrating the sediment cores collected are shown in Figure 7–9. As encountered in the previous NESP study (Apte et al. 2018), sediment composition was quite varied, ranging from coarse, coral-containing material (e.g. Masig - C and Bramble Cay - E) to fine muds (Boigu and Saibai sites).

The concentrations of metals in sediment cores showed no consistent trends with depth. This is illustrated by particulate copper depth profiles in Figure 7-10. There was no indication of any consistent surface enrichment of copper which would be indicative of recent deposition of sediments containing elevated copper concentrations (i.e. mine-derived sediments). The same pattern was observed in the NESP 2016 survey data (Apte et al. 2018).

The trends in the distribution of eight particulate metals with location are shown in Figure 7–11. Similar to the previous trends observed for metals in waters and suspended sediments, the highest metal concentrations were found at the northern sites around Boigu, Saibai and south of Daru. The only exception was particulate cadmium which did not display a noticeable trend with location.

Figure 7–9: Examples of fine sediment cores taken at Boigu (left) and Saibai (middle and right).
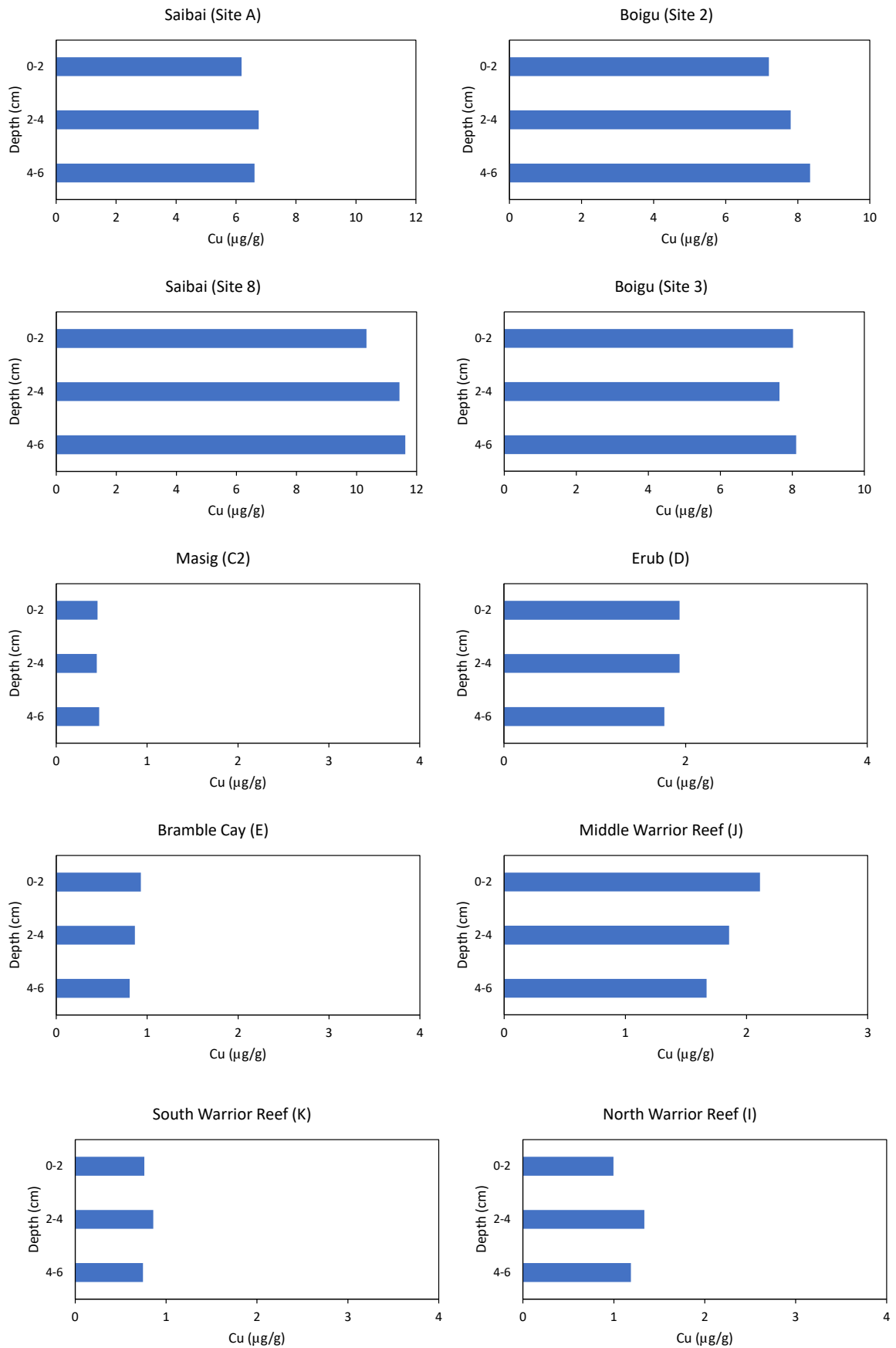
Figure 7–10: Example of sediment core profiles obtained in 2020: particulate copper (Cu).

Table 7–10: Benthic trace element concentrations (Torres Strait Regional survey, Oct/Nov 2020). Figures in red exceed the ANZG sediment quality guideline value. Note: Al – aluminium, Ca – calcium, Fe – iron, S – sulfur, Mn – Manganese, Ag – silver, As – arsenic, Cd – cadmium, Co – cobalt, Cr – chromium, Cu – copper, Mo – Molybdenum, Ni – nickel, Pb – lead, U – uranium, V – vanadium, Zn – zinc.

Location	Sample	Depth	Al	Ca	Fe	S	Mn	Ag	As	Cd	Co	Cr	Cu	Mo	Ni	Pb	U	V	Zn
		(cm)	(mg/g)				(µg/g)												
Masig	C2	0-2	0.57	370	0.56	1.54	19.0	0.004	1.28	0.02	0.13	2.31	0.45	0.13	0.97	0.53	3.27	2.1	1.4
Masig	C2	2-4	0.71	372	0.58	1.50	19.1	0.005	1.08	0.01	0.18	2.46	0.45	0.11	0.99	0.50	3.20	2.5	1.1
Masig	C2	4-6	0.64	376	0.58	1.44	20.4	0.01	1.10	0.04	0.20	2.5	0.47	0.10	1.01	0.49	3.20	3.0	1.4
Masig	C	0-2	2.36	328	4.71	2.01	58.3	0.01	3.77	0.02	1.04	7.8	1.19	0.25	3.63	1.96	2.24	6.3	7.3
Erub	D	0-2	3.66	321	3.89	1.82	58.3	0.01	4.13	0.05	1.33	10.8	1.93	0.31	5.85	1.72	2.08	11.4	6.7
Erub	D	2-4	2.42	340	3.72	1.79	56.5	0.01	4.36	0.07	1.44	10.1	1.93	0.32	5.84	1.77	2.28	9.8	6.0
Erub	D	4-6	2.42	332	3.71	1.87	62.5	0.01	4.35	0.05	1.29	9.8	1.77	0.30	5.47	1.77	2.31	8.9	6.0
Bramble Cay	E	0-2	0.27	352	0.34	1.24	13.0	0.01	0.74	0.03	0.13	1.79	0.93	0.10	0.84	0.60	1.75	1.8	1.3
Bramble Cay	E	2-4	0.29	358	0.29	1.22	10.9	0.01	0.86	0.04	0.12	1.64	0.86	0.08	0.73	0.54	1.93	1.9	1.2
Bramble Cay	E	4-6	0.28	358	0.27	1.27	10.6	0.01	0.90	0.02	0.09	1.67	0.81	0.07	0.68	0.52	1.98	2.0	0.95
S. of Daru	F	Surface	8.72	202	47.9	1.15	1090	0.01	84	0.05	12.5	22.6	5.69	2.07	15.7	15.2	1.30	97.4	44.0
N. Warrior R	I	0-2	1.23	357	1.24	1.33	33.0	0.01	1.75	0.03	0.30	5.5	0.99	0.10	1.37	0.90	2.32	3.9	2.5
N. Warrior R	I	2-4	1.42	353	1.35	1.43	35.9	0.01	1.98	0.05	0.34	6.0	1.34	0.11	1.66	0.94	2.45	4.5	2.4
N. Warrior R	I	4-6	1.00	338	1.18	1.39	34.6	0.02	1.83	0.06	0.28	5.63	1.19	0.11	1.46	0.86	2.48	3.6	2.03
M. Warrior R	J	0-2	3.21	330	2.96	2.00	43.9	0.02	2.48	0.05	1.01	7.2	2.11	0.21	3.57	1.53	2.49	8.7	4.8
M. Warrior R	J	2-4	4.36	322	3.44	2.09	49.9	0.02	2.06	0.05	0.95	8.6	1.86	0.20	3.54	1.50	2.34	9.0	8.0
M. Warrior R	J	4-6	3.26	335	2.89	1.91	42.5	0.02	1.85	0.04	0.81	7.1	1.67	0.23	3.19	1.26	2.04	7.5	4.8
S. Warrior R	K	0-2	0.76	345	1.15	1.76	48.7	0.01	1.92	0.04	0.27	3.7	0.76	0.14	1.25	1.15	2.26	2.8	1.6
S. Warrior R	K	2-4	1.40	352	1.42	1.78	53.1	0.01	2.03	0.02	0.37	4.4	0.86	0.15	1.51	1.24	2.21	4.0	2.3
S. Warrior R	K	4-6	1.02	349	1.22	1.84	49.2	0.01	1.78	0.03	0.32	3.9	0.75	0.15	1.34	1.23	2.15	3.2	1.9
	DGV		-	-	-	-	-	1	20	1.5	-	80	65	-	21	50	-	-	200

Table 7–11: Benthic sediment metals data, Saibai and Boigu Islands survey, November 2020. Figures in red exceed the ANZG sediment quality guideline value. Note: Al – aluminium, Ca – calcium, Fe – iron, S – sulfur, Mn – Manganese, Ag – silver, As – arsenic, Cd – cadmium, Co – cobalt, Cr – chromium, Cu – copper, Mo – Molybdenum, Ni – nickel, Pb – lead, U – uranium, V – vanadium, Zn – zinc.

Site	Depth (cm)	Al	Ca	Fe	S	Mn	Ag	As	Cd	Co	Cr	Cu	Mo	Ni	Pb	U	V	Zn
Saibai		(mg/g)				(µg/g)												
S1	0-2	12.7	125	32.3	0.88	403	0.02	26.1	0.04	12.1	20.7	7.82	0.49	20.3	12.5	0.89	58.8	45.9
S1	2-4	12.6	122	30.9	0.84	365	0.01	25.4	0.03	11.3	20.3	7.01	0.46	20.1	12.3	0.92	51.7	45.3
S1	4-6	15.0	116	30.5	0.94	361	0.02	21.7	0.03	11.3	22.7	7.88	0.45	20.6	12.4	1.06	54.7	47.4
Site 8	0-2	17.9	159	38.1	1.04	454	0.02	24.5	0.08	10.7	29.8	10.3	0.76	18.4	14.3	1.12	77.5	56.0
Site 8	2-4	12.0	114	32.1	1.19	319	0.02	17.9	0.03	10.6	24.4	11.4	0.57	19.5	13.5	1.34	51.9	50.9
Site 8	4-6	12.3	114	31.7	1.21	313	0.02	15.4	0.03	10.7	24.3	11.6	0.55	19.7	13.4	1.34	49.4	49.5
Site A	0-2	10.5	245	33.7	0.50	624	0.01	78.9	0.05	8.83	15.6	6.18	0.95	13.5	13.2	1.16	70.6	27.9
Site A	2-4	11.5	226	38.0	0.48	603	0.02	79.5	0.04	9.71	18.2	6.75	1.19	14.7	14.7	1.15	78.5	30.9
Site A	4-6	9.1	241	33.7	0.53	496	0.01	68.1	0.06	9.17	16.0	6.62	0.85	14.0	13.8	1.20	66.0	30.2
Boigu																		
Site 2	0-2	13.3	113	27.4	1.06	343	0.02	14.5	0.02	9.99	21.4	7.20	0.36	18.3	10.3	0.91	49.4	44.4
Site 2	2-4	13.1	122	24.8	1.67	312	0.02	12.6	0.02	9.62	20.4	7.80	0.34	17.7	10.1	1.07	42.2	42.7
Site 2	4-6	16.2	120	25.7	1.85	319	0.01	12.5	0.02	10.1	22.8	8.34	0.37	18.7	10.3	1.02	50.5	44.8
Site 3	0-2	15.1	123	25.3	1.88	320	0.01	12.8	0.04	9.87	22.0	8.02	0.33	18.3	10.1	1.01	47.3	44.0
Site 3	2-4	13.9	150	30.2	1.11	328	0.02	18.7	0.03	8.55	23.4	7.64	0.51	15.3	10.7	0.99	60.5	38.6
Site 3	4-6	14.4	146	36.8	1.19	338	0.02	23.6	0.04	9.14	26.6	8.11	0.68	16.0	12.3	1.08	75.5	39.6
Site 3 duplicate	0-2	10.3	126	28.3	1.39	338	0.02	18.3	0.03	9.10	20.6	9.09	0.52	15.8	11.9	0.99	50.1	41.2
Site 3 duplicate	2-4	14.4	141	3.31	1.09	374	0.02	25.3	0.02	9.24	22.7	7.87	0.58	16.5	12.3	1.02	59.2	39.9
Site 3 duplicate	4-6	10.0	131	41.7	1.44	342	0.02	32.0	0.02	10.0	24.7	8.40	1.06	16.5	14.6	1.15	79.7	37.8
DGV		-	-	-	-	-	1	20	1.5	-	80	65	-	21	50	-	-	200
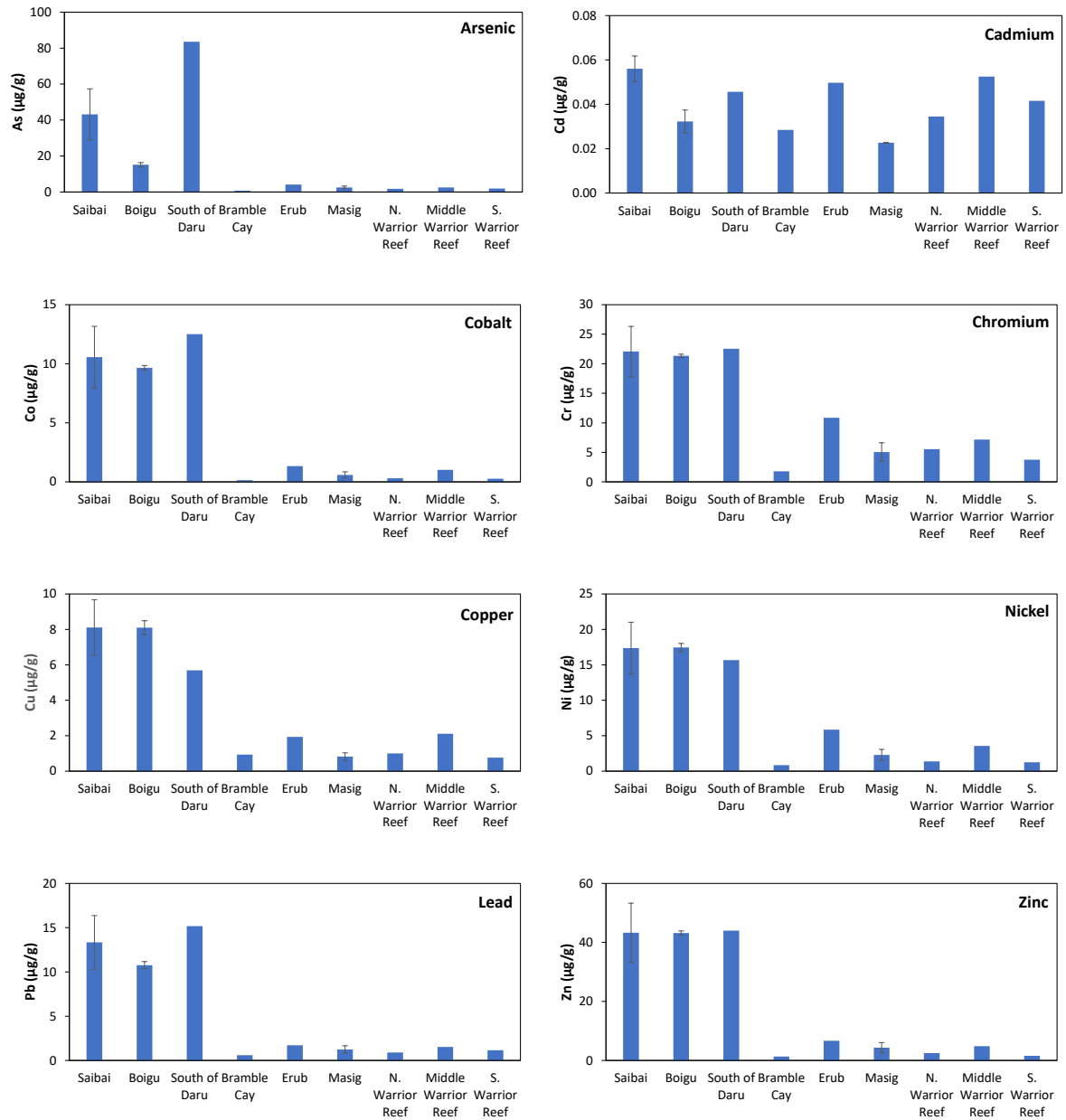
Figure 7–11: Variation of benthic sediment metal concentrations with location (mean ± standard error)

As observed in the previous NESP study (Apte et al. 2018), there were numerous strong correlations (r>0.8) between many of the 65 trace elements measured in sediments indicating common sources. Most of the correlating elements could be separated into two groups. Around 36 elements were enriched in samples from the northern sites including aluminium, iron, copper, cobalt and lead. Particulate calcium, (an indicator of calcium carbonate content), displayed a strong inverse relationship with this group of elements, with the lowest calcium concentrations found at northern sites. A smaller number of elements (strontium, boron, uranium, palladium and ruthenium) correlated strongly with calcium (r>0.8) thus indicating a common marine origin. Cadmium was not strongly correlated with any other element.

The spatial trends observed in particulate metal concentrations can be related to the relative amounts of marine-derived, calcium carbonate dominated particulates which have low metal concentrations, and fine, terrigenous sediments containing far higher concentrations of most trace elements. Not surprisingly, the highest metal particulate concentrations are found in the coastal sediments closest to the PNG mainland which are dominated by fine sediments.

Trace element concentrations in sediments were compared to sediment quality guideline values that apply in Australia (Table 7–10 and Table 7–11). Note that guideline values are not currently available for all metals. The concentrations of most trace elements were generally well below the guideline values, reflecting uncontaminated environments (Table 7–10 and Table 7–11). However, particulate arsenic concentrations exceeded the ANZG (2018) sediment quality guideline values (DGV) at the site South of Daru (F) and in core sections from most of the Saibai and Boigu sampling sites (Table 7–11). The concentrations of arsenic in samples taken at Saibai were higher than observed in the 2016 survey where cores were taken at Site A and Site 8 (Apte et al. 2018), but this is likely to be a result of the more comprehensive coring program around Boigu and Saibai undertaken in the present study which captures environmental variability more accurately.

The particulate arsenic concentrations at the site South of Daru (F) and East Saibai (Site A) also exceeded the ANZG (2018) GV-high value of 70 µg/g which is an indicator of potential toxicity problems but is not intended to be a guideline value for the protection of ecosystems. Given that the arsenic concentrations were fairly uniform throughout the measured core profiles, it is reasonable to assume that these arsenic concentrations reflect natural background mineral enrichment in the area rather than recent contamination. Similarly, particulate nickel concentrations which are approaching DGV concentration in samples from around Boigu and Saibai (Table 7–11) display uniform core profiles that are indicative of natural background mineral enrichment as opposed to recent contamination.

A comparison between the current data and the 2016 NESP benthic sediments data set is shown in Figure 7–12. There was reasonable agreement between the 2016 and 2020 surveys aside from:
- higher particulate arsenic concentrations at East Saibai Site A in 2020
- higher particulate cadmium concentrations at Masig (Site C) and Bramble Cay (Site E) in 2016.

It is unlikely that these differences are the result of differences in sampling or analysis as the same procedures were used in both surveys. Further coring in the area is required to confirm if sediment heterogeneity is the reason for the differences. However, it should be noted that

the ANZG sediment quality framework (2018), recognises that depending on underlying geology, the benthic sediments in some areas will be naturally enriched in trace metals to above guideline values and this natural phenomenon does not necessitate any further management actions.

Three of the sites sampled in the current study were close to the sites sampled during the Torres Strait Baseline Study conducted in the early 1990's (Dight and Gladstone, 1993). Compared to the 2016 and 2020 surveys, the baseline study measured far higher concentrations of copper, chromium, cobalt, nickel, lead and zinc at Bramble Cay (Figure 7–12). For instance, the concentrations of particulate copper measured during the baseline study ranged from 18 to 23 μg/g and were over an order of magnitude high than the concentrations measured in the current study (*Ca*. 1 μg/g). The discrepancy in concentrations was traced to large differences in the amount of fine sediments at the sampling locations. During the baseline study fine sediments (<63 μm diameter) comprised 38-50% of the total sediment mass. This compares to <10% during the NESP surveys. It is not clear why there is such a large difference. The data may reflect geomorphological changes at Bramble Cay over the last 30 years or transient deposition of fine sediments at this location.

Particulate chromium concentrations were consistently higher at all three locations sampled in 1993. When comparing the data it is important to take into account the advances in analytical chemistry techniques that have occurred since the Torres Strait Baseline Study was conducted some 30 years ago. Most of the metals in the baseline study were determined directly without sample digestion by X-ray fluorescence spectrometry (XRF) as compared the current study which used acid digestion followed by ICPMS which is typically one order of magnitude more sensitive. The acid digestion procedure used in the NESP surveys was not designed to solubilise all forms of particulate metals. Metals associated with silicates and refractory elements such as chromium are particularly insoluble, however, for many metals (e.g. copper and zinc) near full recovery from particulates can be expected (Gaudino et al. 2007). For environmental studies which focus on the interactions of particulates with living organisms, the fraction of metals not mobilised by acid digestion is not likely to play a significant environmental role and can be regarded as being biologically inert. The differences in analytical methodologies therefore explains the marked differences in particulate chromium concentrations measured between the two studies.
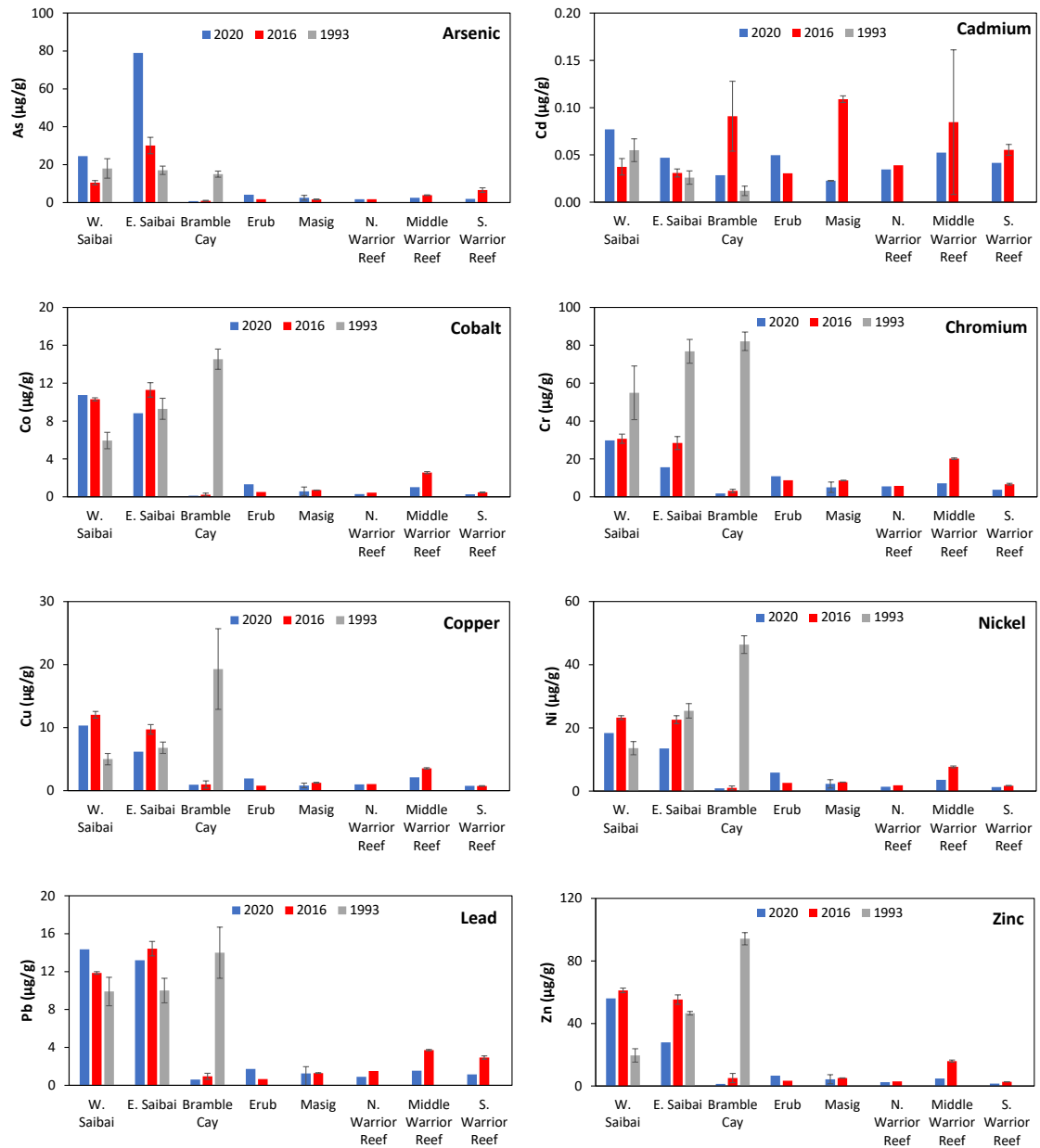
Figure 7–12: Comparison of benthic sediment metal concentrations measured in this study with previous data (mean ± standard deviation): 2016 NESP sampling campaign and three sites from the Torres Strait Baseline Study (Dight and Gladstone, 1993).

Trace elements in total suspended solids

The concentrations of 62 trace elements were measured in suspended sediment samples. The data for the 16 most commonly monitored elements are shown in Table 7–12. The data for all elements and associated laboratory quality control data are available in the eAtlas data repository.

Boigu Site 1 duplicate measurements (TSS = 9.3 mg/L) indicated a relative percentage difference for the replicates in Table 7–12 ranging typically from 2 to 20%. It should be noted that the TSS concentrations in many of the samples collected during the survey were below 4 mg/L (Table 7–12). The determination of particulate trace metals at such low TSS concentrations is challenging and the data will be subject to a greater uncertainty than encountered at higher TSS concentrations.

The variation of TSS elemental concentrations with location is shown for key trace elements in Figure 7–13. Arsenic, cobalt, nickel, aluminium and iron concentrations were highest at the sites around Boigu and Saibai whereas the highest copper and lead concentrations were observed at Bramble Cay, the site closest to the Fly River Estuary. Particulate zinc was also high at Bramble Cay, however, the highest zinc concentration was recorded at Erub. Erub is a volcanic island and the local geology is likely to influence trace element concentrations in the surrounding waters. Aluminium and iron concentrations were also highest around Boigu and Saibai, reflecting their association with fine, terrigenous sediments. By contrast, calcium displayed the opposite trend at Boigu and Saibai which is consistent with a marine origin for this element (i.e. calcium carbonate-based minerals).

A comparison of the TSS data for selected elements with surface layer benthic sediment data from the same or closest location is shown in Figure 7–14. Most of the trace metals show some enrichment in suspended sediments whereas elements such as calcium show an opposite trend with consistently higher concentrations in the benthic sediments. Typically, resuspension events will suspend fine sediments which have higher metal concentrations than the bulk sediments. There are also other potential sources of suspended sediments to the system including the Fly River plume, contributions from coastal rivers to the west of Daru and biogenic material. The relative contributions of these other sources will vary depending on location. It is noteworthy that the data for Bramble Cay (Figure 7–14) indicates very large differences between the TSS metals and benthic metal concentrations for copper and lead which could be associated with contributions from the Fly River plume. The same trends were observed in the earlier NESP project (Apte et al. 2018).

The current data is compared with TSS data obtained during the 2016 and 2018 NESP surveys in Figure 7–15. Despite the different sources of TSS and the variability of their contributions, there is generally good agreement between the data sets (most elemental concentration data is within a factor of two or better) however there are marked differences between surveys for copper, lead, manganese and zinc at the Bramble Cay site where the metal concentrations recorded from the current study are much higher compared to other locations in the Torres Strait. These differences may be related to the temporal variability of sediment contributions from the Fly River plume to the suspended sediment load at this site.

Discussion of the results in comparison with concentrations found in other locations and in the previous studies in the Torres Strait is included in Section 8.2.

Table 7–12: TSS-bound metal concentrations for the Saibai and Boigu Islands survey November 2020 (Nov 2020) and Torres Strait Regional survey October/November 2020 (Oct/Nov 20). Note: Al – aluminium, Fe – iron, S – sulfur, Ca – calcium, As – arsenic, Cd – cadmium, Co – cobalt, Cr – chromium, Cu – copper, Mn – Manganese, Mo – Molybdenum, Ni – nickel, Pb – lead, V – vanadium, Zn – zinc, U – uranium.

Survey	Location	Sample	TSS	Al	Fe	S	Ca	As	Cd	Co	Cr	Cu	Mn	Mo	Ni	Pb	V	Zn	U
			(mg/L)	(mg/g)				(µg/g)											
Nov 2020	Boigu	Site 1	9.3	17.7	34.0	2.5	50.1	17	<1	13	36	24	566	1.6	35	22	49	151	0.81
Nov 2020	Boigu	Site 1 duplicate	-	24.4	35.8	3.2	50.1	13	<1	14	34	19	568	0.5	33	20	62	131	0.80
Nov 2020	Boigu	Site 1 Mean	9.3	21.1	34.9	2.9	50.1	15	<1	14	35	22	567	1	34	21	55	141	1
Nov 2020	Saibai	Site 8	25	22.9	36.9	2.3	56.8	15	<0.3	14	36	32	541	1	32	22	59	153	1
Nov 2020	Saibai	S3	15	26	32.8	2.1	81.3	13	<0.4	20	37	29	502	0.6	31	17	65	103	0.94
Oct/Nov 2020	East of Saibai	G	3.7	14.1	11.7	5.7	138	3	1	2	38	<9	239	0.6	18	22	24	50	1.8
Oct/Nov 2020	South of Daru	F	1.0	12.9	15.3	13.1	25.2	6	<1	6	<21	21	554	2	18	15	46	45	0.56
Oct/Nov 2020	Bramble Cay	E	1.0	12.1	13.8	13.5	22.4	9	<1	8	<27	76	605	3	18	37	35	167	0.5
Oct/Nov 2020	Erub	D	0.3	5.0	9.6	8.6	181	9	<3	<4	<67	<43	155	7	23	30	<12	173	2
Oct/Nov 2020	North Warrior Reef	I1	2.0	12.9	9.93	7.47	132	4	1	<1	25	<10	148	1	11	27	23	43	1.6
Oct/Nov 2020	Middle Warrior Reef	J	6.0	13.1	11.4	5.59	207	5	<0.5	2.9	34	<6	167	0.9	13	6	23	36	2.9

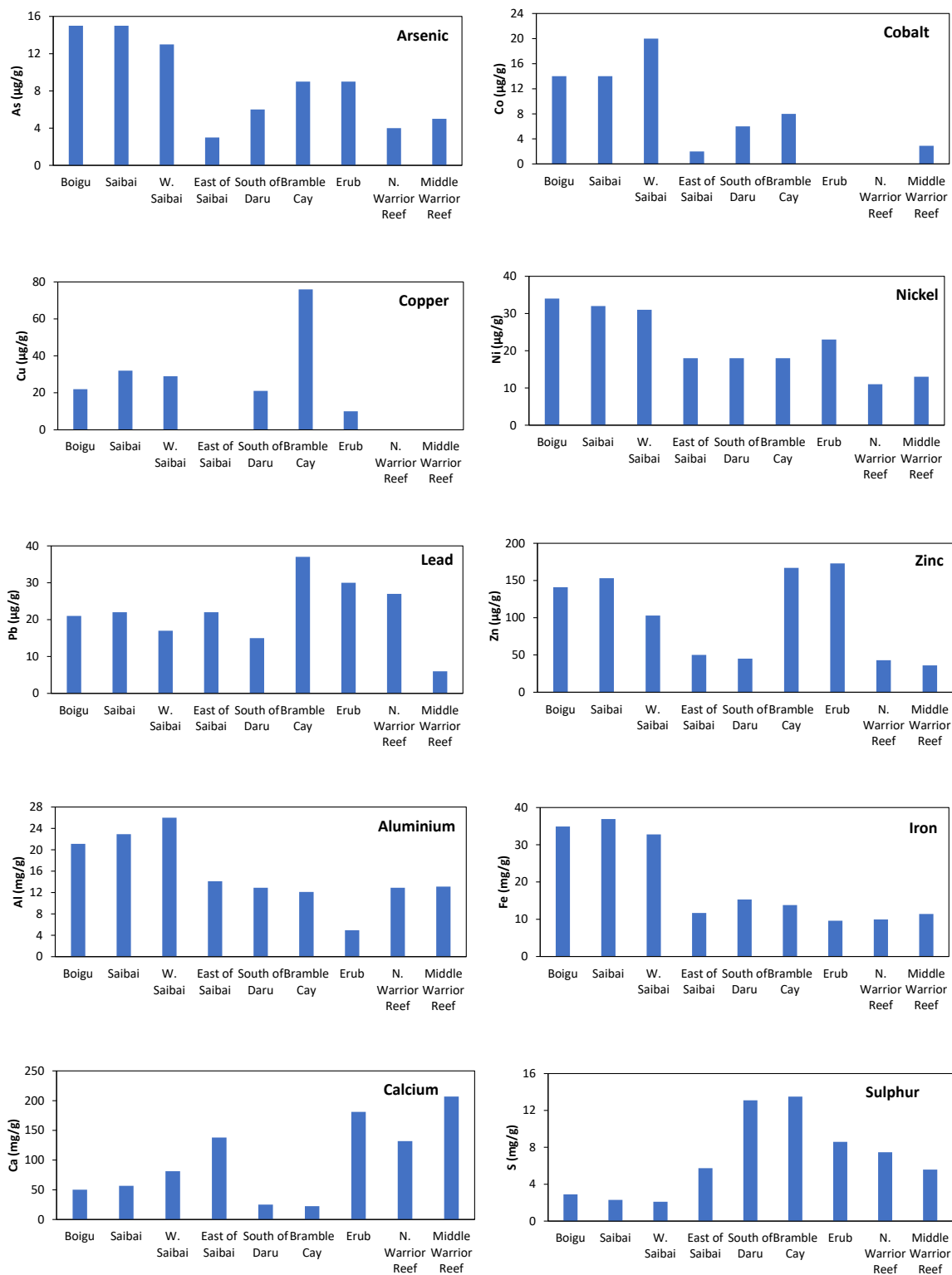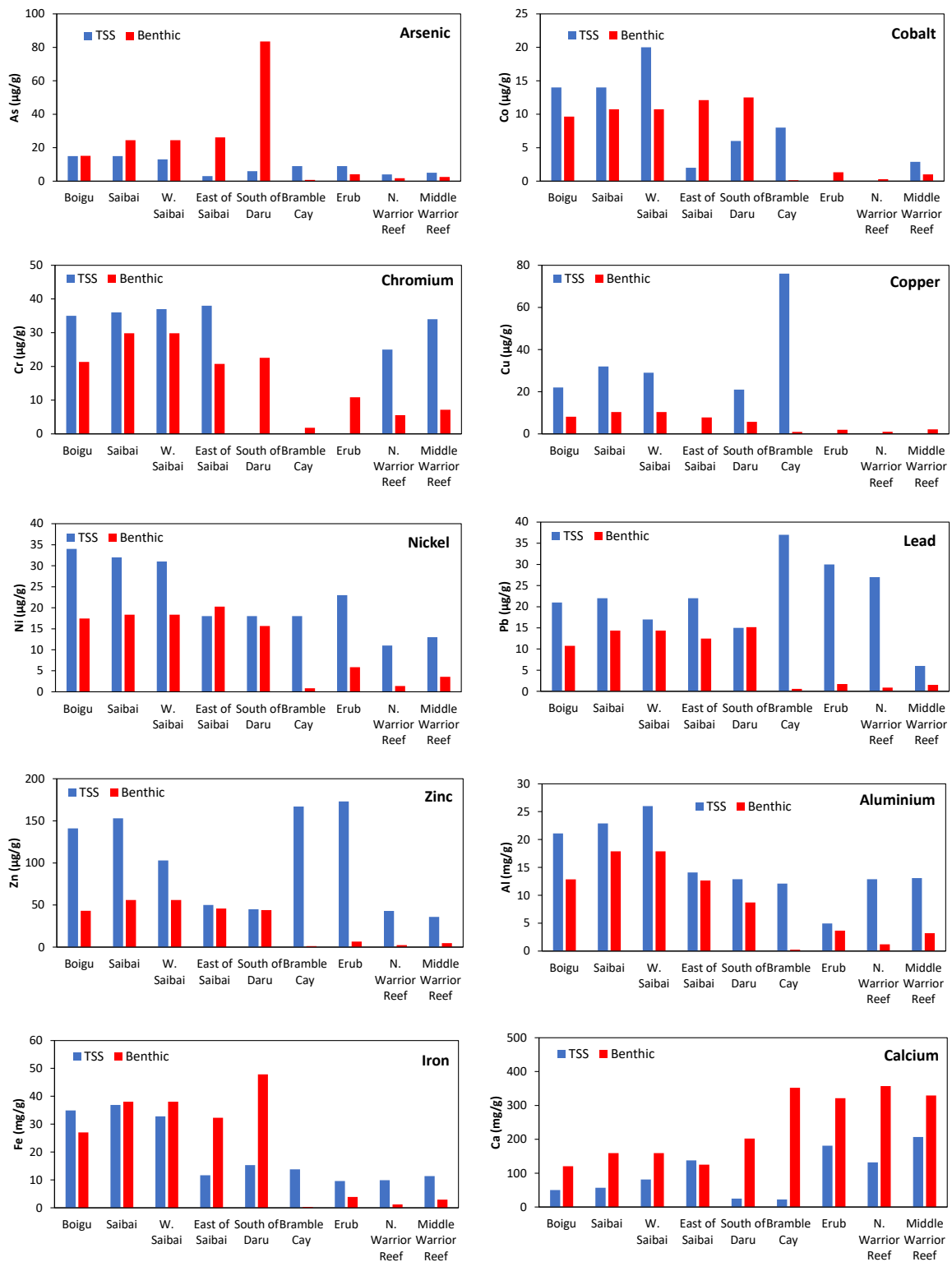**Figure 7–13: Variation of TSS trace metal concentrations with location (data below detection limit not shown).**

Figure 7–14: Comparison of TSS trace metal concentrations with surface sediment concentrations at each site (data below detection limit not shown).
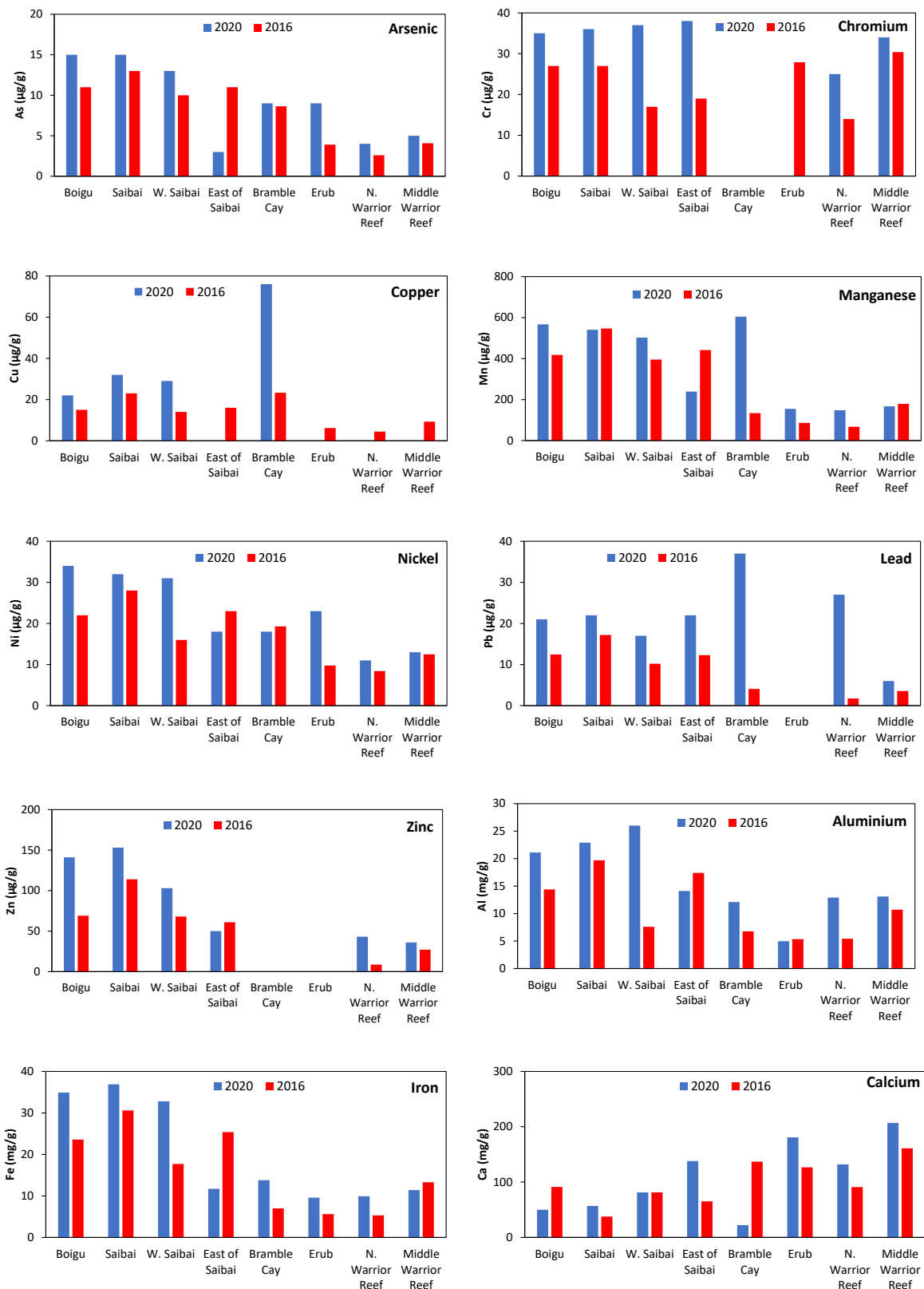
Figure 7–15: Comparison of TSS trace metal concentrations obtained in 2020 with the previous NESP survey data (2016). Data below detection limit not shown.

7.3.2 Tracing mine-derived sediments

Method validation results

SEM images obtained for the validation test samples are shown in Figure 7–16. Note the distinctly lighter colour of the denser sulphide mineral particles compared to the natural sediment background. The EDS layered element maps for the validation samples are shown in Figure 7–17. The detection of pyrite or chalcopyrite particles which were added to the samples is clearly indicated in all images aside from the sediment control by particles yellow or white coloration in the images.

Application to sediments

The list of samples analysed is presented in Table 7–13. The samples comprised 5 suspended sediment samples and 18 benthic sediment core slices. The samples were taken during the 2020 sampling campaigns and also included archived sediment samples from the November 2016 field campaign. The samples spanned a range of sites where elevated copper concentrations have been detected including Saibai, Boigu, Bramble Cay and the Warrior Reef. It was not possible to analyse TSS samples having very low solids concentrations (e.g. <10 mg/L) as the samples did not contain sufficient solids material for accurate analysis.

Examples of SEM images obtained for the samples analysed are shown in Figure 7–18 with a larger range of images presented in Appendix A. It is noteworthy that the images obtained have a low abundance of <2 μm size particles which demonstrates the effectiveness of the clay removal step. The images show a range of different particle types and morphologies. The differences in morphologies between the samples containing a high proportion of fine sediments (e.g. Boigu and Saibai) from coral dominated sediments (e.g. Bramble Cay and Warrior Reef) are particularly noticeable.

Examples of EDS elemental spectra obtained for an range of samples are shown in Figure 7–19, Figure 7–20 and Figure 7–21 and a comprehensive collection of spectra indicating the detection of target elements shown in Appendix B. Note that EDS detects elements present at significant concentrations (% range) and is ideally suited to detecting mineral particles containing a high abundance of elements such as copper, sulphur and iron.

The mineral particles detected by SEM/EDS are summarised in Table 7–14 and Table 7–15. Particles containing copper, iron and sulphur (indicative of the copper sulphide minerals such as chalcopyrite or bornite) were detected in four TSS samples from the Boigu and Saibai region and in two benthic sediment surface samples from Saibai and the Warrior Reef. The diameter of the particles containing Cu, Fe and S ranged from 4 to 30 microns with many being embedded in larger sediment particles.

Iron and sulphur containing particles were detected in three benthic sediment samples originating from Saibai and Bramble Cay. The detection of particles containing iron and sulphur alone, does not necessarily indicate a mine-related origin as pyrite and other iron sulphide minerals may naturally occur in coastal sediments.

A number of particles containing detectable amounts of elements such as Ti, V and Zr were also detected in some benthic sediment samples and these are also listed in Table 7–15. The associated minerals are not likely to be of mine origin but were noted for scientific interest.

Their detection is consistent with the known presence of mineral sands in the Gulf of Papua which are enriched in elements such as titanium and zirconium (Mayur Resources 2021).

At this stage the occurrence of low concentrations of mineral particles containing Cu, Fe and S (indicative of chalcopyrite or bornite) cannot be conclusively linked to a mine origin. However, their detection particularly in suspended sediments is consistent with transport of some mine-derived materials from the Fly River. Further application of the tracer techniques to sediments from the Fly River is required to provide further evidence on the origin of these particles.

Chalcopyrite
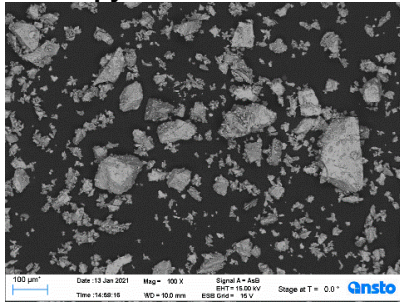
Pyrite

10% chalcopyrite
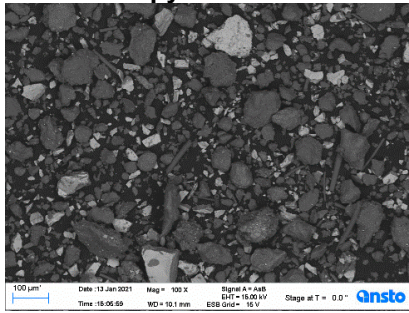
10% pyrite
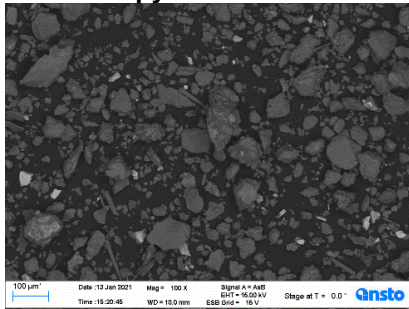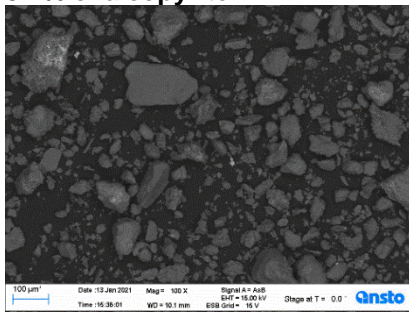
1% chalcopyrite

1% pyrite

0.1% chalcopyrite

0.1% pyrite

Control sediment
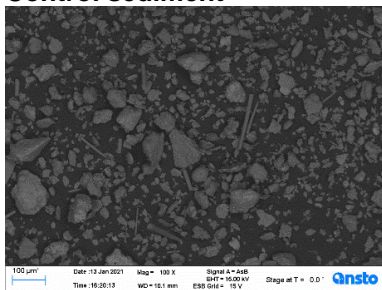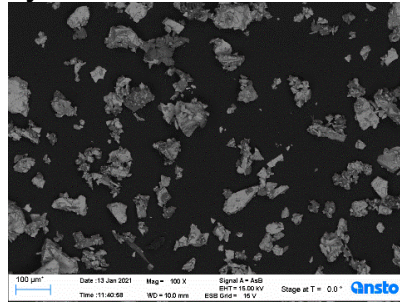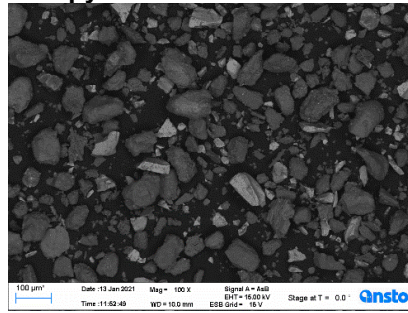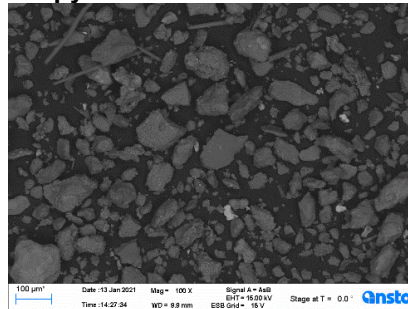
Figure 7–16: SEM images of the processed mineral/sediment mixtures. Note the lighter colours indicate the presence of dense minerals such as metal sulphides.

10% chalcopyrite
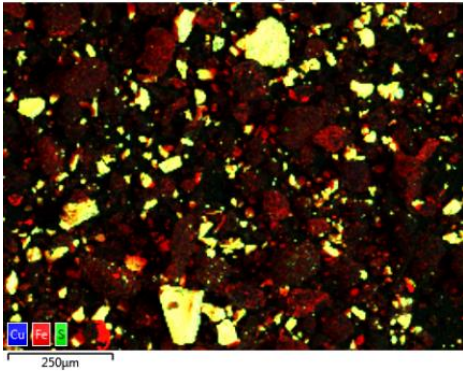
10% pyrite
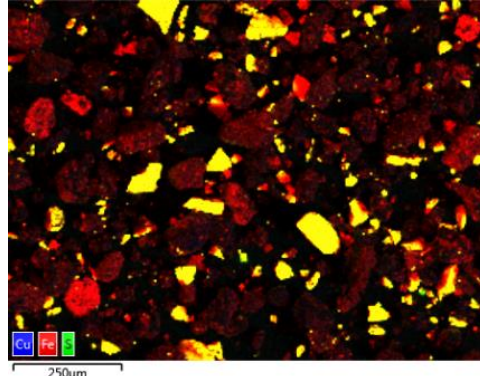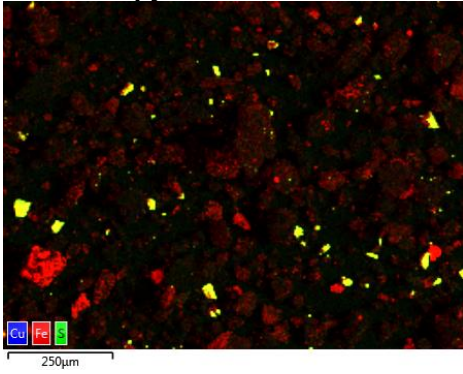
1% chalcopyrite
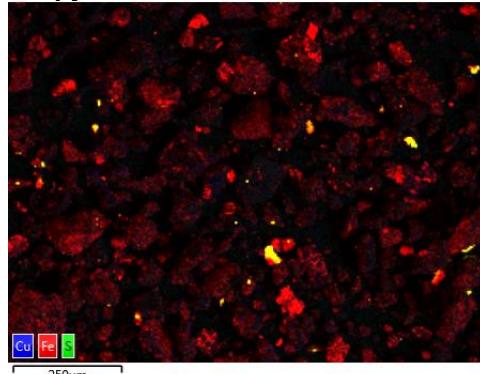
1% pyrite

0.1% chalcopyrite
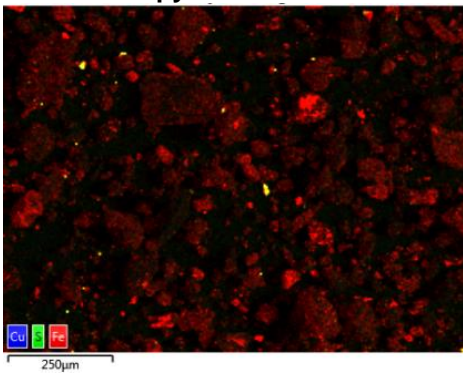
0.1% pyrite
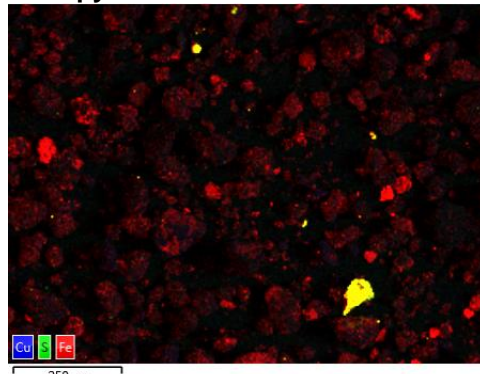
Control sediment
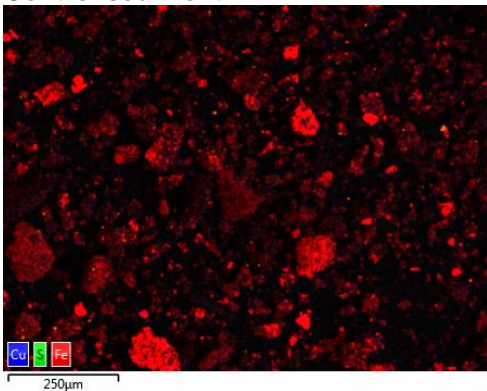
Figure 7–17: EDS maps of the processed mineral/sediment mixtures. Note the lighter colours (e.g. yellow) indicate the presence of, iron and sulphur and copper.

Table 7–13: List of sediment samples analysed by SEM.

Location	Survey	Sample	
TSS samples			
Boigu	December 2019	B6	
Boigu	December 2019	B8	
Boigu	December 2019	B9	
Saibai	December 2019	Site A	
Saibai	December 2019	S4	
Benthic sediments			**Core slice**
Saibai	November 2020	Site 1	0-2 cm
Boigu	November 2020	Site 2	0-2 cm
Boigu	November 2020	Site 3	0-2 cm
Saibai	November 2020	Site 8	0-2 cm
Saibai	November 2020	Site A	0-2 cm
Saibai	October 2016	Site A core 1	0-2 cm
Saibai	October 2016	Site A core 1	2-4 cm
Saibai	October 2016	Site A core 2	0-2 cm
Saibai	October 2016	Site A core 2	2-4 cm
Saibai	October 2016	Site A core 2	4-6 cm
Saibai	October 2016	Site A core 3	0-2 cm
Saibai	October 2016	Site A core 3	2-4 cm
Saibai	October 2016	Site A core 3	4-6 cm
Warrior Reef	October 2016	Site E	Surface layer 1
Warrior Reef	October 2016	Site E	Surface layer 2
Warrior Reef	October 2016	Site E	Surface layer 3
Bramble Cay	Oct/Nov 2020	Site E	0-2 cm
South of Daru	Oct/Nov 2020	Site F	Surface layer

Saibai, Site 4 suspended sediment
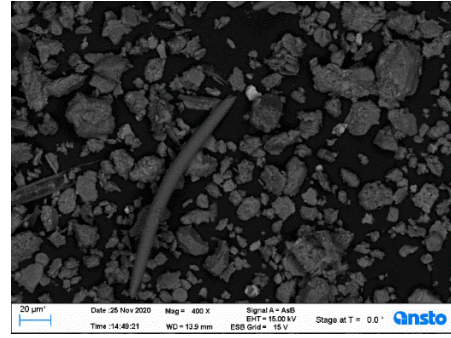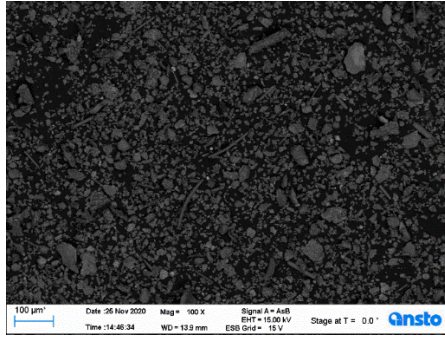
Saibai, Site 8 benthic sediment core: 0-2 cm slice
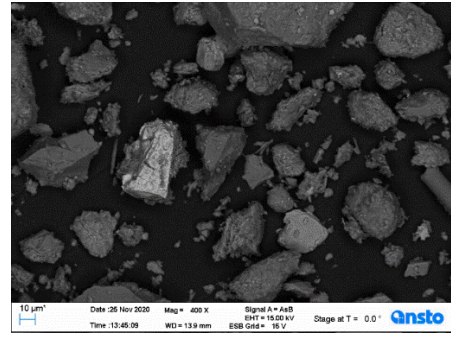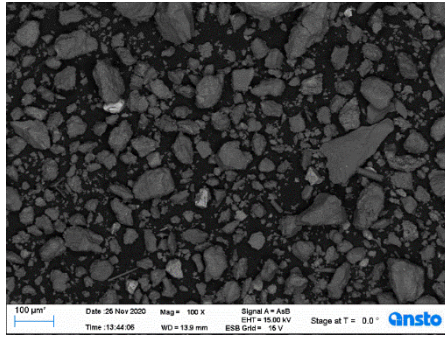
Warrior Reef, Site E benthic sediment core: 0-2 cm slice
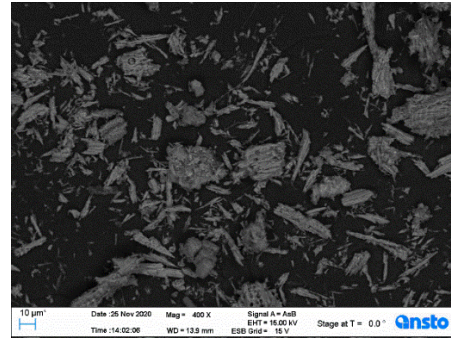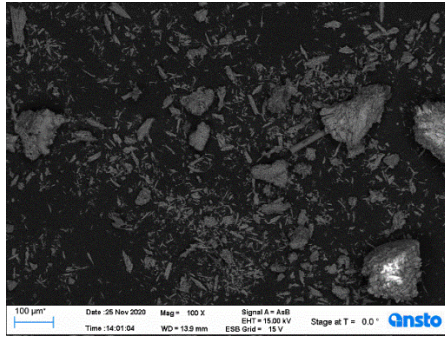
South of Daru, Site F benthic sediment surface layer
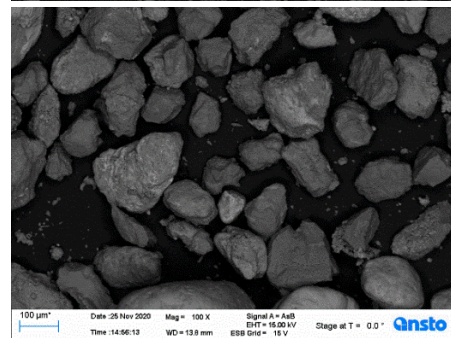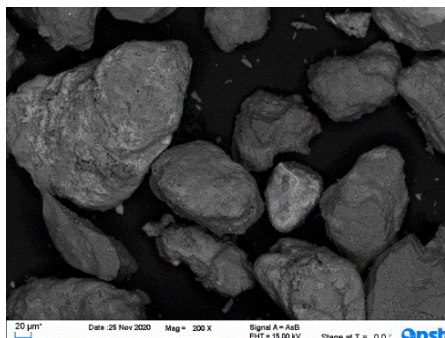
Bramble Cay, Site E#3 benthic sediment surface layer
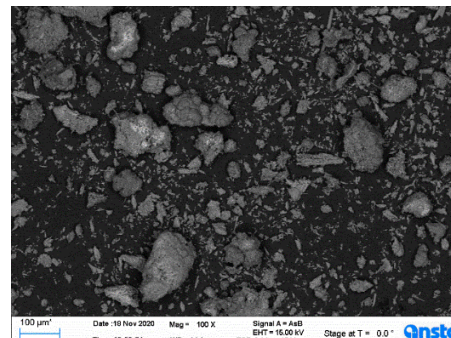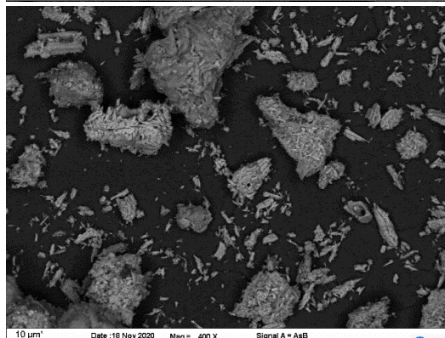
Figure 7–18: Examples of SEM images obtained for the samples analysed.

105

Benthic sediment sample: E3

Warrior Reef, October 2016 survey, Spectra 43 and 44 – copper (Cu), iron (Fe), sulphur (S).
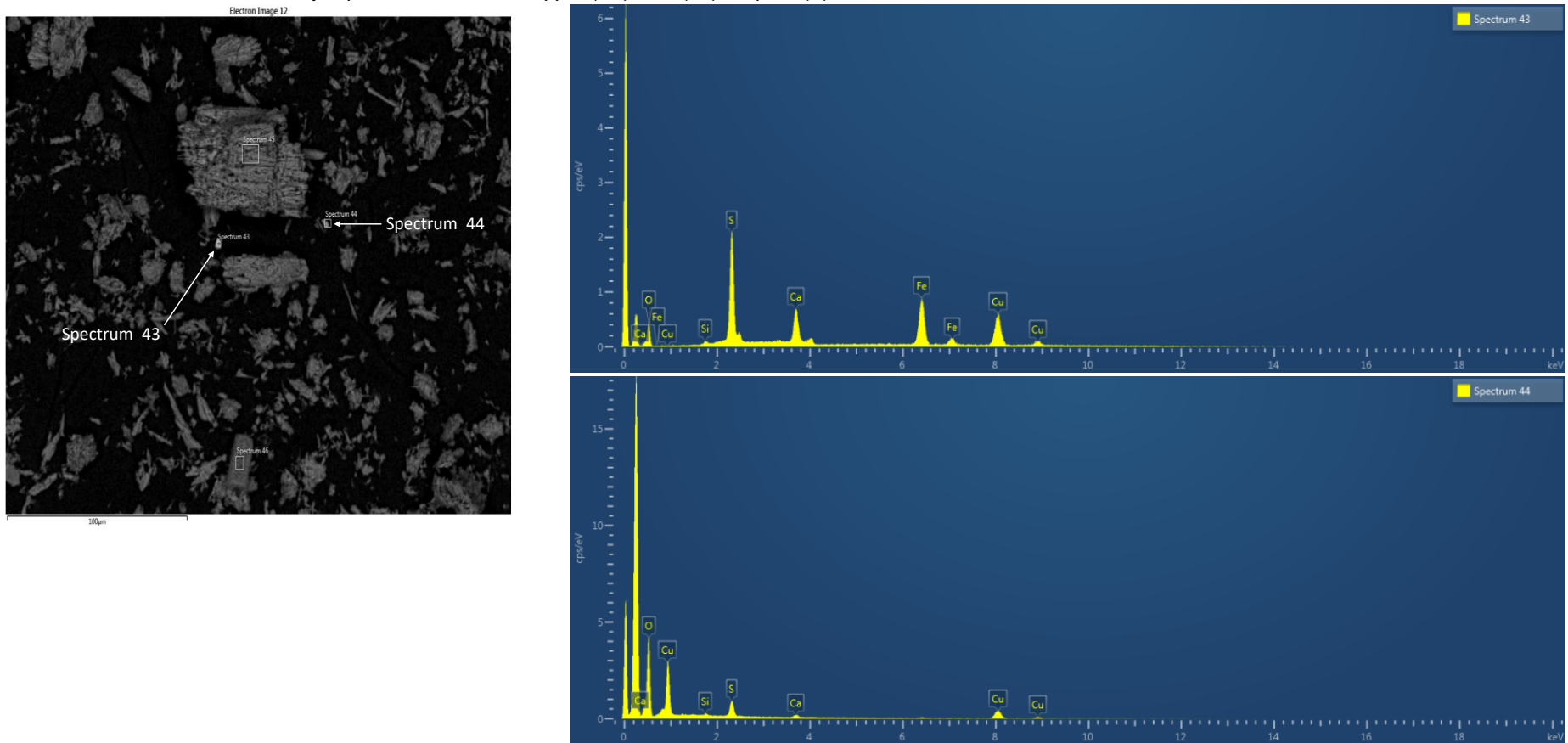
Figure 7–19: Example of EDS spectra obtained: sample E3.

TSS sample: B6

Boigu Island, December 2019 survey, Spectrum 36 copper (Cu), iron (Fe), sulphur (S), spectrum 38 Fe and S.
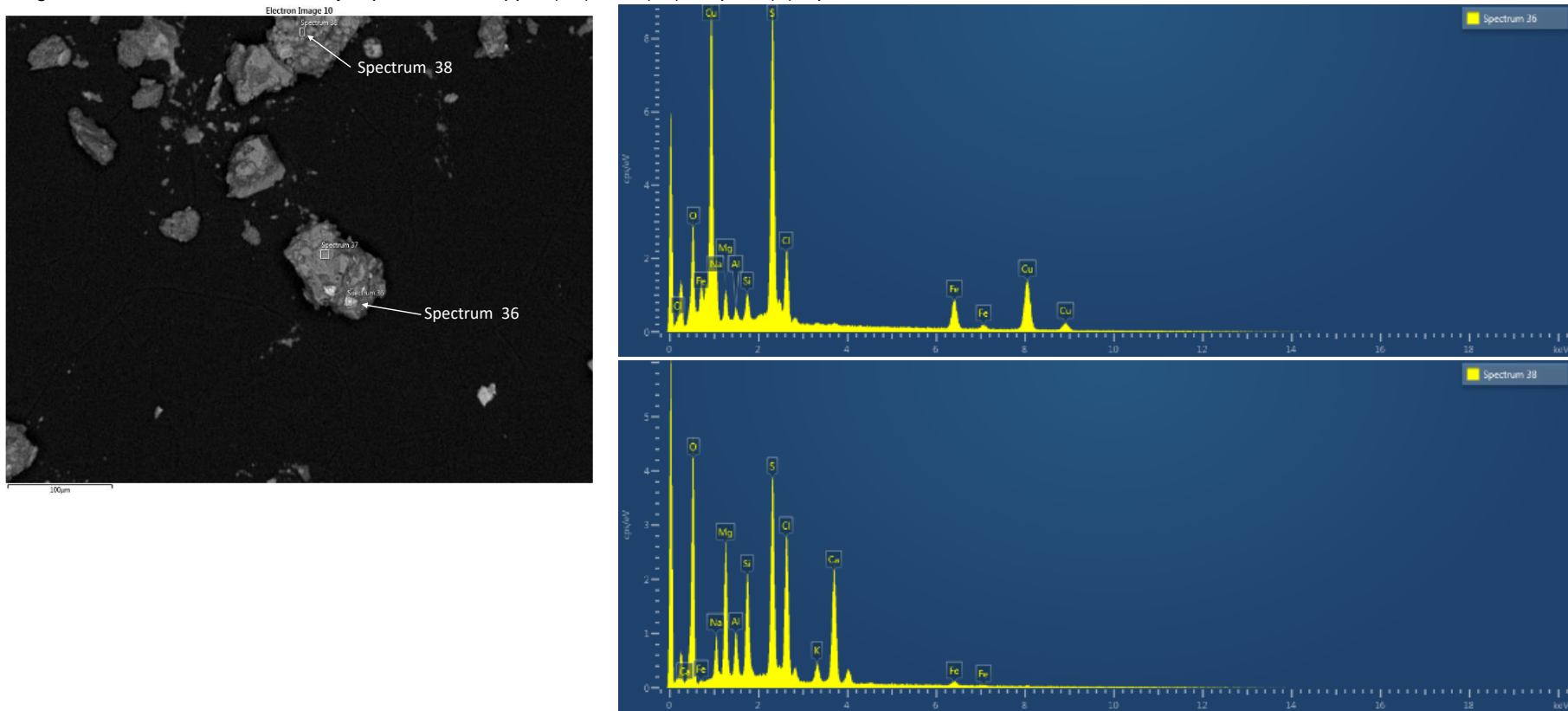
Figure 7–20: Examples of EDS spectra obtained sample B6.

Sample: B9

Boigu Island, December 2019 survey, Spectra 39 and 40 copper (Cu), iron (Fe), sulphur (S).
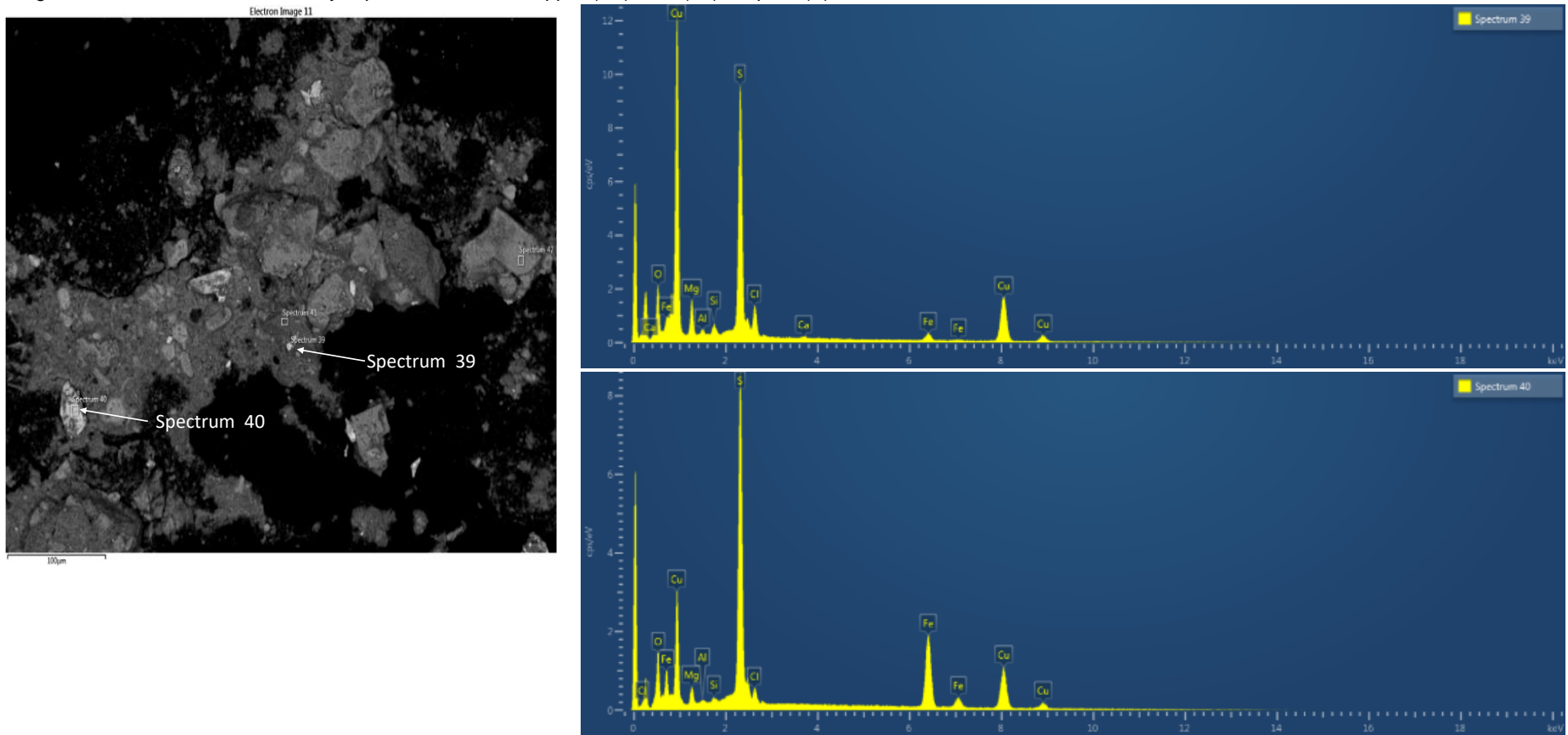
Figure 7–21: Examples of EDS spectra obtained for sample B9.

Table 7–14: Benthic sediment samples with target elements detected by SEM.

Location	Survey	Sample code	Depth	Detected
Boigu	November 2020	Site 2	0-2 cm	Spectrum 5-101 Zirconium (Zr), Spectrum 3-4 – Copper (Cu)
Saibai	November 2020	Site 8	0-2 cm	Spectrum 3-12 contains vanadium (V) and titanium (Ti)
Saibai	November 2020	Site A	0-2 cm	Spectrum 3-16 – Zr detected. Spectrum 3-15 – cerium (Ce), Spectrum 5-86 rare earths, spectrum 5-87 – Ti
Saibai	October 2016	Site A core 1	0-2 cm	Spectrum 5-80 – Ti, Spectrum 5-85 – Cu, S, Spectrum 4-21 high Ti
Saibai	October 2016	Site A core 2	0-2 cm	Spectrum 2-10 light coloured, well-ordered particle containing Ti and some V
Saibai	October 2016	Site A core 2	4-6 cm	Spectrum 2-16 light, rounded particle – FeS
Saibai	October 2016	Site A core 3	0-2 cm	Spectrum 2-26 – V and Ti
Saibai	October 2016	Site A core 3	0-2 cm	Spectrum 4-29 – rare earths, spectrum 4-30 some V, spectrum 4-31 Fe and S
Bramble Cay	Oct/Nov 2020	Site E	0-2 cm	Spectrum 5-62 – Fe, S
Warrior Reef	October 2016	Site E	Surface 3	Spectra 4-43 and 4-44 - Cu, Fe, S, Spectra 5-55 Cu, Fe, S, Spectra 5-54 Fe, S

Table 7–15: TSS samples with target elements detected by SEM.

Location	Survey	Sample code	Detected
Boigu	December 19	B6	Spectrum 4-36 Cu, Fe and S, spectrum 4-38 Fe and S
Saibai	December 19	Site A	Spectrum 4-33 Cu and S, spectrum 4-34 Fe,S
Boigu	December 19	B9	Spectra 4-39 and 4-40 Cu, Fe, S
Boigu	December 19	B8	Spectra 5-44 and 5-45 Ti, spectrum 5-49, 5-50 Cu, Fe, S

7.3.3 Seagrass surveys

2020 studies

The results for 22 trace elements analysed in 46 seagrass samples collected across the region are available in the eAtlas repository along with the laboratory quality control data. The species composition of the seagrasses sampled varied with location (Table 7–16) with *Halodule, Halophila, and Enhalus spp.* dominant at the Boigu and Saibai sampling sites whereas *Cymodocea* and *Thalassia spp.* were found at all of the other sites.

This section focuses on the key metals that are of regulatory interest because of their intrinsic toxicity to marine organisms: arsenic, cadmium, cobalt, chromium, copper, nickel, lead and zinc (ANZG 2018). These elements are often present at elevated concentrations in marine systems owing to anthropogenic contamination. The data is presented in the form of element concentration versus location plots in Figure 7–22 and the complete data set for the contaminants of interest plus iron and manganese in Table 7–16.

The plots (Figure 7–22) indicate markedly higher concentrations of cobalt, chromium, copper, lead and zinc in seagrasses at the Boigu and Saibai sites. The other elements do not display this trend. Copper lead and zinc were also higher at Bramble Cay compared to the remaining sites.

The mean arsenic and cadmium data for the North Warrior Reef site (I) were weighted by two out of the five replicate samples I1 and I2 (Table 7–16) which have far higher concentrations (arsenic: 138 and 123 µg/g, Cadmium: 2.38 and 2.13 µg/g) than the other replicates. Additional tissue subsamples were digested, analysed and confirmed the high concentrations. The concentrations of cadmium in samples I1 and I2 are within the range reported in seagrass studies around the world (Govers et al. 2018, Lewis and Devereux 2009). The elevated arsenic concentrations were higher than, but not appreciably different to seagrass arsenic concentrations of up to 86 µg/g dry wt measured at Bathurst Bay in the GBR (Haynes 2001). Bathurst Bay is also a relatively pristine marine location. The maximum value for arsenic in seagrass leaves reported by Lewis and Devereux (2009) in their review of metals in seagrasses from across the world was 21 µg/g (*Posidonia oceanica,* Mediterranean Sea). The benthic sediment metals data did not indicate any elevated concentrations of arsenic or cadmium at site I and previous measurements of dissolved arsenic and cadmium concentrations in this area were in the typical range expected for coastal seawater (Apte et al. 2018). Samples I1 and I2 were identified as *Cymodocea serrulata* which is the same species sampled and analysed in Bathurst Bay (Haynes 2001). It appears that the reasons for high arsenic and cadmium bioaccumulation are related to the physiology of the seagrass species rather than the presence of elevated metal concentrations in waters or sediments. The occurrence and physiology of a seagrass species capable of accumulating large concentrations of arsenic and cadmium from relatively uncontaminated environments is worthy of further investigation.

Table 7–16: Trace metal concentrations in seagrasses, 2020 study. Note: As – arsenic, Cd – cadmium, Co – cobalt, Cr – chromium, Fe – iron, Mn – manganese, Ni – nickel, Pb – lead, Zn – zinc.

Location	Site	Species	As	Cd	Co	Cr	Cu	Fe	Mn	Ni	Pb	Zn
			Dry weight (µg/g)									
Saibai	SG2	*Halodule Uninervis (wide leaf morphology)*	28	0.92	2.3	2.8	11.3	7844	206	5.3	1.96	23
Saibai	SG2	*Halophila ovalis*	13	0.58	2.4	5.3	12.6	6275	301	4.2	4.49	16
Saibai	SG2	*Halophila ovalis and Halodule uninervis (wide leaf morphology)*	5.0	0.85	2.7	0.8	11.1	771	160	5.4	0.75	10
Saibai	SG1	*Enhalus acroides*	2.9	0.59	3.5	0.8	13.3	410	152	7.0	0.40	19
Saibai	SG1	*Enhalus acroides*	1.9	1.52	1.3	1.1	16.5	717	165	3.0	0.69	15
Boigu	Intertidal	*Halopohila ovalis and Halodule uninervis (narrow leaf morphology)*	4.0	0.33	1.5	2.3	6.0	3008	278	1.9	2.41	15
Boigu	Intertidal	*Halodule uninervis*	6.7	0.28	4.5	2.3	8.0	4159	686	3.0	4.57	20
East of Saibai	G1	*Cymodocea serrulata*	1.94	1.29	0.46	1.33	9.0	401	57	2.26	0.79	15.2
East of Saibai	G2	*Cymodocea serrulata*	2.22	1.38	0.50	1.84	10.3	576	59	2.56	1.01	16.1
East of Saibai	G3	*Cymodocea serrulata*	3.96	1.24	1.21	6.54	10.9	3022	79	5.66	2.94	23.8
East of Saibai	G4	*Cymodocea serrulata*	1.50	1.14	0.40	1.37	9.31	539	54	2.49	0.89	25.7
East of Saibai	G5	*Thalassia hemprichii*	2.68	1.36	0.61	3.38	8.38	1033	62	3.41	0.76	23.6
Masig	C1	*Thalassia hemprichii*	4.86	0.82	0.19	1.56	6.28	390	25	3.21	0.25	8.12
Masig	C2	*Thalassia hemprichii*	8.39	1.04	0.20	1.32	5.94	320	24	3.69	0.49	6.85
Masig	C3	*Thalassia hemprichii*	7.22	0.86	0.06	0.72	5.93	164	15	3.64	0.30	8.95
Masig	C4	*Thalassia hemprichii*	4.72	1.05	0.15	0.83	5.61	196	23	3.28	0.13	5.97
Masig	C5	*Thalassia hemprichii*	5.31	0.80	0.19	1.25	5.15	321	22	3.01	0.18	6.63
Bramble Cay	E1	*Thalassia hemprichii*	1.50	1.05	0.53	0.31	11.4	266	32	3.45	0.61	14.2
Bramble Cay	E2	*Thalassia hemprichii*	1.93	1.40	0.25	0.53	9.5	494	61	1.80	5.28	17.1
Bramble Cay	E2	*Thalassia hemprichii*	2.00	1.25	0.32	1.01	7.58	832	59	1.90	4.99	17.5
Bramble Cay	E3	*Thalassia hemprichii*	2.05	0.87	0.43	0.41	11.0	198	35	3.66	1.51	13.3
Bramble Cay	E4	*Cymodocea rotundata, Thalassia hemprichii*	1.66	1.10	0.58	1.03	10.8	679	42	3.26	0.57	12.0

Location	Site	Species	As	Cd	Co	Cr	Cu	Fe	Mn	Ni	Pb	Zn
			Dry weight (µg/g)									
Bramble Cay	E5	*Thalassia hemprichii, Cymodocea rotundata*	1.60	0.92	0.27	0.48	10.2	320	44	2.22	0.39	11.7
Bramble Cay	E5	*Thalassia hemprichii, Cymodocea rotundata*	1.58	0.75	0.18	<0.3	10.2	127	47	2.38	0.21	18.2
Erub	D1	*Thalassia hemprichii*	5.70	0.96	0.15	0.59	4.75	102	19	4.99	0.42	6.32
Erub	D2	*Thalassia hemprichii*	3.60	1.16	0.13	0.55	6.15	138	21	4.94	0.33	4.29
Erub	D3	*Thalassia hemprichii*	7.32	1.09	0.20	0.84	5.41	119	26	5.11	0.35	4.56
Erub	D4	*Thalassia hemprichii*	2.94	1.09	0.11	0.44	5.22	145	20	4.91	0.10	4.68
Erub	D5	*Thalassia hemprichii*	4.36	0.96	0.17	0.42	4.89	113	19	5.38	0.91	5.45
M. Warrior Reef	J1	*Thalassia hemprichii*	2.02	0.96	0.21	0.79	6.60	335	39	3.79	0.45	6.02
M. Warrior Reef	J2	*Thalassia hemprichii*	3.51	0.99	0.17	0.18	7.31	197	39	3.41	0.84	9.28
M. Warrior Reef	J3	*Thalassia hemprichii*	4.19	1.11	0.18	0.10	6.58	125	73	3.27	0.28	4.99
M. Warrior Reef	J4	*Thalassia hemprichii*	2.49	0.65	0.31	2.76	4.68	1134	53	1.74	1.06	9.25
M. Warrior Reef	J5	*Thalassia hemprichii*	5.06	0.92	0.19	0.50	6.95	210	61	3.37	0.35	5.87
M. Warrior Reef	J6	*Thalassia hemprichii*	7.17	1.29	0.22	0.71	6.59	347	60	4.32	0.55	5.86
N. Warrior Reef	I1	Cymodocea serrulata	138	2.38	0.26	1.84	6.42	783	58	2.72	0.48	7.03
N. Warrior Reef	I2	*Cymodocea serrulata, Halophila decipiens*	123	2.13	0.21	0.82	5.33	339	59	1.85	0.62	5.77
N. Warrior Reef	I3	*Thalassia hemprichii*	20.9	0.99	0.19	1.03	6.63	508	63	1.38	0.62	5.81
N. Warrior Reef	I3	*Thalassia hemprichii*	16.5	0.98	0.15	0.50	6.05	263	68	1.37	0.68	5.94
N. Warrior Reef	I4	*Cymodocea serrulata*	4.51	0.92	0.09	0.09	5.70	161	77	0.96	0.32	4.58
N. Warrior Reef	I5	*Thalassia hemprichii*	10.6	1.15	0.13	0.77	5.13	342	53	1.09	0.66	6.39
S. Warrior Reef	K1	*Cymodocea serrulata*	3.30	0.66	0.13	0.32	4.88	184	54	1.52	0.24	6.25
S. Warrior Reef	K2	*Cymodocea serrulata*	2.78	0.69	0.10	0.05	5.43	126	48	1.32	0.32	7.17
S. Warrior Reef	K3	*Cymodocea serrulata*	2.99	0.53	0.11	0.23	5.05	198	49	1.16	0.41	6.28
S. Warrior Reef	K3	*Cymodocea serrulata*	4.15	0.73	0.14	0.25	6.07	160	47	1.59	0.61	5.97
S. Warrior Reef	K5	*Cymodocea serrulata*	3.44	0.73	0.22	1.26	4.14	532	77	1.52	0.46	7.53
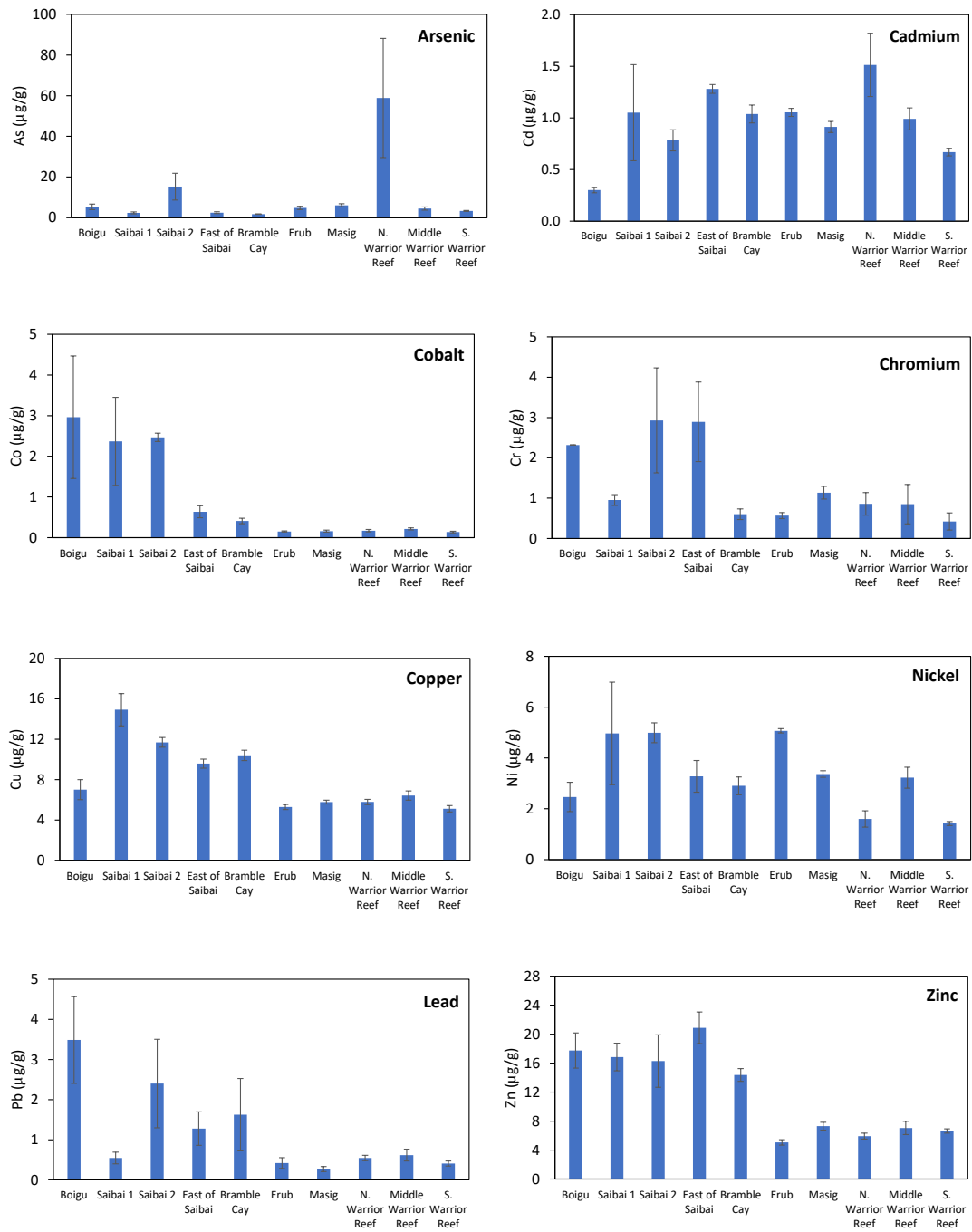
Figure 7–22: Seagrass trace metal concentrations versus location (mean± S.E., µg/g dry weight).

Pearson correlation coefficients indicated many statistically significant correlations between the trace elements in the seagrass samples (n=46, r>0.29, p<0.05). However most of these associations were relatively weak (r<0.5) and were not of value in terms of establishing functional relationships that relate to metal uptake. The strongest correlations were observed for manganese vs cobalt (r= 0.855) and copper vs zinc (r= 0.680). The scatter plots illustrating the linear relationships between these elements are shown in Figure 7–23. The association between manganese and cobalt is interesting as these elements are also known to be closely associated in marine sediments and their porewaters (Heggie and Lewis 1984, Stockdale et al. 2010).
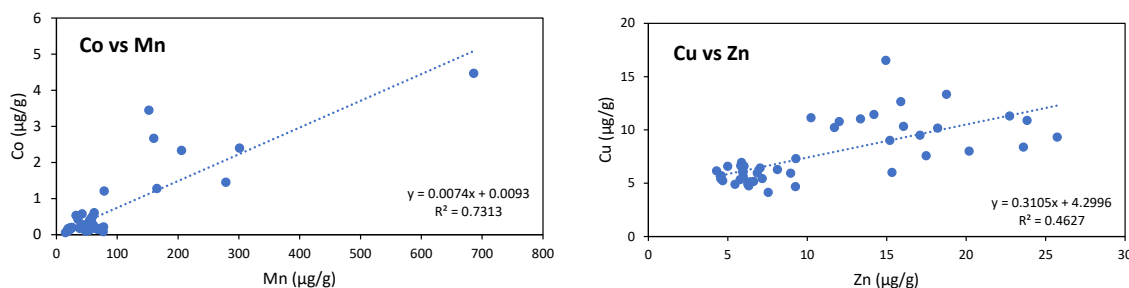
Figure 7–23: Key relationships observed between metals in the seagrass samples analysed.

Given that similar spatial trends were observed with a number of metals in benthic sediment (i.e. elevated concentrations around Saibai and Boigu), the relationship between the seagrass and sediment data was explored. This was achieved by comparing the mean seagrass metal concentrations at each site against the corresponding mean sediment metal concentrations. Only two statistically significant linear correlations were identified: cobalt (r =0.978, p<0.05, n=6) and chromium (r=0.869, p<0.05, n=6). The data for these metals are plotted in Figure 7–24.

The observation of simple relationships with the total metal content of the sediments is useful in terms of providing a proxy for seagrass metal concentrations and also confirming the consistency of the data sets. In practice, the bioaccumulation of trace metals by seagrasses will be influenced by a number of factors including the speciation and bioavailability of metals in the sediments and their concentrations in porewaters, so strong relationships with the total metal concentrations in sediment are not necessarily expected.

Copper, lead and zinc which were also elevated in samples from around Boigu and Saibai displayed moderate correlations with the corresponding sediment metal concentrations (r values of 0.597, 0.586 and 0.795 respectively) but these were not statistically significant. It is likely that the relationships for these metals would be stronger if other sediment measurements that are more closely related to metal bioavailability in sediments were utilised such as weak acid extractable metals or porewater metal concentrations.

Arsenic and nickel concentrations in benthic sediments were typically one order of magnitude higher at the Boigu and Saibai sites compared to the other locations (Table 7–11) however, there was no corresponding increase in seagrass metal concentrations (Table 7–16 and Figure 7–22). This suggests that either the forms of these metals in the sediments at Boigu and Saibai

have limited bioavailability or seagrasses regulate the concentrations of these elements in their tissues (Bonanno & Di Martino 2016, Marín-Guirao et al. 2005).
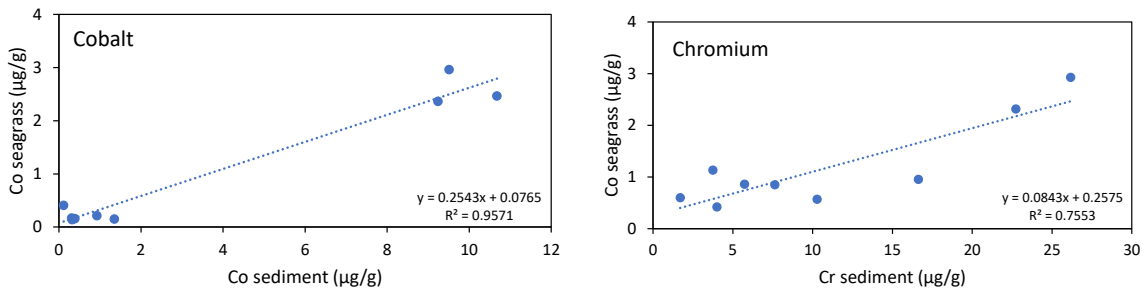
Figure 7–24: Relationships observed between cobalt and chromium in seagrass and their corresponding benthic sediment metal concentrations at each sampling location.

Torres Strait regional assessment

A comparison was made between the three data sets that are available for trace elements in seagrasses: the current study, the Torres Strait Baseline Study (Dight and Gladstone 1993) and NESP TWQ Hub Project 2.2.1 (Waterhouse et al. 2018).

The Torres Strait Baseline Study acquired data in 1991 and 1992 that determined the extent of influence of Fly River discharge and the status of trace metals within the Torres Strait using a range of techniques. NESP TWQ Hub Project 2.2.1 undertook a small scoping study in October 2016 to estimate the spatial and temporal extent of exposure of seagrasses in the Torres Strait to Fly River discharge. Sampling was constrained to three sites around Saibai Island and the Warrior Reefs. The current study built on the recommendations of Waterhouse et al. (2018) and collected seagrass samples from a variety of sites across the region, however, travel restrictions due to COVID-19 guidelines, prevented the collection of temporal samples. Due to the relatively small sample sizes (Torres Strait Baseline Study n = 46, NESP TWQ Hub Project 2.2.1 study n=21 and current study n=46), grouping sites together into relative exposure areas (defined in Waterhouse et al. 2018 and discussed further in Section 8.3) allowed for comparison of seagrass trace metal concentrations from two previous studies. Table 7-17 displays the sites from each study and their allocation to the relative exposure areas.

Table 7–17: Sites from the different studies allocated to Areas of Exposure as defined in Waterhouse et al. (2018). Torres Strait Baseline Study - Dight and Gladstone (1993); 2016 – NESP Project 2.2.1 - Waterhouse et al. (2018); 2020 – this study.

Study	Relative exposure area		
	High	**Moderate**	**Low**
2020	Saibai 1	Masig	Southern Warrior
	Saibai 2	Erub	
	Boigu	North Warrior	
	East of Saibai	Middle Warrior	
	Bramble Cay		
2016	SG (Saibai)	E (North Warrior)	
		G (South Warrior)	
Torres Strait Baseline Study	KoKope Reef	Campbell Island (Tappoear Island)	Dungeness Reef

To detect any differences between the three studies in the region, ANOVAs were performed on the key trace elements (Table 7–18). With the exception of chromium, nickel and zinc, metal concentrations were not significantly different between the three studies.

Table 7–18: Analysis of Variance Table between three regional Torres Strait studies (Torres Strait Baseline Study, NESP Project 2.2.1 and NESP Project 5.14) for each trace element of interest. DF = (degrees of freedom), MS = mean sums of squares, F = ratio between groups and the level of significance, * p<0.05 displayed.

Trace element	DF	MS	F	Significance
Arsenic	2	55.217	1.479	0.313
Cadmium	2	0.045	1.209	0.373
Cobalt	2	3.645	1.753	0.265
Chromium	2	9.970	16.226	0.007*
Copper	2	7.746	2.527	0.174
Nickel	2	4.133	31.310	0.001*
Lead	2	1.214	3.628	0.106
Zinc	2	324.313	19.441	0.004*

Results of a Scheffe test for chromium, nickel and zinc (Figure 7–25) showed that the 2016 results (Waterhouse et al. 2018) were significantly higher than the Torres Strait Baseline Study (Dight and Gladstone 1993) and the current study. The observed differences for these metals may be associated with factors such as differences in seagrass species and their condition (Bonanno and Orlando-Bonaca 2017, 2018, Schlacher-Hoenlinger and Schlacher (1998).
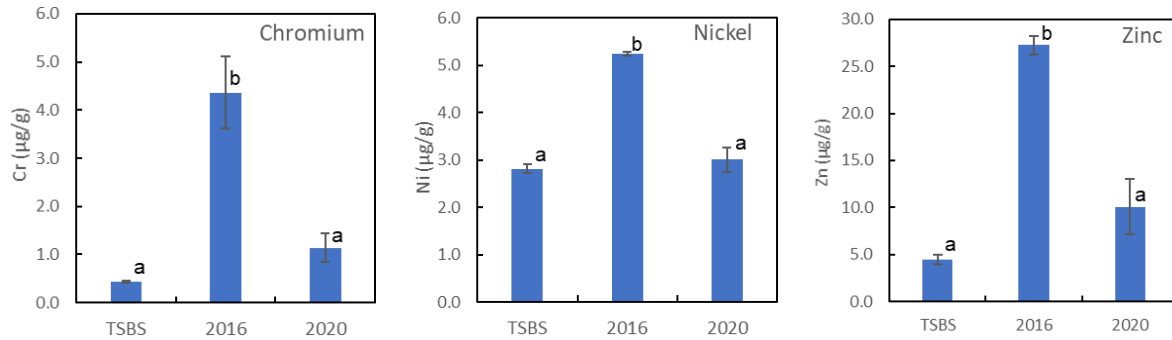
Figure 7–25: Significant differences between studies for chromium, nickel and zinc (mean ± S.E.). Different letters (a and b) depict which studies are significantly different from each other. TSBS - Torres Strait Baseline Study.

Discussion of the seagrass results in comparison to results from other studies is presented in Section 8.2.4.

7.4 Conclusions and recommendations

The current investigations have provided further information on the distribution of trace elements in the Torres Strait which support the findings of the previous NESP geochemistry investigation (Apte et al. 2018). Water quality across the Torres Strait is generally very good, however elevated concentrations of some trace elements are observed in waters, sediments and seagrasses of the NE of the Torres Strait including Bramble Cay and also around the northern Warrior Reefs, Boigu and Saibai Islands.

The enrichment of metals in waters and sediments in the Boigu and Saibai region is likely to result from natural inputs of metals from the PNG mainland such as river runoff from various coastal rivers which are periodically augmented by contributions from the Fly River plume. The relative contributions from these sources is hard to assess without data on the contributions of metals from the PNG coastal rivers in the Boigu/Saibai region. Sediment core data indicates relatively homogenous distributions of metals with depth and does not indicate increases in metals concentrations with time. Sulphide mineral particles indicative of mine-derived sediments were detected in suspended sediment particles in samples from Boigu and Saibai but confirmation of their origin requires further work.

In general terms, seagrass trace metal concentrations in the Torres Strait showed a decrease in a gradient away from the PNG coastline. Seagrass trace metal concentrations tended to be significantly higher in the NE Torres Strait (Bramble Cay), and then Boigu and Saibai to the west. Markedly higher concentrations of cobalt, chromium, copper, lead and zinc were found in seagrasses from the Boigu and Saibai sites. Copper lead and zinc were also higher at Bramble Cay compared to the remaining sites. These results are in broad agreement with the patterns of the metal analysis in water, TSS and benthic sediment. Of the eight trace metals of interest only three (chromium, nickel, zinc) were significantly different between previous studies with the 2016 values being higher than either the Torres Strait Baseline Study or current study. This is possibly a factor of limited spatial coverage and samples numbers collected during the 2016 survey. Even with these differences, at a Torres Strait regional level,

seagrass trace element concentrations are generally low compared with literature values reported for elsewhere (see Section 8.2.4).

Future geochemical investigations in Torres Strait should focus primarily on the NE Torres Strait, Warrior Reef and the Saibai/Boigu region. It is recommended that further work is required on the following aspects:

1. Understanding the inputs of metals from the PNG mainland around Boigu and Saibai (e.g. temporal sampling of local rivers and the Fly River) and Australia.
2. Understanding the temporal variations in dissolved metals and suspended sediments at locations such as Bramble Cay would provide a better understanding of exposure to elevated metal concentrations and their associated impacts.
3. Conducting transect surveys from the southern channel of the Fly River Estuary to Bramble Cay would improve our understanding of how metal concentrations in water and suspended sediments change with distance from the estuary.

These are described further in Section 8.5.

PART C: INTEGRATED FINDINGS

8.0   DISCUSSION

8.1 The extent of the influence of the Fly River discharge in the Torres Strait

8.1.1 Multiannual patterns

The remote sensing analysis provided further evidence that habitats located in the NE corner of the Torres Strait Protected Zone, including the northern Warrior Reef, as far west as Saibai Island and as far east as Bramble Cay are located in an area of higher potential exposure to waters and sediments from the Fly River. The source of highly turbid waters cannot, however, be fully attributed to the Fly River and is likely to include other sources of sediments associated with the smaller streams (including the likely influence of the Wassi Kussa and Mai Kussa Rivers around Boigu Island), as well as resuspension of sediment deposited in the Torres Strait mud wedge via currents, wind and wave action (Ayukai and Wolanski 1997; Harris et al. 2004; Heap et al. 2005; Waterhouse et al. 2018).

The influence of the Fly River on Bramble Cay appears to be enhanced by trade winds and several satellites images have captured intermittent influence of the Fly River plume on Bramble Cay during the trade wind season. Luminescent lines indicating exposure to terrestrial organic matter have been previously observed in corals from Bramble Cay back to 1781 (Lough 2016), which along with earlier field observations (described below) confirmed a very likely plume influence at this site.

In the middle of the Torres Strait, the presence of moderately turbid water masses was most likely associated with calcareous sediments flowing through the Warrior Reef or a mixture of terrigenous and carbonate suspended sediments closer to the coast (e.g., Harris 1988). Calcareous sediments sometimes mixed with the terrigenous sediments originating from the Fly River and/or resuspended from the Torres Strait mud wedge; complicating the optical and colour signature of coastal waters around Boigu, Saibai and the northern Warrior Reef. On the Eastern side, the Ugar, Masig and Poruma Island sites were predominantly exposed to less turbid waters.

The hydrodynamic and mud transport modelling identified a turbid coastal boundary layer along the PNG coast of the Torres Strait with maximum turbidity found inshore and decreasing seaward. The turbid coastal boundary layer is patchy due to the existence of a persistent mud wedge along the PNG coast which is resuspended by tidal currents, wind and waves especially during strong wind events. The model demonstrated that polluted new mud intrudes into Torres Strait from the Fly River discharge and is diluted by the non-polluted mud of the mud wedge. Daru and Bristow Islands, located close to the PNG coast, form a hydrodynamic barrier that restricts the water circulation and slows down the intrusion of Fly River contaminated material further west into the Torres Strait.

The model predicted that about 9% of the Fly River mud flux enters the Torres Strait through the Southern Channel of the Fly River estuary, the closest channel to Torres Strait, which is

similar to the estimate of 11% of previous studies (Harris et al. 2004). However, these predictions must be seen as qualitative in the absence of field data describing mud dynamics in Torres Strait. Despite these limitations, there is confidence in the results as long as the main assumption – that the physical properties of erosion and settling of the mud in Torres Strait are the same as those in the Fly River estuary – is valid.

8.1.2 Seasonal patterns

The remote sensing data showed that the Fly River plume intruded into the Torres Strait most extensively during the SE trade wind season and less so during the monsoon season. This was in agreement with hydrodynamic and sediment modelling results for the region (Li et al. 2017; Martins and Wolanski 2015; Wolanski et al. 2013, 2021; and Section 0 in this report), field salinity records (Waterhouse et al. 2018 and Section 3.0 in this report) and field observations (Harris et al. 1993 and Sections 0 and 7.0 of this report). There was also a good spatial match between the 2019-2020 SSC-salinity plots and satellite plumes boundaries (Section 0).

The new satellite analyses supported previous studies and hypotheses suggesting that currents in the Torres Strait reverse seasonally, with flow being predominantly westwards during the SE trade wind season (negative mean sea level) and driving PNG turbid river into the Torres Strait (Harris 1994; Li et al. 2017; Wolanski et al. 2013a, 2013b). Satellite and *in-situ* logger data collected as part of this study suggested that, during the trade wind period, the Fly River intrusion in the Torres Strait Protected Area is greater between June and September and at a maximum in July - August. The contribution of the Wassi Kussa and Mai Kussa Rivers also varied seasonally and, in the satellite database, was at a maximum around May to August. In the middle of Torres Strait, positive turbidity anomalies were measured east of the central islands in January and February, in the middle of the Torres Strait in May and April and then west of the central Islands in April to August.

8.1.3 Additional evidence

Historical field data sets (also used to support development of the original hydrodynamic model - Li et al. 2013) highlight the agreement with the results of the current study, providing further confidence in the conclusions. Oceanographic studies of the salinity plumes in the Torres Strait have been carried out in 1979, the 1980s and 1990s. In these studies, the lower salinity plume was observed to be always vertically well-mixed throughout the water column (Wolanski et al. 1984; Wolanski et al. 1994, 1999). The plume intrusion was observed to be most intense during the SE trade wind season (April-September) and the least intense during the rest of the year. For example, the time-series of salinity at a nominal 5 m depth at mooring sites in the Great North East Channel and Bramble Cay showed that: (1) the Fly River plume intrusion in the Torres Strait was a permanent feature as exemplified by lower salinity in the east than in the west (Figure 8–1) and (2) that the salinity, hence plume intrusion, varied in time.
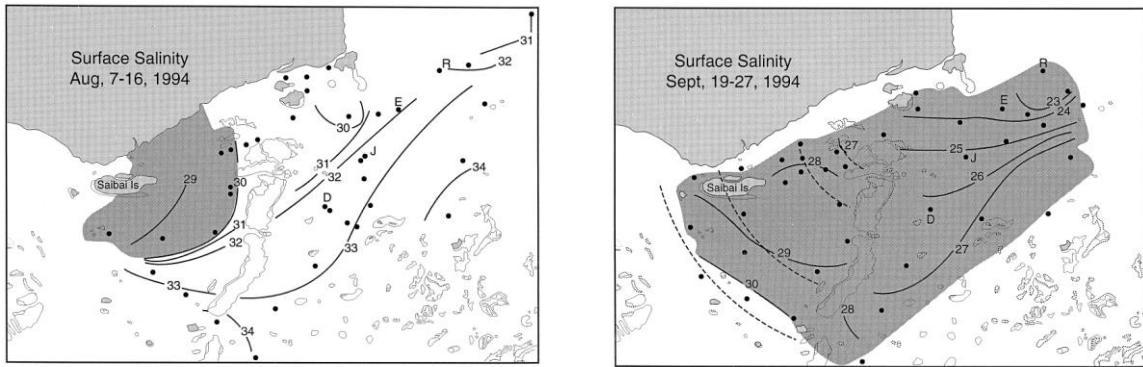
Figure 8–1: Surface salinity distribution in Torres Strait in August and September 1994. Data from Wolanski et al. (1999).

Field studies Ayukai and Wolanski (1997) also provided evidence of reduced surface salinity and reduced light penetration, assumed to be associated with increased turbidity, in the Torres Strait. Figure 8–2 shows a gradient of increasing salinity and light penetration away from the Fly River mouth to the south, and more gradually to the west. Bramble Cay, in the top left of both figures, is located in a convergence area of the lower salinity and light penetration.
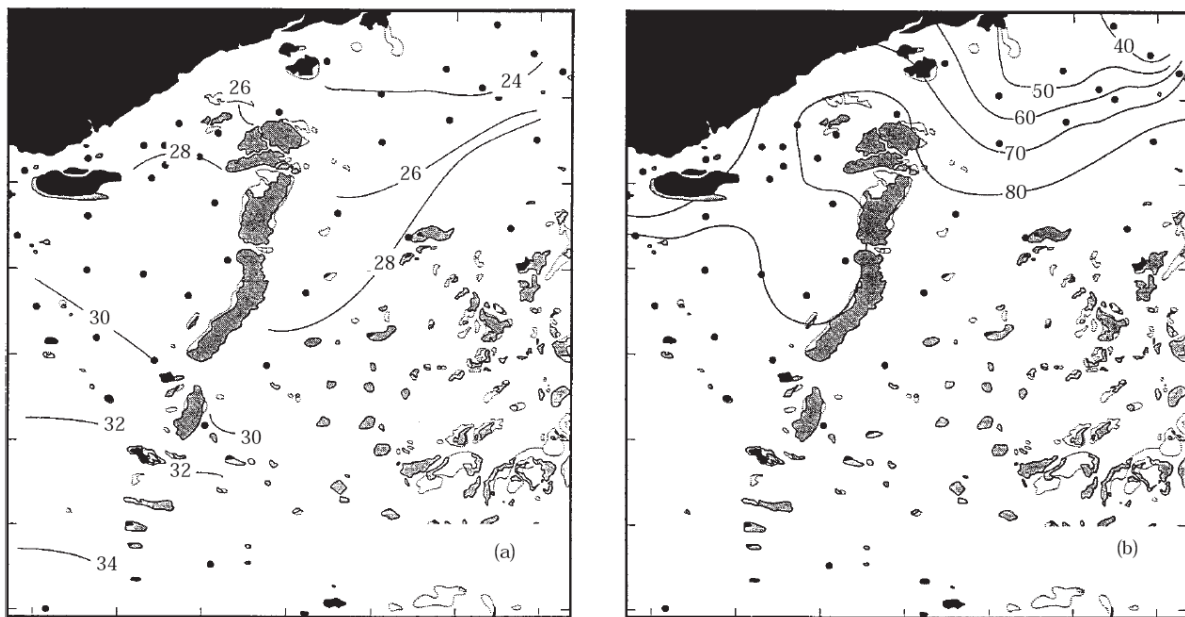
Figure 8–2: Surface salinity (left) and light penetration (right) at the sea surface measured in the Torres Strait in September 1994. Source: Ayukai and Wolanski (1997).

The potential exposure of Bramble Cay to more turbid waters is also supported by earlier NESP datasets and historic studies. Deployment of continuous turbidity loggers at Bramble Cay (2017 to 2018) showed higher than expected levels of turbidity (average of 10.7 NTU) for a remote offshore reef (as compared to offshore reefs in the GBR that average 0–3 NTU and near-shore reefs that average 3-5 NTU in the dry season and a maximum of 10-15 NTU in the wet season). The observed patterns of turbidity at Bramble Cay were correlated with wind speed and most likely represent local wind driven resuspension of *in-situ* material and not episodic movement of material from the (Fly River) north. The exception is a peak in turbidity observed in June 2017 that seems to be unrelated to local environmental conditions. Analysis

of satellite images in this period shows evidence of Fly River discharge entering the region. The presence of fine terrestrial material at Bramble Cay indicates that there is long-term transport of material from PNG as the nearest source. However, this may be via more complex long-term transport mechanisms rather than short-term episodic events, which in turn will have implications for the potential transport of contaminants into the area.

Additional examples of the Fly River plume reaching Bramble Cay, particularly during the SE trade wind seasons, was also provided in Section 0. For example, Figure 6–12d on 12 October 2019 showed an example of when the Fly River plume was large and extended well offshore in the Gulf of Papua, reaching Bramble Cay.

While the new data in this study provides further evidence of the potential exposure of the Warrior Reefs to Fly River waters, the likely degree of exposure is still poorly understood. The additional logger measuring turbidity and salinity at the northern Warrior Reefs (2019-2020) provided valuable, but inconclusive, data. The logger data showed generally low turbidity levels. However, seasonal patterns were evident in the dataset – with an increase in turbidity and a decrease in salinity (typical of a turbid plume influence), as well as lower temperatures and salinity from around May to September (SE trade winds). The patterns of salinity could not be explained by localised rainfall or run-off and may indicate the influence of diluted plume waters. The salinity levels showed a strong monthly cycle with low salinity events coinciding with the tidal cycle (spring tides). The link is not fully understood, but the reductions in salinity may represent water from coastal PNG coming down into the northern Warrior Reefs driven by tidal forcing. The logger site at Kokope Reef (northern Warrior Reefs) is only approximately 20 km from mainland PNG (directly north), and for context, the Fly River mouth is approximately 60 km to the east, and Wassi Kussa River is approximately 110km to the east. The decadal median assessment of the remote sensing of colour classes to derive water types (Figure 6–6) concluded that the northern Warrior Reefs were regularly exposed to Secondary waters, indicating a regular occurrence of moderately turbid waters in this area. As identified above, the source of turbidity could be linked to several factors including Fly River discharge, smaller coastal PNG streams and resuspension of sediment deposited in the Torres Strait mud wedge via currents, wind and wave action (Ayukai and Wolanski 1997; Harris et al. 2004; Heap et al. 2005).

From an ecosystem perspective, analysis of the frequency of exposure of coral reef and seagrass habitats to waters with higher turbidity using remote sensing data in Waterhouse et al. (2018) identified that habitats around Saibai and Boigu Islands were most frequently exposed to turbid waters, compared to islands in the central areas of the Torres Strait such as Warraber, Iama and Poruma. Habitats around the northern Warrior Reefs, Erub and Mer were also exposed to turbid waters, although less frequently than Boigu and Saibai. Frequent pulses of higher turbidity were observed at the Bramble Cay coral reef site. Importantly, the latter sites all have healthy coral reefs with high coral cover and low macroalgae cover (as described in Waterhouse et al. 2018).

8.2 Assessment of mining-derived contaminants

Metal concentrations in waters and sediments are generally low across most of the Torres Strait with higher concentrations observed around the Boigu/Saibai region, Bramble Cay and the Warrior Reef.

The concurrent elevation of metals in waters, benthic sediments and suspended sediments is illustrated graphically for copper in Figure 8–3. The relationship between suspended and benthic sediment concentrations is most likely a consequence of frequent sediment resuspension and settling events. The association between dissolved and particulate copper concentrations may reflect release of metals from the sediments into solution. Additionally to these internal cycling processes, some sites will also receive inputs from external sources, namely the Fly River plume and also other inputs from other rivers draining the Southern Fly district. The importance of external sources of metals is amply demonstrated by the suspended solids data from Bramble Cay which indicates a significant enrichment of copper relative to the concentrations of particulate copper in benthic sediments at that site (Table 8–1). Given the proximity of this site to mouth the Fly River estuary it is highly likely the suspended sediments observed at Bramble Cay originate from the estuary. The differences between the different suspended sediment samples is also illustrated by the partition coefficients, Kd (Table 8–1) with the highest values being observed at Bramble Cay.
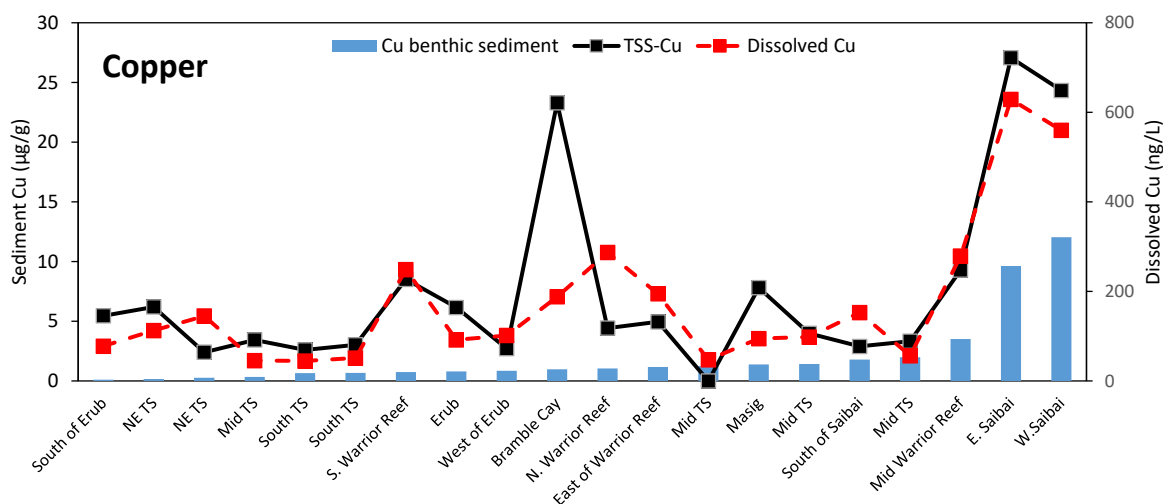
Figure 8–3: Benthic, suspended and dissolved copper (Cu) concentrations at the 2016 sampling sites. Note the lines connecting the data points are there to emphasise trends and do not imply the data sets are continuous.

Table 8–1: Comparison of copper concentrations around Boigu/Saibai and Bramble Cay with those in the Fly River Estuary (data are means where replicates exist). Cu – copper, Kd - light

Site	Dissolved Cu (ng/L)	TSS-Cu (µg/g)	Benthic particulate Cu (µg/g)	Kd (L/g)	Notes	Source
Fly River Estuary	553	45	-	81	Southern channel, n=4, >32 PSU	Angel et al. (2020)
Boigu/Saibai	389	17	11	44	June 2018	Apte et al. (2018)
Boigu/Saibai	442	25	8.2	57	November 2020	This study
Bramble Cay	188	23.3	1	124	October 2016	Apte et al. (2018)
Bramble Cay	-	76	0.9		November 2020	This study
Bramble Cay	310	28	-	90		Angel et al. (2020)

8.2.1 Dissolved metal concentrations

Table 8-2 summarises the concentrations of key dissolved trace metals measured in the NESP studies (this report and Apte et al. 2018) compared to typical concentrations at other marine locations both within Australia and across the world. This compilation includes recent data for the Fly River Estuary and the NE Torres Strait from Angel et al. (2020). The metal concentrations in the southern and eastern Torres Strait are consistent with uncontaminated locations such as the southern GBR (Angel et al. 2010b) and the northern Australia coast (Munksgaard and Parry 2001). Higher concentrations of dissolved copper and lead are observed in the NE Torres Strait (including the Warrior Reef and Bramble Cay) and in the coastal waters around Boigu and Saibai.

Elevated concentrations of trace metals were confined to the northern parts of the Torres Strait, but it is important to put these concentrations in the context of results of other locations around the world, and results found in similar locations. The concentrations of dissolved trace metals found around the NE Torres Strait, Boigu and Saibai are higher than that found in other Australian coastal environments, especially for cobalt and cadmium, but are far lower than the concentrations observed in contaminated locations such as industrialised harbours.

As noted previously, the concentrations of dissolved trace metals measured in the Torres Strait were all below the ANG default guideline values for 95% species protection which are the main guideline values applied in Australia for coastal management (ANZG 2018). However, the concentrations of dissolved copper consistently exceeded the very stringent ANG guideline value of 99% that is applicable for pristine, uncontaminated waters in the Boigu and Saibai region. The next step in the Australian water quality management strategy (ANZG 2018) is to examine the bioavailability of metals exceeding guideline values. It is well understood that the toxicity and bioavailability of dissolved copper in marine waters is strongly influenced by complexation with dissolved organic matter. Given the presence of dissolved organic matter in waters draining from the coastal rivers and marshes around Boigu and Saibai, it is highly likely that a large proportion of dissolved copper is present as non-bioavailable organic complexes. It is therefore recommended that the speciation (i.e. extent of organic matter complexation) of dissolved copper in the Saibai and Boigu region are investigated by applying chemical speciation techniques such as the Chelex column method (Bowles et al. 2006) or diffusive gradients in thin films (also referred to as 'DGT') coupled with ultratrace analysis (Twiss and Moffett 2002).

Table 8–2: Comparison of dissolved metal concentrations measured in the current study with other locations.

Location	Cadmium (ng/L)	Copper (ng/L)	Nickel (ng/L)	Lead (ng/L)	Zinc (ng/L)	References
Saibai/Boigu region (mean)	4.9	413	166	6	56	This study and Apte et al. (2018)
Torres Strait – south and east (mean)	1.8	130	132	3.8	41	Apte et al. (2018)
NE Torres Strait	2.2	263	138	8	55	Angel et al. (2020)
Torres Strait	2.1	199	188	-	-	Apte and Day 1998
Outer Fly Estuary (southern channel, n=4, >32 PSU	4.6	553	177	9	42	Angel et al. (2020)
Uncontaminated locations[1]						
Southern Great Barrier Reef QLD	<1.5	40	150	<10	40	Angel et al. (2010b)
NSW coast (ng/L)	2.5	30	180	10	<22	Apte et al. (1998)
Northern Australia coast	2.1	151	116	<2	18	Munksgaard and Parry (2001)
Contaminated locations						
Sydney Harbour	40	932	175	-	3270	Hatje et al. (2003)
Humber estuary, UK	80	180	2500	-	3000	Comber et al. (1995)
Scheldt estuary, Netherlands	15	750	1000	-	1000	Baeyens et al. (1998)
San Francisco Bay estuary, USA	22	315	140	-	160	Sanudo-Wilhelmy et al. (1996)

[1]The reference location values are the typical dissolved metal concentrations found in waters with salinities >30‰

Distribution of dissolved copper

Aside from the collection of data around Boigu and Saibai in December 2019, it was not possible to collect further dissolved metals data during this project owing to the COVID pandemic which resulted in cancellation of a major field trip planned for March 2020. Nevertheless, the dissolved metals data from December 2019 was consistent with data collected in October 2016 and June 2018 of elevated dissolved metal concentrations in the Saibai/Boigu region. Note that only benthic sediments were analysed for trace metal concentrations in the Torres Strait Baseline Study.

This section revisits the 2016 data set for dissolved metals (Apte et al. 2018) and specifically focuses on dissolved copper as it is well established that this metal is the major aquatic contaminant originating from the Ok Tedi mine (Bolton 2009).

The spatial distribution of dissolved copper concentrations (ng/L) determined during the October 2016 survey is shown in Figure 8–4. Based on previous studies of dissolved metal concentrations in Pacific coastal waters around Eastern Australia (Angel et al. 2010b; Apte et al. 1998), the 'background' concentration of dissolved copper in uncontaminated waters is typically less than 50 ng/L. The dotted line marked on the map, approximately midway between

Thursday Island and the PNG mainland, is an approximate boundary delineating background marine copper concentrations from those showing some elevation in concentration.
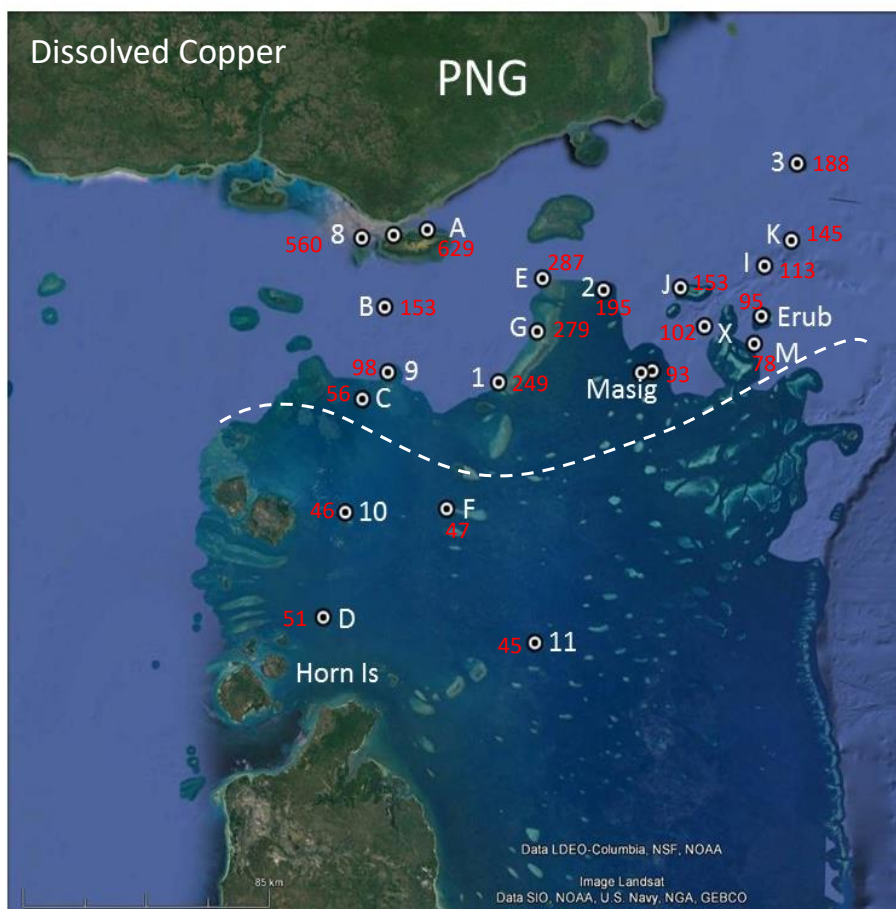
Figure 8–4: Map showing the distribution of dissolved copper (ng/L) determined during the October 2016 survey. The dotted line represents a proposed boundary delineating background marine copper concentrations (south) from those showing some elevation in concentration. The measured dissolved copper concnetrations are marked in red.

As noted earlier the highest copper concentrations (along with other metals) were found around Saibai. However the second highest group of dissolved copper concentrations were at four sites around the Warrior Reefs (sites E, G, 1 and 2, Figure 8–4) and the next highest at Bramble Cay (Site 3). This was surprising, as it was expected that the samples closest to the mouth of the Fly River (i.e. Bramble Cay) would contain the highest copper concentration. This interesting feature of the data could be explained by the known complex water movements through the Torres Strait and/or freshwater contributions from PNG coastal rivers between Boigu and Daru. At this stage the metal contributions from Southern Fly district rivers are unknown and need to be quantified. It was not possible to investigate this issue in the current NESP project as international field work is beyond the scope of the program.

8.2.2 Benthic sediments

The previous NESP investigations (Apte et al. 2018) focused on mapping the distributions of trace elements across the Torres Strait and identified a south to north concentration gradient with the highest metal concentrations observed around Boigu and Saibai, consistent with presence of metal-bearing, terrigenous fine sediments. The additional sediment core data

collected in the current study confirms these observations. Particulate arsenic concentrations above Australian sediment quality guideline values (ANZG 2108) were measured at sites around Boigu and Saibai, however as noted earlier, this is most likely a consequence of natural background enrichment of these metals rather than recent contamination events.

The observed metal concentrations are strongly influenced by sediment composition, and in this system, most notably by the proportion of calcareous sediments relative to fine terrigenous sediments. With the exception of cadmium and uranium, calcareous sediments contain negligible concentrations of metals and can be regarded as a solid diluent for terrigenous sediments. In order to get a better view of the fine sediment distribution across the region, the particulate copper data was corrected to remove the mass contribution from calcium carbonate. A similar approach as used by Heap et al. (2007). The calcium carbonate content of the benthic sediment samples was calculated from the particulate calcium data. It was assumed that all of the calcium present in the sediment was associated with carbonate. The metal concentration data was then adjusting by subtracting the mass of calcium carbonate in each sample from the total sample mass to give the mass of non-carbonate sediment material. Particulate metal concentrations were then recalculated. The calculated calcium carbonate content of the sediment samples ranged from 26 to 93% of total mass.

A comparison of the original data with the calcium carbonate corrected data for copper is shown in Figure 8–5. The corrected data reveals a clearer gradient in particulate copper concentrations across the study area. The highest concentrations were found in the northern sites around Saibai and Bramble Cay. Higher copper concentrations were also observed around the northern Warrior Reef. The presence of a significant north- south gradient following correction for calcareous sediments indicates the non-calcareous sediments occurring in the south are of different composition (e.g. marine sands) and have a lower copper concentration than the terrigenous sediments to the north.

It is noteworthy that even with calcium carbonate correction, the benthic sediment copper concentrations are lower than the current copper concentrations in TSS samples from the Fly River Estuary (Table 8–1). This suggests that the benthic sediments are dominated by historic deposition of fine sediments rather than contaminated sediments from the Fly River over the last 35 years. This view is supported by the mine-derived sediment tracer data which does not consistently indicate any recent accumulation of sulphide minerals which are likely to be of mine origin such as chalcopyrite in benthic sediments. The modelling data presented in Section 0 also predicts that that it will take nearly a century for large scale transport of mud from the Fly Estuary to Saibai Island. The time scales to reach Boigu Island are much larger.
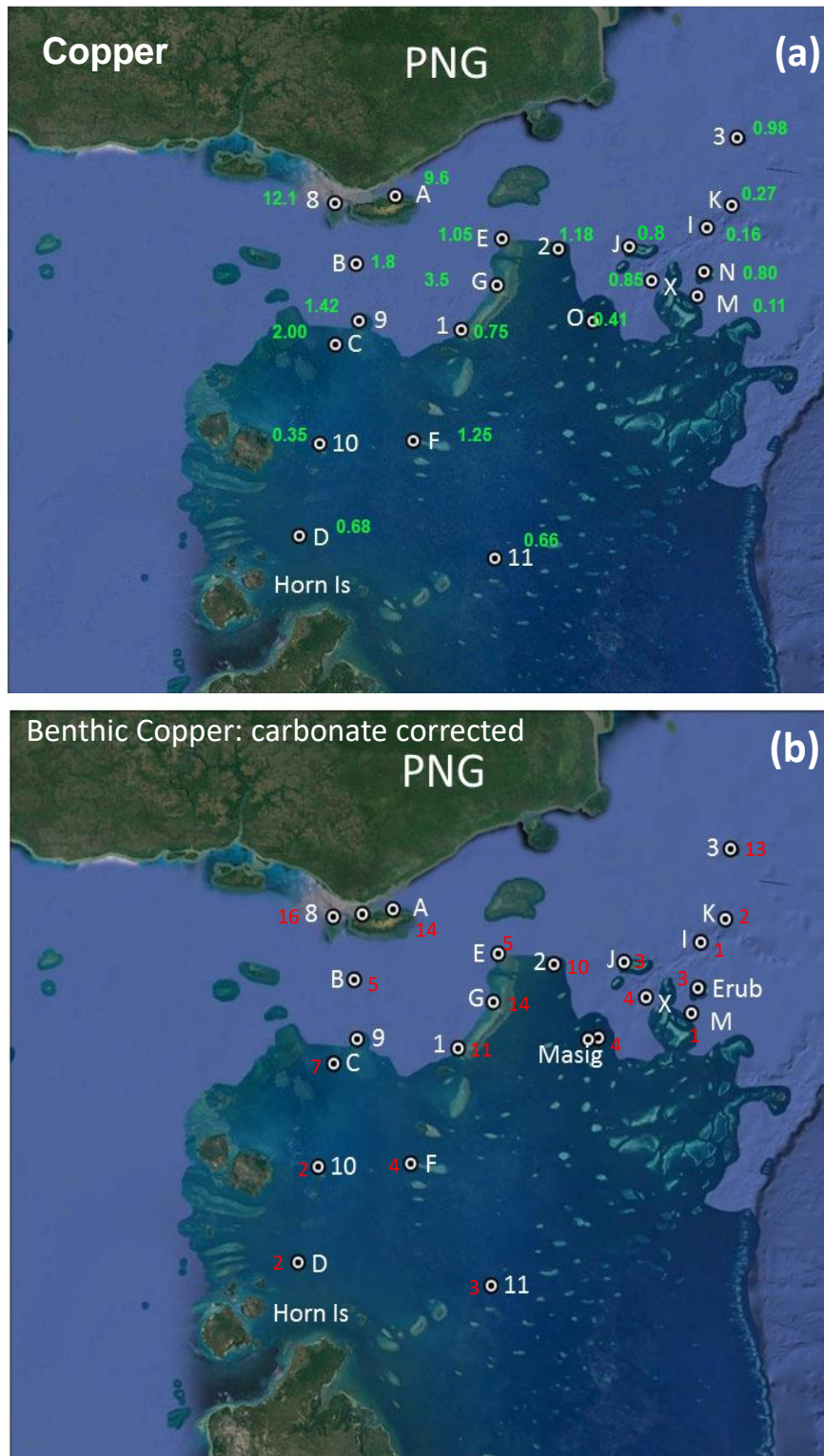
Figure 8–5: Particulate copper concentrations (µg/g) in benthic sediments, October 2016. (a) total copper concentrations, (b) copper concentrations in non carbonaceous sediment (corrected for calcium carbonate).

8.2.3 Suspended sediments

In order to understand the distributions of terrigenous fine sediments in the Torres Strait, it was necessary to separate out the influence of calcium carbonate minerals which are of marine

origin. The carbonate correction procedure used to correct the benthic sediment data was also applied to the data for all suspended sediment samples collected during the two NESP studies (2016 to 2020). The carbonate content of suspended sediments varied from 3 to 61% for the complete data set with the highest calcium carbonate samples found in the south. As noted earlier, the distribution of metals in suspended sediments followed the similar pattern to dissolved copper and particulate copper in benthic sediments, with the highest concentrations found around Boigu, Saibai and Bramble Cay. Even with calcium carbonate correction, the data showed a strong south to north concentration gradient (Figure 8–6). This indicated that the differences in copper concentration were not just accounted for by variations in calcium carbonate content. As noted for benthic sediments, the type of fine sediment materials in suspension must also be different in the south.

It should be noted that sediment samples in this project were collected under relatively calm conditions and the calcium carbonate content may not be representative of more turbulent conditions where resuspension of larger quantities of carbonaceous material is expected.

A comparison of recent suspended sediment copper concentrations in the Fly River estuary (Angel et al. 2020), Boigu/Saibai and Bramble Cay is shown in Table 8–1. Note that the current concentrations of copper in the Fly River estuary are far higher than observed in the samples from the Torres Strait. This confirms significant dilution of Fly River sediments/waters with sediments/water of much lower metal concentrations. This could be achieved by deposition and remobilisation processes which facilitate the mixing of new sediments with older deposits or mixing of the Fly River sediments with sediments introduced from other terrestrial sources.

In an attempt to understand the potential contributions of suspended sediments derived from the Fly River estuary, the ratios of copper to various trace elements (Cu/Al, Cu/Fe and Cu/Mn) sediments were examined and compared to the same ratios derived from recent suspended sediment data from the Fly River estuary (Angel et al. 2014, Angel et al. 2020). The ratios for the whole TSS data set from 2016 to 2020 are presented in Figure 8-7. Most sites including those around Saibai and Boigu have elemental ratios lower than those found in the Fly River estuary. This indicates that either the suspended sediments do not originate from the Fly River or that they have been mixed with sediments from another origin (e.g. resuspended sediments). However, a number of sites in the NE Torres Strait including Bramble Cay (2, 3, K and I) consistently have ratios higher than in the Fly River estuary. This suggests that suspended sediments undergo fractionation when transported from the estuary over extended distances. The concentrations of copper were retained in the suspended sediments, whereas the concentrations of elements such as aluminium, iron and manganese declined. This is most likely associated with differential settling of clay particles and associated trace elements which typically flocculate and settle in highly saline waters. It also suggests that the particulate forms of copper have different physico-chemical properties than other trace metals that reduces the tendency of the particles to settle from solution.

The data to date does not suggest that elemental concentrations have significantly increased in sediments from the Saibai and Boigu region as a consequence of mine-derived sediments. However this does not preclude the presence of relatively small amounts of mine-derived materials. An additional line of evidence is provided by the mineral tracer studies. Particles of containing both copper, sulphur and iron (most likely chalcopyrite) were detected in suspended sediment samples from Boigu and Saibai which suggests some transport of mine-derived

materials to this area. However this should be regarded as preliminary data. Ideally, transect samples taken from the freshwater regions of the Fly River to the outer parts of the estuary need to be analysed to confirm the source of the sulphide mineral particles.
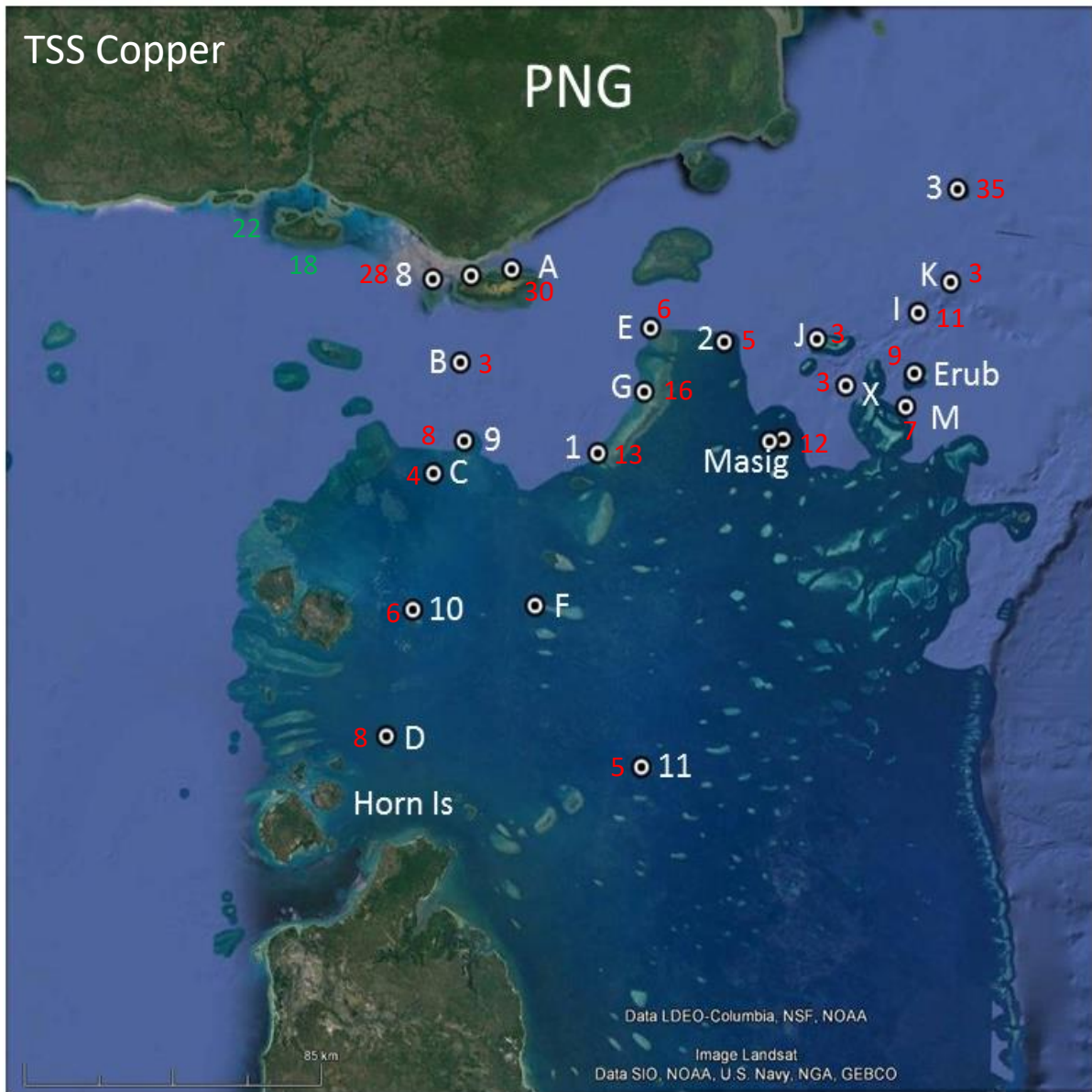
Figure 8–6: Map showing the distribution of suspended sediment associated copper (2016 survey). Units are µg/g. Note that the data has been corrected by subtracting the calcium carbonate content. The data points for Boigu (in green) were collected in June 2018.
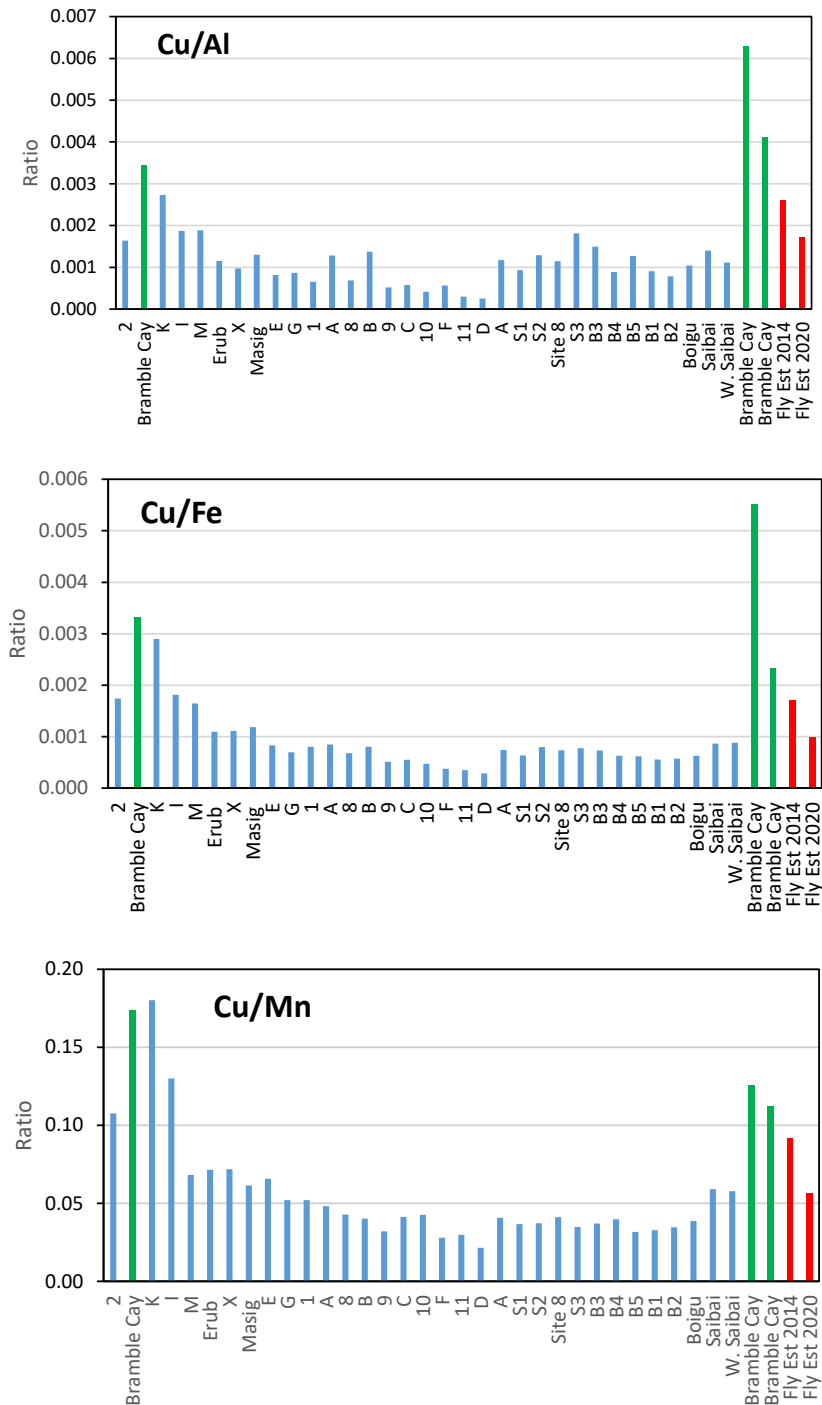
Figure 8–7: Elemental ratios for suspended sediment samples collected during the study, 2016 to 2020. The red bars are the mean ratios for the Fly River estuary based on data collected by Angel et al. (2014, 2020). The green bars denote Bramble Cay. Note: Cu – copper, Al – aluminium, Fe – iron, Mn – manganese.

8.2.4 Seagrass trace metal concentrations

Guidelines have not yet been developed to identify environmentally acceptable ranges of trace element concentrations in seagrass. To determine the status of trace elements in seagrass for the Torres Strait in the context of other locations, the data from this study was compared to published data sets from within Australia and internationally. Comparison studies were chosen on the premise that they were:

- regionally relevant (far northern GBR, Haynes 2001). This study includes sites from a range of locations including those in developed areas such as Gladstone Harbour, Port of Townsville and the Cairns Inlet, so the undeveloped areas in the far northern GBR including Lloyd Bay, Princess Charlotte Bay, Flinders Island, Bathurst Bay were averaged;
- from a second area in the northern GBR that was considered pristine and used as reference site for turtle foraging (Howick Islands, Thomas et al. 2020);
- a receiving body of water to a highly modified urbanised catchment (Sydney, Australia; Birch et al. 2018), and
- concentrations derived from a literature review on global unpolluted sites (Govers et al. 2014).

As shown in Table 8–3 and Figure 8-8, the Torres Strait regional concentrations were generally similar to, or below the concentrations found in other locations that are typically described as unpolluted in the literature. Torres Strait seagrass trace element concentrations were:

- All lower than the unpolluted global averages (Govers et al. 2014).

- Variable when compared with Far Northern GBR concentrations (Haynes 2001). The average concentrations of copper and cadmium in all Torres Strait studies were higher than in the far northern GBR. The results for cobalt, nickel and zinc were also higher in the 2016 Torres Strait study.

- Variable when compared with GBR unpolluted concentrations (Howick Islands, Thomas et al. 2020): All Torres Strait concentrations for arsenic and chromium were lower, copper and zinc were higher, and cobalt and nickel levels for 2016 and 2020 were higher than those recorded at Howick Islands.

- Generally lower than the modified urban catchment concentrations (Birch et al. 2018), with the exception of nickel that was higher in all three Torres Strait studies, and higher concentrations for cobalt and chromium in 2016.

Table 8–3: Seagrass leaf trace element concentrations from this study compared to seagrass leaf metal concentrations reported in the literature

Trace Element	Torres Strait Studies[1]			Literature Values[2]			
	1993	2016	2020	Global unpolluted	Far northern GBR	GBR, unpolluted	Urban catchment
Arsenic	1.88	4.06	5.31	-	29.9	5.97	17.9
Cadmium	0.85	0.66	1.01	1.41	0.16	0.203	-
Cobalt	0.18	3.26	0.62	-	1.61	0.523	2.93
Chromium	0.44	4.72	1.21	11.4	12.3	5.42	3.03
Copper	5.15	8.67	7.66	9.12	3.13	2.47	36.5
Nickel	2.81	5.27	3.12	7.97	4.02	3.04	2.47
Lead	0.35	1.89	1.04	5.16	4.88	1.12	53.3
Zinc	4.43	27.73	10.83	44.6	14.6	BD	192.3

[1]Torres Strait Studies are based on regional mean results. 1993 is the Torres Strait Baseline Study - Dight and Gladstone (1993), 2016 - Waterhouse et al. (2018), 2020 is the current study.
[2]Global unpolluted - Govers et al. (2014), Far northern GBR - Haynes (2001), unpolluted (Howick Islands) - Thomas et al. (2020), Urban catchment (Sydney, Australia) - Birch et al. (2018)
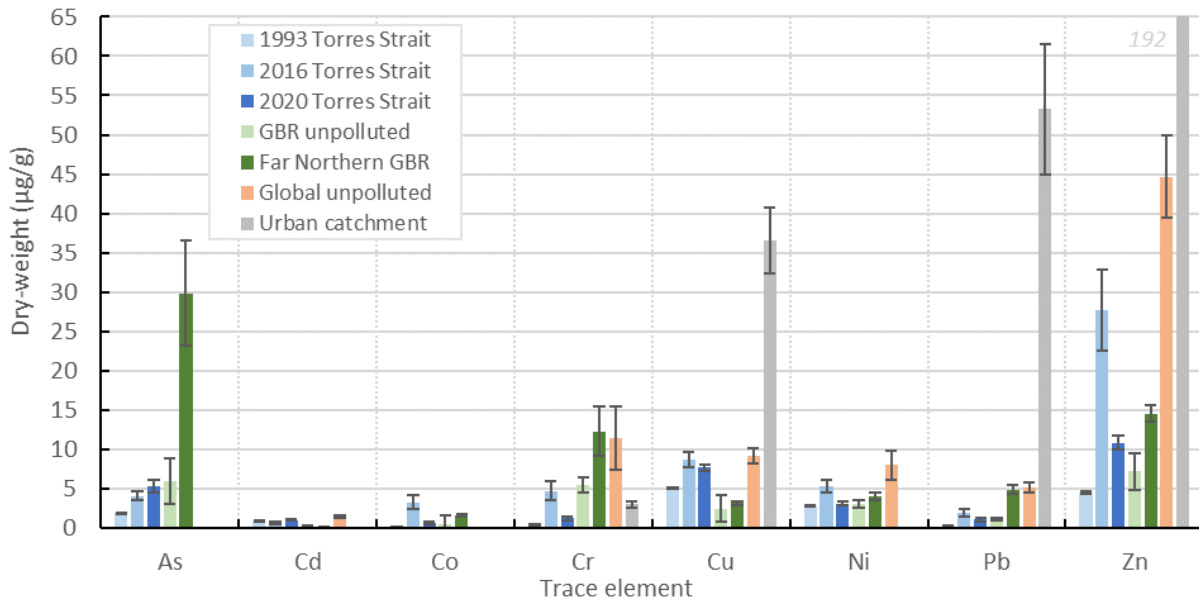
Figure 8–8: Comparison of Torres Strait studies on trace element content of seagrass leaves against the literature values. Global unpolluted - Govers et al. (2014), Far Northern GBR - Haynes (2001), GBR unpolluted (Howick Islands) - Thomas et al. (2020), Urban catchment (Sydney, Australia) - Birch et al. (2018). Note that the y-axis was limited to 65 μg/g to show the differences between studies, limiting the full extent of the Zinc result for the Urban catchment (192 μg/g). Note: As – arsenic, Cd – cadmium, Co – cobalt, Cr – chromium, Fe – iron, Mn – manganese, Ni – nickel, Pb – lead, Zn – zinc.

Many factors can affect metal concentrations measured in seagrass (Thomas et al. 2020). Factors can include sampling intensity, timing of sampling, analytical procedures; relative concentration of other metals in the plant and the surrounding environment; as well as the species, part, and age of plant analysed (Kirkby 2012). Consequently, any comparisons or conclusions between studies should be made with caution as the above comparison studies have their idiosyncrasies. For example, the trace metal values in this study were also derived from whole plants not just the leaves as in the current study. Thomas et al. (2020) while being a reference site, was analysing macrophytes as turtle forage which included both seagrass and algae, which may alter the results. The seagrass meadows sampled in Birch et al. (2018) were temperate species, and the global unpolluted sites of Govers et al. (2014), were heavily biased to areas and species found in the Mediterranean. In general, there are limited published studies assessing trace elements in seagrass, and particularly, in tropical waters. The value of this dataset in building a benchmark for other marine assessments should be recognised.

While parts of the northern Torres Strait show elevated concentrations of trace metals in water, sediment and seagrass, the concentrations are relatively low in comparison to other locations, and typically comparable to those in other unpolluted environments. It is unlikely that seagrass metal concentrations will change with time unless there is first a significant increase in water or sediment metal concentrations. Given this is unlikely, follow-up monitoring of seagrass metal concentrations on its own is therefore regarded as a low priority.

8.3 Exposure assessment

To draw the multiple lines of evidence into a collective view, a combined assessment of the metal analysis in the water column, sediments and seagrass, remote sensing analysis of water

quality exposure, *in-situ* salinity and turbidity, hydrodynamic and mud transport modelling and published literature was conducted in Waterhouse et al. (2018) to (i) provide an overview of the current understanding of the processes affecting the fate and transport of waters and sediments derived from the Fly River in the Torres Strait; and (ii) identify the areas within the Torres Strait that are most likely to be influenced from Fly River discharges. A summary of this assessment is provided in Appendix D.

The key findings of the assessment were:
- Multi-annual (2008 to 2018) frequency of exposure maps illustrated an inshore to offshore spatial pattern, with the highest frequency of the Primary water type (i.e., more turbid conditions) in the coastal areas, and offshore areas most frequently exposed only to the Tertiary water type (see explanation of water types in Section 6).
- Assessment of the frequency of exposure of coral reefs and seagrass habitats (including subtidal, intertidal and NW Torres Strait seagrasses) to turbid waters (2008–2018) showed that the majority of the coral reef and seagrass habitat areas across the Torres Strait are exposed to turbid Primary and Secondary water types (CC1–5) less than 50% of the time, except for the NW Torres Strait seagrass area. In this area, approximately 71% (273 km^2) of the habitat area was exposed frequently (50 to 90% of the time) and 29% (110 km^2) was exposed to turbid waters very frequently (90–100%).
- Spatial analysis of the frequency of exposure of 10 selected coral reef and seagrass habitat sites to in the northern and central Torres Strait Primary and Secondary waters revealed that habitats at Boigu and Saibai Islands experience the greatest exposure to turbid waters. Habitats around the northern Warrior Reefs, Erub and Mer are also exposed to turbid waters, although less frequently. Importantly, these are sites that have healthy coral reefs with high coral cover and low macroalgae cover, making them at high risk of ecological impacts, however, the evidence to date does not indicate residual impacts from previous (potential) exposures to Fly River plumes.

Further analysis of the results of the trace metal data collected in this study was conducted to confirm the previous definition of the exposure areas. The data support the observations made previously (Apte et al. 2018). The latest results support the zones defined in the previous assessment, however, interpretation of additional water and sediment data provided in this report provided a better understanding of trace metal distributions in the Torres Strait. In particular, Masig was assessed as being in a transitional area, and was assessed as moderate to low relative exposure area (rather than moderate in the previous assessment).

To assess the seagrass results, ANOVAs were performed on the key trace elements of interest (Table 8–4) to assess the differences between areas of relative exposure in the current study. With the exception of arsenic and cadmium, all trace metals returned a significant result between areas of exposure. A Scheffe test was performed *post hoc* on the significant results showing which areas of exposure were significantly different from each other. Of those significant ANOVA results, all trace elements were significantly higher in the High exposure area along the northern areas of the study area from Bramble Cay to Boigu, with the exception of nickel (Figure 8–9). For nickel, grouping of the data in the Highest and Moderate exposure areas showed that the concentrations were significantly higher than in the Lowest exposure area.

Table 8–4: Results of the Analysis of Variance between Areas of Exposure, 2020. DF = (degrees of freedom), MS = mean sums of squares, F = ratio between groups and the level of significance, * p<0.05 displayed.

Trace element	DF	MS	F-Ratio	Significance
As	2	1059.378	1.562	0.221
Cd	2	0.392	2.947	0.063
Co	2	6.566	10.176	0.000*
Cr	2	6.114	4.295	0.020*
Cu	2	122.464	48.236	0.000*
Ni	2	8.213	4.455	0.017*
Pb	2	10.855	8.385	0.001*
Zn	2	653.352	71.467	0.000*
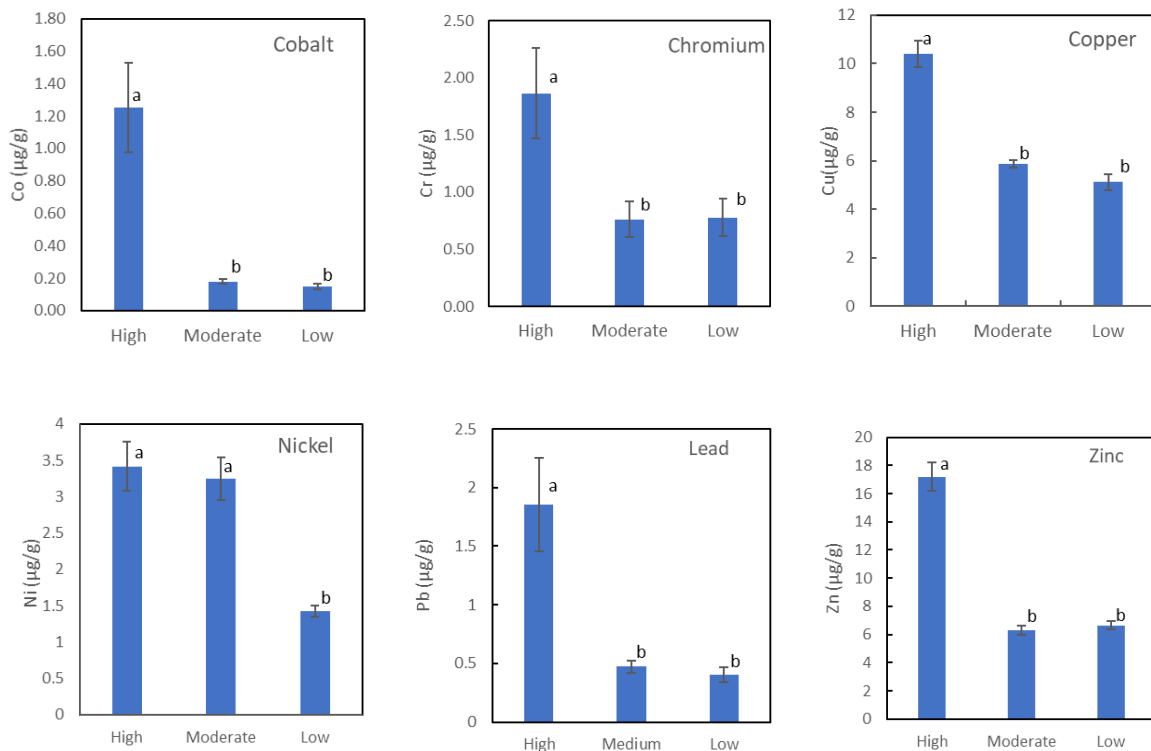
Figure 8–9: Significant differences between areas of exposure for seagrass trace elements in the 2020 study (mean ± S.E.). Different letters (a or b) depict the significantly different groups.

These results support the zones defined in the previous assessment and do not require any changes to the spatial areas of exposure. However, in the previous study, it was noted that further evidence was required to support the conclusions regarding the potential exposure to Fly River waters at Bramble Cay and the Warrior Reefs. The new results, and additional evidence highlighted in Section 0, provides greater confidence in these results.

Table 8–5 summarises the assessment information used to derive six 'areas of relative exposure' with different characteristics in the Torres Strait. For each zone, assessments are provided for:

a) Exposure to Fly River discharge and/or derived sediments: A Relative Assessment Score (Highest, Moderate, Lowest) was allocated based on expert assessment of the results of the in-situ data (loggers and salinity), hydrodynamic and sediment transport modelling, remote sensing and additional historical evidence. A confidence assessment of High, Moderate or Low was determined using expert elicitation of the lead researchers.

b) Mine-derived pollution: A Relative Assessment Score (Highest, Moderate, Lowest) was allocated based on statistical analysis (presented in previous sections) and expert assessment of the results of trace metals in sediment, water and seagrass the results. A confidence assessment of High, Moderate or Low was determined using expert elicitation of the lead researchers.

c) Potential threats: Ecological significance and confidence was assessed as High, Moderate or Low using expert elicitation of the lead researchers, based on the presence of key ecosystems (see Appendix D), relative exposure and trace metal results.

d) Overall assessment: Synthesis of the above assessments defined the following groupings:

- Exposure to Fly River discharge. Elevated trace metal concentrations, above guideline values. Ecological risk likely, but high uncertainty.
- Exposure to diluted Fly River discharge. Slightly elevated or elevated trace metal concentrations, but below guideline values. Ecological risk likely to be low, but high uncertainty.
- Low exposure, low trace metal levels, low ecological risk.

Potential areas for further investigation were identified.

The highest relative exposure areas (to freshwater, turbid waters and trace metals) were located in North East (Bramble Cay - Zone 1) and North West (Saibai, Boigu - Zone 3). While the North Central areas (Warrior Reefs - Zone 2) were also considered to be within a higher area of exposure, the results indicated that the degree of exposure here was less than that measured Saibai and Boigu islands (Z one 3) and Bramble Cay (Zone 1). In addition, some uncertainty remains around the source of influence for the northern Warrior Reefs (Zone 2) as this influence appears to be intermittent and could be driven from the east or west. Despite these differences, Zone 2 was still allocated in the highest relative exposure category relative to other locations. The North Central–south area (Masig and Ugar - Zone 4) was considered to be a transitional area, and was therefore assessed as moderate to low exposure. The Central (Iama, Warraber, Poruma – Zone 5) and South East areas (Erub, Mer – Zone 6) were the lowest exposure areas, indicating limited or no evidence of Fly River discharge influencing these areas. These results are illustrated in Figure 8-10.

It is important to reiterate that even the highest concentrations of dissolved trace metals measured in the study were below the ANZG default guideline values for 95% species protection. Of particular note, the concentrations of dissolved copper detected in the Boigu and Saibai regions consistently exceeded the Australian and New Zealand Guideline Value of 99% that is applicable for pristine, uncontaminated water. The Overall Assessment, synthesising the above results and adding an assessment of Ecological significance, took this into account. None of the zones were assessed as being in the highest Overall Assessment category as the ecological significance of the results in all locations was assessed as being relatively low to moderate, and with low data confidence. Zone 1, Zone 2 and Zone 3 were in the moderate

category, Zone 4 was in the moderate to lowest category, and Zone 5 and 6 were in the lowest category.

The greatest confidence in datasets was in the exposure assessment at Bramble Cay (which is supported by the salinity and turbidity data, modelling, remote sensing and historic coral cores) and the trace metal results in Zone 5 and Zone 6 (southernmost areas - Iama, Warraber, Poruma, Erub and Mer) due to there being no evidence of elevated trace metals in any of the surveys. The lowest confidence in datasets was in the exposure assessment in Zone 4 (Masig and Ugar) due to variable results, and the Ecological significance assessment for Zones 1 to 4 due to the lack of data on ecosystem condition. The higher confidence in Zones 5 and 6 simply reflected the exposure and trace metal results. The uncertainty in the Ecological significance assessments also highlights the limits on the scope of this study which did not include quantification of the cause/effect links of the Fly River discharge on ecosystem health in the Torres Strait. As a result of these limitations, none of the zones were assessed as being in a High overall assessment category. However, the assessment provides a valuable preliminary assessment for environmental managers to identify areas of potential concern.

The Ok Tedi mine is scheduled to cease mining and mineral processing in 2024 (OTML 2021). Following mine closure, inputs of mine-derived sediment to the river system will cease, however the mine wastes stored in the Fly River in the river bed and on the floodplain, will work their way through the system for decades to follow. Nevertheless, it is highly unlikely that sediment loads and copper concentrations will further increase in the Fly River and it is therefore reasonable to assume that over this time period that trace metals concentrations in the Torres Strait will not increase. Assuming mine closure goes ahead as planned, mine-derived sediment inputs into the Gulf of Papua and Torres Strait will decline over a timescale of decades.

Results from this project underline the importance of integration of data from a range of sources to provide a comprehensive assessment of water quality and environmental conditions. In this study, the remote sensing data utilised results from the *in-situ* monitoring studies (salinity*, in-situ* loggers and metals) to strengthen the conclusions by providing match up of results with satellite images and verification of the potential source of influence. Furthermore, the modelling also cross referenced the remote sensing outputs, and *in-situ* data. Without these links between datasets, the ability to draw the conclusions with a relatively high level of confidence would not be possible. This study also highlights the value of long-term datasets, and the important role that the Torres Strait Baseline Study played in setting a baseline for comparison of results in the region. It has demonstrated that the multiple lines of evidence approach to exposure assessment is essential in remote, complex and data poor marine environments such as the Torres Strait.

Table 8–5: Summary of the lines of evidence assessing the intrusion of Fly River waters into the Torres Strait.

Relative assessment score	Confidence in dataset/assessment	Assessment
● Highest	▪▪▪ High	◆ Exposure to Fly River discharge. Elevated trace metal concentrations, above guideline values. Ecological risk likely , but high uncertainty. **Further investigation recommended.**
● Moderate	▪▪ Moderate	◆ Exposure to diluted Fly River discharge. Slighly elevated or elevated trace metal concentrations, but below guideline values. Ecological risk likely to be low, but high uncertainty. **Further investigation recommended.**
● Lowest	▪ Low	◆ Low exposure, low trace metal levels, low ecological risk. **No need for further investigations***

* Further investigations include: Examination of biological indicators + Salinity monitoring + Long-term continuous in-situ measurements of temperature, salinity and turbidity supported by satellite data and sediment transport modelling + Periodic monitoring (every five to ten years) of water and sediment quality including trace metal analysis.

Zone	In-situ data – loggers and salinity	Modelling data suggests that:	Remote sensing data suggests that:	Additional evidence	Metals in sediment, water & seagrass	Ecological significance	Overall assessment
1 — North central (Warrior Reef)	Pulses of low salinity water detected, appear correlated to monthly tidal flows and may represent low salinity PNG coastal water intruding down to the northern Warrior Reefs.	The influence of Fly River waters is a common occurrence during the SE trade wind season.	The influence of Fly River waters is likely to reach the Warrior Reefs during the SE trade wind season.	Oceanographic studies in April-May 1982 and August-September 1994 show a major intrusion of Fly River water and mud at Warrior Reef.	Some evidence of slightly elevated trace metal concentrations in benthic sediments, waters and suspended sediments. Relatively low trace metals concentrations in seagrass - consistent with other unpolluted environments.	Presence of key ecosystems (coral, seagrass). Dissolved trace metals below guideline values for species protection.	Very likely periodic influence of Fly River waters during the SE trade wind season. Turbid plume waters likely diluted (low salinity, higher but still moderate turbidity levels). Measurable likely influence of contaminated materials. Ecological significance likely to be low, but there is high uncertainty in this assessment.
	Exposure to Fly River discharge and/or derived sediments				*Mine derived pollution*	*Potential threats*	
	● ▪▪▫				● ▪▪▫	● ▪▫▫	◆
2 — North east (Bramble Cay)	Higher than expected levels of field turbidity and exposure to turbid waters in satellite data for a remote offshore reef.	The influence of Fly River waters is a common occurrence throughout the year, but especially in the SE trade wind season with events lasting 2-3 weeks.	Intermittent influence of the Fly River plume on Bramble Cay captured by medium resolution (MODIS and Sentinel) and high resolution satellite images (Sentinel-2) during the trade wind season. Period of highest exposure is likely between June and September.	Coral cores showed freshwater influence and several pulses of freshwater each year (1781-1993). Oceanographic studies in April-May 1982 and August-September 1994 show a major intrusion of Fly River water and mud.	Elevated dissolved copper and elevated suspended sediment associated copper concentrations detected. Also some evidence of elevated trace metal concentrations in benthic sediments. Some elevation of trace metals (copper, silver, lead, zinc) in seagrass.	Presence of Key ecosystems (coral, seagrass) + fisheries. Dissolved trace metals below guideline values for species protection.	Regular 'pulses' of Fly River waters potentially driven by wind intensity and direction (inter-annual variability) with higher chance of exposure during periods of intense SE trade winds. Measurable likely influence of contaminated materials. Ecological significance likely to be low, but there is high uncertainty in this assessment.
	Exposure to Fly River discharge and/or derived sediments				*Mine derived pollution*	*Potential threats*	
	● ▪▪▪				● ▪▪▫	● ▪▫▫	◆
3 — North west (Boigu, Saibai)	Lower field salinity and higher salinity ranges measured.	The influence of Fly River waters is a common occurrence during the SE trade wind season. Signature diluted at Boigu Island.	The influence of Fly River waters is likely to reach Saibai Island. Wassi Kussa and Mai Kussa Rivers likely contribute to turbidity levels in the areas east and west of Boigu Island. The contribution of Mai and Wassi Kussa rivers varied seasonally and is expected to reach a maximum around May to August with turbid riverine water mainly flowing westward during this period.	An oceanographic study in April-May 1982 and August-September 1994 show a major intrusion of Fly River water and mud. Historically, extensive salinity intrusion in August-September 1994.	Elevated trace metal concentrations in waters and sediments. Highest metal concentrations in waters and sediments detected in this zone. Highest concentrations of several metals, including copper, lead and zinc, in seagrass found in this area.	Presence of Key ecosystems (coral, seagrass). Dissolved copper concentrations exceed the 99% species protection guideline value indicating some potential stress on ecosystems.	Likely influence of Fly River waters and mud at Saibai but this is diluted by the original mud along the PNG coast; potential influence of Fly River waters at Boigu but likely highly diluted. The time scale of influence of contaminated materials may be 100 years. Likely influence of southern PNG mainland inputs (especially at Boigu – Mai and Wassi Kussa rivers) requires quantification. Ecological significance likely to be low, but there is high uncertainty in this assessment.
	Exposure to Fly River discharge and/or derived sediments				*Mine derived pollution*	*Potential threats*	
	● ▪▪▫				● ▪▪▫	● ▪▫▫	◆

Relative assessment score

- 🟠 Highest
- 🟡 Moderate
- 🔵 Lowest

Confidence in dataset/assessment

- ▪▪▪ High
- ▪▪ Moderate
- ▪ Low

Assessment

- 🔶 Exposure to Fly River discharge. Elevated trace metal concentrations, above guideline values. Ecological risk likely, but high uncertainty. *Further investigation recommended.*
- 🔶 Exposure to diluted Fly River discharge. Slighly elevated or elevated trace metal concentrations, but below guideline values. Ecological risk likely to be low, but high uncertainty. *Further investigation recommended.*
- 🔷 Low exposure, low trace metal levels, low ecological risk. *No need for further investigations**

* Further investigations include: Examination of biological indicators + Salinity monitoring + Long-term continuous in-situ measurements of temperature, salinity and turbidity supported by satellite data and sediment transport modelling + Periodic monitoring (every five to ten years) of water and sediment quality including trace metal analysis.

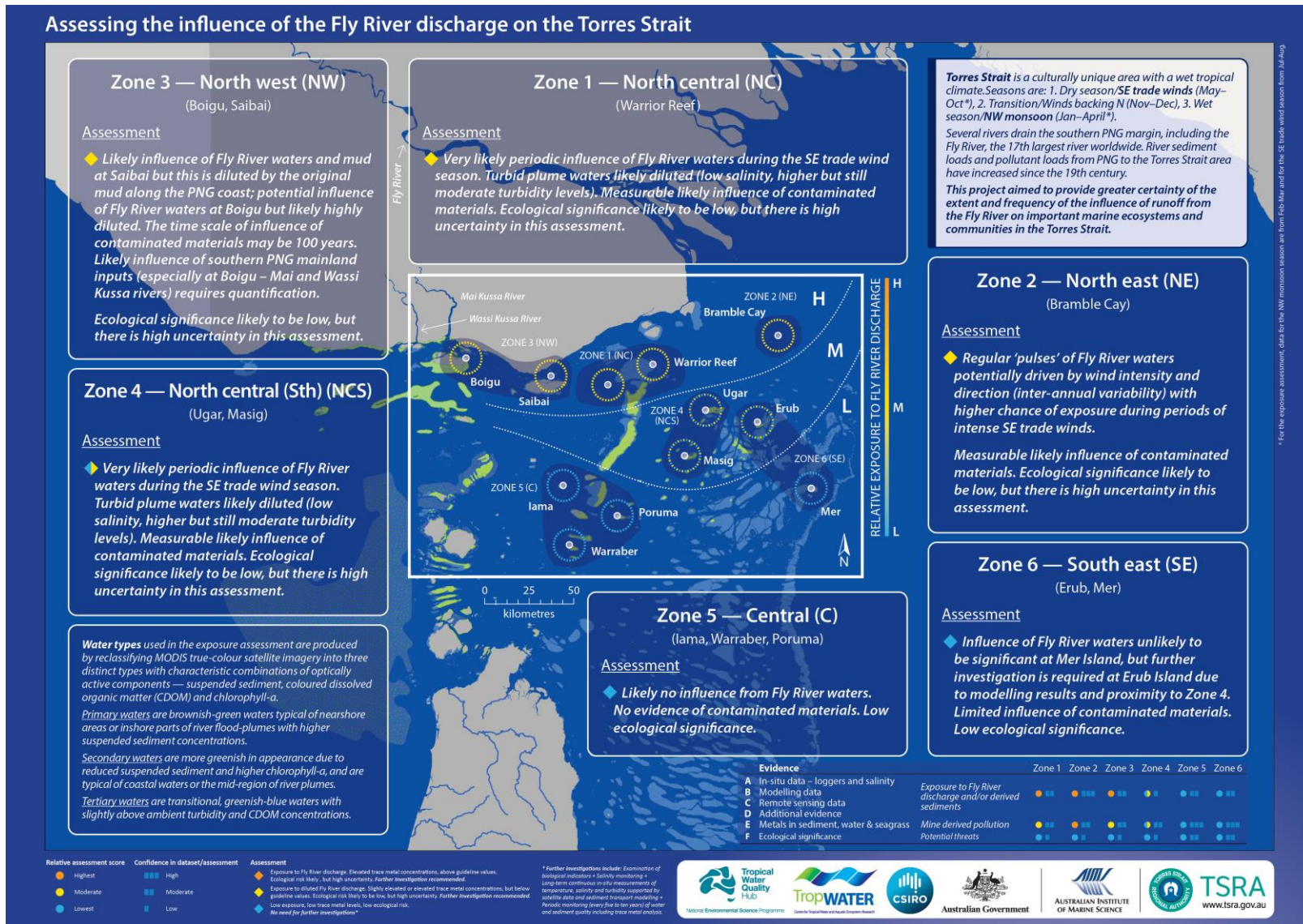| Zone	In-situ data – loggers and salinity	Modelling data suggests that:	Remote sensing data suggests that:	Additional evidence	Metals in sediment, water & seagrass	Ecological significance	Overall assessment
4 — North central (south) **(Ugar, Masig)**	Salinity measurements at Masig Island are similar to average values for marine waters. Occasional reductions in salinity (to 33 PSU) were measured in the SE trade wind seasons.	Frequent intrusion of Fly River water, but diluted with seawater. Probably minimal Fly River mud reaches there.	Limited exposure to turbid waters and greatest variability between years in the SE trade wind season.	Oceanographic studies in 1979, 1981, 1982 and 1994 shows a frequent intrusion of the Fly River plume, but well diluted by oceanic water.	Some evidence of elevated trace metal concentrations in waters. Relatively low trace metals concentrations in sediments and seagrass - consistent with other unpolluted environments.	Presence of Key ecosystems (coral, seagrass) + fisheries. Dissolved trace metals below guideline values for species protection.	Likely event-driven influence of Fly River waters in the SE trade wind season, likely to be highly diluted with seawater. Comparison of salinity data with local rainfall data and satellite images and modelling results indicate that the periods of lower salinity may be influenced by Fly River waters. Small influence of water-borne contaminated materials. Ecological significance likely to be low, but there is high uncertainty in this assessment.
	Exposure to Fly River discharge and/or derived sediments 🟡🔵 ▪▫▫				*Mine derived pollution* 🟡🔵 ▪▪	*Potential threats* 🔵 ▪▫	🔶
5 — Central **(Iama, Warraber, Poruma)**	Highest mean salinities and lowest salinity ranges were measured at these sites. Data indicates minimal freshwater inputs.	Minimal intrusion of Fly River water.	Very limited exposure to turbid waters.	Oceanographic studies in 1979, 1981, 1982 and 1994 shows an intrusion of the Fly River plume highly diluted by oceanic water.	No evidence of elevated trace metal concentrations in waters and sediments. Relatively low trace metals concentrations in seagrass - consistent with other unpolluted environments.	Presence of Key ecosystems (coral, seagrass). Dissolved trace metals below guideline values for species protection.	Likely no influence from Fly River waters. No evidence of contaminated materials. Low ecological significance.
	Exposure to Fly River discharge and/or derived sediments 🔵 ▪▪▫				*Mine derived pollution* 🔵 ▪▪▪	*Potential threats* 🔵 ▪▪▫	🔷
6 — South east **(Erub, Mer)**	Insufficient salinity measurements collected to undertake assessment.	Limited Fly River water reaches Erub Island.	Limited exposure to turbid waters and greatest variability between years in the SE trade wind season.	Coral cores showed no freshwater influence at Erub (1781-1993). Previous modelling studies (1979, 1981, 1982 and 1994) show no intrusion of Fly River waters at Mer Island, but a more frequent intrusion of Fly River water at Erub Island (but no mud), and it was well diluted with seawater.	No evidence of elevated trace metal concentrations in waters and sediments. Relatively low trace metals concentrations in seagrass - consistent with other unpolluted environments.	Presence of Key ecosystems (coral, seagrass). Dissolved trace metals below guideline values for species protection.	Influence of Fly River waters unlikely to be significant at Mer Island, but further investigation is required at Erub Island due to modelling results and proximity to Zone 4. Limited influence of contaminated materials. Low ecological significance.
	Exposure to Fly River discharge and/or derived sediments 🔵 ▪▪▫				*Mine derived pollution* 🔵 ▪▪▪	*Potential threats* 🔵 ▪▪▫	🔷

Figure 8–10: Map illustrating the key lines of evidence assessing the influence of Fly River discharge in the Torres Strait.

8.4 Conclusions

The current study, and the evidence from the first NESP studies (Apte et al. 2018 and Waterhouse et al. 2018), have provided significant advances in the knowledge of the influence of the Fly River discharge in the Torres Strait. The specific conclusions are:

1. Data collected through salinity monitoring, turbidity loggers, remote sensing and modelling predictions further confirmed previous findings that habitats located in the northeast corner of the Torres Strait Protected Zone, including the northern Warrior Reef, as far west as Saibai Island and as far east as Bramble Cay, are located in an area of higher exposure to sediments from the Fly River. The evidence also reinforced that there is a turbid coastal boundary layer along the PNG coast of the Torres Strait with maximum turbidity found inshore and decreasing seaward.

2. The source of highly turbid Torres Strait waters cannot be fully attributed to the Fly River and is likely to include other sources of sediments associated with smaller streams (including the Wassi Kussa and Mai Kussa Rivers around Boigu Island), as well as resuspension of sediment deposited in the Torres Strait mud wedge via currents, wind and wave action.

3. The Fly River plume intruded into the Torres Strait to the greatest extent during the southeast trade wind season and less so during the monsoon season. Satellite images and logger data collected at Warrior Reef suggested that the plume intrusion is greater between June and September, with a likely maximum in July to August.

4. Salinity at the northern Warrior reef monitoring site showed a strong monthly cycle with low salinity events that cannot be explained by localised rainfall or run-off. These may represent tidally driven brackish waters from coastal PNG flowing into the northern Warrior Reef area.

5. Sediment transport modelling demonstrated that contaminated new mud intrudes Torres Strait from the Fly River discharge and is diluted by the non-contaminated mud of the long-term mud wedge. Daru and Bristow Islands, located close to the PNG coast, form a hydrodynamic barrier that restricts the circulation pattern and slows down the intrusion of Fly River contaminated material further west into the Torres Strait. The time scales for the pollution spread in Torres Strait are probably of the order of 100 years.

6. Water quality across the Torres Strait is generally very good, however elevated concentrations of some trace metals are observed in waters, sediments and seagrasses in the northeast areas of the Torres Strait including Bramble Cay and also around the northern Warrior Reefs, Boigu and Saibai Islands. The highest copper concentrations (along with other metals) were found around Saibai Island. The concentrations of dissolved trace metals measured in the Torres Strait were all below the Australia and New Zealand marine water quality guideline values for 95% species protection which are the main guideline values applied in Australia for coastal management. However, the concentrations of dissolved copper detected in the Boigu and Saibai regions consistently exceeded the Australian and New Zealand Guideline Value of 99% that is applicable for pristine, uncontaminated waters. This is significant because copper is the primary trace metal of concern that is linked to the Ok Tedi mine discharge. It is important to note that the concentrations of dissolved copper measured in the Torres Strait are orders of magnitude below those reported to cause direct impacts on coral and seagrass ecosystems.

7. The enrichment of metals in waters and sediments in the Boigu and Saibai region is likely to result from natural inputs of metals from the PNG mainland such as river runoff

from various coastal rivers which are periodically augmented by contributions from the Fly River plume. The relative contributions from these sources is hard to assess without data on the contributions of metals from the PNG coastal rivers in the Boigu/Saibai region. Sediment core data indicates relatively homogenous distributions of metals with depth and does not indicate increases in metals concentrations with time. Sulphide mineral particles indicative of mine-derived sediments were detected in suspended sediment particles in samples from Boigu and Saibai but confirmation of their origin requires further work.

8. The concentrations of dissolved trace metals found around the northeast Torres Strait, Boigu and Saibai are higher than those found in other Australian coastal environments, especially for cobalt and cadmium, but are far lower than the concentrations observed in contaminated locations such as industrialised harbours.

9. The elevation of metal concentrations in the northeast Torres Strait at locations such as Bramble Cay is most likely associated with the influence of the Fly River plume. This is evident from the elevated dissolved copper concentrations and copper concentrations in suspended sediments. The association is also supported by salinity and turbidity logger data and remote sensing results. However, benthic sediments do not appear to be accumulating mine-derived contaminants as only extremely low particulate trace metal concentrations were detectable along with an absence of sulphide mineral particles (used for tracing). This is also consistent with the findings from the hydrodynamic and mud transport modelling.

10. Seagrass trace metal concentrations were significantly higher in the northeast Torres Strait (Bramble Cay), and then Boigu and Saibai islands. Markedly higher concentrations of cobalt, chromium, copper, lead and zinc were found in seagrasses from the Boigu and Saibai sites. Copper lead and zinc were also higher at Bramble Cay compared to the remaining sites. These results are in broad agreement with the patterns of the metal analysis in water, suspended sediments and benthic sediment. Seagrass trace element concentrations were generally low compared with literature values reported for other unpolluted environments.

11. Comparison of benthic sediment metals data collected over the course of the NESP Tropical Water Quality Hub Torres Strait projects (2016 to 2020) with data from the Torres Strait Baseline Study conducted in the early 1990's did not suggest any marked increase in metals concentrations that could be associated with mine-derived sediment inputs. Indeed the recent concentrations of copper (indicative of mine-related inputs) in sediments measured at Bramble Cay, the monitoring site closest to the mouth of the Fly River, were over an order of magnitude lower than measured during the baseline study. This difference was linked to the presence of a far larger proportion of fine sediments at Bramble Cay during the baseline study compared to the current day. The data may reflect geomorphological changes at Bramble Cay over the last 30 years or transient deposition of fine sediments at this location.

12. Based on multiple lines of evidence derived from the investigations conducted, six 'areas of relative exposure' to Fly River discharge were defined (Table i). The highest relative exposure areas (to freshwater, turbid waters and trace metals) were located in North East (Bramble Cay - Zone 1) and North West (Saibai, Boigu - Zone 3). While the North Central areas (Warrior Reefs - Zone 2) were also within the higher area of exposure, the degree of exposure - and link to the Fly River specifically - was lower than Saibai and Boigu islands (Zone 3) and Bramble Cay (Zone 1), but still high relative to other areas. The North Central–south area (Masig and Ugar - Zone 4) was

considered to be a transitional area and was therefore assessed as moderate to low exposure. The Central (Iama, Warraber, Poruma – Zone 5) and South East areas (Erub, Mer – Zone 6) were the lowest exposure areas, with limited or no evidence of Fly River discharge influencing these areas. Data confidence varied for each zone and assessment (Table i). This was a *relative* assessment of the exposure of the Torres Strait region to Fly River discharge, and even the highest concentrations of dissolved trace metals measured in the study were below the ANZG default guideline values for 95% species protection. However, the concentrations of dissolved copper detected in the Boigu and Saibai regions consistently exceeded the Australian and New Zealand Guideline Value of 99% that is applicable for pristine, uncontaminated water. An Overall Assessment, synthesising the above results and adding an assessment of Ecological significance, took this into account. None of the zones were assessed as being in the highest Overall Assessment category as the ecological significance of the results in all locations was assessed as being relatively low to moderate, and with low data confidence. Zone 1, Zone 2 and Zone 3 were in the moderate category, Zone 4 was in the moderate to lowest category, and Zone 5 and 6 were in the lowest category.

Limitations

The recent work confirms that habitats located in the NE corner of the Torres Strait Protected Zone including Bramble Cay, north of Masig Island and as far northwest as Saibai Island, are located in an area of higher exposure to brackish and turbid waters from, the Fly River, as well as from/or derived from local PNG river discharges. Despite the increased sediment load, water and sediment quality is generally very good across the region, however, increased metal concentrations in waters and sediments were observed in the northern Torres Strait, and particularly around Boigu and Saibai islands, Bramble Cay and to a lesser extent, the northern Warrior Reefs. The additional data in this study confirmed that runoff from the PNG mainland may also be a factor influencing metal concentrations around Boigu and Saibai islands, and that the influence of the Fly River to Boigu Island is likely to be limited.

Salinity monitoring in the region provided a valuable additional line of evidence in conjunction with the satellite images. The data supported conclusions about the areas in the region that are most likely influenced by land based freshwater discharges either from the Fly River or runoff from the adjacent PNG mainland. Participation of the TSRA Rangers in the salinity monitoring strengthened the local engagement in the study and provided a mechanism for regular contact. It also provided an opportunity to train the Rangers in water quality monitoring techniques and improve their understanding of the issues driving the project scope. It is recommended that this would be a valuable component of the study to be continued, but only if other monitoring including the remote sensing and *in-situ* loggers are also supported, as these three components strongly complemented each other. Several visits to local communities provided feedback of the project results have provided an opportunity to extend the project learnings and interact with the key end users of the research. Final community feedback sessions are planned in April/May 2021.

The *in-situ* loggers were a highly valuable project component but difficult to service logistically, resulting in some gaps in the datasets. The new data at the Warrior Reefs revealed patterns that were partially qualified with the remote sensing data. However, the unexpected low salinity events that appear to be linked to the tidal cycles at the northern Warrior Reefs shows that understanding of the systems is still incomplete. This reflects the complex nature of the

oceanography in this region. Overall, the loggers demonstrated the utility of long-term observations in understanding the observed patterns and so there is ongoing value in continuing these observations and the platforms that provide them. While addition of logger instruments at Saibai Island was recommended for the current study, this was not installed due to logistical constraints and selection of a suitable location. This still remains a priority for any future work. Ongoing deployment of a network of continuous loggers that measure salinity, temperature and turbidity would assist in further qualification of the likely sources of elevated turbidity and low salinity peaks across the Torres Strait. Instrumentation at Bramble Cay, the Warrior Reefs and Saibai Island remain a priority. Addition of instrumentation around Daru would assist to better quantify the link between Fly River inputs and the results in these locations.

The results of the modelling provide predictions of the net flux of mud transport from the Fly River into the Torres Strait, with a long-term outlook of net mud movement. Extension of the modelling domain to include Bramble Cay would be valuable to estimate the proportion of Fly River material that is transported to that area. The confidence in the modelling results would be improved by further validation data. In particular, future work should focus on collecting *in-situ* suspended sediment concentration measurements across turbidity gradients and moored nephelometer data to further verify the mud model. The *in-situ* salinity, temperature and turbidity data collected at Warrior Reef were successful to support the large-scale trends defined by the satellite colour class images. This type of continuous measurement is highly valuable in the remote Torres Strait area to support the satellite information, as well as current modelling effort in the region (Wolanski et al. 2021 and Section 0).

The remote sensing data provided a long term, large scale dataset to underpin the improved understanding of Fly River discharges, turbidity patterns and preliminary estimates of suspended sediment concentrations. The application of the water type analysis extended from the GBR also supported the definition of areas of relative area to turbid waters. Dense cloud cover in the study area allowed the capture of satellite information about 50% of the time and it is likely that some large sediment plumes associated with rough weather may have been missed. However, the spatial and temporal trends in water composition described in this study were consistent with other evidence collected in the Gulf of Papua-Torres Strait region, suggesting that the cloud cover did not substantially alter the data interpretation.

Preliminary validation exercises provided confidence in the colour and turbidity trends described in this report. However, the validation of the TSS algorithm trialed was inconclusive due to the limited number of field data coincident to cloud free satellite acquisition. This empirical algorithm is likely to underestimate suspended sediment concentrations in the most turbid part of the study area, including the Torres Strait mud wedge and the Fly River estuary and to be more accurate in the lower concentration ranges (this study and Wolanski et al. 2021). Investment in local suspended sediment concentrations observations across turbidity gradients would help improving the accuracy of the satellite estimations and allow developing more complex satellite retrieval models. The remoteness and high cloud cover of the study areas, however, limits the ability to collect more field data concurrent to the satellite overpass. It is impossible to fully separate direct riverine plume influence from sediment resuspension in the true colour and colour class satellite maps and it may be challenging to develop a fully validated satellite SSC algorithm for the large-scale study area due to the above limitations. However, this study underlined the value of combining satellite information and continuous (or

regular) salinity and turbidity measurements at smaller scale / key site locations. Further analyses of sentinel-3 Forel-Ule images and high resolution sentinel-2 images, combined with field Forel-Ule measurements (smartphone application) and logger data would help better illustrating fine-scale coastal processes and turbidity exposure around key locations such as Bramble Cay, Saibai Island and the Warrior Reef.

The COVID-19 restrictions resulted in a significant and highly effective collaborative effort between CSIRO, AIMS and JCU and TSRA which enabled some field work to be completed in 2020. Ongoing collaboration with TSRA and the Ranger teams has been a major positive outcome of the NESP Tropical Water Quality Hub research, with benefits highlighted in relation to the salinity monitoring above. The teams also assisted with the sample collection for trace metal analysis in 2016, 2019 and 2020 which added significant value to the projects, both in terms of local engagement and in overcoming logistical challenges.

8.5 Recommendations

1. Future water quality monitoring of the Torres Strait would be best conducted jointly between Australia and PNG. This would allow access to areas such as the rivers that drain the Southern Fly district and also enable monitoring of the sources of mine derived contamination that originate from the Fly River. It is also important to track changes of mining operations in PNG such as mine expansions and shutdowns and use this information as a trigger to inform future monitoring.
2. Future sediment and water quality monitoring should focus on Bramble Cay, the Warrior Reef complex and the PNG coastline (Daru to Boigu). Prior to long term monitoring, a pilot study should assess temporal variability (e.g. seasonal variations) and spatial heterogeneity at these locations. Given the slow rates of sediment accumulation, a monitoring frequency of every 5 to 10 years would be sufficient to track environmental change.
3. Further field monitoring should be conducted to explain the low salinity events observed at the northern Warrior Reef. This information would enable a better understanding of water circulation and a better understanding of the freshwater contributions from the rivers in the Southern Fly district.
4. This study has illustrated the benefits of utilising multiple lines of evidence (e.g. field monitoring, remote sensing, modelling, biomonitoring and geochemical investigations) to assess environmental impacts. It is recommended that future studies adopt this integrative approach.
5. Involvement of local Rangers has also provided significant benefits to the project in terms of access to local support, and engagement and upskilling of the Ranger teams; continuation of their involvement is recommended in any future monitoring programs.

REFERENCES

Álvarez-Romero, J., Devlin, M., da Silva, E., Petus, C., Ban, N., Pressey, R., Kool, J., Roberts, J., Cerdeira-Estrada, S., Wenger, A., & Brodie, J. (2013). A novel approach to model exposure of coastal-marine ecosystems to riverine flood plumes based on remote sensing techniques. *Journal of Environmental Management*, 119, 194-207.

Angel, B.M, Apte, S.C., Simpson, S.L., Jarolimek, C.V., & Jung, R.F. (2010a*). Behaviour of copper in the Fly River Estuary, Papua New Guinea*. CSIRO Water for a Healthy Country Technical Report. Prepared for Ok Tedi Mining Ltd, 45 pp.

Angel, B.M., Hales, L.T., Simpson, S.L., Apte, S.C., Chariton, A.A., Shearer, D.A., & Jolley, D.F. (2010b). Spatial variability of cadmium, copper, manganese, nickel and zinc in the Port Curtis Estuary, Queensland, Australia. *Marine and Freshwater Research*, 61, 170-183.

Angel, B.M., Apte, S.C., Simpson, S.L., Jarolimek, C.V., & King, J.J. (2014). *The behaviour of trace metals in the Fly Estuary, Papua New Guinea*. CSIRO Water for a Healthy Country Technical report EP14897, 91 pp.

Angel, B.M., Jarolimek, C.V. King, J.J., Mudaliar, P., & Apte, S.C. (2020). *Evaluation of trace metal concentrations in the Fly Estuary and nearby waters of the Gulf of Papua and the Torres Strait, Papua New Guinea*. Land and Water report, CSIRO, Australia.

Anthony, K.R.N. (2000). Enhanced particle-feeding capacity of corals on turbid reefs (Great Barrier Reef, Australia). *Coral Reefs*, 19(1), 59-67.

Anthony, K.R.N., & Fabricius, K.E. (2000). Shifting roles of heterotrophy and autotrophy in coral energetics under varying turbidity. *Journal of Experimental Marine Biology and Ecology*, 252, 221-253.

ANZG (2018). *Australian and New Zealand Guidelines for Fresh and Marine Water Quality*. Australian and New Zealand Governments and Australian state and territory governments, Canberra ACT, Australia. Available at www.waterquality.gov.au/anz-guidelines. Last accessed 6 September 2019.

Apte, S.C. (2009). Biogeochemistry of copper in the Fly River. In B.R. Bolton (Ed.), *The Fly River Papua New Guinea. Environmental studies in an impacted tropical river system*. Developments in Earth & Environmental Sciences, 9. (pp. 321-373). Elsevier B.V.

Apte, S.C., & Day, G.M. (1998). Dissolved metal concentrations in the Torres Strait and Gulf of Papua. *Marine Pollution Bulletin*, 30, 298-304.

Apte, S.C., Batley, G.E., Szymczak, R., Rendell, P.S., Lee, R., & Waite, T.D. (1998). Baseline trace metal concentrations in New South Wales coastal waters. *Marine Freshwater Research*, 49, 203-214

Australian Government (2014, 18 July 2014). The context of water planning in Queensland. 2015. http://archive.nwc.gov.au/library/topic/planning/report-card/queensland.

Apte, S.C., Angel, B.M., Hunter, C., Jarolimek, C.V., Chariton, A.A., King J., & Murphy, N. (2018). *Impacts of mine-derived contaminants on Torres Strait environments and communities.* Report to the National Environmental Science Program. Reef and Rainforest Research Centre Limited, Cairns (128 pp.).

Ayukai, T., & Wolanski, E. (1997). Importance of biologically mediated removal of fine sediments from the Fly River plume, Papua New Guinea. *Estuarine, Coastal and Shelf Science*, 44, 629-639.

Baeyens, W., Goeyens, M., Monteny, F., & Elskens, M. (1998). Effect of organic complexation on the behaviour of dissolved cadmium, copper, and zinc in the Scheldt estuary. *Hydrobiologia*, 366, 15-43.

Bainbridge, S.J., Berkelmans, R., Sweatman, H., & Weeks, S. (2015). *Monitoring the health of Torres Strait Reefs – Final Report*. Report to the National Environmental Research Program. Reef and Rainforest Research Centre Limited, Cairns, 93 pp.

Bainbridge, Z., Lewis, S., Bartley, R., Fabricius, K., Collier, C., Waterhouse, J., Garzon-Garcia, A., Robson, B., Burton, J., Wenger, A., & Brodie, J. (2018). Fine sediment and particulate organic matter: A review and case study on ridge-to-reef transport, transformations, fates, and impacts on marine ecosystems. *Marine Pollution Bulletin*, 135, 1205–1220.

Baird, M.E., Wild-Allen, K.A., Parslow, J., Mongin, M., Robson, B., Skerratt, J., Rizwi, F., SojaWo´znaik, M., Jones, E., Herzfeld, M., Margvelashvili, N., Andrewartha, J., Langlais, C., Adams, M.P., Cherukuru, N., Gustafsson, M., Hadley, S., Ralph, P.J., Rosebrock, U., Schroeder, T., Laiolo, L., Harrison, D., & Steven, A.D.L. 2020a. CSIRO Environmental Modelling Suite (EMS): Scientific description of the optical and biogeochemical models (vB3p0). *Geoscientific Model Development,* 13, 4503–4553.

Baird, M. E., Adams, M. P., Andrewartha, J., Herzfeld, M., Jones, E., Margvelashvili, N., Mongin, M., Rizwi, F., Robson, B., Skerratt, J., Steven, A.D., Wild-Allen, Karen A., & Soja-Wozniak, M. (2020b). Additional processes and diagnostic variables in the CSIRO *Environmental Modelling Suite*, 38 pp.

Baird, M.E., Adams, M.P., Andrewartha, J., Cherukuru, N., Gustafsson, M., Hadley, S., Herzfeld, M., Jones, E., Margvelashvili, N., Mongin, M., Parlsow, J., Ralph, P.J., Rizwi, F., Robson, B., Rosebrock, U., Sakov, P , Schroeder, T., Skerratt, J, Steven, A.D.L., & Wild-Allen K.A. (2017). *Appendix B: CSIRO Environmental Modelling Suite: Scientific description of the optical, carbon chemistry and biogeochemical models (BGC1p0)*, 131 pp. URL: https://research.csiro.au/ereefs/wp-content/uploads/sites/34/2015/08/eReefsOpticalBGCframeBGC1p0.pdf

Banc-Prandi, G., & Fine, M. (2019). Copper enrichment reduces thermal tolerance of the highly resistant Red Sea coral *Stylophora pistillata*. *Coral Reefs*, 38(2), 285-296.

Bégin, C., Schelten, C.K., Nugues, M.M., Hawkins, J., Roberts, C., & Côté, I.M. (2016). Effects of protection and sediment stress on coral reefs in Saint Lucia. *PloS ONE*, 11(2), p.e0146855.

Benfares, R., Seridi, H., Belkacem, Y., Inal, A. (2015). Heavy metal bioaccumulation in Brown algae Cystoseira compressa in Algerian coasts, Mediterranean Sea. Environ. Process., 2 (2015), pp. 429-439.

Bessell-Browne, P., Negri, A., Fisher, R., Clode, P.L., & Jones, R. (2017). Impacts of light limitation on corals and crustose coralline algae. *Science Reports*, 7(1), 11553. doi: 10.1038/s41598-017-11783-z.

Birch, G.F., Cox, B.M., & Besley, C.H (2018). Metal concentrations in seagrass (Halophila ovalis) tissue and ambient sediment in a highly modified estuarine environment (Sydney estuary, Australia). *Marine Pollution Bulletin*, 131, 130-141.

Birkeland, C. (1988). *Geographic comparisons of coral-reef community processes*. In Choat, J.H., D. Barnes, MA. Borowitzka, J.C. Coll, P.J.Davies, P. Flood, B.G. Hatcher, D. Hopley, P.A. Hutchings, D. Kinsey, G.R. Orme, M. Pichon, P.F. Sale, P. Sammarco, C.C. Wallace, C. Wilkinson, E. Wolanski and O. Bellwood (eds.) Proceedings of the 6th International Coral Reef Symposium: Vol. 1: Plenary Addresses and Status review. Townsville, Australia. pp. 211-220.

Biscéré, T., Lorrain, A., Rodolfo-Metalpa, R., Gilbert, A., Wright, A., Devissi, C., Peignon, C., Farman, R., Duvieilbourg, E., Payri, C., & Houlbrèque, F. (2017). Nickel and ocean warming affect scleractinian coral growth. *Marine Pollution Bulletin*, 120(1-2), 250-258.

Bolton, B. (2008). *The Fly River, Papua New Guinea: Environmental Studies in an Impacted Tropical River System*. Elsevier, Amsterdam, 620 pp.

Bonanno, G., & Orlando-Bonaca, M. (2017). Trace elements in Mediterranean seagrasses: accumulation, tolerance and biomonitoring. A review. *Marine Pollution Bulletin*, 125(1-2), 8-18.

Bonanno, G., & Orlando-Bonaca, M. (2018). Trace elements in Mediterranean seagrasses and macroalgae. A review. *Science of The Total Environment*, 618, 1152-1159.

Bonanno, G., & Di Martino, V. (2106). Seagrass *Cymodocea nodosa* as a trace element biomonitor: bioaccumulation patterns and biomonitoring uses. *Journal of Geochemical Exploration*. 169, 43-49. doi.org/10.1016/j.gexplo.2016.07.010

Bowles, K.C., Apte, S.C., Batley, G.E., Hales, L.T., & Rogers, N.J. (2006). A rapid Chelex column method for the determination of metal speciation in natural waters. *Analytica Chimica Acta*, 558, 237-245. doi.org/10.1016/j.aca.2005.10.071

Brackup, I., Capone, D.G. (1985). The effect of several metal and organic pollutants on nitrogen fixation (acetylene reduction) by the roots and rhizomes of *Zostera marina*. Journal of Experimental Botany 25, 145-151.

Butler, J.R.A., Bohensky, E., Skewes, T., Maru, Y., Busilacchi, S., Rochester, W., Katzfey, J., & Wise, R.M. (2015). *Drivers of change in the Torres Strait region: status and trends*. Report to National Environmental Research Program. Reef & Rainforest Research Centre Limited, Cairns, 60 pp.

Canestrelli, A., Fagherazzi, S., Defina, A., & Lanzoni, S. (2010). Tidal hydrodynamics and erosional power in the Fly River delta, Papua New Guinea. *Journal of Geophysical Research*, 115, F04033. doi.org/10.1029/2009JF001355

Carter, A.B., & Rasheed, M.A. (2016). *Assessment of key dugong and turtle seagrass resources in north-west Torres Strait*. Report to the National Environmental Science Programme and Torres Strait Regional Authority. Reef and Rainforest Research Centre Limited, Cairns, 40 pp.

Carter, A.B., & Rasheed, M.A. (2018). *Torres Strait Seagrass Long-term Monitoring: Dugong Sanctuary, Dungeness Reef and Orman Reefs*., Centre for Tropical Water & Aquatic Ecosystems, Research Report No. 18/17, James Cook University, Cairns, 35 pp.

Carter, A.B., Taylor, H.A., & Rasheed, M.A. (2014). *Torres Strait mapping: Seagrass consolidation, 2002–2014*. JCU Publication, Report no. 14/55, Centre for Tropical Water & Aquatic Ecosystem Research, Cairns, 47 pp.

Carter, A.B., Mellors, J.M., & Rasheed, M.A. (2018). *Torres Strait Seagrass 2018 Report Card. Centre for Tropical Water & Aquatic Ecosystems*, Research Publication 18/25, James Cook University, Cairns, 65 pp.

Carter, A.B., Mellors, J.M., Whap, T., Hoffmann, L.R., & Rasheed, M.A. (2020). '*Torres Strait Seagrass 2020 Report Card*'. Centre for Tropical Water & Aquatic Ecosystem Research Publication 20/24, James Cook University, Cairns, 62 pp.

Chartrand, K.M., Szabó, M., Sinutok, S., Rasheed, M.A., & Ralph, P.J. (2018). Living at the margins – The response of deep-water seagrasses to light and temperature renders them susceptible to acute impacts. *Marine Environmental Research*, 136, 126–138.

Coles, R.G. McKenzie, L.J., & Campbell S.J. (2002). Chapter 11: The seagrasses of eastern Australia. In: *The World Atlas of Seagrasses*: Present Status and Future Conservation, eds. E.P. Green, F.T. Short, M.D. Spalding. University of California Press, pp. 119-133.

Collier, C., & Waycott, M. (2009). *Drivers of change to seagrass distributions and communities on the Great Barrier Reef: Literature Review and Gaps Analysis*. Report to the Marine and Tropical Sciences Research Facility. Reef and Rainforest Research Centre Limited, Cairns 55 pp.

Collier, C.J., Lavery, P.S., Ralph, P.J., & Masini, R.J. (2009). Shade-induced response and recovery of the seagrass *Posidonia sinuosa*. *Journal of Experimental Marine Biology and Ecology*, 370(1-2), 89-103.

Collier, C.J., Waycott, M., & McKenzie, L.J. (2012). Light thresholds derived from seagrass loss in the coastal zone of the northern Great Barrier Reef, Australia. *Ecological Indicators*, 23, 211–219.

Collier, C.J., Adams, M., Langlois, L., Waycott, M., O'Brien, K., Maxwell, P., & McKenzie, L. (2016). Thresholds for morphological response to light reduction for four tropical seagrass species. *Ecological Indicators*, 67, 358–366.

Comber, S., Gunn, A., & Whalley, C. (1995). Comparison of the partitioning of trace metals in the Humber and Mersey Estuaries. *Marine Pollution Bulletin*, 30, 851-860.

Cresswell, T. (2012). *Sources and mechanisms of metal bioaccumulation in the Lagaip/Strickland Rivers, Papua New Guinea*. PhD thesis, RMIT University, Melbourne. 269 pp.

Crockett, J. S., Nittrouer, C.A., Ogston, A.S., Walsh, J.P., Naar, D., & Donahue, B. (2008). Morphology and filling of incised submarine valleys on the continental shelf near the mouth of the Fly River, Gulf of Papua. *Journal of Geophysical Research,* 113, F01512.

Crockett, J.S., Nittrouer, C.A., Ogston, A.S., & Goni, M.A. (2009). Variable Styles of Sediment Accumulation Impacting Strata Formation on a Clinoform: Gulf of Papua, Papua New Guinea. In: *The Fly River: natural and human aspects of a complex fluvial system*. B.R. Bolton (Ed.), Elsevier, Amsterdam, 620 pp.

De'ath, G., & Fabricius, K. (2010). Water quality as a regional driver of coral biodiversity and macroalgae on the Great Barrier Reef. *Ecological Applications*, 20, 840-850.

de Bakker, D., van Duyl, F.C., Bak, R.P.M., Nugues, M.M., Nieuwland, G., & Meesters, E.H. (2017). 40 Years of benthic community change on the Caribbean reefs of Curaçao and Bonaire: the rise of slimy cyanobacterial mats. *Coral Reefs*, 36, 355-367. doi.org/10.1007/S00338-016-1534-9.

Devlin, M., Petus, C., Teixeira da Silva, E., Tracey. D., Wolff, N., Waterhouse, J., & Brodie, J. (2015). Water quality and river plume monitoring in the Great Barrier Reef: An overview of methods based on ocean colour satellite data. *Remote Sensing*, 7, 12909-12941. doi: 10.3390/rs71012909

Dietrich, W.E., Day, G.M., & Parker, G. (1999). The Fly River, Papua New Guinea: Inferences about river dynamics, floodplain sedimentation and fate of sediment, *In: Varieties of Fluvial Form*, eds. A. J. Miller, A. Gupta. New York, John Wiley, pp. 345-376.

Dight, I.J., & Gladstone, W. (1993). *Torres Strait baseline study: pilot study final report June 1993*. Great Barrier Reef Marine Park Authority Research Publication No. 29. Townsville, Great Barrier Reef Marine Park Authority.

Doxaran, D., Froidefond, J.-M., & Castaing, P. (2003). Remote-sensing reflectance of turbid sediment-dominated waters. Reduction of sediment type variations and changing illumination conditions effects by use of reflectance ratios. *Applied Optics,* 42, 2623–2634.

Dorji, P., Fearns, P., & Broomhall, M. (2016). A semi-analytic model for estimating total suspended sediment concentration in turbid coastal waters of northern Western Australia using MODIS-Aqua 250 m data. *Remote sensing,* 8(7), 556.

Duckworth, A., Giofre, N., & Jones, R. (2017). Coral morphology and sedimentation. *Marine Pollution Bulletin*, 125 (1–2), 289–300.

Duke, N.C., Burrows, D., & Mackenzie, J.R. (2015). *Mangrove and freshwater wetland habitat status of the Torres Strait Islands. Biodiversity, biomass and changing condition of wetlands*. Report to the National Environmental Research Program. Reef and Rainforest Research Centre Limited, Cairns, 100 pp.

Erftemeijer, P.L., Riegl A., Hoeksema B.W., & Todd, P.A. (2012). Environmental impacts of dredging and other sediment disturbances on corals: A review. *Marine Pollution Bulletin*, 64, 1737–1765.

Fabricius, K., De'ath, G., McCook, L., Turak, E., & Williams, D.M.c.B. (2005). Changes in algal, coral, and fish assemblages along water quality gradients on the inshore Great Barrier Reef. *Marine Pollution Bulletin*, 51, 384-398.

Fabricius, K.E., Logan, M., Weeks, S., & Brodie, J. (2014). The effects of river run-off on water clarity across the central Great Barrier Reef. *Marine Pollution Bulletin*, 84, 191–200.

Fabricius, K.E., Logan, M., Weeks, S.J., Lewis, S.E., & Brodie, J. (2016). Changes in water clarity related to river discharges on the Great Barrier Reef continental shelf: 2002-2013. *Estuarine, Coastal and Shelf Science*, 173, A1–A5.

Ferguson, A.J.P., Gruber, R., Potts, J., Wright, A., Welsh, D.T., & Scanes, P. (2017). Oxygen and carbon metabolism of *Zostera muelleri* across a depth gradient – implications for resilience and blue carbon. *Estuarine Coastal Shelf Science*, 187, 216–230.

Ferrier-Pages, C., Schoelzke, V., Jaubert, J., Muscatine, L., & Hoegh-Guldberg, O. (2001) Response of a scleractinian coral *Stylophora pistillata*, to iron and nitrate enrichment. *Journal of Experimental Marine Biology and Ecology*, 259, 249–261.

Fuentes, M.M.P.B., Bell, I., Hagihara, R., Hamann, M., Hazel, J., Huth, A., Seminoff, J.A., Sobtzick, S., & Marsh, H. (2015). Improving in-water estimates of marine turtle abundance by adjusting aerial survey counts for perception and availability biases. *Journal of Experimental Marine Biology and Ecology*, 471, 77-83.

Galloway, W.E. (1975). Process framework for describing the morphologic and stratigraphic evolution of a deltaic depositional system, *In: Deltas: Models for exploration*, ed. M. L. Broussard. Houston: Houston Geological Society, pp. 87-98.

Gaudino, S., Galas, C., Belli, M., Barbizzi, S., de Zorzi, P., Jacimovic, R., Jeran, Z., Pati, A., & Sansone, U., (2007). The role of different soil sample digestion methods on trace elements analysis: a comparison of ICP-MS and INAA measurement results. Accreditation and Quality Assurance, 12, 84–93. doi.org/10.1007/s00769-006-0238-1

Gissi, F., Stauber, J., Reichelt-Brushett, A., Harrison, P.L. & Jolley, D.F. (2017). Inhibition in fertilisation of coral gametes following exposure to nickel and copper. *Ecotoxicology and Environmental Safety*, 145, 32-41.

Gladstone, W. (1996). *Trace metals in sediments, indicator organisms and traditional seafoods of the Torres Strait*. Great Barrier Reef Marine Park Authority, Townsville. http://hdl.handle.net/11017/262

Govers, L.L., Lamers, L.P.M., Bouma, T.J., Eygensteyn, J., de Brouwer, J.H.F., Hendriks, A.J., Huijbers, C.M., & van Katwijk, M.M. (2014). Seagrasses as indicators for coastal trace metal pollution: a global meta-analysis serving as a benchmark, and a Caribbean case study. *Environmental Pollution*, 195, 210-217. doi.org/10.1016/j.envpol.2014.08.028.

Great Barrier Reef Marine Park Authority [GBRMPA] (2010). Water Quality Guidelines for the Great Barrier Reef Marine Park. Great Barrier Reef Marine Park Authority, Townsville. 99 pp.

Gruber, R., Waterhouse, J., Logan, M., Petus, C., Howley, C., Lewis, S., Tracey, D., Langlois, L., Tonin, H., Skuza, M., Costello, P., Davidson, J., Gunn, K., Lefevre, C., Moran, D., Robson, B., Shanahan, M., Zagorskis, I., Shellberg, J., & Neilen, A. (2020). *Marine Monitoring Program: Annual Report for Inshore Water Quality Monitoring 2018-19*. Report for the Great Barrier Reef Marine Park Authority, Great Barrier Reef Marine Park Authority, Townsville.

Hamann, M., Smith, J. Preston S., & Fuentes, M.M.P.B. (2015a). *Nesting green turtles of Torres Strait*. Report to the National Environmental Research Program. Reef and Rainforest Research Centre Limited, Cairns, 13 pp.

Hamann, M., Smith, J., & Preston, S. (2015b). *Flatback turtles of Torres Strait*. Report to the National Environmental Research Program. Reef and Rainforest Research Centre Limited, Cairns, 8 pp.

Harris, P.T. (1994). Comparison of tropical, carbonate and temperate, siliciclastic tidally dominated sedimentary deposits: examples from the Australian continental shelf. *Australian Journal of Earth Sciences,* 41(3), 241-254.

Harris, P. T. (1988). Sediments, bedforms and bedload transport pathways on the continental shelf adjacent to Torres Strait, Australia—Papua New Guinea. Continental Shelf Research, 8(8), 979-1003.Harris, P.T., Baker, E.K., Cole, A.R., Short, S.A. (1993). A preliminary study of sedimentation in the tidally dominated Fly River Delta, Gulf of Papua. *Continental Shelf Research*, 13, 441–472.

Harris, P.T., Heap, A., Passlow, V., Hughes, M., Porter-Smith, R., Beaman, R.J., Hemer, M., Daniell, J., Buchanan, C., Watson, T., Collins, D., Bleakley, N., Anderson, O., & King, A. (2004). *Cross-shelf sediment transport in the Torres Strait - Gulf of Papua region: RV Franklin cruise 01/02, January-February, 2002*. Geoscience Australia, Canberra.

Hatje, V., Apte, S.C., Hales, L.T., & Birch, G. (2003). Dissolved trace metal distributions in Port Jackson estuary (Sydney Harbour), Australia. *Marine Pollution Bulletin*, 46, 719-730.

Haynes, D. (2001). *Pesticide and heavy metal concentrations in Great Barrier reef sediment, seagrass and dugongs (Dugong dugon)*. Unpublished PhD thesis, University of Queensland. 216 pp.

Haywood, M.D.E., Browne, M., Skewes, T., Rochester, W., McLeod, I., Pitcher, R., Dennis, D., Dunn, J., Cheers, S., & Wassenberg, T. (2007). *Improved knowledge of Torres Strait seabed biota and reef habitats*. Report to the Marine and Tropical Sciences Research Facility. Reef and Rainforest Research Centre Limited, Cairns, 115 pp.

Haywood, M.D.E., Pitcher, C.R., Ellis, N., Wassenberg, T.J., Smith, G., Forcey, K., McLeod, I., Carter, A., Strickland, C., & Coles, R. (2008). Mapping and characterisation of the inter-reefal benthic assemblages of the Torres Strait. *Continental Shelf Research*, 28, 2304-2316.

Heap, A.D., Hemer, M., Daniell, J., Mathews, E., Harris, P.T., Kerville, S., & O'Grady, L. (2005). *Biophysical Processes in the Torres Strait Marine Ecosystem – post cruise report*. Geoscience Australia, Record 2005/11, 112 pp.

Hedley, J.D., McMahon, K., & Fearns, P. (2014). Seagrass canopy photosynthetic response is a function of canopy density and light environment: a model for *Amphibolis griffithii. PloS ONE*, 9(10), p.e111454.

Heggie D, & Lewis T (1984). Cobalt in pore waters of marine sediments. *Nature,* 311, 453–455.

Lewis, M.A. & Devereux, R. (2009). Nonnutrient anthropogenic chemicals in seagrass ecosystems: fate and effects. *Environmental Toxicology and Chemistry*. 28,644-661.

Hemer, M., Harris, P.T., Coleman, R., & Hunter, J. (2004). Sediment mobility due to currents and waves in the Torres Strait–Gulf of Papua region. *Continental Shelf Research*, 24(9), 2297-2316. doi: 10.1016/j.csr.2004.07.011.

Hughes, T.P., Kerry, J.T., Álvarez-Noriega, M., Álvarez-Romero, J.G., Anderson, K.D., Baird, A.H., Babcock, R.C., Beger, M., Bellwood, D.R., Berkelmans, R., & Bridge, T.C. (2017). Global warming and recurrent mass bleaching of corals. *Nature*, 543(7645), 373.

Hughes, T., Kerry, J., & Simpson, T. (2018a). Large-scale bleaching of corals on the Great Barrier Reef. *Ecology*, 99, 501-501.

Hughes, T.P., Kerry, J.T., Baird, A.H., Connolly, S.R., Dietzel, A., Eakin, C.M., Heron, S.F., Hoey, A.S., Hoogenboom, M.O., Liu, G., & McWilliam, M.J. (2018b). Global warming transforms coral reef assemblages. *Nature*, 556(7702), 492.

Humanes, A., Ricardo, G.F., Willis, B.L., Fabricius, K.E., & Negri , A.P. (2017a). Cumulative effects of suspended sediments, organic nutrients and temperature stress on early life history stages of the coral *Acropora tenuis*. *Scientific Reports*, 7, 44101.

Humanes, A., Fink, A., Willis, B.L., Fabricius, K.E., de Beer, D., & Negri, A.P. (2017b). Effects of suspended sediments and nutrient enrichment on juvenile corals. *Marine Pollution Bulletin*, 125(1-2), 166-175.

Johnson, J.E., Welch, D.J., Marshall, P.A., Day, J., Marshall, N., Steinberg, C.R., Benthuysen, J.A., Sun, C., Brodie, J., Marsh, H., Hamann, M., & Simpfendorfer, C. (2018). *Characterising the values and connectivity of the northeast Australia seascape: Great Barrier Reef, Torres Strait, Coral Sea and Great Sandy Strait*. Report to the National Environmental Science Program. Reef and Rainforest Research Centre Limited, Cairns, 81pp.

Jones, R., Ricardo, G.F., & Negri, A.P. (2015). Effects of sediments on the reproductive cycle of corals. *Marine Pollution Bulletin*, 100(1), 13–33.

Kilminster, K., McMahon, K., Waycott, M., Kendrick, G.A., Scanes, P., McKenzie, L., O'Brien, K.R., Lyons, M., Ferguson, A., Maxwell, P., Glasby, T., & Udy, J. (2015). Unravelling complexity in seagrass systems for management: Australia as a microcosm. *Science of the Total Environment*, 534, 97–109.

Kirkby, E. (2012). Introduction, definition and classification of nutrients. P. Marschner (Ed.), *Marschner's Mineral Nutrition of Higher Plants*, Academic Press, London, UK (2012), pp. 3-5, 10.1016/B978-0-12-384905-2.00001-7

Lewis, M.A., &Devereux, R. (2009). Non-nutrient anthropogenic chemicals in seagrass ecosystems: fate and effects. *Environmental Toxicology and Chemistry,* 28, 644-661.

Li, Y., Martins, F., & Wolanski, E. (2017). Sensitivity analysis of the physical dynamics of the Fly River plume in Torres Strait. *Estuarine, Coastal and Shelf Science*, 194, 84-91.

Lough, J.M. (2016). *Coral core records of the north-east Torres Strait*. Report to the National Environmental Science Programme. Reef and Rainforest Research Centre Limited, Cairns, 24 pp. http://nesptropical.edu.au/wp-content/uploads/2017/01/NESP-TWQ-2.2.1-INTERIM-REPORT-1.pdf

Mallela, J., Roberts, C., Harrod, C., & Goldspink, C.R. (2007). Distributional patterns and community structure of Caribbean coral reef fishes within a river-impacted bay. *Journal of Fish Biology*, 70, 523-537.

Marín-Guirao, L., Atucha, A.M., Barba, J.L, Martínez López, E., & García Fernández, A.J. (2005). Effects of mining wastes on a seagrass ecosystem: metal accumulation and bioavailability, seagrass dynamics and associated community structure. Marine Environmental Research, 60(3), 317-337. doi.org/10.1016/j.marenvres.2004.11.002

Martins, F., & Wolanski, E. (2015). *The pattern and intrusion of the Fly River flood plume to the Gulf of Papua and the Torres Strait: Preliminary numerical modelling results.* TropWATER Report 38/15, James Cook University, Townsville, Australia, 25 pp.

Mayur Resources (2021). Orokolo Bay industrial sands project. Retrieved from: https://mayurresources.com/minerals/

McKenzie, L., Yoshida, R., Grech, A., & Coles, R. (2010). *Queensland seagrasses. Status 2010 – Torres Strait and East Coast.* Fisheries Queensland (DEEDI), Cairns, 6 pp.

McMahon, K., Collier, C., & Lavery, P.S. (2013). Identifying robust bioindicators of light stress in seagrasses: a meta-analysis. *Ecological Indicators*, 30, 7-15.

Mehta, A.J. (2013). *Nearshore and Estuarine Cohesive Sediment Transport.* American Geophysical Union, 582 pp.

Milliman, J.D., & Syvitski, J.P.M. (1992). Geomorphic/ tectonic control of sediment discharge to the ocean: the importance of small mountainous rivers. *Journal of Geology,* 100, 525-544.

Munksgaard, N.C., & Parry, D.L. (2001). Trace metals, arsenic and lead isotopes in dissolved and particulate phases of North Australian coastal and estuarine seawater. *Marine Chemistry*, 75(3), 165-184.

Núñez-Nogueira, G., Pérez-López, A. & Santos-Córdova, J.M. (2019). As, Cr, Hg, Pb, and Cd Concentrations and Bioaccumulation in the Dugong *Dugong dugon* and Manatee *Trichechus manatus*: A Review of Body Burdens and Distribution. *International Journal of Environmental Research and Public Health*, 16(3), 404.

O'Brien, K.R., Adams, M.P., Ferguson, A.J.P., Villarreal-Samper, J., Maxwell, P.S., Baird, M.E., & Collier, C.J. (2018a). Chapter 10 Seagrass resistance to light deprivation. In (Eds) A.W.D. Larkum, G. Kendrick and P.J. Ralph. *Seagrasses of Australia: Structure*, Ecology and Conservation, pp 287-311. Springer, Cham. ISBN 978-3-319-71354-0.

O'Brien, K.R., Waycott, M., Maxwell, P., Kendrick, G.A., Udy, J.W., Ferguson, A.J.P., Kilminster, K., Scanes, P., McKenzie, L.J., McMahon, K., Adams, M.P., Samper-Villarreal, J., Collier, C., Lyons, M., Mumby, P.J., Radke, L., Christianen, M.J.A., & Dennison, W.C. (2018b). Seagrass ecosystem trajectory depends on the relative timescales of resistance, recovery and disturbance. *Marine Pollution Bulletin,* 134, 166-176.

OTML (2021). Mine closure. https://oktedi.com/who-we-are/our-history/mine-closure/

Peters, E.C., Gassman, N.J., Firman, J.C., Richmond, R.H. & Power, E.A. (1997), Ecotoxicology of tropical marine ecosystems. *Environmental Toxicology and Chemistry*, 16, 12-40. doi.org/10.1002/etc.5620160103

Petus, C., Chust, G., Gohin, F., Doxaran, D., Froidefond, J.-M., & Sagarminaga, Y. (2010). Estimating turbidity and total suspended matter in the Adour River plume (South Bay of Biscay) using MODIS 250-m imagery. *Continental Shelf Research,* 30, 379-392.

Petus, C., Collier, C., Devlin, M., Rasheed, M., & McKenna, S. (2014). Using MODIS data for understanding changes in seagrass meadow health: a case study in the Great Barrier Reef (Australia). *Marine Environment Research*, 98, 68–85.

Petus, C., Waterhouse, J., & Brodie, J. (2018). *Using MODIS satellite imagery to provide a large-scale baseline of the composition of coastal waters and the Fly River plume in the Gulf of Papua - Torres Strait (GPTorres Strait) regions*, Technical Report to the National Environmental Research Program, Tropical System Hub, 32 pp.

Petus, C., Waterhouse, J., Lewis, S., Vacher, M., Tracey, D., & Devlin, M. (2019). A flood of information: Using Sentinel-3 water colour products to assure continuity in the monitoring of water quality trends in the Great Barrier Reef (Australia). *Journal of Environmental Management,* 2548, 109255.

Petus, C., Waterhouse, J., Tracey, D., Brodie, J., et al., (manuscript in preparation). Monitoring sediment distribution and potentially polluted riverine runoff in a data-limited environment: insights from satellite images in the remote Torres Strait.

Pitarch, J., van der Woerd, H. J., Brewin, R. J., & Zielinski, O. (2019). Optical properties of Forel-Ule water types deduced from 15 years of global satellite ocean color observations. *Remote Sensing of Environment*, 231, 111249.

Poiner, I.R., & Peterkin, C. (1996). Seagrasses. In: *The State of the Marine Environment Report for Australia. Technical Annex: 1,* eds. L.P. Zann, P. Kailola, P. Townsville, Australia: Great Barrier Reef Marine Park Authority, pp. 40-45.

Poppe, L.J., Paskevich, V.F., Hathaway, J.C., & Blackwood D.S. (2001). *A Laboratory Manual for X-Ray Powder Diffraction*. US Geological Survey Open-File Report 01-041. https://pubs.usgs.gov/of/2001/of01-041/index.htm Last accessed 16 February 2021.

Pratchett, M.S., Hoogenboom, M.O. (2019). Chapter 11, Disturbances and pressures to coral reefs. In: (Ed.) P. Hutchings, M. Kingsford, O. Hoegh-Guldberg. The Great Barrier Reef: Biology, Environment and Management. p.131. CRC Press, ISBN 9780367174286.

Reichelt-Brushett, A.J., & Harrison, P.L. (2000). The effect of copper on the settlement success of larvae from the scleractinian coral *Acropora tennis*. *Marine Pollution Bulletin* 41(7–12), 385–391.

Reichelt-Brushett, A.J., & Harrison, P.L. (2005). The effects of selected trace metals on fertilization success of several scleractinian coral species. *Coral Reefs* 24, 524–534.

Reichelt-Brushett, A., & Hudspith, M. (2016). The effects of metals of emerging concern on the fertilisation success of gametes of the tropical scleractinian coral *Platygyra daedalea*. *Chemosphere*, 150, 398-406.

Richmond, R.H., Tisthammer, K.H. & Spies, N.P., (2018). The effects of anthropogenic stressors on reproduction and recruitment of corals and reef organisms. *Frontiers in Marine Science*, 5, p.226.

Rodriguez, I.B., Lin, S., Ho, J., & Ho, T.Y. (2016). Effects of trace metal concentrations on the growth of the coral endosymbiont *Symbiodinium kawagutii*. *Frontiers in Microbiology*, 7, p.82. DOI=10.3389/fmicb.2016.00082.

Sabdono, A. (2009). Heavy metal levels and their potential toxic effect on coral Galaxea fascicularis from Java Sea, Indonesia. *Research Journal of Environmental Sciences* 3(1), 96–102.

Salomons, W., & Eagle, A. M. (1990) Hydrology, sedimentology and the fate and distribution of copper in mine-related discharges in the Fly River system, Papua New Guinea. *The Science of the Total Environment,* 97/98, 315-334.

Sanudo-Wilhelmy, S., Rivera-Duarte, I., & Flegal, A. (1996). Distribution of colloidal trace metals in the San Fransisco Bay estuary. *Geochimica et Cosmochimica Acta*, 60, 4933-4944.

Schlacher-Hoenlinger, M., & Schlacher, T. (1998). Accumulation, contamination, and seasonal variability of trace metals in the coastal zone – patterns in a seagrass meadow from the Mediterranean. *Marine Biology* 131**,** 401–410. doi.org/10.1007/s002270050333

Simpson, S.L., & Batley, G.E. (2016). *Sediment Quality Assessment: A Practical Handbook*. CSIRO Publishing, Melbourne, Victoria.

Smith, G.W., Kozuchi, A.M., & Hayasaka, S.S. (1982). Heavy metal sensitivity of seagrass rhizoplane and sediment bacteria. Botanica Marina XXV, 19-24.

Sobtzick, S., Hagihara, R., Penrose, H., Grech, A., Cleguer, C., & Marsh, H. (2014). *An assessment of the distribution and abundance of dugongs in the Northern Great Barrier Reef and Torres Strait*. A Report for the Department of the Environment, National Environmental Research Program (NERP). August 2014.

Statton, J., McMahon, K., Lavery, P., & Kendrick, G.A. (2018). Determining light stress responses for a tropical multi-species seagrass assemblage. *Marine Pollution Bulletin,* 128, 508–518.

Stockdale, A., Davison, W., Zhang, H., & Hamilton Taylor J. (2010). The association of cobalt with Iron and Manganese (oxyhydr)oxides in marine sediment. *Aquatic Geochemistry,* 16, 575–585. doi.org/10.1007/s10498-010-9092-1

Sweatman, H., Johns, K., Jonker, M., Miller, I., & Osborne, K. (2015). *Report on second monitoring field trip to Torres Strait, January 2014*. Report to the National Environmental Research Program. Reef and Rainforest Research Centre Limited, Cairns, 10 + iv pp.

Thomas, C.R., Bennett, W.W., Garcia, C., Simmonds, A., Honchin, C., Turner, R., Madden & Hof, C.A. (2020). Coastal bays and coral cays: Multi-element study of *Chelonia mydas* forage in the Great Barrier Reef (2015-2017). *Science of the Total Environment,* 740 : 140042. doi.org/J0.\016/j.scitotenv2020.140042

Torres Strait Regional Authority [TSRA] (2016b). *Torres Strait Long Term Coral Reef Monitoring Project 2015-2016*. Author: Simpson, T. Published by the Torres Strait Regional Authority Land and Sea Management Unit, Thursday Island, Queensland. (56 pp).

Torres Strait Regional Authority [TSRA] (2016a). *Land and Sea Management Strategy for Torres Strait 2016-2036*. Report prepared by the Land and Sea Management Unit, Torres Strait Regional Authority, June 2016, 104 pp.

Thomas, C.R., Bennett, W., Simmonds, A., Turner, R., Honchin, C., Madden Hof, C.A., Bell, I., & Brodie, J.E. (2018). Metal screening in turtle forage, sediment, seagrass and river water of the Great Barrier Reef, pp 37 – 78. Chapter 3 In: *Rivers to Reef to Turtles Project Final Report, WWF, Australia*. 192 pp. https://www.wwf.org.au/ArticleDocuments/394/WWF_RRT.pdf.aspx

Twiss, M.R., & Moffett, J.W. (2002). Comparison of Copper Speciation in Coastal Marine Waters Measured Using Analytical Voltammetry and Diffusion Gradient in Thin-Film Techniques. *Environmental Science & Technology,* 2002 36(5), 1061-1068. DOI: 10.1021/es0016553

Van der Woerd, H.J., & Wernand, M.R., 2015. True colour classification of natural waters with medium-spectral resolution satellites: SeaWiFS, MODIS, MERIS and OLCI. 2015. *Sensors* 15, 25663–25680. doi.org/10.3339/s151025663 .

Van der Woerd, J.H., & Wernand, R.M., 2018. Hue-angle product for low to medium spatial resolution optical satellite sensors. *Remote Sensing,* 10, 180.

Vonk, J.A., Smulders, F.O., Christianen, M.J., & Govers, L.L. (2018). Seagrass leaf element content: A global overview. *Marine Pollution Bulletin*, 134, 123-133.

Ward, T.J. (1989). The accumulation and effects of metals in seagrass habitats. In Biology of seagrasses: a treatise on the biology of seagrasses with special reference to the Australian region. Eds. A. W. D. Larkum, A. J. McComb, and S. A. Shepherd. Elsevier, Amsterdam. pp. 797-820.

Ward, T.J., Correll, R.B., & Anderson, R.B. (1986). Distribution of cadmium, lead and zinc amongst the marine sediments, seagrasses and fauna, and the selection of sentinel accumulators near a lead smelter in South Australia. Australian Journal of Marine and Freshwater Research 37, 567-585.

Waterhouse, J., Brodie, J., Wolanski, E., Petus, C., Higham, W., & Armstrong, T. (2013). *Hazard assessment of water quality threats to Torres Strait marine waters and ecosystems*. Report to the National Environmental Research Program. Reef and Rainforest Research Centre Limited, Cairns, 70 pp.

Waterhouse, J., Apte, S.C., Brodie, J., Hunter, C., Petus, C., Bainbridge, S., Wolanski, E., Dafforn, K.A., Lough, J., Tracey, D., Johnson, J.E., Angel, B.M., Jarolimek, C.V., Chariton, A.A., & Murphy, N. (2019). *Identifying water quality and ecosystem health threats to the Torres Strait from runoff arising from mine-derived pollution of the Fly River: Synthesis Report for NESP Project 2.2.1 and NESP Project 2.2.2*. Report to the National Environmental Science Programme. Reef and Rainforest Research Centre Limited, Cairns 25 pp.

Waterhouse, J., Petus, C., Bainbridge, S., Birrer, S.C., Brodie, J., Chariton, A.C., Dafforn, K.A., Johnson, J.E., Johnston, E.L., Li, Y., Lough, J., Martins, F., O'Brien, D., Tracey, D., & Wolanski, E. (2018). *Identifying the water quality and ecosystem health threats to the Torres Strait and Far Northern Great Barrier Reef arising from runoff of the Fly River*. Report to the National Environmental Science Programme. Reef and Rainforest Research Centre Limited, Cairns, 157 pages.

Welch, D.J., & Johnson, J.E. (2013). *Assessing the vulnerability of Torres Strait fisheries and supporting habitats to climate change*. Report to the Australian Fisheries Management Authority. C2O Fisheries, Australia, 114 pp.

Wells, J.N., & Rasheed, M.A. (2017). *Port of Townsville Annual Seagrass Monitoring and Baseline Survey: September - October 2016*. James Cook University, Centre for Tropical Water & Aquatic Ecosystem Research (TropWATER), Cairns, 54 pp.

Wenger, A.S., & McCormick, M.I. (2016). Determining trigger values of suspended sediment for behavioral changes in a coral reef fish. *Marine Pollution Bulletin,* http://dx.doi.org/10.1016/j.marpolbul.2013.02.014

Wenger, A.S., Fabricius, K.E., Jones, G.P., & Brodie, J.E. (2015). Effects of sedimentation, eutrophication, and chemical pollution on coral reef fishes. Chapter 15 in *Ecology of fishes on coral reefs*, p145. Cambridge University Press.

Wenger, A.S., Harvey, E., Wilson, S., Rawson, C., Newman, S.J., Clarke, D., Saunders, B.J., Browne, N., Travers, M.J., McIlwain, J.L., Erftemeijer, P.L.A., Hobbs, J.-P.A., McLean,

D., Depczynski, M., & Evans, R.D. (2017). A critical analysis of the direct effects of dredging on fish. *Fish,* doi.org/10.1111/faf.12218.

Wolanski, E., Ridd, P., King, B., & Trenorden, M. (1992). *Predictions of the fate of mine-derived Copper, Fly River estuary and Gulf of Papua, Papua New Guinea*. A report prepared for Ok Tedi Mining Limited by the Australian Institute of Marine Science. 23 pp. + 13 Figures.

Wolanski, E., King, B., & Galloway, D. (1995a). Dynamics of the turbidity maximum in the Fly River estuary, Papua New Guinea. *Estuarine Coastal Shelf Science*, 40, 321-337.

Wolanski, E., Spagnol, S., King, B., Galloway, D., & McAllister, F. (1995b). *Fly River plume intrusion in Torres Strait*. A report prepared for Ok Tedi Mining Limited. Australian Institute of Marine Science, July 1995.

Wolanski, E., King, B., & Galloway, D. (1997). Salinity intrusion into the Fly River estuary, Papua New Guinea *Journal of Coastal Research*, 13, 185-212.

Wolanski, E., Spagnol, S., & King, B. (1999). Patchiness in the Fly River plume, Papua New Guinea. *Journal of Marine Systems*, 18, 369-381.

Wolanski, E., Lambrechts, J., Thomas, C.J., & Deleersnijder, E. (2013b). *A high-resolution model of the water circulation in Torres Strait*. NERP project 4.4 Report. TropWATER, James Cook University, Townsville, Australia.

Wolanski, E., Lambrechts, J., Thomas, C., & Deleersnijder, E. (2013a). The net water circulation through Torres Strait. *Continental Shelf Research*, 64, 66-74.

Wolanski, E., Petus, C., Lambrechts, J., Brodie, J., Waterhouse, J., Tracey, D. (2021). The intrusion of polluted Fly River mud into Torres Strait. Marine Pollution Bulletin https://doi.org/10.1016/j.marpolbul.2021.112243

Woods, R.M., Baird, A.H., Mizerek, T.L., & Madin, J.S. (2016). Environmental factors limiting fertilisation and larval success in corals. *Coral Reefs*, 35(4), 1433-1440.

APPENDIX A: SUMMARY OF ANALYTICAL PROCEDURES

A-1 General analytical procedures

High purity deionised water was obtained from a Milli-Q system (18 MΩ.cm conductivity, Millipore, Australia) and was used throughout the study. Plasticware used for metals analyses was acid-washed prior to use by soaking for a minimum of 24 h in 10% (v/v) analytical reagent (AR) or nitric acid (Merck Tracepur) followed by rising with copious quantities of deionised water.

A-2 Preparation of trace metal sample bottles

One-litre low-density polyethylene (Nalgene) bottles used for all metals analyses other than mercury were cleaned using a three-stage sequence in clean room laboratories at CSIRO Lucas Heights. First, the bottles and lids were submerged for a minimum of 2 h in 2% v/v Extran detergent solution, followed by rinsing the outside and inside at least five times with deionised water. The bottles were then soaked for a minimum of 24 h in 10% nitric acid (Merck, AR grade) contained in a covered plastic tank. They were then rinsed five times with deionised water and filled with 1% high purity nitric acid (Merck Tracepur), capped and left to stand for at least 48 h. After this time the bottles were rinsed five times with deionised water, 'double-bagged' in two polyethylene zip-lock bags, and stored in sealed containers to avoid contamination during transportation to the field.

For TSS-bound metals analyses, five-litre low-density polyethylene (Nalgene) bottles were used that underwent the same three-stage sequence washing procedure as used for the one-litre Nalgene bottles.

Fluorinated ethylene propylene (FEP) bottles were used for the collection of water samples for mercury analysis and were cleaned using the following four step procedure. Each bottle and lid was soaked for at least 2 h in 1% v/v Extran detergent solution, followed by rinsing the outside and inside at least five times with deionised water. The bottles and lids were then soaked in acidified (0.2% v/v nitric acid) seawater for at least one day, followed by rinsing the outside and inside at least five times with deionised water. Each bottle was then filled with 50% v/v AR grade nitric acid, capped and left to stand for at least 3 days in clean zip-lock bags. The outside and inside of each bottle were rinsed at least five times with deionised water, and the bottles filled with 10% v/v hydrochloric acid (Merck Tracepur) and left to stand for at least 3 days. Finally each bottle and lid was rinsed on the outside and inside at least five times with deionised water and placed inside two polyethylene zip-lock bags for transportation to the field.

A-3 Analysis of metals in water samples

Dissolved cadmium, cobalt, copper, nickel, lead, and zinc
Dissolved cadmium, cobalt, copper, nickel, lead and zinc (Cd, Co, Cu, Ni, Pb and Zn) in filtered samples were analysed by complexation and solvent extraction, followed by quantitation of the pre-concentrated metals by Inductively Coupled Plasma-Mass Spectrometry (ICP-MS). The extraction procedure allowed the pre-concentration of metals by a factor of 25, thus allowing more accurate quantification. A dithiocarbamate complexation/solvent extraction method

based on the procedure described by Magnusson and Westerlund (1981) was employed. The major differences were the use of a combined sodium bicarbonate buffer/ammonium pyrrolidine dithiocarbamate reagent (Apte and Gunn 1987) and 1,1,1-trichloroethane as the extraction solvent in place of Freon. In brief, sample aliquots (250 mL) were buffered to pH 5 by the addition of the combined reagent and extracted into two 10 mL portions of triple-distilled trichloroethane. The extracts were combined and the metals back-extracted into 1 mL of concentrated nitric acid (Merck Tracepur). The back extracts were diluted to a final volume of 10 mL by addition of deionised water and analysed by ICP-MS (Agilent 8800) using the instrument operating conditions recommended by the manufacturer. For quality control purposes a portion of the certified reference seawater NASS-6 (National Research Council (NRC), Canada) CRM was analysed in every sample batch.

Dissolved aluminium and iron concentrations were measured directly on portions of acidified filtered waters by Inductively Coupled Plasma-Atomic Emission Spectrometry (ICP-AES) (Varian 730 ES) by the method of standard addition. The concentrations of dissolved chromium were measured directly by ICP-MS (Agilent 7500CE) following three-fold dilution with 0.2% v/v nitric acid and calibration against standards prepared from certified stocks (Choice Analytical).

Dissolved organic carbon (DOC)

DOC was measured on aliquots of filtered samples collected during the June 2018 survey using a Shimadzu TOC-LCSH Total Organic Carbon Analyser using the procedures recommended by the manufacturer.

Analytical methods for measuring metals in TSS and benthic sediments

The benthic sediment samples were freeze-dried (Christ Alpha 1-2 LD plus) before chemical analysis. The freeze-dried sediments were disaggregated by gentle grinding using an acid washed agate mortar and pestle.

TSS and benthic sediments were digested in pre-cleaned TFM^{TM} fluoropolymer digestion vessels using aqua regia digestions in a microwave-assisted reaction system (MARS, CEM). The membrane filters containing the suspended sediments or aliquots of the benthic sediment samples (0.5 g) were transferred into the MARS digestion vessels and subjected to pressurised digestion. The method involved adding 9 mL of concentrated nitric acid (Merck Tracepur) and 3 mL of concentrated hydrochloric acid (Merck Tracepur) to each digestion vessel and heating at high pressure in a MARS digestion system for 4.5 minutes at 175°C. Once cool, the digest vessels were vented followed by dilution of the digest to a final volume of 40 mL using deionised water. The masses of the empty vessel, the vessel plus sample, and the vessel plus sample and acid mixture before and after heating were recorded to allow calculation of a dilution factor used in the determination of metal concentrations in the initial undiluted sample. For quality control purposes, portions of the certified reference sediments ERM-CC018 (IRMM) and PACS-3 (NRC Canada) were analysed in each sample batch. All particulate metals concentrations data is reported as dry sediment mass.

It should be noted that the analytical method applied does not measure all forms of particulate metals, rather the portion of metal that is released into solution (recoverable) during the acid-digestion procedure. Metals associated with silicates and refractory elements such as chromium are likely to be underestimated, however, for many metals (e.g. copper and zinc) near full recovery from particulates can be expected. For environmental studies which focus

on the interactions of particulates with living organisms, the fraction of metals not mobilised by acid digestion is not likely to play a significant role and can be regarded as being inert. For the purposes of simplification, the term particulate metals is used in this report to denote the total recoverable metals.

Seagrass metal analysis

Sediment was rinsed from the seagrass leaves with Milli-Q® water before a minimum of 200 mg of seagrass was weighed for each sample. The seagrass was then freeze dried using a Christ Alpha 1-2 LD Freeze Dryer. The dried seagrass samples were digested by high pressure/temperature nitric acid microwave digestion using a CEM MARS6 Microwave. Metals were quantified by Inductively coupled plasma mass spectrometry (ICP-MS) using an Agilent 8800 ICP-MS. The certified reference material BCR-279 (sea lettuce) was digested and analysed with the samples as a check on accuracy.

A-4 References

Apte, S.C., & Gunn, A.M. (1987). Rapid determination of copper, nickel, lead and cadmium in small samples of estuarine waters by liquid/liquid extraction and electrothermal atomic absorption spectrometry. *Analytica Chimica Acta*, 93,147-156.

Magnusson, B., & Westerlund, S. (1981). Solvent extraction procedures combined with back-extraction for trace metal determinations by atomic absorption spectrometry. *Analytica Chimica Acta,* 131, 63-72.

APPENDIX B: ELECTRON MICROGRAPHS OF SEDIMENT SAMPLES

Key

Location	Source	Type of sample	Sample code	Core slice
Boigu	CSIRO Survey Dec 19	TSS	B8	
Saibai	CSIRO Survey Dec 19	TSS	S4	
Boigu	JCU Nov 20 survey	Benthic	Site 3	0-2 cm
Saibai	JCU Nov 20 survey	Benthic	Site 8	0-2 cm
Saibai	NESP Oct 16 survey	Benthic	Site A core 3	0-2 cm
Saibai	NESP Oct 16 survey	Benthic	Site A core 3	2-4 cm
Saibai	NESP Oct 16 survey	Benthic	Site A core 3	4-6 cm
Warrior Reef	NESP Oct 16 survey	Benthic (coral reef)	Site E	Bag 3
Bramble Cay	AIMS Nov 20 Survey	Benthic	Site E	0-2 cm
S of Daru	AIMS Nov 20 Survey	Benthic	Site F	Surface layer

Boigu, Site B8 suspended sediment
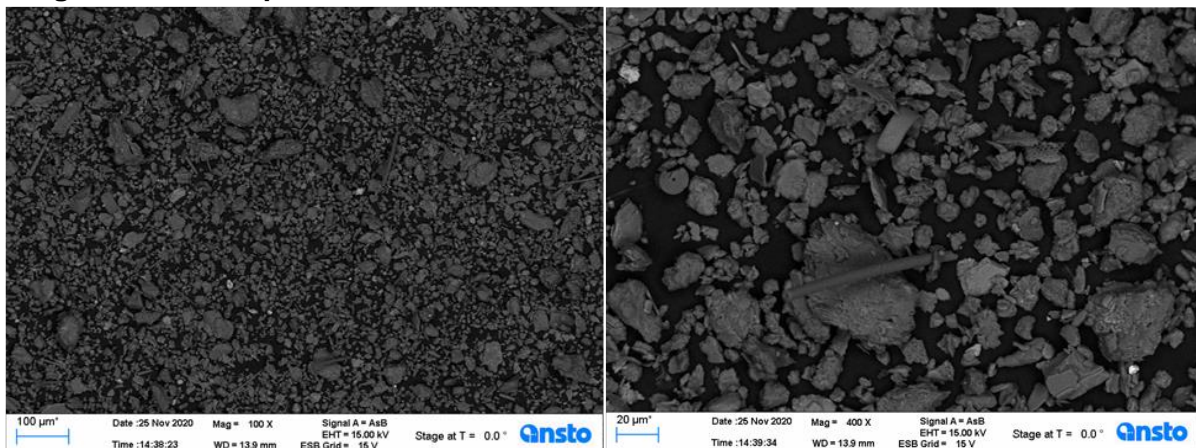
Saibai, Site 4 suspended sediment
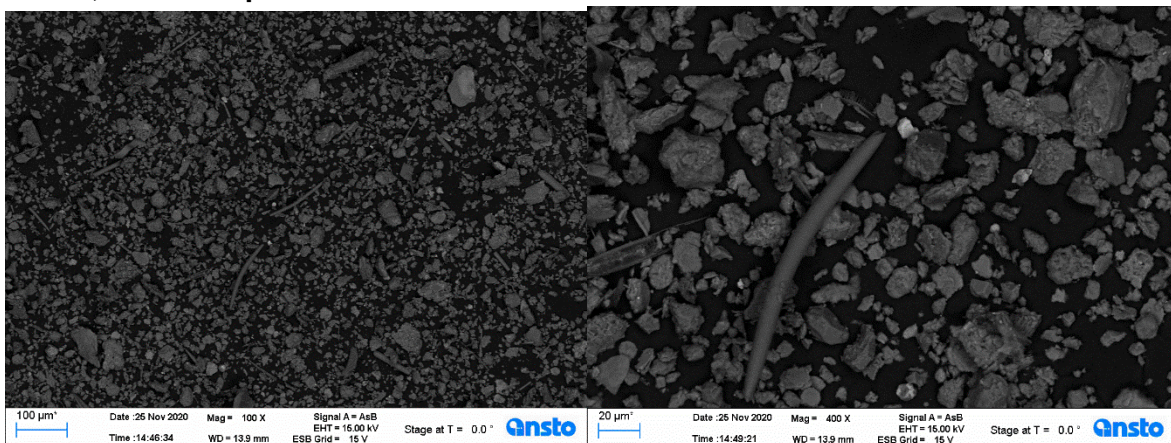
Boigu, Site 3 benthic sediment core: 0-2 cm slice
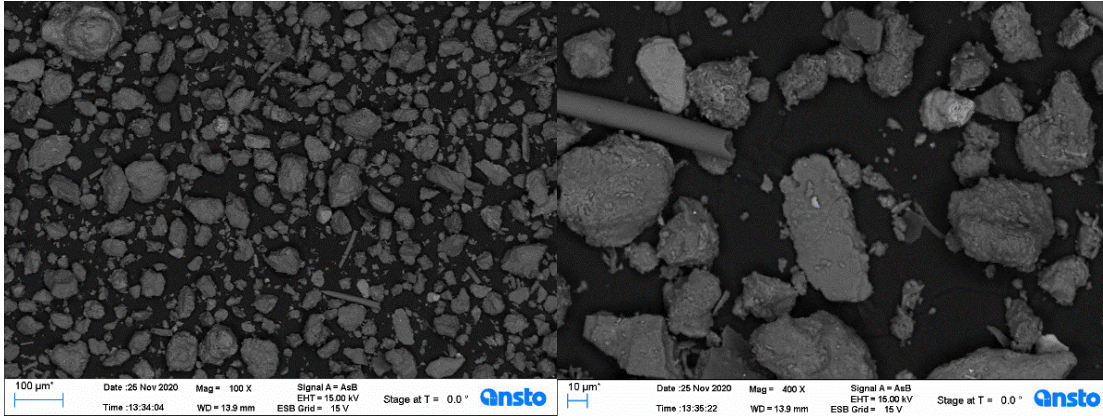
Saibai, Site 8 benthic sediment core: 0-2 cm slice
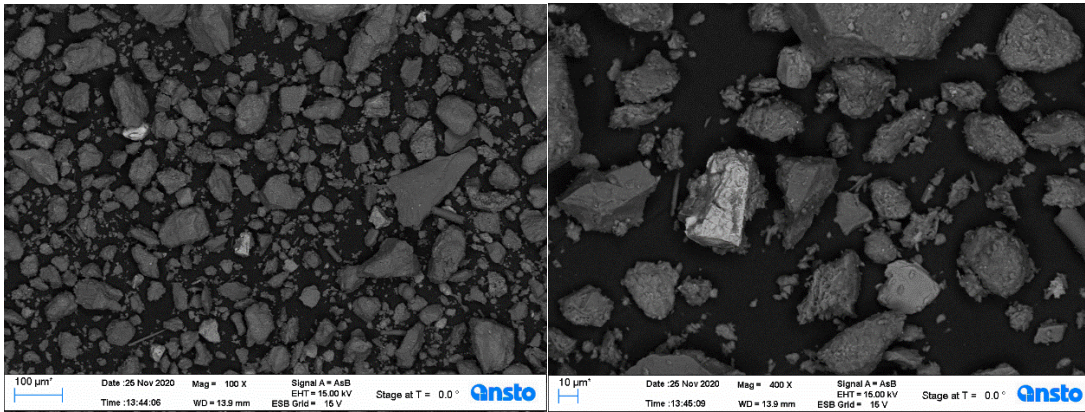
Warrior Reef, Site E benthic sediment core: 0-2 cm slice
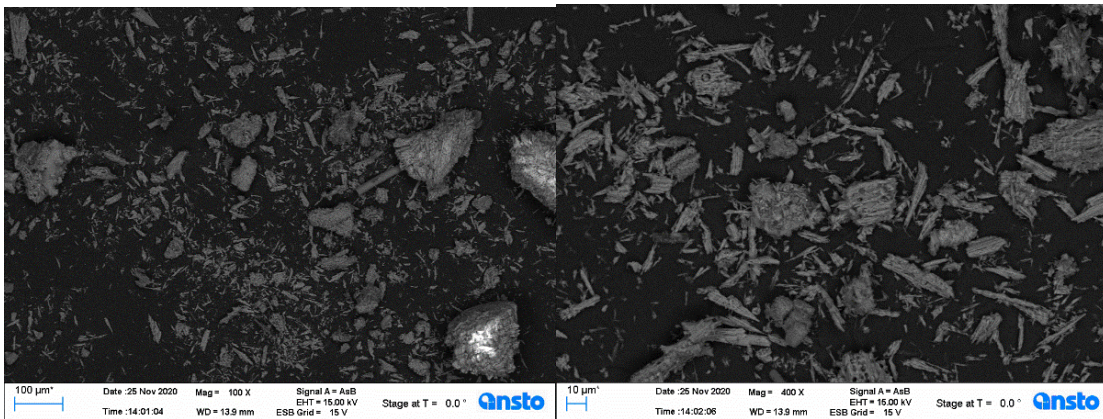
South of Daru, Site F benthic sediment surface layer
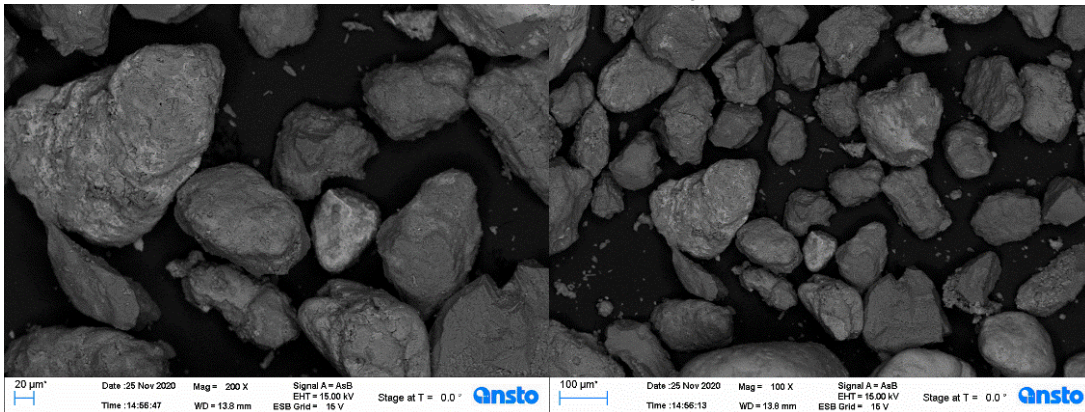
Saibai, Site A3 benthic sediment core: 0-2 cm slice
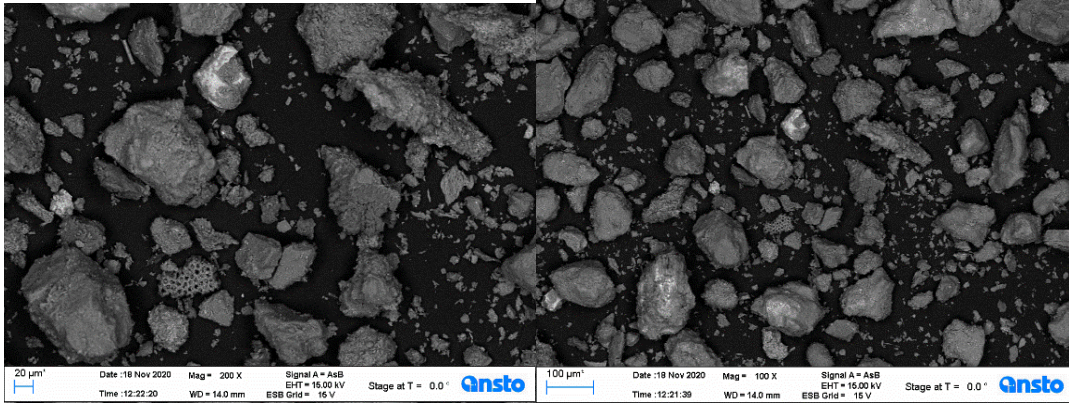
Saibai, Site A3 benthic sediment core: 2-4 cm slice
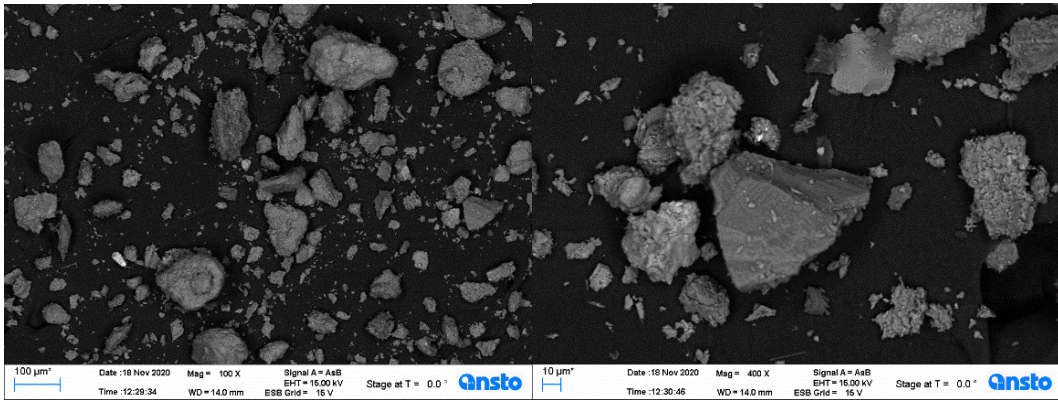
Saibai, Site A3 benthic sediment core: 4-6 cm slice
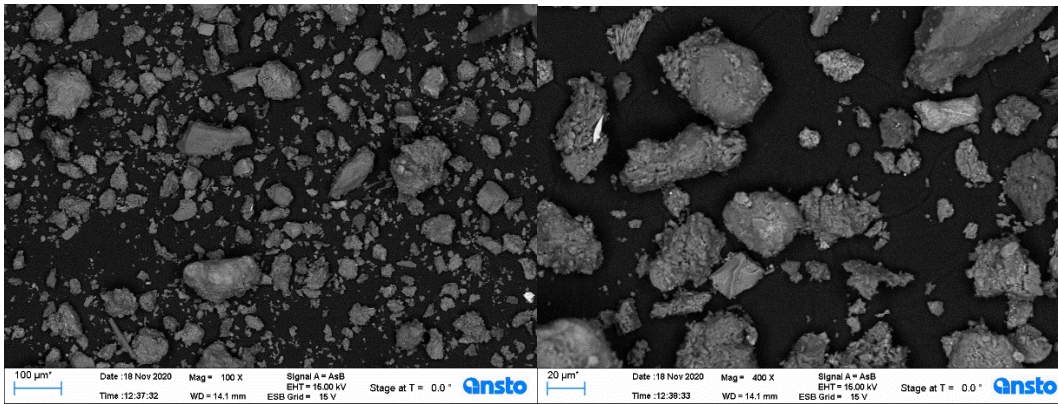
Bramble Cay, Site E#3 benthic sediment surface layer
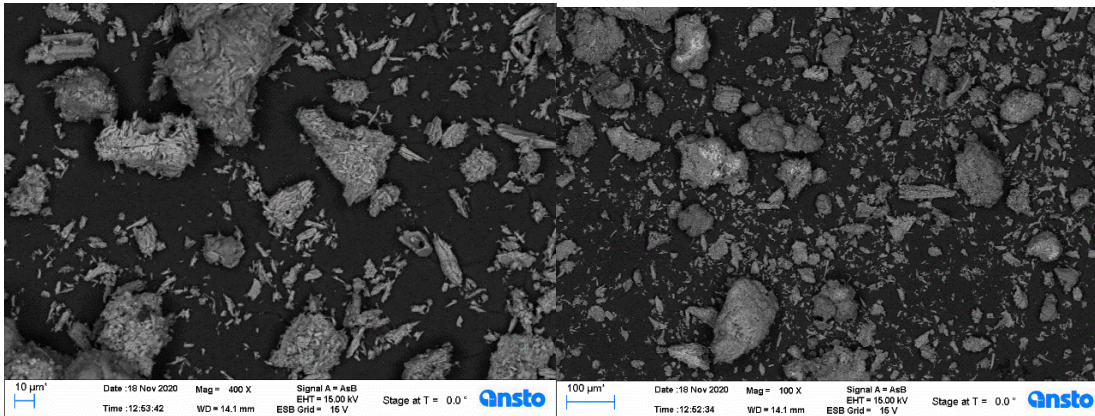
APPENDIX C: SEDIMENT SAMPLE ENERGY DISPERSIVE X-RAY SPECTROSCOPY (EDS) SPECTRA

A1 0-2

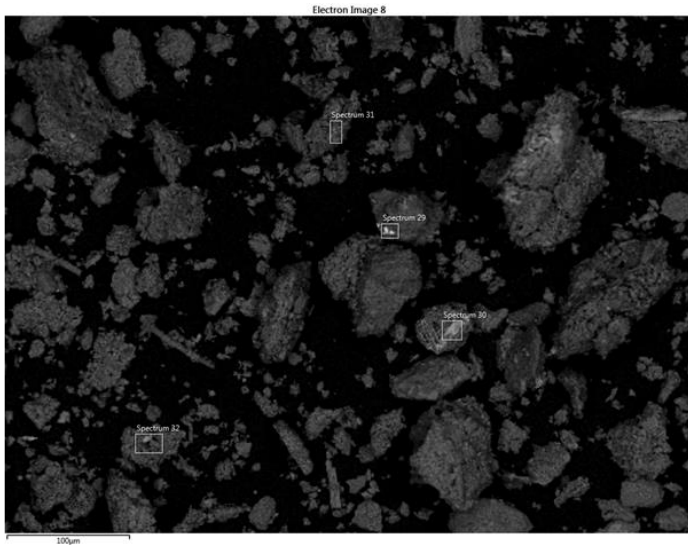| Saibai	NESP Oct 16 survey	Site A core 1	0-2 cm	Spectrum 80 – Ti, Spectrum 85 – Cu, S, Spectrum 21 Ti
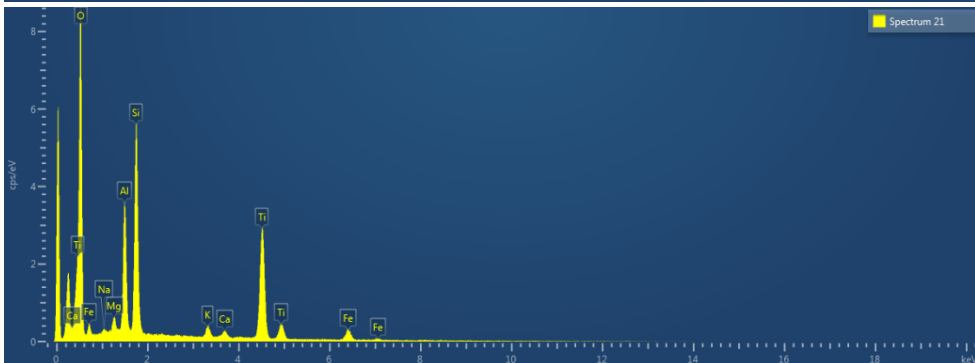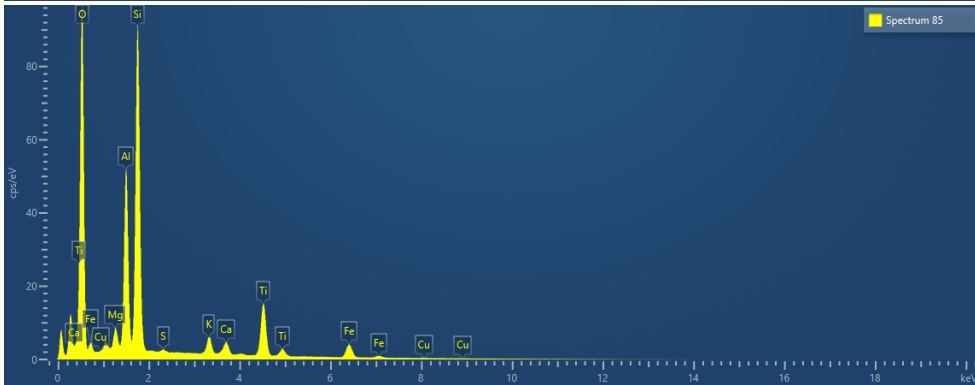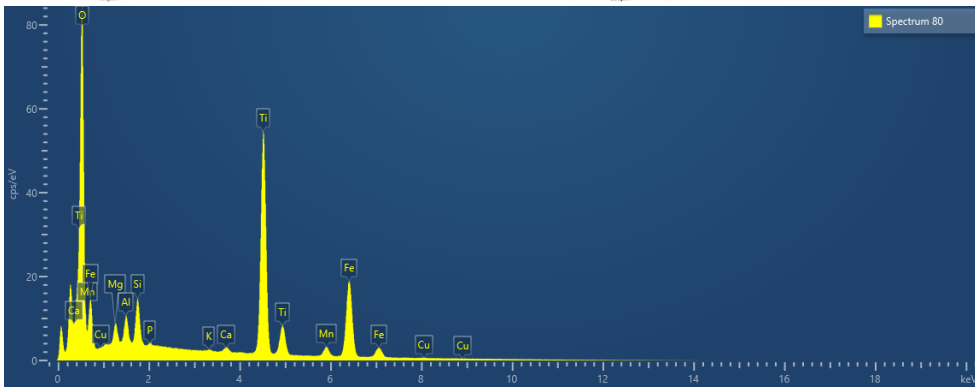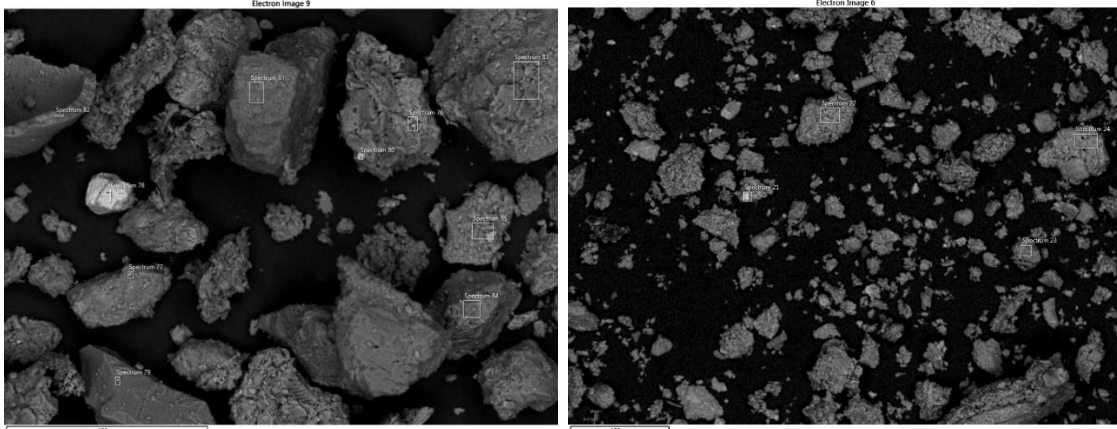
Sample: A2 4-6

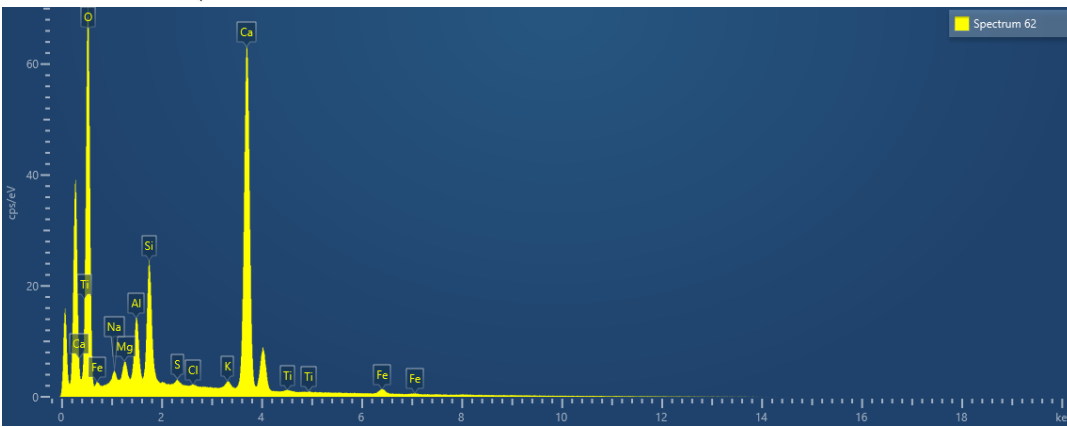| Saibai	NESP Oct 16 survey	Site A core 2	4-6 cm	Spectrum 16 light, rounded particle – FeS

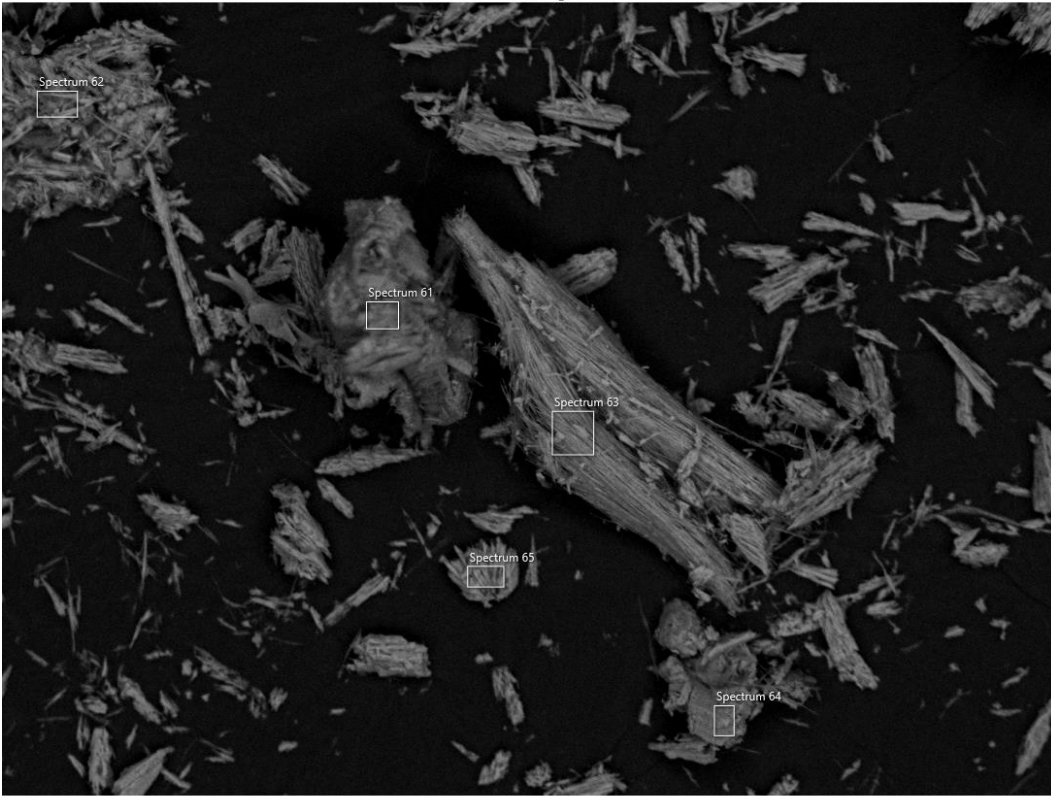Electron Image 5
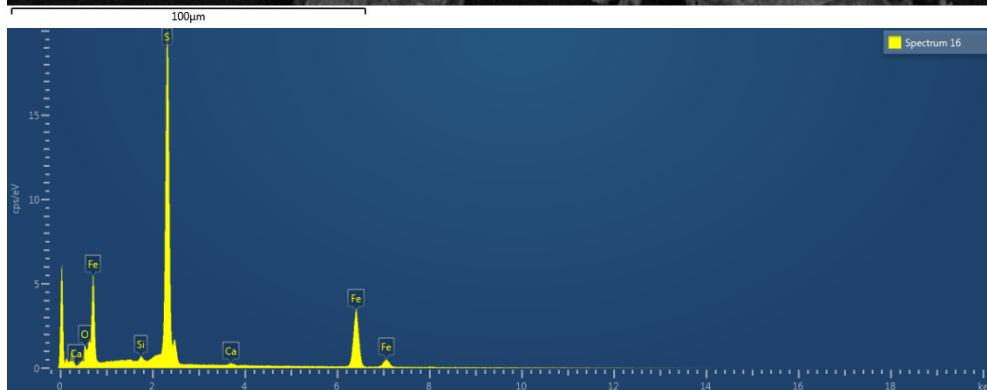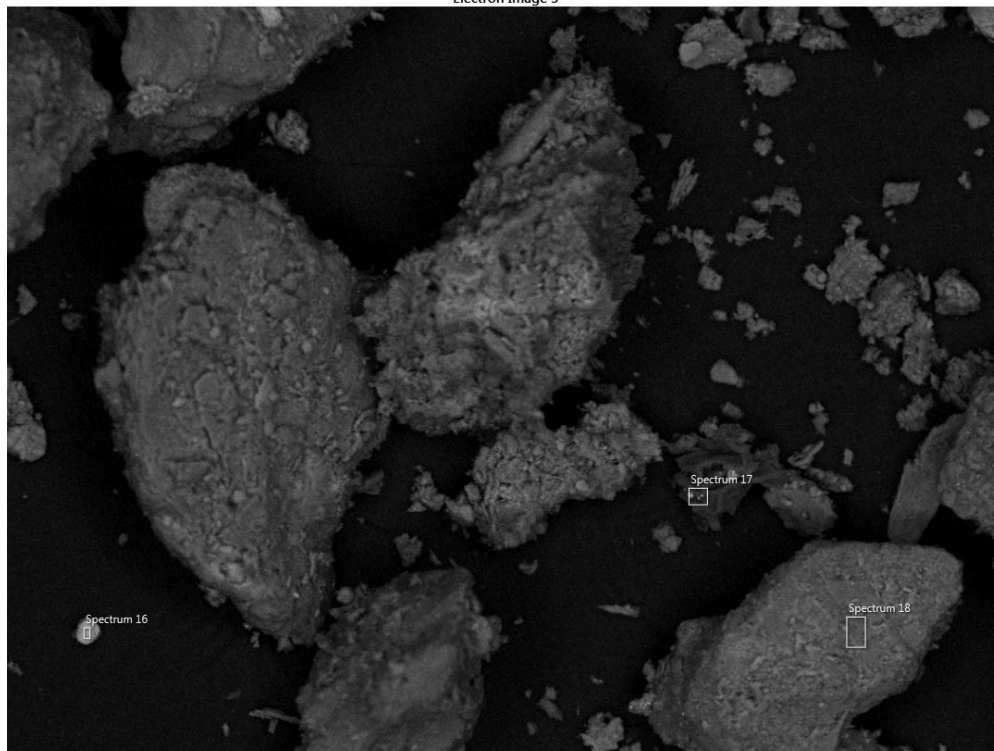
Sample: A3 0-2

| Saibai	NESP Oct 16 survey	Site A core 3	0-2 cm	Spectrum 29 – rare earths, spectrum 30 V, spectrum 31 Fe and S
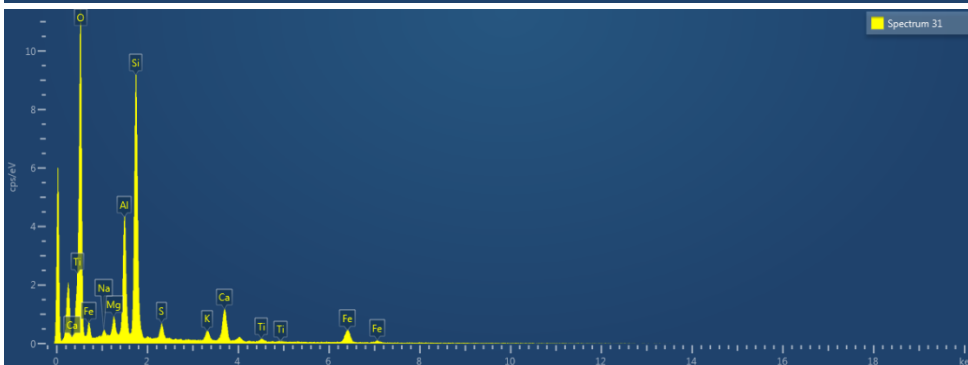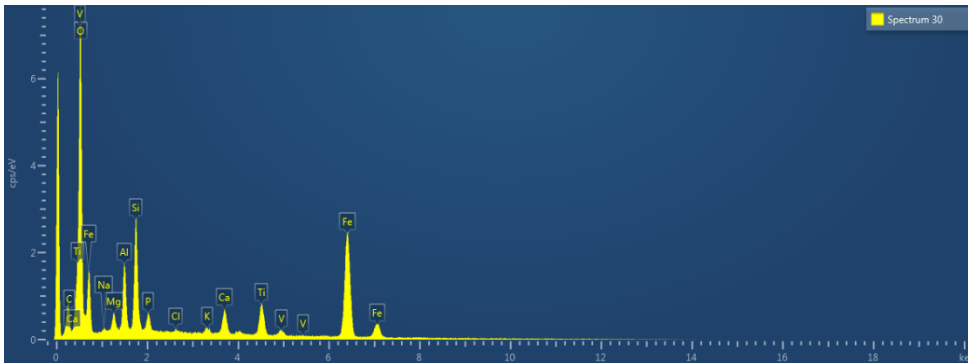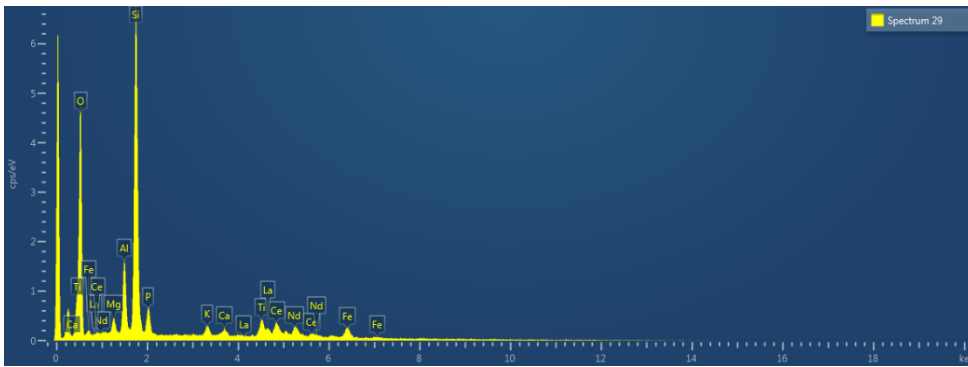
E 0-2

Bramble Cay	AIMS Nov 20 Survey	Site E	0-2 cm	Spectrum 62 – Fe, S

Electron Image 7

Sample: E3

Warrior Reef	NESP Oct 16 survey	Site E	Surface 3	Spectra 43 and 44 - Cu, Fe, S, Spectra 55 Cu, Fe, S, Spectra 54 Fe, S

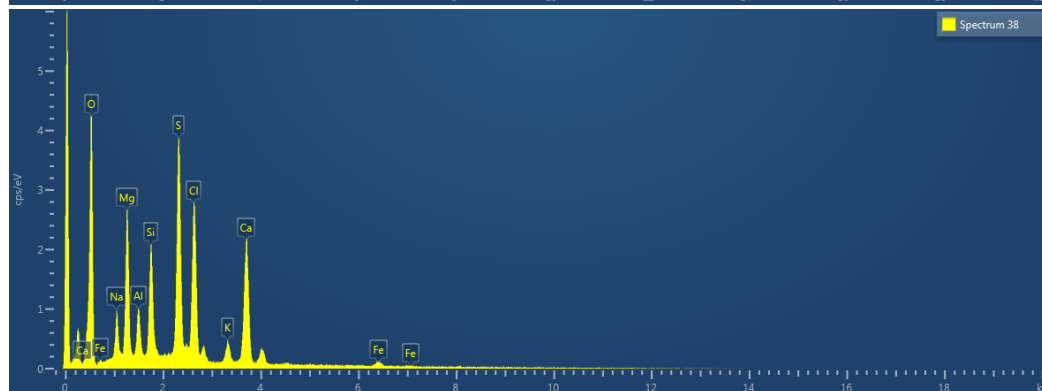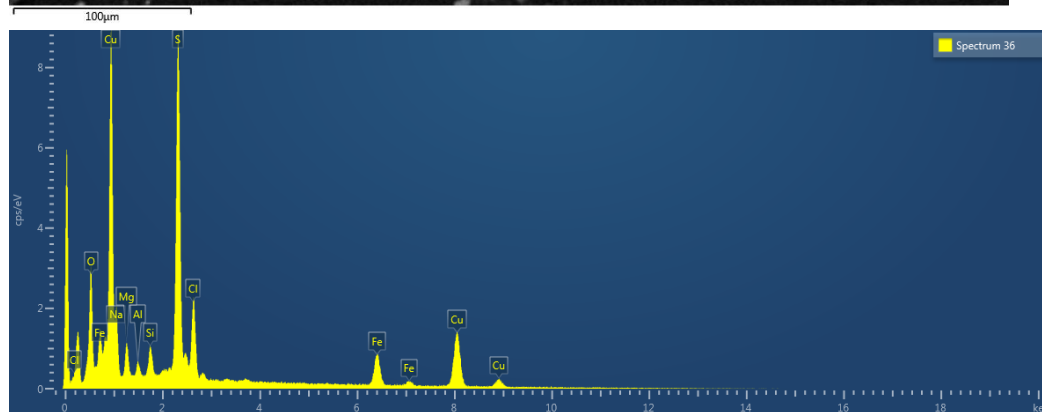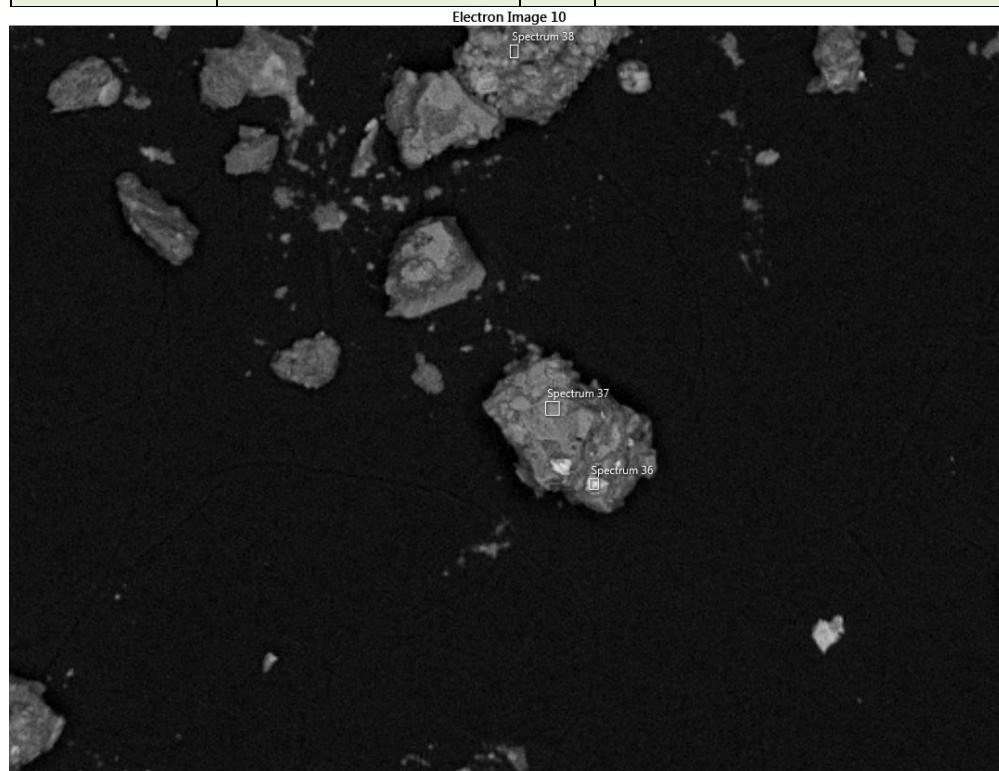| Warrior Reef	NESP Oct 16 survey	Site E	Surface 3	Spectra 43 and 44 - Cu, Fe, S, Spectra 55 Cu, Fe, S, Spectra 54 Fe, S
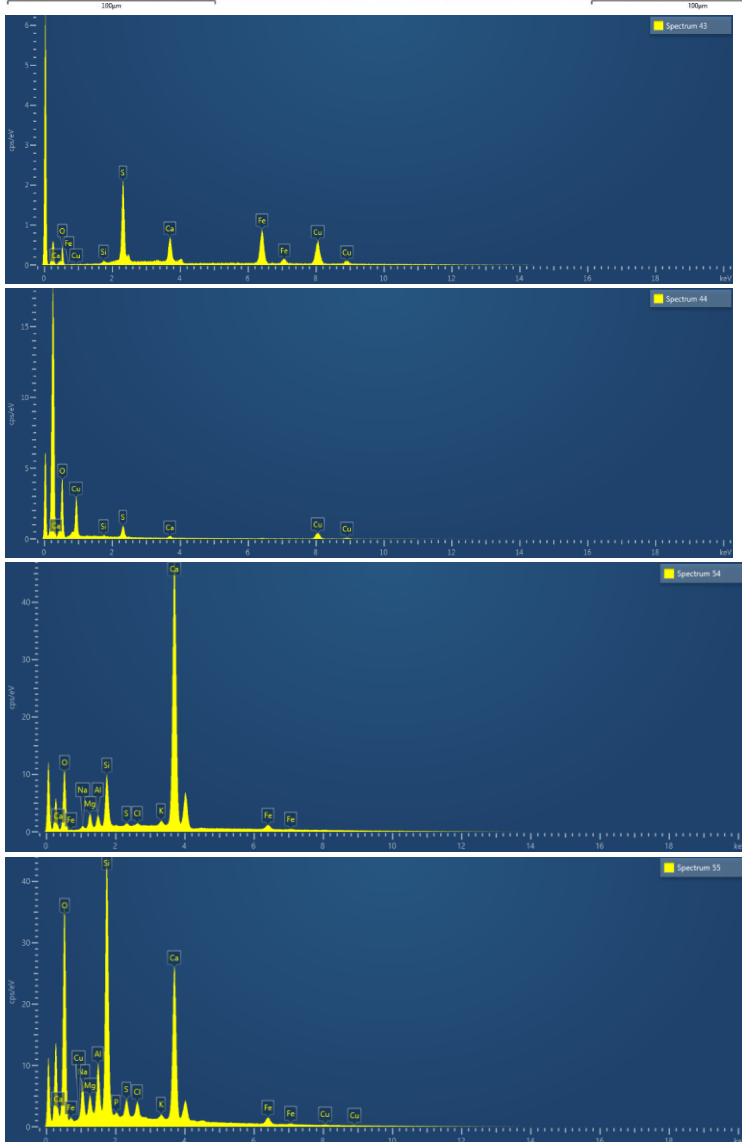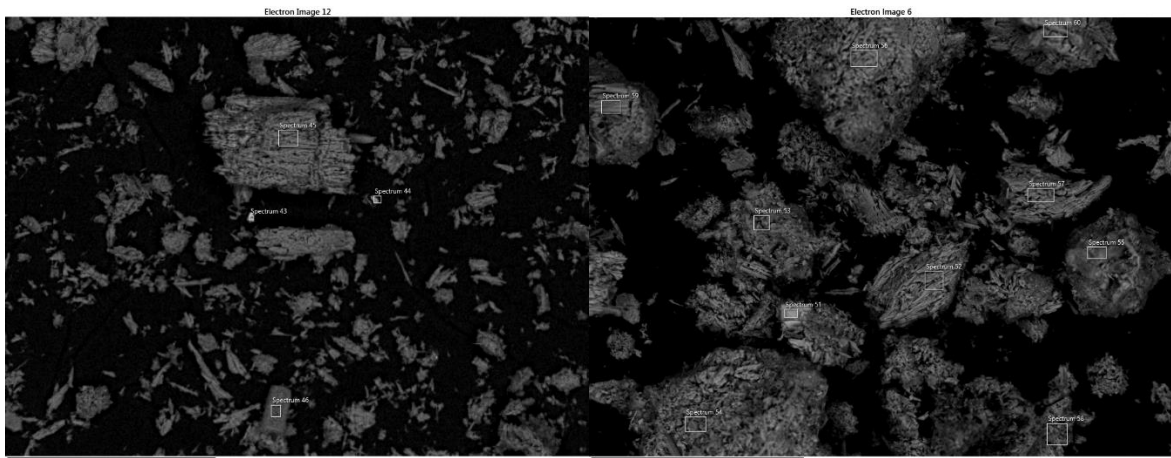
TSS samples

Sample: B6

Boigu Dec 19	CSIRO Survey Dec 19	B6	Spectrum 36 Cu, Fe, S, spectrum 38 Fe and S

Sample: Site A

Saibai Dec 19	CSIRO Survey Dec 19	Site A	Spectrum 33 Cu and S, spectrum 34 Fe,S
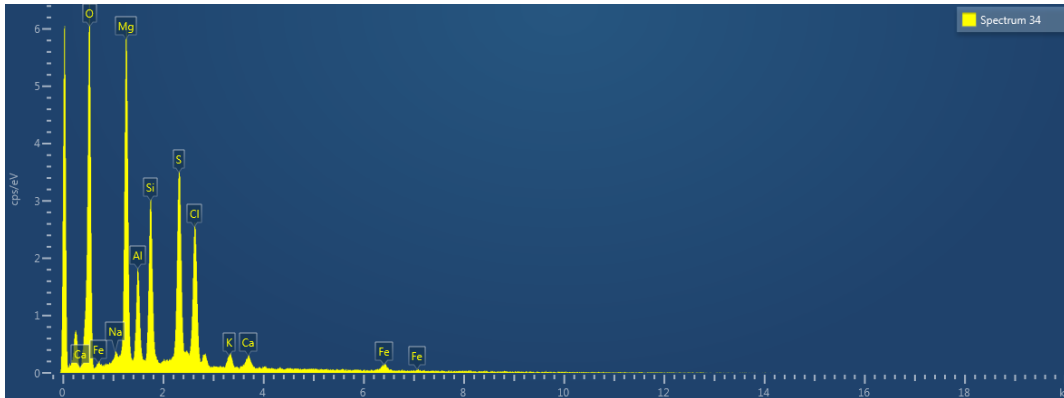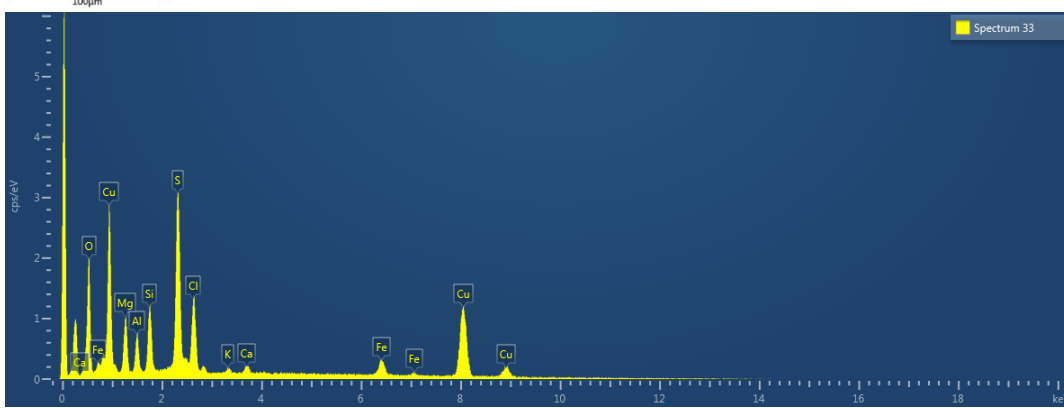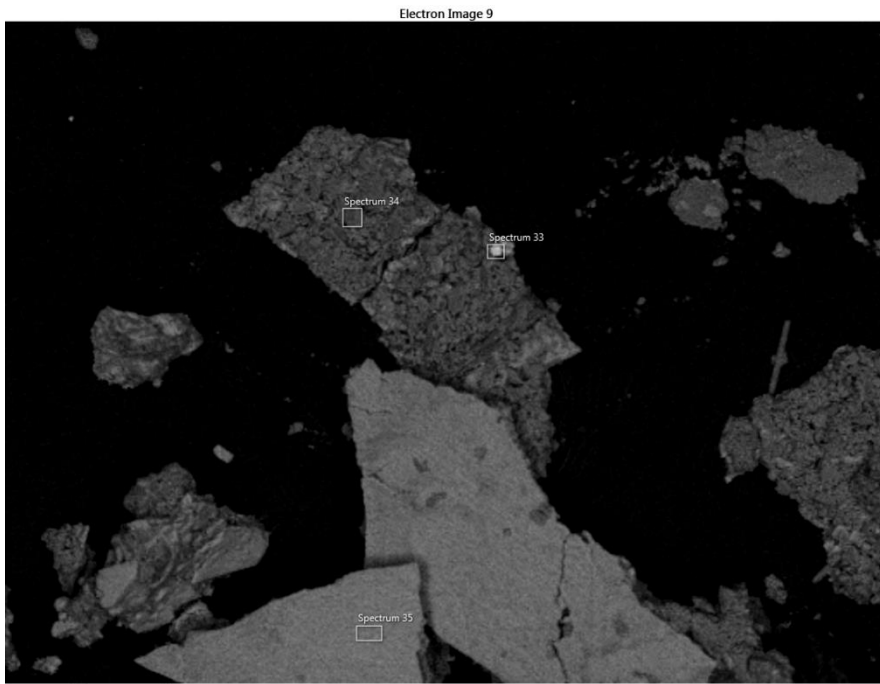
Sample: B9

Boigu Dec 19	CSIRO Survey Dec 19	B9	Spectra 39 and 40 Cu, Fe, S
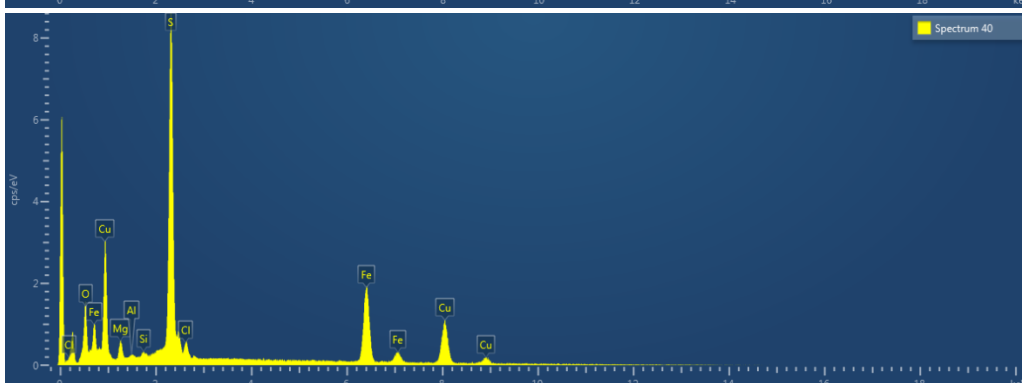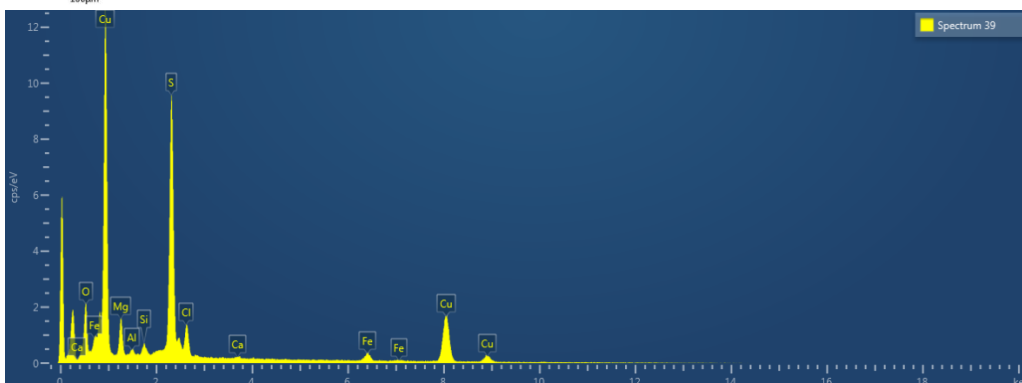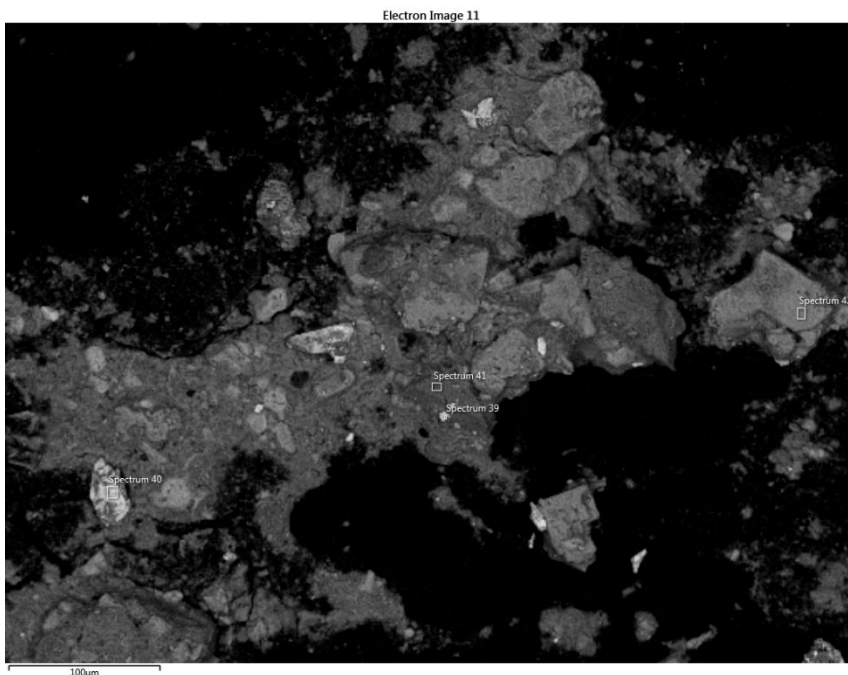
B8

Boigu Dec 19	CSIRO Survey Dec 19	B8	Spectra 44 and 45 Ti, spectrum 49, 50 Cu, Fe, S,
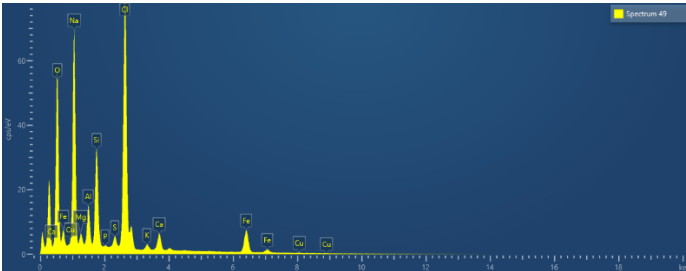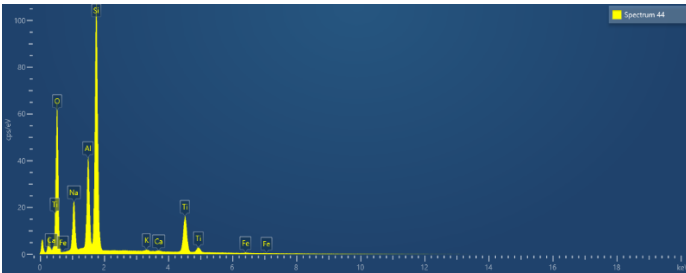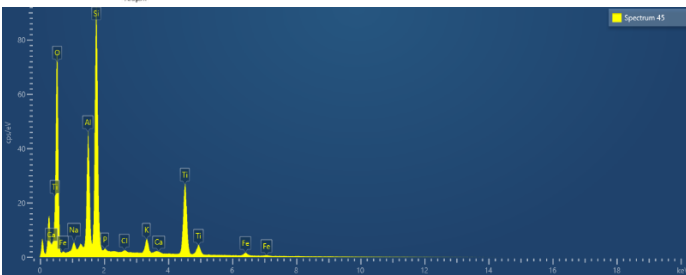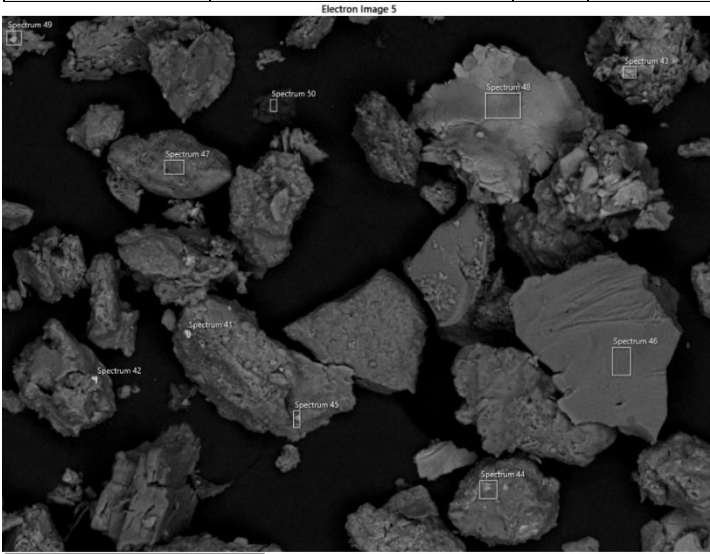
APPENDIX D: FURTHER BACKGROUND TO THE REGIONAL EXPOSURE ASSESSMENT

D-1 Background

Waterhouse et al. (2018) (Section 4.6) included an assessment to map the frequency of exposure of reef and seagrass habitats to turbid waters using the classification of remote sensing true colour images into water type classifications, and develop a potential exposure map for the region. Using evidence from other NESP 2.2.1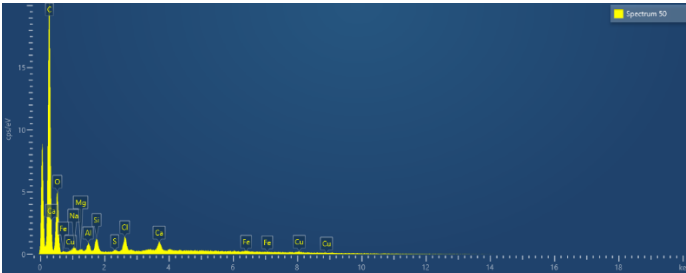 project components, a qualitative assessment of the potential contribution of the Fly River to the areas of greatest exposure to turbid waters was undertaken. This work is extracted here to support the exposure assessment presented in Section 8.3.

The frequency of exposure of waters, coral reefs and seagrass habitats to turbid waters in the Torres Strait was assessed using the daily colour class maps (six distinct colours) produced via the remote sensing analysis for 2008 to 2018. Here it was recognised that turbid conditions can be driven by resuspension and/or the influence of Fly River discharge under certain conditions and/or the influence of the southern PNG rivers (e.g. Wassi Kussa and Mai Kussa rivers at certain sites around Boigu and Saibai islands).

D-2 Overview of methods

The full methods are described in Waterhouse et al. (2018) Section 4.6. The study used daily MODIS satellite true colour imagery and a semi-automated colour classification technique developed for the Great Barrier Reef (Álvarez-Romero et al. 2013; Devlin et al. 2015) and fully described in Section 6.

Seven complete years (2008 to 2017[5] but excluding 2011 and 2012 due to NASA data issues) of daily colour class (CC) maps of the Torres Strait region were produced to generate water type maps (used here and in Section 6). Water type mapping is a tool used to characterise large areas in terms of predicted water quality conditions. The colour classification captures colour gradients occurring in coastal and marine waters and aims to summarise typical changing water quality along- and cross-shore through the classification into Primary (turbid, sediment-dominated), Secondary (less turbid, dominant to moderate concentrations of Chl-a and finer sediments) and Tertiary (slightly above ambient turbidity and Chl-a concentrations) water types. A full description of the Primary, Secondary and Tertiary water type characteristics is shown in Section 6. Water type maps were used to assess the frequency of occurrence of each water type at different temporal and geographical scales and to evaluate the frequency of exposure of coral reefs and seagrass habitats to turbid waters in the Torres Strait.

Annual and multi-annual frequency maps were generated from the daily CC maps for each of the CC1 to 6, as well as 1–4 combined (Primary water type), 1–5 (Primary plus Secondary water types) and 1–6 combined. The water type frequency was defined as the total number of

---

[5] For all annual and seasonal frequency maps and figures, only complete years/seasons were used, i.e. 2009–2017 (excluding 2011 and 2012) for annual, 2008–2017 for Jul–Aug (excluding 2011) and 2009–2018 (excluding 2011 and 2012) for Feb–Mar.

days per year exposed to a given water type divided by the number of data days (non-cloud) recorded per year, resulting in a normalised frequency on a scale from 0 to 1. An annual 'cloud frequency' raster was also produced, calculated as the number of cloud-masked days per pixel divided by the total number of daily rasters available for the year.

The annual and multi-annual frequency maps were analysed as follows:

1. *Seagrass and coral reef exposure (whole Torres Strait scale)*: extraction of pixel counts of percent frequency of exposure for primary (CC1–4), secondary waters (CC5) in 10% frequency increments—multi-annually (decadal average) as well as for July–August (within the SE trade wind season), February–March (within the monsoon season) and annually. As previously described, these data are for surrounding waters greater than 1 px from benthic features and within 1 km.

2. *Exposure at different habitat sites across the Torres Strait*: extraction of the frequency of exposure to the six CCs at different sites in the northern Torres Strait—multi-annually (decadal average) as well as for July–August, February–March and annually (Appendix 2C). The data were analysed at 10 sites where the SLIM hydrodynamic modelling, remote sensing or other studies indicated potential influence from Fly River plume waters, and/or where coral reef and seagrass data were available (Table D1).

3. *Exposure at different potential zones of influence*: the sites where finally grouped into six different potential zones of influence based on their geographical location and their likely exposure to Fly River waters, defined as exposure to Fly River plume waters and subsequent resuspension. The mean exposure (1 km radius) to Primary, Secondary, Tertiary and marine waters was extracted into the different zones of influence. Analyses were performed at different temporal scales: multi-annually (decadal average) as well as for July–August (within the SE trade wind season), February–March (within the monsoon season) and annually.

The assessment area is shown by the full extent of the map in Figure D1, encompassing the area west to Kawa Island, south to Beresford Shoals, north to Poruma Island and east of Mer (between 142.015°E to 144.295°E and 8.860°S to 10.354°S). This area includes 2,952km^2 of mapped coral reefs and 1,337km^2 of mapped seagrass meadows. The habitat data included in the assessment was:

- Coral reefs: mapped coral reefs (AIMS, Lawrey and Stewart 2016); and
- Seagrass: intertidal seagrass (Carter et al. 2014), subtidal seagrass (Carter et al. 2014), NW Torres Strait seagrass (Carter and Rasheed 2016) and subtidal seagrass presence/absence (Hayward et al. 2008).
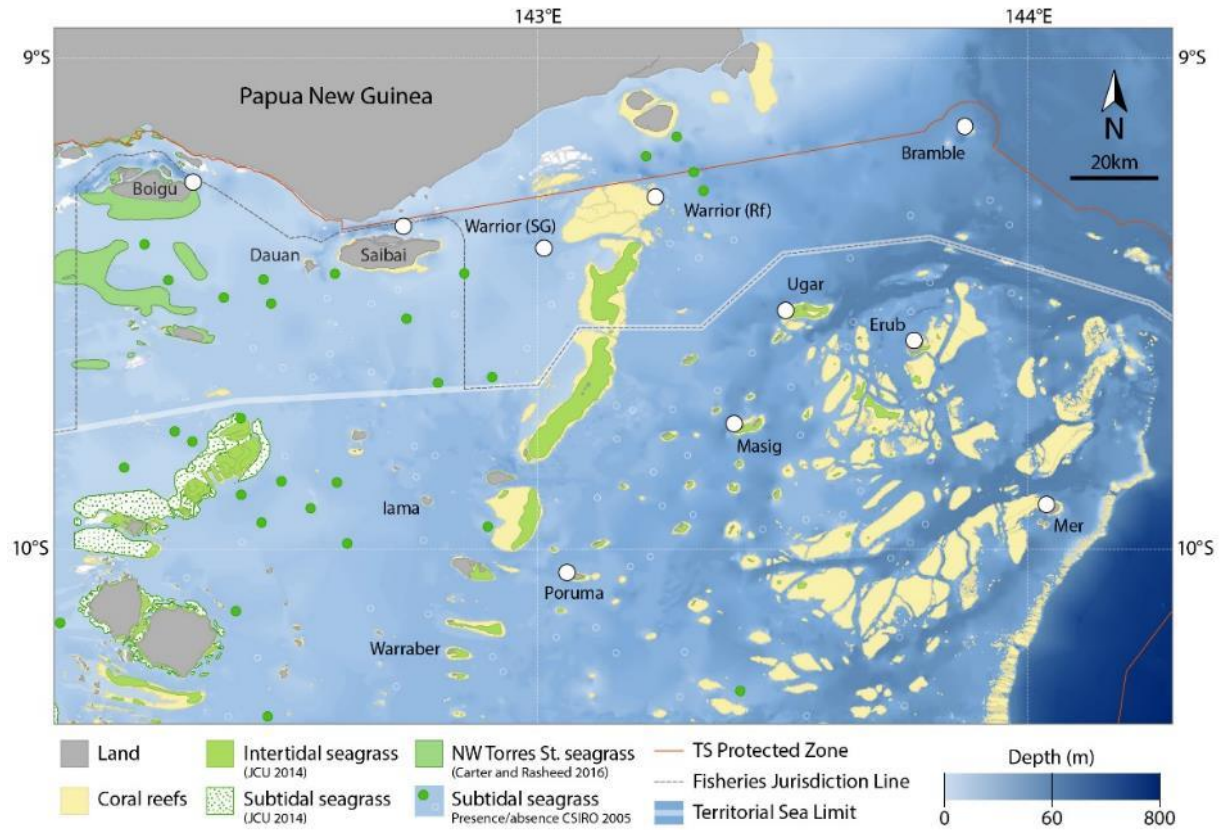
Figure D1: Location of the Torres Strait coral reefs, seagrass beds and habitat sites selected for the risk assessment (white dots) (between 142.015°E to 144.295°E and 8.860°S to 10.354°S). Map prepared by D. Tracey, TropWATER JCU using datasets from GBRMPA, Carter et al. (2014), Hayward et al. (2008) and Carter and Rasheed (2016).

Table D1: Habitat (coral reef and seagrass) sites selected for the risk assessment (and corresponding monitoring codes where relevant) and potential zone of influence: Zone 1: North, 2: North East, 3: North West, 4: South, 5: Central and 6: East. Note: SG = seagrass site; RF = reef site. The site names correspond to the TSRA coral reef monitoring locations.

Site	Lat	Long	Habitat type	Zone	Description and evidence from other studies: Coral cores (CC), *In-situ* loggers (L), Remote Sensing (RS), Modelling (M) and Bibliography (B)
Warrior Reef (SG)	9.42	143.05	seagrass	1	Very likely influence of Fly River waters (B, M, RS)
Warrior Reef (RF)	9.28	143.24	reef	1	Very likely influence of Fly River waters (B, M, RS)
Bramble Cay	9.14	143.87	reef	2	Several pulses of freshwater each year, likely from the Fly River (CC, L, RS)
Boigu	9.28	142.3	seagrass	3	Potential influence of Fly River (B, M, RS) and very likely influence of southern PNG rivers (RS)
Saibai	9.36	142.77	reef	3	Likely influence of Fly River (B, M, RS) and likely influence of southern PNG rivers (RS)
Poruma (P1R1)	10.05	143.06	reef	4	Low risk of influence from Fly River (B, M, RS)

Site	Lat	Long	Habitat type	Zone	Description and evidence from other studies: Coral cores (CC), *In-situ* loggers (L), Remote Sensing (RS), Modelling (M) and Bibliography (B)
Ugar (U1R1)	9.51	143.51	reef	5	Low risk of influence from Fly River (B, M, RS)
Masig (Y1R1)	9.75	143.4	reef	5	Low risk of influence from Fly River (B, M, RS)
Erub (E2R1)	9.58	143.77	reef	6	Low risk of influence from Fly River (B, M, RS, CC)
Mer (M3R1)	9.91	144.04	reef	6	Low risk of influence from Fly River (B, M, RS)

D-3 Results

Long-term patterns

Multi-annual frequency maps

Multi-annual frequency maps (2009–2017, excluding 2011 and 2012) combine the outputs from annual assessments to generate a longer-term assessment of water quality conditions in the region. These maps illustrated an inshore to offshore spatial pattern, with the highest frequency of the Primary water type (i.e., more turbid conditions) in the coastal areas and offshore areas most frequently exposed only to the Tertiary water type (Figure D2).

To assist with interpretation of the data, the frequency of exposure to turbid waters has been grouped into categories based on the decadal average: Infrequently (0–10% of the time), occasionally (10–50% of the time), frequently (50–90% of the time) and very frequently (90–100% of the time).
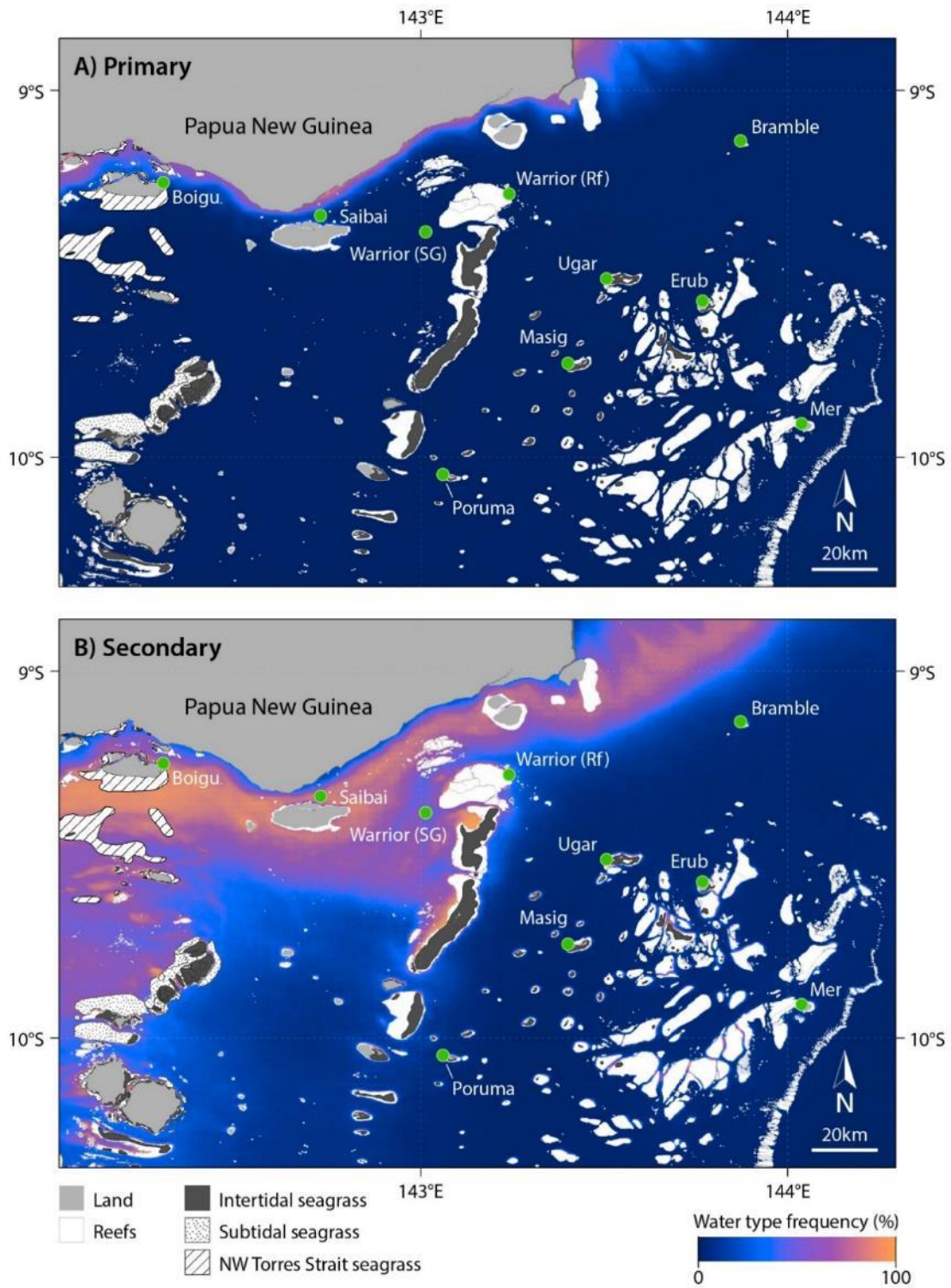
Figure continued below

Figure D2: Maps showing the multiannual frequency (2009–2017, excluding 2011 and 2012) of A) Primary water type (CC1–4), B) Secondary water type (CC5) and C) Tertiary water type (CC6) as well as D) cloud frequency occurrence; where the highest frequency is shown in orange and the lowest frequency is shown in blue. Maps prepared by D. Tracey, TropWATER JCU using datasets from GBRMPA, Carter et al. (2014), Hayward et al. (2008) and Carter and Rasheed (2016).
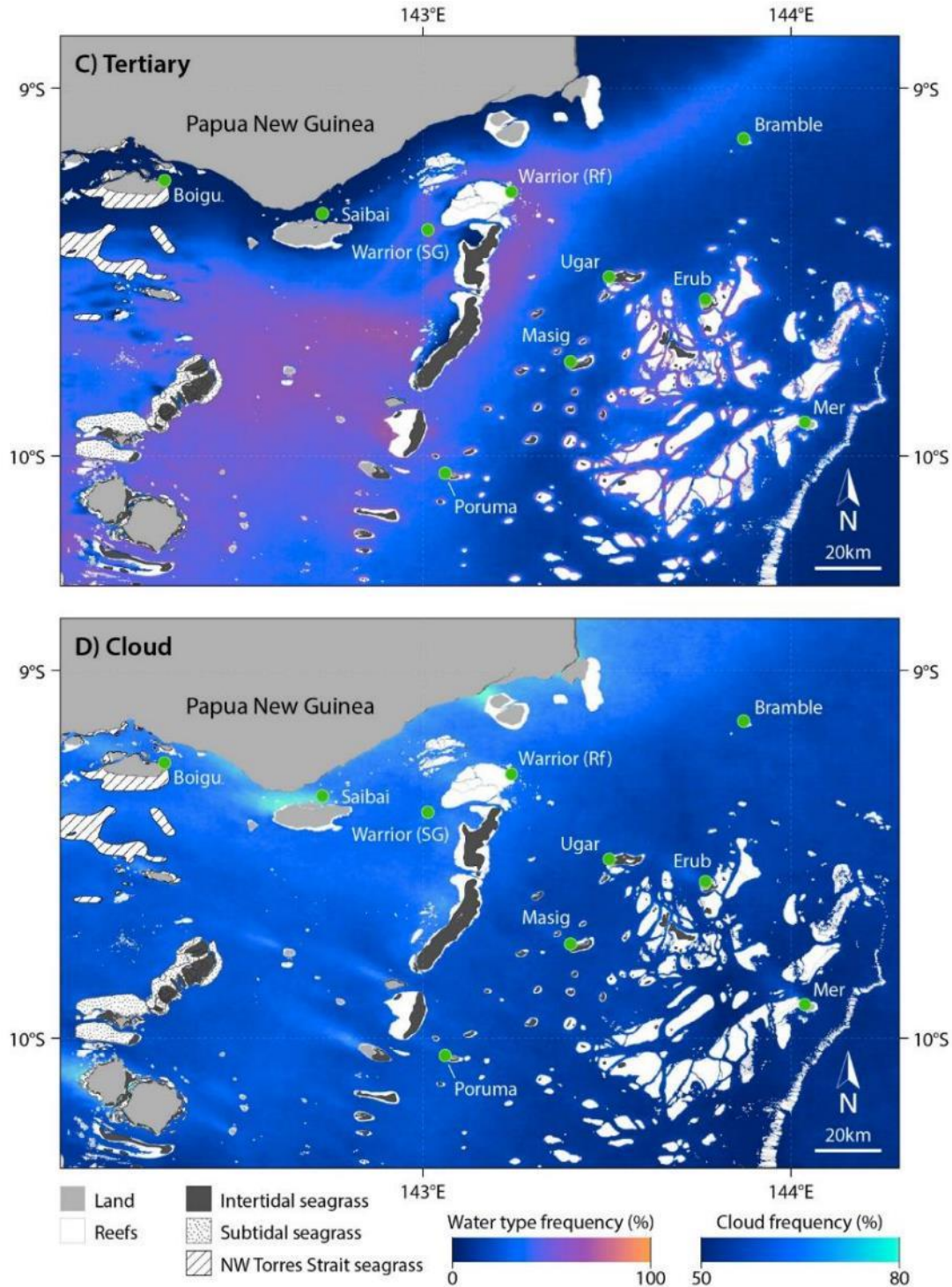
Figure D2: Maps showing the multiannual frequency (2009–2017, excluding 2011 and 2012) of A) Primary water type (CC1–4), B) Secondary water type (CC5) and C) Tertiary water type (CC6) where the highest frequency is shown in orange and the lowest frequency is shown in blue; and D) cloud frequency occurrence where the highest frequency is shown in aqua and the lowest frequency is shown in blue.
Maps prepared by D. Tracey, TropWATER JCU using datasets from GBRMPA, Carter et al. (2014), Hayward et al. (2008) and Carter and Rasheed (2016).

The multi-annual frequency analysis of the occurrence of clouds showed the highest cloud frequency at the Saibai and Boigu Islands and Warrior Reef sites (Figure D2 and Table D2) and typically greater or similar cloud frequency during July–August (within the SE trade wind

season) and February–March (within the monsoon season) in most locations (based on multi-annual average conditions—this varies between years).

Table D2: Frequency of cloud cover in the daily images for each of the assessment sites (average % of total number of days in 2008–2018).

|	Boigu	Bramble Cay	Erub (E2R1)	Masig (Y1R1)	Mer (M3R1)	Poruma (P1R1)	Saibai	Ugar (U1R1)	Warrior Reef RF	Warrior Reef SG
Annual	64.7	60.3	61.0	59.8	61.7	63.4	71.3	59.9	66.1	64.6
July-August	70.3	66.7	60.4	62.1	64.4	65.6	80.9	65.6	73.1	72.2
February-March	71.7	58.0	61.4	61.9	64.5	68.1	74.0	61.6	61.5	63.1

Coral reef and seagrass exposure (whole Torres Strait scale)

The assessment of the areas of coral reef and seagrass habitats (shown in Figure D2) exposed to Primary and Secondary water types combined (CC1–5) between 2009 and 2017 is shown in Table D3 and Figure D3. In summary, 53% (or 1,573 km^2) of coral reef area was exposed to Primary and Secondary waters infrequently (0–10% of the time, decadal average) and only approximately 3% (or 89 km^2) of coral reef area was exposed to turbid waters very frequently (90–100% of the time) (Table D3).

Intertidal seagrass habitats show greater frequency of exposure to turbid waters, with 11.9% (or 67 km^2) of habitat area being exposed to Primary and Secondary waters infrequently (0–10% of the time), and 63% (or 354 km^2) of area exposed occasionally to turbid waters (10–50% of the time). However, only approximately 2.4% (or 14 km^2) of intertidal seagrass area is exposed to turbid waters very frequently (90–100%).

The subtidal seagrass also showed greater frequency of exposure to turbid waters, with 0.2% (or 1 km^2) of habitat area being exposed to Primary and Secondary waters infrequently (0–10% of the time), and 54% (or 212 km^2) of area being exposed occasionally (10–50% of the time) to turbid waters. However, only approximately 0.9% (or 3 km^2) of subtidal seagrass area was exposed to turbid waters very frequently (90–100%).

Finally, the NW Torres Strait seagrasses showed the greatest frequency of exposure of all habitats. None of the habitat area was exposed to Primary and Secondary waters less than 50% of the time. Approximately 71% (273 km^2) of habitat area was exposed frequently (50 to 90% of the time) and 29% (110 km^2) of the NW Torres Strait seagrass area was very frequently (90–100%) exposed to turbid waters.

Table D3: Exposure (area km² and % of habitat area) of coral reef, intertidal and subtidal seagrass habitats to Primary and Secondary (CC1–5) waters between 2008 and 2018.

Frequency of exposure:	0-10%	10-20%	30-30%	30-40%	40-50%	50-60%	60-70%	70-80%	80-90%	90-100%
Habitat	Area of habitat exposed to primary or secondary waters (km²)									
Coral reefs	1573	456	227	177	123	88	80	67	72	89
Intertidal seagrass	67	94	89	99	72	47	35	27	18	14
Subtidal seagrass	1	21	58	67	66	52	49	53	22	3
NW Torres St. seagrass	0	0	0	0	0	50	64	81	78	110

Frequency of exposure:	0-10%	10-20%	30-30%	30-40%	40-50%	50-60%	60-70%	70-80%	80-90%	90-100%
Habitat	Percentage of habitat area exposed to primary or secondary waters (%)									
Coral reefs	53.3	15.4	7.7	6.0	4.2	3.0	2.7	2.3	2.4	3.0
Intertidal seagrass	11.9	16.7	15.9	17.7	12.8	8.3	6.2	4.9	3.2	2.4
Subtidal seagrass	0.2	5.4	14.8	17.1	16.9	13.2	12.4	13.6	5.6	0.9
NW Torres St. seagrass	0.0	0.0	0.0	0.0	0.0	13.0	16.8	21.1	20.3	28.8

■ >50% of habitat area   ■ 10-50% of habitat area   □ <10% of habitat area

Coral reefs (2952 km²)   Intertidal seagrass (562 km²)   Subtidal seagrass (393 km²)   NW Torres Strait seagrass (382 km²)

Frequency of exposure
0-10%   50-60%
10-20%   60-70%
20-30%   70-80%
30-40%   80-90%
40-50%   90-100%

Note: Habitat areas are calculated between 142.015°E to 144.295°E and 8.860°S to 10.354"S.
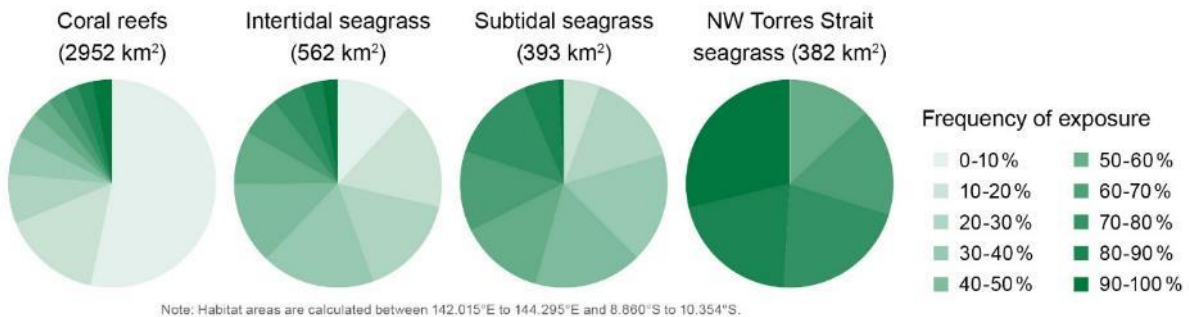
Figure D3: Exposure (area km2) of coral reef, intertidal and subtidal seagrass habitats to Primary and Secondary (CC1–5) waters between 2008 and 2018 (excluding 2011 and 2012).

Exposure at different habitat sites

Figure D3 shows the average long-term (2008 to 2018) frequency of exposure to each CC for each of the habitat sites. The average (decadal) exposure to the most turbid CCs (CC1–4 or Primary water type) decreased from the most northern to the sites further south. The greatest frequency of exposure to Primary waters was measured at Saibai and Boigu Islands, the northern sites (Figure D3, top graph); exposure at the more southern sites (Figure D3, bottom graph) was greatest at Erub Island. The Warrior Reef sites, and Saibai, Boigu, Erub and Mer Island sites were predominantly exposed to Secondary waters (CC5, ≥ 50% of the time), with the greatest frequency of exposure to Secondary waters also measured at Saibai and Boigu Islands (84% of the time). The Ugar, Masig and Poruma Island sites were predominantly exposed to Tertiary waters (CC6, ≥ 50% of the time). Bramble Island was exposed 26%, 38% and 34% of the time to Secondary, Tertiary and marine waters, respectively.
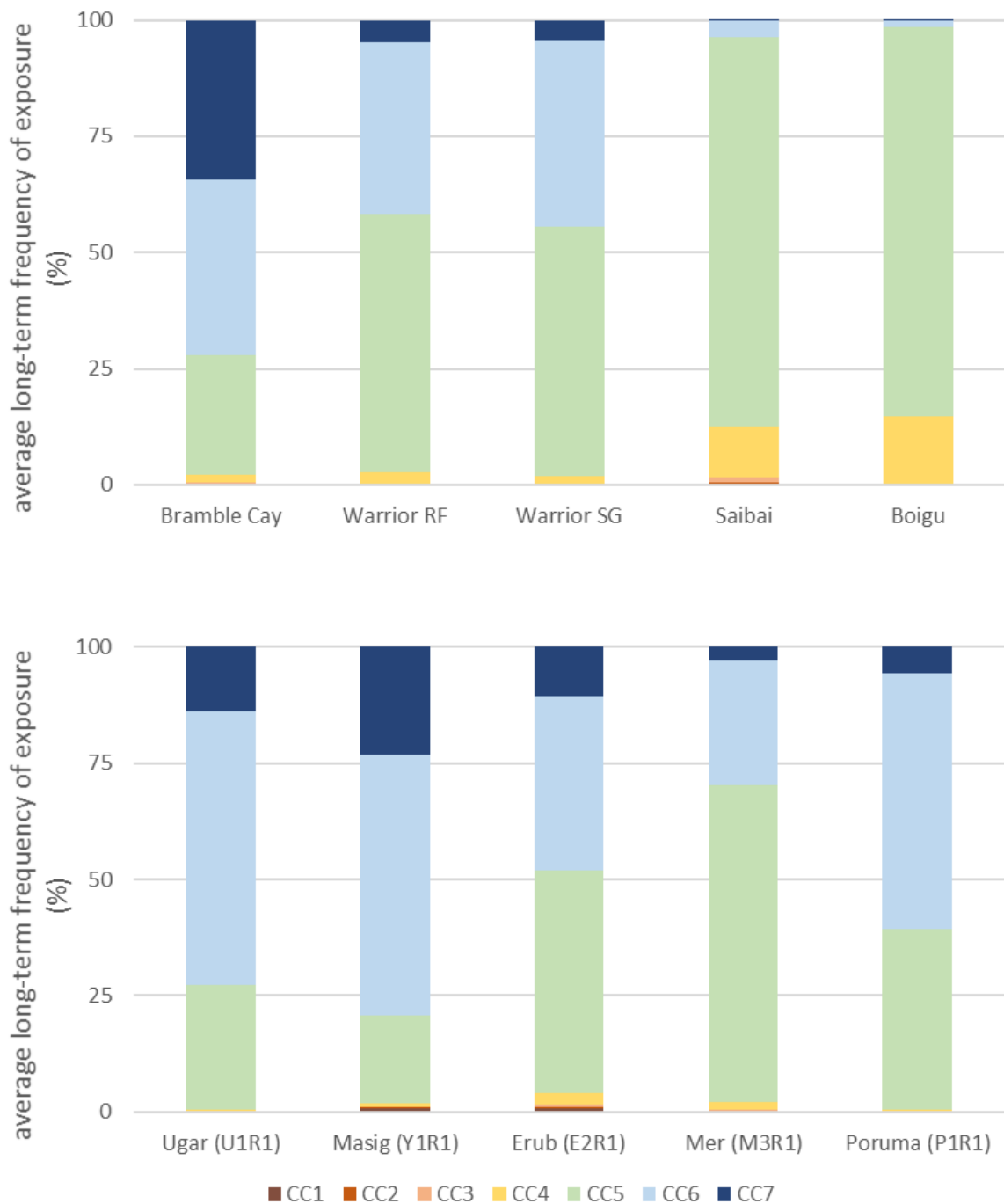
Figure D3: Long-term frequency (decadal mean, 2008–2018) of exposure to different CCs (CC1 to CC6) at the selected coral reef and seagrass monitoring sites in the northern Torres Strait (Table D1). Site codes in brackets after each site name (TSRA 2016): Top graph: Northern sites, bottom graph: Central sites. The water type frequency was defined as the total number of days per year exposed to a given water type divided by the number of data days (non-cloud) recorded per year, resulting in a normalised frequency on a scale from 0 to 1. Locations of the sites are presented in Figure D1.

Exposure to different potential zones of influence

Six potential zones of influence for the assessment area have been defined based on the results of the potential influence of the Fly River discharge in other sections of this report. The results for these zones are shown in Figure . The zonal results support the findings at the habitat site level presented above. The greatest frequency of exposure to Primary waters (CC1–4) was measured in the NW zone (3) and the greatest frequency of exposure to Secondary waters (CC5) was in the NW and North zones (3 and 1). The North and Central zones (1 and 5) had the greatest exposure to Tertiary waters (CC6) and the eastern zones (2 and 6) were the most often classified as marine waters (CC7).

This supports the premise that habitats in the northern Torres Strait are exposed more frequently to turbid waters than habitats in the south (Figure D4, Zones 1 and 3). The source cannot, however, be directly attributed to the Fly River and may include other coastal rivers (e.g. Wassi Kussa River at Boigu Island) and resuspension of sediment via currents, wind and wave action (e.g. at Erub, Masig and Mer Islands).

Potential links to ecosystem health

As noted above, the habitat sites for this analysis were selected from locations that are regularly monitored either by TSRA as part of their Coral Reef Monitoring Program or by TropWATER as part of ongoing seagrass health assessments (Carter and Rasheed 2016; TSRA 2016). However, it is difficult to make any causal links between the exposure results and ecosystem health assessments.

While the monitoring results from the 2015–2016 surveys conducted by the TSRA coral reef program (TSRA 2016) provide some indication of reef condition when compared with GBR long-term standards (Table D4), additional survey data are required to make any assessment of reef condition against the frequency of exposure to Primary and Secondary waters. ***The exposure results are only included here as an example of how this data could be considered in the future with longer term datasets.*** The lowest hard coral cover was monitored at Ugar Island (between 18.7% and 24.7%) and also the highest macroalgae cover (17.2%). Ugar Island had among the lowest frequency of exposure to Primary waters (CC1–4, Figure D2), indicating that turbidity is not likely to be the main driver of low coral cover in this location.

All other sites surveyed had moderate to high coral cover and low macroalgae cover (Table D4), which is consistent with previous surveys that recorded generally high cover (< 30%), particularly on the eastern Warrior Reefs (up to 47%) (Haywood et al. 2007; Sweatman et al. 2015; note that this is the most recent published data available). Other indicators generally associated with exposure to turbidity—such as coral disease—were also low and within a range generally considered healthy (see Thompson et al. 2017).

Table D4: Summary results from the Torres Strait coral reef monitoring surveys 2015–2016 (TSRA 2016). Colour shading: Green = high; Orange = moderate.

Location	Long term exposure results – average frequency		Hard coral cover (average %)	Comparison with GBR standards	Macroalgae cover (average %)	Comparison with GBR standards	Coral disease (average affected %)
	Primary	**Secondary**					
Poruma	0.50	38.82	27.3 – 50.9		7.5		n.d.
Masig	1.95	18.85	44.2 – 44.3		3.3		8.1
Ugar	0.49	26.79	18.7 – 24.7		17.2		0.2
Erub	4.14	47.78	27.7 – 34.2		2.5		1.3
Mer	2.13	68.05	41.8 – 48.1		3.1		0.3

Surveys in 2013 recorded 279 species of coral with massive corals locally dominant on the Warrior Reefs (Haywood et al. 2007; Osborne et al. 2013) and species richness varying along an east-west gradient, with the *Acroporidae* and *Pocilloporidae* coral families having higher richness on the eastern reefs (Osborne et al. 2013). These results indicate that the species richness of coral communities in the Torres Strait may reflect an east-west gradient in turbidity and wave exposure (Osborne et al. 2013).

While the exposure results provide a preliminary estimate of the spatial extent of exposure of habitats in the Torres Strait to turbid waters, **no direct link between exposure to river plume waters and reef condition can be made with these data at this stage.**
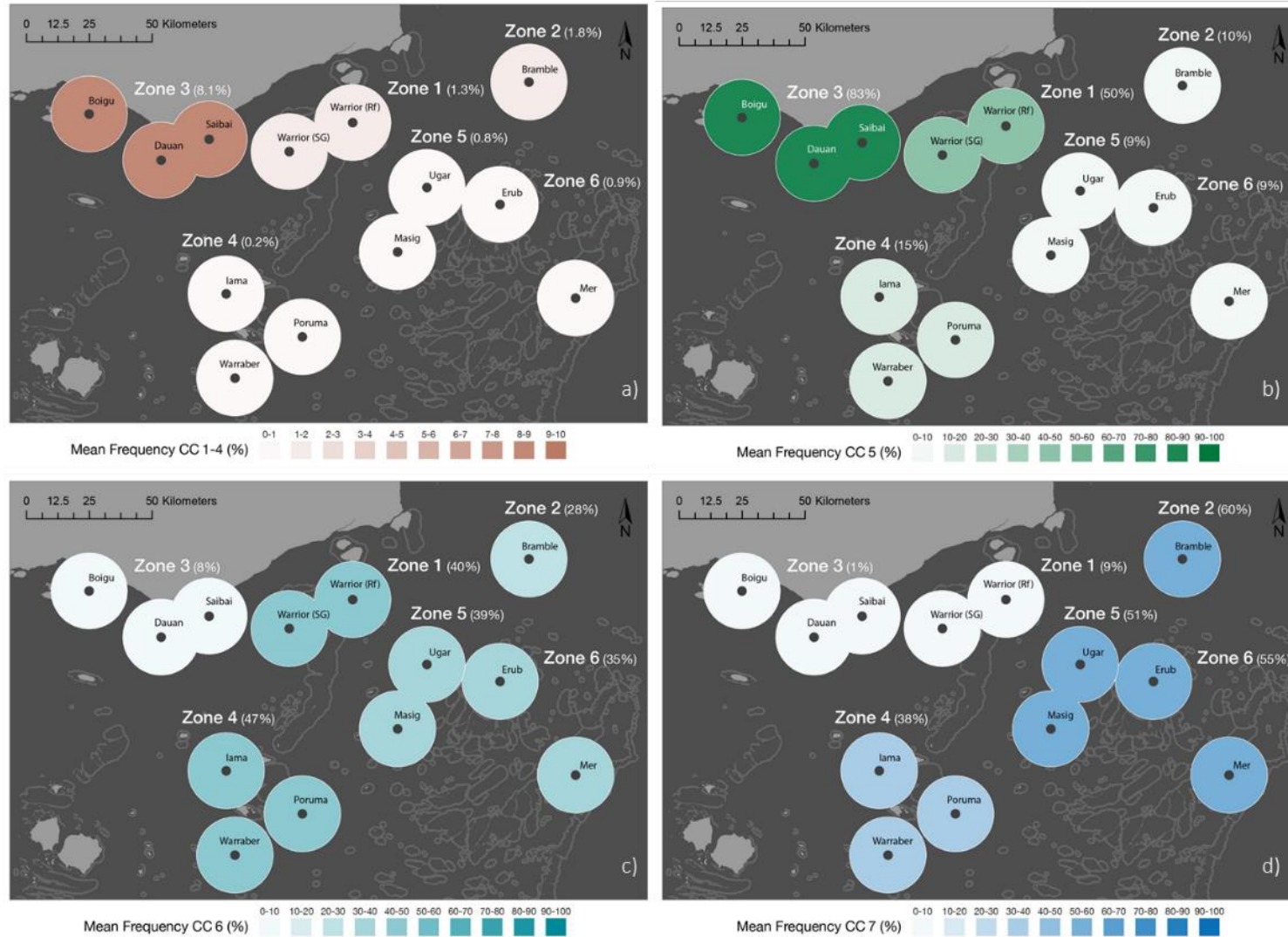
Figure D4: Spatial analysis of the mean frequency of exposure of habitat sites (1 km radius) to Primary (CC1–4), Secondary (CC5), Tertiary (CC6) and marine waters (CC7) into different zones of influence as defined in Table D1. Zone 1: North; Zone 2: North East; Zone 3: North West; Zone 4: South; Zone 5: Central and Zone 6: Eastern. Maps prepared by D. Tracey, TropWATER JCU.

Annual and seasonal patterns

In specific years and seasons, the Torres Strait reefs and seagrasses had a higher frequency of exposure to turbid waters, as shown by the exposure assessments for July–August (within SE trade wind season), February–March (within monsoon season) and annual periods at the (i) habitats (whole of Torres Strait scale), (ii) habitat sites and (iii) zonal geographical scales in the Appendices in Waterhouse et al. (2018). These variations are expected **given the seasonal nature of turbidity, in part driven by trade winds and resuspension** of the muddy carbonate sediments found around northern islands and reefs (Sweatman and Berkelmans 2012)**.**

Examples of observations are provided below.

For the **whole of Torres Strait scale habitat assessment** (coral reefs, intertidal seagrass and subtidal seagrass) there were clear examples of patterns across habitats such as:

1. While there was limited and infrequent exposure to Primary waters in all assessment periods for all habitats, some exposure was evident for coral reefs in all years where data was available. For coral reefs and intertidal seagrass, the area of exposure to Primary waters (while limited) was greatest during July–August 2008 and February–March 2009 and 2013.
2. The area of exposure to Primary and Secondary waters was greatest in February–March for all years for all habitats. The exception was for subtidal seagrass during July–August 2008 when the results were comparable.
3. For July–August and February–March, the greatest frequency and areas of exposure for all habitats typically occurred in 2008 and 2015. In February–March, reduced frequency exposure was evident in 2017 and 2018 compared to other years.

Further analysis of these preliminary results is required to understand the potential environmental drivers of the seasonal and inter-annual variability in exposure. In particular, Fly River discharge data would be highly valuable.

For the **habitat assessment** there were clear examples of differences between sites including:

- **Boigu and Saibai Islands** – dominated by Primary and Secondary waters. Greatest frequency of exposure to Primary waters of all sites, with greatest exposure in February–March. Primary waters evident in all years (where data available) in February–March except for 2009. Some occurrence of Tertiary waters in July–August. Greatest variability between years in July–August.
- **Warrior Reefs (seagrass and reef sites)** – dominated by Secondary waters and, to a lesser extent, Tertiary waters, with some exposure to Primary waters in February–March in most years where data was available, and in July–August in 2008 and 2015. Patterns between seasons and between years are reasonably consistent.
- **Erub and Poruma Islands and Mer** – dominated by Secondary waters, particularly in February–March, and Tertiary waters in July–August. Some limited exposure to Primary waters in some years, particularly in February–March.
- **Masig and Ugar Islands** – dominated by Tertiary waters and, to a lesser extent, Secondary waters, with very limited exposure to Primary waters, predominantly in February–March. Greatest variability between years in July–August.
- **Bramble Cay** – dominated by Tertiary and marine waters and, to a lesser extent, Secondary waters, with limited exposure to Primary waters in some years,

predominantly in February–March. Patterns between seasons and between years are reasonably consistent.

As above, further analysis of these results is required to understand the potential environmental drivers of the seasonal and inter-annual variability in exposure, which may include local wind and wave action and currents, and could be done to some extent with the hydrodynamic model. Cloud coverage interferes with image collection and can influence the results by providing a bias towards the period where there is lower cloud cover. Again, Fly River discharge data would be highly valuable. Updated ecosystem condition data would also be required.

A preliminary analysis of the correlation between frequency of exposure at the habitat sites and the annual NINO3.4 sea surface temperature anomaly (NINO3.4, index for ENSO events) was also undertaken. It showed weak negative relationships between annual NINO3.4 and the annual frequency of exposure to Primary (CC1–4) and Secondary (CC5) water types, with the strongest correlation observed at Bramble Cay ($r^2 = 0.5$, $p < 0.1$) and Masig Island ($r^2 = 0.3$, $p < 0.1$). However, further analysis of this result, as well as of the exposure datasets is required to understand potential environmental drivers of the seasonal and inter-annual variability in exposure to turbid waters. Furthermore, cloud coverage interferes with image collection and can influence the results by providing a bias towards periods where there is lower cloud cover, which is typically associated with less rainfall (Table D2).

D-4 Conclusions

The results of the frequency of habitat exposure to river plume waters identifies some coral reef and seagrass habitats in the northern Torres Strait that are frequently or very frequently exposed to turbid waters. However, at the time, these results were preliminary and further assessment was recommended. These conditions could be driven by resuspension and/or the influence of fluvial discharges from PNG rivers potentially including the Fly River discharge under certain conditions. It is therefore important to identify the source of Primary (CC1–4) and Secondary (CC5) waters at specific sites by combining sediment and water sampling with habitat health surveys to provide more insight into whether the discharge from the Fly River is likely to be a major driver of the condition of coral reef and seagrass habitats in the northern areas of the Torres Strait.

D-5 References

Álvarez-Romero, J., Devlin, M., da Silva, E., Petus, C., Ban, N., Pressey, R., Kool, J., Roberts, J., Cerdeira-Estrada, S., Wenger, A., & Brodie, J. (2013). A novel approach to model exposure of coastal-marine ecosystems to riverine flood plumes based on remote sensing techniques. Journal of Environmental Management, 119, 194-207.

Carter, A.B., Taylor, H.A., & Rasheed, M.A. (2014). Torres Strait mapping: Seagrass consolidation, 2002–2014. JCU Publication, Report no. 14/55, Centre for Tropical Water & Aquatic Ecosystem Research, Cairns, 47pp.

Carter, A.B., & Rasheed, M.A. (2018). Torres Strait Seagrass Long-term Monitoring: Dugong Sanctuary, Dungeness Reef and Orman Reefs., Centre for Tropical Water & Aquatic Ecosystems, Research Report No. 18/17, James Cook University, Cairns, 35 pp.

Devlin, M., Petus, C., Teixeira da Silva, E., Tracey. D., Wolff, N., Waterhouse, J., & Brodie, J. (2015). Water quality and river plume monitoring in the Great Barrier Reef: An overview of methods based on ocean colour satellite data. Remote Sensing, 7, 12909-12941. doi: 10.3390/rs71012909

Haywood, M.D.E., Browne, M., Skewes, T., Rochester, W., McLeod, I., Pitcher, R., Dennis, D., Dunn, J., Cheers, S., & Wassenberg, T. (2007). Improved knowledge of Torres Strait seabed biota and reef habitats. Report to the Marine and Tropical Sciences Research Facility. Reef and Rainforest Research Centre Limited, Cairns, 115pp.

Haywood, M.D.E., Pitcher, C.R., Ellis, N., Wassenberg, T. J., Smith, G., Forcey, K., McLeod, I., Carter, A., Strickland, C., & Coles, R. (2008). Mapping and characterisation of the inter-reefal benthic assemblages of the Torres Strait. Continental Shelf Research, 28, 2304-2316.

Osborne, K., Miller, I., Johns, K., Jonker, M., & Sweatman, H. (2013). Preliminary report on surveys of biodiversity of fishes and corals in Torres Strait. Australian Institute of Marine Science, Townsville, Australia.

Sweatman, H., & Berkelmans, R. (2012). Summary of existing information on coral reef communities of the Torres Strait. NERP Project 2.3 Report, Australian Institute of Marine Science, Townsville, 7pp.

Thompson, A., Costello, P., Davidson, J., Logan, M., Coleman, G., Gunn, K., & Schaffelke, B. (2017). Marine monitoring program. Annual Report for inshore coral reef monitoring: 2015 to 2016. Report for the Great Barrier Reef Marine Park Authority, Great Barrier Reef Marine Park Authority, Townsville, 133pp.

Torres Strait Regional Authority (TSRA) (2016). Torres Strait Long Term Coral Reef Monitoring Project 2015-2016. Author: Simpson, T. Published by the Torres Strait Regional Authority Land and Sea Management Unit, Thursday Island, Queensland. (56pp).